UNIVERSITAT DE BARCELONA

Facultat de Química

DEPARTAMENT DE QUÍMICA FÍSICA

Laboratori d'Electroquímica dels Materials i del Medi Ambient

ELECTROCHEMICAL ADVANCED OXIDATION PROCESSES FOR THE REMOVAL OF THE DRUGS PARACETAMOL, CLOFIBRIC ACID AND CHLOROPHENE FROM WATERS

DOCTORAL THESIS

Ignacio SIRÉS SADORNIL

Barcelona, november 2006

UNIVERSITAT DE BARCELONA

PART B

RESULTATS I DISCUSSIÓ

RESULTS AND DISCUSSION

7. DESTRUCCIÓ D'UN FÀRMAC ANTIINFLAMATORI NO ESTEROÍDIC: PARACETAMOL

/ *DESTRUCTION OF A NON-STEROIDAL ANTIINFLAMMATORY DRUG: PARACETAMOL*

This chapter is devoted to the study of the degradation of the non-steroidal antiinflammatory drug (NSAID) paracetamol. It is divided into three parts: (i) an introduction giving an overview on the characteristics of paracetamol, its environmental relevance and some results published in literature on its destruction, (ii) the results obtained for the destruction of this drug by electro-Fenton and photoelectro-Fenton processes, and (iii) the results obtained by anodic oxidation.

7.1. CARACTERÍSTIQUES DEL PARACETAMOL / *CHARACTERISTICS OF PARACETAMOL*

Paracetamol (Figure 7.-1), known as *acetaminophen* in the United States, is a non-steroidal anti-inflammatory drug (NSAID) belonging to the chemical family of aromatic amides. It is classified as a common analgesic and antipyretic drug, analogous to acetylsalicylic acid. In fact, it is the most widely used over-the-counter analgesic in USA, with production of 3600 tons in 2002 [345]. Paracetamol is a metabolite of phenacetine, a very commonly used analgesic in past years. Due to the fact that phenacetine is really toxic at therapeutical dosage and since it is metabolized to paracetamol, phenacetine is no longer used at present.

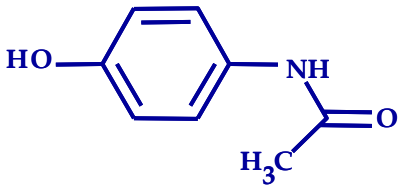

Figure 7.-1 Paracetamol.

Paracetamol is usually a white crystalline powder, odourless and bitter-tasted. Saturated solutions are slightly acid. It is soluble in acetone, hardly soluble in ether or benzene and highly soluble in water as shown in Table 7.-1. Some of the most remarkable properties of paracetamol are also given in Table 7.-1.

It is worth noting that some chemicals serve double duty as both drugs and pest-control agents. For example, warfarin can act as a rat poison as well as an anticoagulant, and triclosan is a general biocide and a gingivitis agent used in toothpaste. Similarly, paracetamol is frequently used for control of Brown Tree snakes: *Boiga irregularis*, native to eastern Indonesia, became invasive pests on Guam starting in the 1940's/1950's. Without natural predators, the Brown Tree snake's population in Guam is estimated at upwards of 15.000 per square mile, causing

extensive economic losses. No effective control was achieved until discovering that paracetamol can kill them within three days [346]. Other uses include the manufacturing wastes of azoic dyes and chemical products for photographic purposes [347].

Table 7.-1 Paracetamol data [348].

CAS number	103-90-2
Generic names	4-Hydroxyacetanilide 4-Acetamidophenol Acetaminophenol
Trade names	APAP, Disprol, Panadol, Tylenol
Molecular formula	$C_8H_9NO_2$
Molecular mass (g mol^{-1})	151.17
Melting point (°C)	169-171
Boiling point (°C)	> 500
Solubility in H_2O (g L^{-1})$_{20\ °C}$	14
Density (g cm^{-3})$_{21\ °C}$	1.293
pK_a	9.71-9.84

Paracetamol is a safe drug when consumed at therapeutic dosages, since it is metabolized to labile sulphate and glucuronide conjugates for excretion (55-60% administered paracetamol is excreted as a conjugated species). Its action mechanism implies the inhibition of cyclooxygenases at central nervous system, what highens the pain threshold. However, at certain concentrations paracetamol can be bioactivated by cytochromes P450, which are a superfamily of monooxygenases that are responsible for the metabolism of various endogenous and exogenous compounds, then causing severe hepatotoxicity [349, 350], as well as other additional effects. At this point, Paracelsus' theorem can be reminded:

> *"All substances are poisons, there is none that is not a poison. The right dose differentiates a poison and a remedy."*

Paracetamol is a well-known pain reliever, but at the same time when reaching a certain dosage it can effectively control Brown Tree Snakes or cause hepatotoxicity in human beings. Considering this theorem in combination with the fact that the environment contains countless organisms with different sensitivities leads to the hypothesis that medicines may also pose a risk for the environment.

In 1994, 153.9-million paracetamol doses were prescribed. It has been previously said that the key for considering PPCPs as a matter of ecological concern is their continous introduction in the environment due to their widespread huge usage. Undoubtedly, in spite of being considered as readily degradable ($t_{1/2}$ < 1 day), the enormous amount of paracetamol which is manufactured and released to the environment can pose a risk, yet unknown at present, to both humans and animals. Indeed, paracetamol occupies almost 50% of market shares in analgesic-antipyretic field of the world and its demand can be up to 70000 tons annually. At present, the international demand is growing at 15% of annual increasing rate. It is forecast that in 2010 the annual consumption all over the world will be over 100000 tons. More information on paracetamol sales data is available through several books [351, 352].

Some environmental studies have reported the presence of paracetamol up to 6 μg L^{-1} in European STPs effluents, while its presence in surface waters has not been documented [353]. In USA it has been found at μg L^{-1}-level in 17% of studied streams and at ng L^{-1}-level in untreated sewage waters, with a maximum of 10 μg L^{-1} in natural waters [27]. Among 139 surveyed streams in USA, paracetamol has been identified as one of the most frequently detected anthropogenic compounds. In UK, paracetamol was included in a top 10 list according to its risk characterisation ratio, obtained by using its Predicted Environmental Concentration (PEC) and Predicted No-Effect Concentration (PNEC) [354].

Before carrying out the present thesis, some previous studies on the degradation of paracetamol had been performed by Vogna et al. [355] and Andreozzi et al. [356] by means of ozonation and H_2O_2/UV in the pH range 2.0-5.5. A detailed discussion about the intermediates formed in both cases is carried out by these authors. Despite the fact that these procedures can be applied to destroy the parent molecule, the maximum mineralization achieved is around 30-40%, so more effective methods must be tested to avoid widespread contamination. In this sense, the electrochemical processes can be an environmentally friendly alternative, as shown later.

On the other hand, some papers have appeared simultaneously as well as after publishing the results got in this thesis. This fact clearly reflects the great interest about the role of PPCPs in the environment, and about paracetamol in particular.
Bobu et al. [357] have reported the percentage of paracetamol conversion by applying several AOPs for 30 min: foto-Fenton (99.55%), UV/O_3 (52.54%), O_3 (42.67%) and H_2O_2/UV (11.96%). However, the maximum mineralization degree achieved is around 50% corresponding to ozonation processes. Again, more powerful processes are needed if complete conversion into CO_2, H_2O and inorganic ions is desired.

In our laboratory, the limitations of simple ozonation and photolytic ozonation (O_3/UV) have been overcome by means of catalyzed ozonation with Fe^{2+}, Cu^{2+} and UVA light [194]. More than 83% of mineralization is attained with the catalyzed methods. As proved for electro-Fenton and photoelectro-Fenton processes shown in section 7.2 of this thesis, the highest oxidizing power is just achieved by combining Fe^{2+}, Cu^{2+} and UVA light.

Transformation of paracetamol by chlorination has been studied by Bedner et al. [345] to simulate wastewater disinfection and understand the toxicological nature of the chlorine-transformation products. Worrisome chlorination products such as *N*-acetyl-*p*-benzoquinone imine, which is the toxicant associated with lethality in

paracetamol overdoses, have been characterized. Due to its lack of stability, the imine readily hydrolyzes to the toxicant 1,4-benzoquinone in aqueous solution.

Finally, Bunce et al. [358] have compared the electro-oxidation process (i.e., anodic oxidation process) of paracetamol by using BDD, Ti/SnO_2 and Ti/IrO_2 anodes, working in an electrochemical reactor. The former two ones led to electrochemical combustion, whereas in the latter *p*-benzoquinone was the exclusive product except at very long electrolysis times. As it has been already argued in this thesis, the difference can be explained in terms of the different mechanisms of oxidation: selective conversion at Ti/IrO_2 anode through the action of hydroxyl radicals in the form of 'superoxides' such as Ti/IrO_x, vs. non-selective combustion involving physisorbed hydroxyl radicals at BDD and Ti/SnO_2.

In this work, paracetamol decay and mineralization have been studied by different EAOPs such as electro-Fenton (EF) and photoelectro-Fenton (PEF) with a Pt anode and an O_2-diffusion cathode, and anodic oxidation with both Pt and BDD anodes.

7.2. TRACTAMENT MITJANÇANT ELECTRO-FENTON I FOTOELECTRO-FENTON / *TREATMENT BY ELECTRO-FENTON AND PHOTOELECTRO-FENTON*

7.2.1. Finalitat del treball / *Aim of the work*

A fundamental task (not shown in the related papers) must be carried out before starting with the study on the degradation and mineralization of paracetamol by electro-Fenton and photoelectro-Fenton processes using an O_2-diffusion cathode.
In order to assess the ability of the C_{black}-PTFE O_2-diffusion cathode to electrogenerate hydrogen peroxide, several solutions containing 100 mL of 0.05 M Na_2SO_4 at pH 3.0 and at 35 ºC have been electrolyzed by applying a constant current, in the presence and absence of catalysts (Fe^{2+}, Cu^{2+} and UVA light). The experimental setup consists of an open undivided thermostated conic electrolytic cell, where a Pt anode and an O_2-diffusion cathode are placed as shown in Figure 6.-3. The H_2O_2 concentration accumulated in each solution during the electrolysis has been determined by the spectrophotometric measurement of the absorbance of the colored complex formed between Ti(IV) and H_2O_2 at λ = 408 nm (more detailed in section 6.3).

The results in Figure 7.-2 show some trends that can be accounted for by:

(i) The cathode generates H_2O_2 through Reaction 5.-47, and the amount of accumulated H_2O_2 is higher when the applied current intensity rises. After a while, a steady state is reached because H_2O_2 formation rate at the cathode (Reaction 5.-47) and H_2O_2 destruction rate at the anode (Reaction 5.-48 and Reaction 5.-49) become equal. This steady concentration in the absence of catalysts is about 13, 40 and 60 mM, at 100, 300 and 450 mA, respectively. That's to say, the maximum H_2O_2 concentration achieved is approximately proportional to the applied current intensity. This behavior agrees with the fact that both Reaction 5.-47 and Reaction 5.-48 verify a first-order kinetics.

(ii) As Fe^{2+}, Cu^{2+} or UVA light are being used as catalyst at a certain current intensity (300 mA in Figure 7.-2), accumulated H_2O_2 concentration decreases due to its growing disappearance caused by its destruction through Fenton's reactions (Reaction 5.-3 and Reaction 5.-4), photo-Fenton reaction (Reaction 5.-23), co-catalyzed Fenton reactions (Reactions 5.-28 to 5.-31) and H_2O_2 photolysis (Reaction 5.-25 and Reaction 5.-26), being the latter two reactions given to a very low extent. These are the main reactions, which in the presence of an organic pollutant R make it possible the mineralization process thanks to the electrogenerated hydroxyl radicals ($^{\bullet}OH$), and to the less powerful agent hydroperoxyl radical ($HO_2^{\bullet}$).

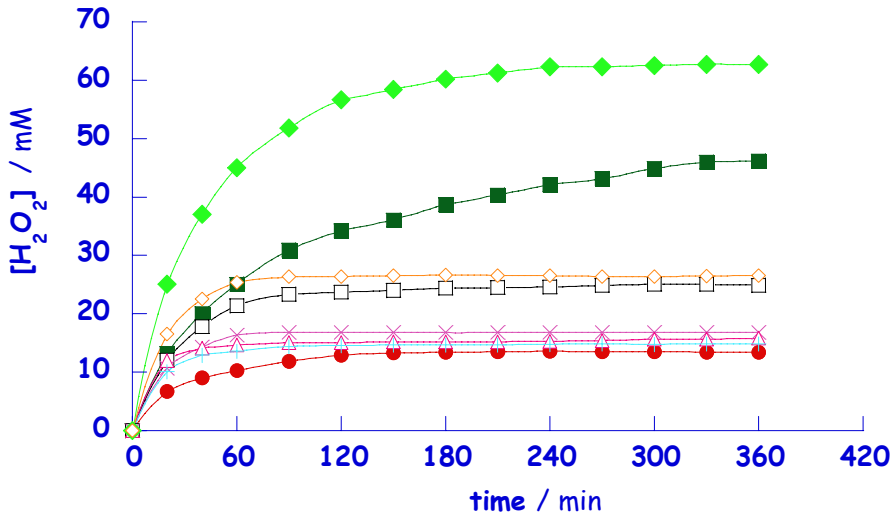

Figure 7.-2 Accumulated H_2O_2 concentration vs. electrolysis time, for the system Pt/O_2-diffusion cathode. The initial 100-mL solution contained 0.05 M Na_2SO_4 at pH = 3.0 and at 35 °C.
(♦, ■, ●) without catalyst, (◊, □) 1.0 mM Fe^{2+} (EF), (×) 1.0 mM Fe^{2+} under UVA irradiation (PEF), (Δ) 1.0 mM Fe^{2+} and 0.25 mM Cu^{2+} (co-catalyzed EF) and (+) latter solution under UVA irradiation (co-catalyzed PEF).
I applied: (♦, ◊) 450 mA, (■, □, ×, Δ, +) 300 mA and (●) 100 mA.

Once the proper performance of the cathode was assured, the EF and PEF processes using a 3-cm^2 Pt anode and a 3-cm^2 O_2-diffusion cathode were applied in order to remove paracetamol from the initial solutions.

At the beginning, the aim was just assuring that these EAOPs were able to face a largely discussed problem such as pharmaceuticals in the environment. In order to assess the performance of EF and PEF processes when dealing with paracetamol, 100-mL solutions containing 157 mg L^{-1} paracetamol (i.e., 100 mg L^{-1} TOC) and 0.05 M Na_2SO_4 as supporting electrolyte, at pH 3.0 and at 35 ºC, were electrolyzed for 6 h at 100 mA. TOC abatement analyses were done in the absence and presence of catalysts (1.0 mM Fe^{2+} and/or 0.25 mM Cu^{2+} and/or UVA light). In additon, paracetamol kinetics as well as final carboxylic acids evolution were studied.

After the considerations carried out in the previous paragraph, the oxidation ability of different systems was tested through the TOC abatement of paracetamol solutions under the same conditions, but applying 300 mA. In the absence of catalysts the process is called anodic oxidation (AO) with H_2O_2 electrogeneration. Afterwards the same experiment was done in presence of catalysts: UVA light irradiation (AO with UVA light), Cu^{2+} with or without UVA light (*Fenton-like* processes), Fe^{2+} with or without UVA light (PEF and EF, respectively), and Fe^{2+} + Cu^{2+} with or without UVA light (co-catalyzed PEF and co-catalyzed EF, repectively).

Then, the influence of the variation of several experimental parameters was studied. Firstly, the effect of current on the oxidation ability of each catalyzed method (containing 1.0 mM Fe^{2+} and/or 1.0 mM Cu^{2+} and/or UVA light) was examined by electrolyzing solutions under the experimental conditions already described, at 33, 100 and 150 mA cm^{-2}. Secondly, the effect of pH was clarified by treating solutions containing 157 mg L^{-1} of drug solutions at initial pH between 2.0 and 6.0, for the system 1.0 mM Fe^{2+} + 1.0 mM Cu^{2+} + UVA light. Thirdly, the influence of Fe^{2+} and Cu^{2+} concentrations was tested by electrolyzing 157 mg L^{-1} of drug solutions of pH 3.0 containing both ions in the range 0.25-1.0 mM at 100 mA cm^{-2} under UVA irradiation. And lastly, the oxidation ability of the system 1.0 mM Fe^{2+} + 1.0 mM Cu^{2+} + UVA light to degrade drug solutions of pH 3.0 at 100 mA cm^{-2} up to nearly 1 g L^{-1} was examined.

Once the optimal conditions were defined through the TOC decay analysis, the evolution of inorganic ions was studied to determine the loss of initial nitrogen of paracetamol in the form of NH_4^+ and NO_3^- ions. In this sense, the aforementioned catalyzed solutions (with 1.0 mM Fe^{2+} and/or 1.0 mM Cu^{2+} and/or UVA light) were electrolyzed for 6 h at 300 mA under the experimental conditions pointed out above.

Having concluded with the TOC decay analysis, chromatographic techniques were used to identify the stable intermediates formed during paracetamol mineralization. GC-MS allowed the detection of some of the intermediates, and both reversed-phase chromatography and ion-exclusion chromatography were used in order to identify the aromatics and the aliphatic carboxylics, respectively. Several experiments involving the degradation of intermediates were also carried out to clearly establish the degradation pathway: solutions containing 50 mg L^{-1} of ketomalonic, maleic and fumaric acids, with 1.0 mM Fe^{2+} + 1.0 mM Cu^{2+} + UVA light, were electrolyzed at pH 3.0 and at 300 mA. In an analogous way, 50 mg L^{-1} of acetamide were treated.

Once the identification of peaks was made, a 157 mg L^{-1} paracetamol solution of pH 3.0 at 35 °C was degraded by all catalyzed and uncatalyzed systems previously described, at 100 mA cm^{-2}, and the evolution of the drug concentration and its oxidation intermediates was determined as a function of the electrolysis time.

Finally, considering all the intermediates that were found, a general reaction scheme for the mineralization of paracetamol in acid media by all indirect electro-oxidation methods with H_2O_2 electrogeneration under action of Fe^{2+}, Cu^{2+} and UVA light as catalysts could be proposed.

The thorough results of this section are included in the following papers (Paper 1-2):

1. Sirés, I., Arias, C., Cabot, P.L., Centellas, F., Rodríguez, R.M., Garrido, J.A., Brillas, E., Paracetamol mineralization by advanced electrochemical oxidation processes for wastewater treatment. *Environ. Chem.* **1** (2004) 26-28.

2. Sirés, I., Garrido, J.A., Rodríguez, R.M., Cabot, P.L., Centellas, F., Arias, C., Brillas, E., Electrochemical degradation of paracetamol from water by catalytic action of Fe^{2+}, Cu^{2+}, and UVA light on electrogenerated hydrogen peroxide. *J. Electrochem. Soc.* **153** (2006) D1-D9.

The following presentations in a congress are related to this work:

A. Brillas, E., **Sirés, I.**, Arias, C., Cabot, P.L., Centellas, F., Rodríguez, R.M., Garrido, J.A., Mineralization of Paracetamol by Photoelectro-Fenton, Vol. 1, pages 101-102, 3rd European Meeting on Solar chemistry and Photocatalysis: Environmental Applications (SPEA-3), Universitat de Barcelona, Barcelona, Spain, 30 June - 2 July 2004. (Poster presentation)

B. Sirés, I., Garrido, J.A., Rodríguez, R.M., Cabot, P.L., Centellas, F., Arias, C., Brillas, E., Mineralización del paracetamol en medio ácido usando cátodos de difusión de oxígeno: acción catalítica de Fe^{2+}, Cu^{2+} y luz UVA sobre el peróxido de hidrógeno electrogenerado, Vol. 1, page 515, XXX Reunión Bienal de la RSEQ (XXVII Reunión del Grupo Especializado de Electroquímica de la RSEQ), Lugo, Spain, 19-23 September 2005. (Poster presentation)

UNIVERSITAT DE BARCELONA

ARTICLE 1 / *PAPER 1*

Paracetamol mineralization by advanced electrochemical oxidation processes for wastewater treatment

Rapid Communication

CSIRO PUBLISHING

I. Sirés et al., *Environ. Chem.* **2004**, *1*, 26–28. doi:10.1071/EN04018

www.publish.csiro.au/journals/env

Paracetamol Mineralization by Advanced Electrochemical Oxidation Processes for Wastewater Treatment

Ignasi Sirés,[A] *Conchita Arias*,[A] *Pere Lluís Cabot*,[A] *Francesc Centellas*,[A] *Rosa María Rodríguez*,[A] *José Antonio Garrido*,[A] *and Enric Brillas*[A,B]

[A] Laboratori de Ciència i Tecnologia Electroquímica de Materials (LCTEM), Departament de Química Física, Universitat de Barcelona, 08028 Barcelona, Spain.

[B] Corresponding author (e-mail: brillas@ub.edu).

Environmental Context. *Even after passing through water treatment plants, discarded pharmaceuticals have been linked with poisoning aquatic life. A simple and reliable method for treating household wastewater would alleviate this issue. Using the common pain reliever paracetamol as a model, the simple combination of dissolved iron and copper with ultraviolet light is shown to fully decompose ('mineralize') this drug into simple inorganic components, which represents an improvement over current treatments with ozone or peroxides, that achieve only partial mineralization.*

Abstract. Paracetamol solutions at pH 3.0 have been efficiently mineralized by environmentally clean electrochemical methods such as electro-Fenton and photoelectro-Fenton processes using a cell with a Pt anode and an O_2-diffusion cathode for H_2O_2 electrogeneration. This species reacts with added Fe^{2+} giving hydroxyl radical as main oxidant. Photoelectro-Fenton with Fe^{2+}, Cu^{2+}, and UVA light as catalysts leads to complete mineralization due to the removal of the final carboxylic acids (oxalic and oxamic). When catalysts are used separately, both acids or part of them remain in solution, giving a partial (>65%) mineralization.

Keywords. catalysis — drugs — electrochemistry — oxidation — water treatment

Manuscript received: 29 March 2004.
Final version: 5 May 2004.

In recent years, many pharmaceutical drugs have been found as minor pollutants, with concentrations less than 10 $\mu g\,L^{-1}$, in European and North American surface and groundwaters, sewage treatments plant (STP) effluents, and drinking water.[1–4] The pollution of natural waters with these compounds has to be avoided, because it is suspected that, at least, they can exert toxic effects to aquatic organisms and contribute to the development of multi-resistant strains of bacteria.[5] Recent papers[1,4–8] have demonstrated that several drugs can be successfully removed in aqueous medium by ozonation and advanced oxidation processes (AOPs), such as O_3/H_2O_2, H_2O_2/UV, and H_2O_2/Fe^{2+}/UV, being proposed as environmentally clean treatments for STP wastewaters containing such products. Paracetamol, *N*-(4-hydroxyphenyl)acetamide, has been detected in STP effluents up to 6 $\mu g\,L^{-1}$.[7] However, this drug only undergoes partial mineralization (conversion into carbon dioxide, water, and inorganic ions) of 30% and 40% from ozonation and H_2O_2/UV systems, respectively, in the pH range 2.0–5.5.[7] This paper reports preliminary results on the greater, and even total, mineralization of acidic paracetamol solutions obtained using advanced electrochemical oxidation processes (AEOPs), such as the electro-Fenton and photoelectro-Fenton treatments, which are more potent yet environmentally clean methods based on H_2O_2 electrogeneration and the catalytic effect of Fe^{2+}, Cu^{2+}, and/or UVA (300–400 nm) light.

A solution of paracetamol (100 mL at 157 $mg\,L^{-1}$, equivalent to 100 $mg\,L^{-1}$ total organic carbon (TOC)) in sodium sulfate (0.05 M at pH 3.0) was initially electrolyzed at a low current (100 mA) for six hours in an open and undivided cell with a platinum anode and an oxygen-diffusion cathode. In this system,[9–11] adsorbed hydroxyl radicals ($OH^{\bullet}$) are produced at the platinum surface from water oxidation by Reaction (1), while hydrogen peroxide is continuously electrogenerated from oxygen reduction at the cathode by Reaction (2). Hydroxyl radicals are a stronger oxidant than hydrogen peroxide, able to react with organics up to their overall mineralization.

$$H_2O \rightarrow OH^{\bullet}_{ads} + H^+ + e^- \quad (1)$$

$$O_{2(g)} + 2H^+ + 2e^- \rightarrow H_2O_2 \quad (2)$$

However, this procedure gives a quite poor mineralization, with a maximum TOC removal of 5% (curve *a* in Fig. 1), indicating a low oxidizing power of hydrogen peroxide and

1448-2517/04/010026

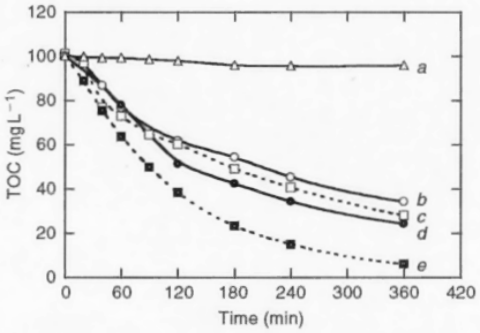

Fig. 1. TOC decrease with electrolysis time for the degradation of a paracetamol solution (100 mL, 157 mg L^{-1}) in Na_2SO_4 (0.05 M, pH 3.0) in a cell with a Pt anode and an O_2-diffusion cathode (both 3 cm^2 area) at 100 mA and 35°C. Catalysts were: (curve *a*, Δ) none; (curve *b*, ○) 1 mM Fe^{2+}; (curve *c*, □) 1 mM Fe^{2+} + 0.25 mM Cu^{2+}; (curve *d*, ●) 1 mM Fe^{2+} + UVA; (curve *e*, ■) 1 mM Fe^{2+} + 0.25 mM Cu^{2+} + UVA.

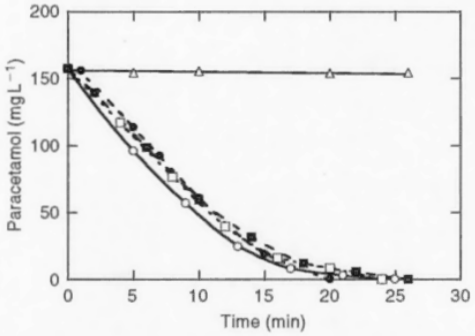

Fig. 2. Paracetamol concentration decrease with electrolysis time for the degradation of the same solution as in Fig. 1. Catalysts were: (○) 1 mM Fe^{2+}; (□) 1 mM Fe^{2+} + 0.25 mM Cu^{2+}; (●) 1 mM Fe^{2+} + UVA; (■) 1 mM Fe^{2+} + 0.25 mM Cu^{2+} + UVA. (Δ) Paracetamol concentration determined when the solution was directly exposed to UVA illumination without current passage.

the generation of a very small hydroxyl radical concentration at the platinum surface.

For the comparative electro-Fenton treatment with addition of 1 mM Fe^{2+} to the solution (curve *b* of Fig. 1), the TOC level rapidly falls for the first hour due to the rapid mineralization of pollutants with $OH^{\bullet}$ produced from the Fenton reaction between the Fe^{2+} catalyst and electrogenerated H_2O_2, Reaction (3):[9–15]

$$Fe^{2+} + H_2O_2 \rightarrow Fe^{3+} + OH^{\bullet} + OH^{-} \qquad (3)$$

At longer times the solution depolluted increasingly slowly, up to a limit of 65% TOC removal, with the formation of products oxidizable only with difficulty, probably complexes of Fe^{3+} with some intermediates (diols, carboxylic acids, and so forth).[16] The catalytic presence of 1 mM Fe^{2+} plus 0.25 mM Cu^{2+} yields a faster degradation rate, reaching 72% TOC removal after 6 h (curve *c* of Fig. 1). This suggests an additional mineralization by reaction of hydroxyl radicals with complexes of Cu^{2+}, competitively formed with those of Fe^{3+}.[11]

The depollution rate is slightly enhanced using photoelectro-Fenton treatment with 1 mM Fe^{2+} under UVA irradiation of the solution (curve *d* of Fig. 1), with 76% of TOC removal after 6 h. This behaviour can be associated with the photodecomposition of some complexes of Fe^{3+}[16] and/or the production of more $OH^{\bullet}$ according to Reaction (3) by additional regeneration of Fe^{2+} from the photoreduction of $Fe(OH)^{2+}$, Reaction (4), the predominant Fe^{3+} species at pH 3.0:[15]

$$Fe(OH)^{2+} + h\nu \rightarrow Fe^{2+} + OH^{\bullet} \qquad (4)$$

In contrast, photoelectro-Fenton treatment with 1 mM Fe^{2+}, 0.25 mM Cu^{2+}, and UVA light is so potent that total mineralization (TOC removal > 95%) is already reached by six hours (curve *e* of Fig. 1).

The kinetics for the reaction of paracetamol with oxidants generated in the above AEOPs was followed using reversed-phase chromatography. Fig. 2 shows a similar rapid drop for

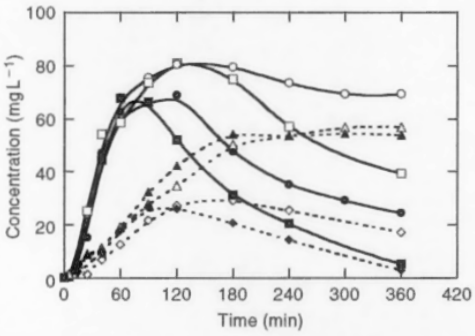

Fig. 3. The concentration of (○, □, ●, ■) oxalic and (Δ, ◇, ▲, ♦) oxamic acids generated as final products during the mineralization of the same paracetamol solution as in Fig. 1. Catalysts were: (○, Δ) 1 mM Fe^{2+}; (□, ◇) 1 mM Fe^{2+} + 0.25 mM Cu^{2+}; (●, ▲) 1 mM Fe^{2+} + UVA; (■, ♦) 1 mM Fe^{2+} + 0.25 mM Cu^{2+} + UVA.

paracetamol concentration by all treatments, with complete removal after 20–25 min. These data cannot be fitted to kinetic equations related to simple reaction orders, which indicates very complex kinetics. Fig. 2 also shows that, as expected, the drug is not photolyzed under UVA illumination. These results confirm that hydroxyl radical produced from Reaction (3) is the main oxidant in all AEOPs.

Electrolyzed solutions were analyzed using ion-exclusion chromatography to detect generated carboxylic acids. Although many of these acids were found in low concentration after 60 min, at longer times only oxalic and oxamic acids were accumulated as final products. Fig. 3 shows a steady concentration of 69 and 57 mg L^{-1} for oxalic and oxamic acids, respectively, from 4 h of electro-Fenton treatment with Fe^{2+}, corresponding to 35 mg L^{-1} of TOC, a value equal to that found for the final electrolyzed solution, as shown by curve *b* of Fig. 1. The latter solution is then mainly composed of a mixture of Fe^{3+}–oxalato and –oxamato complexes, which are not oxidized by $OH^{\bullet}$. As shown in Fig. 3, only oxalic acid is destroyed by photoelectro-Fenton treatment with Fe^{2+}

under the action of UVA light, as expected if Fe^{3+}–oxalato complexes are quickly photodecarboxylated.[16] In contrast, the presence of Fe^{2+} and Cu^{2+} causes the partial destruction of both acids by electro-Fenton and their total removal by photoelectro-Fenton treatments. This positive synergetic effect of Cu^{2+} can be explained by the competitive formation of Cu^{2+}–oxalato and –oxamato complexes, which are destroyed by $OH^{\bullet}$ and accelerate the mineralization process.

We conclude that the combined action of Fe^{2+}, Cu^{2+}, and UVA light in AEOPs based on H_2O_2 electrogeneration allows total mineralization of paracetamol solutions of pH 3.0 at low current. The separate use of catalysts yields an efficient, but partial, depollution, since the final products such as oxalic and oxamic acids are not completely removed. Greater drug mineralization could be achieved by electro-Fenton treatment with Fe^{2+} plus Cu^{2+} if greater amounts of hydroxyl radicals are produced, which enhance the destruction of complexes of Cu^{2+} with the final carboxylic acids. Note that decomposition of accumulated H_2O_2, along with removal of the remaining Fe^{3+} and/or Cu^{2+}, are necessary to dispose of final detoxified solutions. These ions could then be precipitated as hydroxides at pH 8 to be reused.[11] These preliminary results demonstrate that the AEOPs tested are more efficient for paracetamol mineralization than ozonation and AOPs.[7] Further research to find the best operative conditions of all AEOPs for the treatment of wastewaters with this drug is in progress in our laboratory.

Experimental Methods

Paracetamol, oxalic acid, and oxamic acid were reagent grade from Merck and Avocado. Anhydrous sodium sulfate, heptahydrated ferrous sulfate, pentahydrated cupric sulfate, and sulfuric acid were analytical grade from Merck and Fluka. Solutions were prepared with water obtained from a Millipore Milli-Q system (conductivity $< 6 \times 10^{-8}$ S cm^{-1}).

Electrolyses were performed with an Amel 2053 potentiostat–galvanostat. Instruments for measuring solution TOC, drug decay by reversed-phase chromatography, and generated carboxylic acids by ion-exclusion chromatography have been reported.[11] Reversed-phase chromatograms displayed the paracetamol peak at t_r 1.56 min using a 70:30 (v/v) acetonitrile/water mixture at 1.2 mL min^{-1} as the mobile phase. In ion-exclusion chromatography, oxalic (t_r 6.75 min) and oxamic (t_r 9.29 min) acids were quantified using circulating 4 mM H_2SO_4 at 0.6 mL min^{-1}.

The electrolytic cell, containing a 3-cm^2 Pt anode from SEMP and a 3-cm^2 O_2-diffusion carbon–PTFE cathode from E-TEK, has been described.[9,11] The cathode was fed with pure O_2 at 20 mL min^{-1} for H_2O_2 electrogeneration according to Reaction (2). The initial pH, adjusted to 3.0 with 0.05 M H_2SO_4, remained practically constant in all treatments. UVA light was generated with a fluorescent black light/blue tube (6 W, Philips) emitting between 300 and 420 nm (λ_{max} 360 nm) and located 4 cm from the top of the cell.

Acknowledgements

Financial support received from MCYT (Ministerio de Ciencia y Tecnología, Spain) under project BQU2001–3712 and the grant awarded to I.S. by AGAUR (Agència de Gestió d'Ajuts Universitaris i de Recerca, Generalitat de Catalunya) are acknowledged.

References

[1] C. Zwiener, F. H. Frimmel, *Water Res.* **2000**, *34*, 1881. doi:10.1016/S0043-1354(99)00338-3
[2] *Pharmaceuticals and Personal Care Products in the Environment. Scientific and Regulatory Issues* (Eds C. G. Daughton, T. L. Jones-Lepp) **2001** (ACS Symposium Series: Washington, DC).
[3] *Pharmaceuticals in the Environment. Sources, Fate, and Risks* (Ed. K. Kümmerer) **2001** (Springer: Berlin).
[4] T. A. Ternes, M. Meisenheimer, D. McDowell, F. Sacher, H. J. Brauch, B. Haist-Gulde, G. Preuss, U. Wilme, N. Zulei-Seibert, *Environ. Sci. Technol.* **2002**, *36*, 3855. doi:10.1021/ES015757K
[5] I. A. Balcioğlu, M. Ötker, *Chemosphere* **2003**, *50*, 85. doi:10.1016/S0045-6535(02)00534-9
[6] M. M. Huber, S. Canonica, G. Y. Park, U. Von Gunten, *Environ. Sci. Technol.* **2003**, *37*, 1016. doi:10.1021/ES025896H
[7] R. Andreozzi, V. Caprio, R. Marotta, D. Vogna, *Water Res.* **2003**, *37*, 993. doi:10.1016/S0043-1354(02)00460-8
[8] T. A. Ternes, J. Stüber, N. Herrmann, D. McDowell, A. Ried, M. Kampmann, B. Teiser, *Water Res.* **2003**, *37*, 1976. doi:10.1016/S0043-1354(02)00570-5
[9] B. Boye, M. M. Dieng, E. Brillas, *Environ. Sci. Technol.* **2002**, *36*, 3030. doi:10.1021/ES0103391
[10] E. Brillas, P. L. Cabot, J. Casado, in *Chemical Degradation Methods for Wastes and Pollutants. Environmental and Industrial Applications* (Ed. M. Tarr) **2003**, pp. 235–304 (Marcel Dekker: New York, NY).
[11] E. Brillas, M. A. Baños, S. Camps, C. Arias, P. L. Cabot, J. A. Garrido, R. M. Rodríguez, *New J. Chem.* **2004**, *28*, 314. doi:10.1039/B312445B
[12] M. A. Oturan, N. Oturan, C. Lahitte, S. Trevin, *J. Electroanal. Chem.* **2001**, *507*, 96. doi:10.1016/S0022-0728(01)00369-2
[13] A. Ventura, G. Jacquet, A. Bermond, V. Camel, *Water Res.* **2002**, *36*, 3517. doi:10.1016/S0043-1354(02)00064-7
[14] B. Gozmen, M. A. Oturan, N. Oturan, O. Erbatur, *Environ. Sci. Technol.* **2003**, *37*, 3716. doi:10.1021/ES034011E
[15] J. J. Pignatello, *Environ. Sci. Technol.* **1992**, *26*, 944.
[16] Y. Zuo, J. Hoigné, *Environ. Sci. Technol.* **1992**, *26*, 1014.

UNIVERSITAT DE BARCELONA

ARTICLE 2 / *PAPER 2*

Electrochemical degradation of paracetamol from water by catalytic action of Fe^{2+}, Cu^{2+}, and UVA light on electrogenerated hydrogen peroxide

ELEC Mat MA

Journal of The Electrochemical Society, **153** (1) D1-D9 (2006)
0013-4651/2005/153(1)/D1/9/$15.00 © The Electrochemical Society, Inc.

Electrochemical Degradation of Paracetamol from Water by Catalytic Action of Fe^{2+}, Cu^{2+}, and UVA Light on Electrogenerated Hydrogen Peroxide

Ignasi Sirés, José Antonio Garrido, Rosa María Rodríguez, Pere l.luís Cabot,* Francesc Centellas, Conchita Arias, and Enric Brillas[z]

Laboratori de Ciència i Tecnologia Electroquímica de Materials, Departament de Química Física, Facultat de Química, Universitat de Barcelona, 08028 Barcelona, Spain

Acidic aqueous solutions of the drug paracetamol have been degraded by anodic oxidation and indirect electro-oxidation methods using an undivided electrolytic cell with a Pt anode and an O_2-diffusion cathode for H_2O_2 electrogeneration. Anodic oxidation yields low mineralization due to the limited production of oxidant hydroxyl radical ($^{\cdot}OH$) from water oxidation at Pt. The presence of Cu^{2+} as catalyst, with and without (ultraviolet A, UVA) irradiation, slightly enhances the degradation process. In electro-Fenton, much more $^{\cdot}OH$ is produced from Fenton's reaction between added Fe^{2+} and electrogenerated H_2O_2, but stable Fe^{3+} complexes are formed. These species are partially photodecomposed in photoelectro-Fenton under UVA irradiation. The use of Fe^{2+} and Cu^{2+} yields fast decontamination because Cu^{2+} complexes are destroyed. Total mineralization of paracetamol is achieved when Fe^{2+}, Cu^{2+}, and UVA light are combined. The influence of current, pH, and drug concentration upon the efficiency of catalyzed methods is studied. Hydroquinone, *p*-benzoquinone, and carboxylic acids, such as ketomalonic, maleic, fumaric, oxalic, and oxamic, are detected as intermediates. The positive synergetic effect of all catalysts is explained by the oxidation of Cu^{2+}-oxalato and Cu^{2+}-oxamato complexes with $^{\cdot}OH$, along with the photodecarboxylation of Fe^{3+}-oxalato and Fe^{3+}-oxamato complexes by UVA light. NH_4^+ and NO_3^- are released during drug mineralization.
 [DOI: 10.1149/1.2130568]

Manuscript submitted June 6, 2005; revised manuscript received September 2, 2005. Available electronically November 16, 2005.

In recent years indirect electro-oxidation methods with hydrogen peroxide electrogeneration, such as electro-Fenton and photoelectron-Fenton reactions, are being developed for the treatment of toxic organic pollutants in waters.[1-18] These environmentally clean electrochemical techniques are carried out in an electrolytic cell where H_2O_2 is continuously generated in the contaminated solution from the two-electron reduction of O_2 at reticulated vitreous carbon,[1,3,6,7] graphite,[2] mercury pool,[8,13] carbon-felt,[10,11,16,18] and O_2-diffusion[4,5,9,12,14,15,17] cathodes

$$O_2 + 2H^+ + 2e^- \rightarrow H_2O_2 \quad [1]$$

Hydrogen peroxide thus produced is a weak oxidant of organics. In the electro-Fenton reaction, the oxidizing power of this species is enhanced by addition of small amounts of Fe^{2+} as catalyst to the acidic treated solution. Hydroxyl radical ($^{\cdot}OH$) and Fe^{3+} are then generated from the classical Fenton's reaction between Fe^{2+} and H_2O_2 with a second-order rate constant k_2 of 53 $dm^3\ mol^{-1}\ s^{-1}$[19,20]

$$Fe^{2+} + H_2O_2 \rightarrow Fe^{3+} + {}^{\cdot}OH + OH^- \quad [2]$$

An advantage of this method is that Reaction 2 is propagated from Fe^{2+} regeneration, which mainly occurs by reduction of Fe^{3+} species at the cathode or in the medium with H_2O_2. Hydroxyl radical acts as a nonselective, strong oxidant because it is able to react with organics, yielding dehydrogenated or hydroxylated derivatives, until their overall mineralization (conversion into CO_2 and inorganic ions) is achieved.

The photoelectro-Fenton method also involves the irradiation of the solution with (ultraviolet A, UVA) light to favor the regeneration of Fe^{2+} from additional photoreduction of $Fe(OH)^{2+}$, which is the predominant Fe^{3+} species in acid medium[19,20]

$$Fe(OH)^{2+} + h\nu \rightarrow Fe^{2+} + {}^{\cdot}OH \quad [3]$$

Reaction 3 accelerates the production of $^{\cdot}OH$ and, hence, the mineralization of organics. In addition, UVA light can photodecompose complexes of Fe^{3+} with some oxidation products, for example, with oxalic acid.[9,12,14,15,17,21]

Some attempts have also been made to show the possible catalytic effect of Cu^{2+}, alone or combined with Fe^{2+}, on the above procedures. Gözmen et al.[16] have found that bisphenol A in 0.01 M HCl is more rapidly degraded by the electro-Fenton reaction with Fe^{2+} than when electrogenerated H_2O_2 and Cu^{2+} are used. In previous work[17] we have described that addition of Cu^{2+} to nitrobenzene solutions of pH 3.0 accelerates their electro-Fenton and photoelectro-Fenton processes. A positive synergetic effect of Fe^{2+} and Cu^{2+} could then be expected for the degradation of other aromatic compounds in waters using these indirect electro-oxidation systems. At the end of such treatments, the resulting acid effluent should be neutralized up to pH 7–9 for complete decontamination by precipitation of metallic ions in the form of $Fe(OH)_2$, $Fe(OH)_3$, and $Cu(OH)_2$ before disposal. The collected precipitate could even be reused as a catalyst in further processes.

Recently, there is great interest in the environmental relevance of pharmaceutical drugs in waters. This pollution can be due to emission from production sites, direct disposal of overplus drugs in households, excretion after drug administration to humans and animals, and treatments throughout the water in fish farms.[22] A large number of pharmaceutical drugs such as antiinflammatories, analgesics, betablockers, lipid regulators, antibiotics, antiepileptics, and estrogens have been detected as minor pollutants with concentrations $<10\ \mu g\ L^{-1}$ in sewage treatment plant (STP) effluents, surface and ground waters, and even in drinking water.[22-26] Paracetamol [*N*-(4-hydroxyphenyl)acetamide], a common analgesic and antiinflammatory for humans and animals, has been found with concentrations up to 6 $\mu g\ L^{-1}$ in European STP effluents[25] and up to 10 $\mu g\ L^{-1}$ in USA natural waters.[26]

To avoid the potential dangerous accumulation of drugs in the aquatic environment, research efforts are underway to develop powerful oxidation techniques for achieving their destruction. Several works have reported the successful use of ozonation and advanced oxidation processes (AOPs) such as O_3/H_2O_2, H_2O_2/UV, and H_2O_2/Fe^{2+}/UV, with production of $^{\cdot}OH$ as the main oxidant, for the degradation of pharmaceuticals and their metabolites in water.[25,27-30] For paracetamol, a poor mineralization of 30 and 40% is found from O_3 and H_2O_2/UV methods, respectively, in the pH range 2.0–5.5.[25] In both procedures, hydroquinone, 2-hydroxy-4-(*N*-acetyl)aminophenol, 1,2,4-trihydroxybenzene, maleic acid, and oxalic acid are detected as intermediates. In previous work,[31] we have studied the direct anodic oxidation of solutions containing paracetamol concentrations up to 1 $g\ L^{-1}$ in the pH range 2.0–12.0 using an electrolytic cell with a Pt or a boron-doped diamond (BDD)

* Electrochemical Society Active Member.
[z] E-mail: brillas@ub.edu

anode and a graphite cathode. Complete mineralization of the drug with release of NH_4^+ and NO_3^- ions was always obtained with the BDD anode due to the great production of oxidant $^{\bullet}OH$ on its surface from water oxidation.[32-35] Under these conditions, the mineralization rate was pH-independent, the paracetamol decay followed a complex kinetics, and only oxalic and oxamic acids were identified as intermediates in all media. Comparative treatment of the same solutions with the Pt anode yielded a quite poor mineralization, because this electrode produces much lower $^{\bullet}OH$ concentration. However, a slow but complete destruction of paracetamol was achieved using the Pt anode following its kinetics as a pseudo first-order reaction with a constant rate independent of pH.

To clarify the possible application of indirect electro-oxidation methods with H_2O_2 electrogeneration to the removal of aromatic drugs from waters, we have carried out a study on the mineralization of paracetamol using Fe^{2+}, Cu^{2+}, and/or UVA light as catalysts. Higher drug concentrations than those found in STP and natural effluents were chosen to better analyze the oxidation ability of these methods. In this paper, we report the degradation of 157 mg L^{-1} paracetamol solutions of pH 3.0 using an undivided cell with a Pt anode and an O_2-diffusion cathode able to generate H_2O_2. A Pt electrode, instead of a BDD one, was preferred as anode because its very low oxidation allows showing an easier and clearer synergetic effect of catalysts on the degradation process. Comparative electrolyses were then performed with this system (anodic oxidation with H_2O_2 electrogeneration) and with UVA light, 1 mM Cu^{2+}, 1 mM Cu^{2+} + UVA light, 1 mM Fe^{2+} (electro-Fenton process), 1 mM Fe^{2+} + UVA light (photoelectro-Fenton process), 1 mM Fe^{2+} + 1 mM Cu^{2+}, and 1 mM Fe^{2+} + 1 mM Cu^{2+} + UVA light. The influence of applied current density, solution pH, and drug concentration upon the behavior of the catalytic methods was also explored. For each method, the drug decay was followed and its stable intermediates were identified and quantified. A reaction scheme for paracetamol mineralization involving the detected by-products is proposed.

Experimental

Reagents.— Paracetamol, hydroquinone, *p*-benzoquinone, acetamide, ketomalonic acid, maleic acid, fumaric acid, oxalic acid, and oxamic acid were reagent grade from Merck, Sigma-Aldrich, and Panreac. Anhydrous sodium sulfate, heptahydrated ferrous sulfate, and pentahydrated cupric sulfate were analytical grade from Fluka. Analytical grade sulfuric acid was purchased from Merck. All solutions were prepared with pure water obtained from a Millipore Milli-Q system with resistivity >18 MΩ cm at 25°C. Organic solvents and other chemicals employed were either high-pressure liquid chromatography (HPLC) or analytical grade from Panreac.

Apparatus.— Electrolyses were performed with an Amel 2053 potentiostat-galvanostat. The mineralization of paracetamol solutions was determined from the abatement of their total organic carbon (TOC), monitored on a Shimadzu VCSN TOC analyzer. Aromatic intermediates were separated and identified by gas chromatography mass spectroscopy (GC-MS) with a Hewlett-Packard system consisting of a HP 5890 Series II gas chromatograph fitted with an HP-5 0.25-μm, 30-m × 0.25-mm column, and coupled to an HP 5989A mass spectrometer operating in EI mode at 70 eV and at 300°C. The paracetamol decay and the evolution of its aromatic intermediates were followed by reversed-phase chromatography using a system composed of a Waters 600 HPLC liquid chromatograph fitted with a Spherisorb ODS2 5 μm, 150 × 4.6 mm column at room temperature, coupled with a Waters 996 photodiode array detector selected at λ = 280 nm and controlled through a Millennium-32 program. Generated carboxylic acids were detected by ion-exclusion chromatography using the above HPLC chromatograph fitted with an Aminex HPX 87H, 300 × 7.8 mm column at 35°C from Bio-Rad and the photodiode array detector selected at λ = 210 nm. NH_4^+ concentration in treated solutions was determined from the standard colorimetric method with Nessler's reagent, using a Unicam UV/vis UV4 spectrophotometer thermostated at 25°C. NO_3^- concentration in the same solutions was obtained by ion chromatography with a Shimadzu LC-10AT(VP) liquid chromatograph coupled with a Metrohm 690 ion chromatograph, fitted with a Hamilton PRP-X 100 10 μm, 150 × 4.1 mm anion column at room temperature and controlled with an HP 35900E interface.

Electrolytic system.— All electrolyses were conducted in an open, undivided, and thermostated glass-cylindrical cell containing 100 mL of solution stirred with a magnetic bar. A 3-cm^2 Pt sheet of 99.99% purity from SEMPSA and a 3-cm^2 carbon-poly(tetrafluoroethylene) (PTFE) electrode from E-TEK were used as the anode and cathode, respectively. The last electrode was fed with pure O_2 at 20 mL min^{-1} to generate continuously H_2O_2 from Reaction 1. The electrolytic setup and the preparation of the O_2-diffusion cathode have been described.[9] For the trials with UVA irradiation, a Philips 6 W fluorescent black light blue tube was placed at the top of the open cell at 7 cm above the solution. The tube emitted UVA light in the wavelength region between 300 and 420 nm, with λ_{max} = 360 nm, supplying a photoionization energy input to the solution of 140 μW cm^{-2}, detected with a NRC 820 laser power meter working at 514 nm.

Comparative degradation of solutions containing 157 mg L^{-1} of paracetamol and 0.05 M Na_2SO_4 of pH 3.0 adjusted with H_2SO_4 was carried out at a constant current density (*j*) of 33, 100, and 150 mA cm^{-2}, applying an average cell voltage of 5.5, 13.0, and 17.5 V, respectively. The catalytic effect of Fe^{2+} and/or Cu^{2+} was studied by adding 1 mM of each ion, because this Fe^{2+} content was very efficient in the electro-Fenton treatment of other aromatics.[9,12,14,15,17] For the electrolyses starting from pH 4.0 and 6.0, the solution pH was regulated within a range of ±0.3 units by adding small volumes of 0.5 M NaOH each 20 min. All trials were carried out at 35°C, which is the maximum temperature to work with the open electrolytic system without significant water evaporation from solution.[12]

Product analysis procedures.— Before analysis, the samples extracted were filtered with 0.45-μm PTFE filters from Whatman. Reproducible TOC values were obtained from analysis of 100-μL aliquots using the standard nonpurgeable organic carbon method. In reversed-phase chromatography, 70:30 (v/v) acetonitrile/water and 95:5 (v/v) 0.1 M HCOOH + NaOH (pH 3.0)/acetonitrile mixtures were employed as mobile phases at 1.2 mL min^{-1}, whereas in ion-exclusion chromatography, the mobile phase was 4 mM H_2SO_4 at 0.6 mL min^{-1}.[1] In both HPLC techniques, 20-μL samples were injected into the chromatograph. NO_3^- concentration was determined using a 90:10 (v/v) 2 mM phthalate buffer (pH 5.0)/acetone mixture as mobile phase at 2 mL min^{-1}. To identify the aromatic products, several paracetamol solutions were electrolyzed during short times and their organic components were extracted three times with 25 mL of CH_2Cl_2. Each collected organic solution was then dried with anhydrous Na_2SO_4, and once filtered, its volume was reduced to about 5 mL to concentrate the remaining products for further analysis by GC-MS.

Results and Discussion

Comparative degradation of paracetamol.— The oxidation ability of the different indirect electro-oxidation treatments was tested by electrolyzing 157 mg L^{-1} paracetamol solutions (equivalent to 100 mg L^{-1} of TOC) of pH 3.0 at 100 mA cm^{-2} and at 35°C for 6 h. In all experiments the solution pH always remained practically constant, reaching a final value between 2.8 and 3.0. The comparative TOC abatement for the above trials is depicted in Fig. 1.

In the electrolytic system, hydrogen peroxide is continuously injected into the solution from Reaction 1, whereas adsorbed $^{\bullet}OH$ is formed on the Pt surface from water oxidation[32-35]

Journal of The Electrochemical Society, **153** (1) D1-D9 (2006)

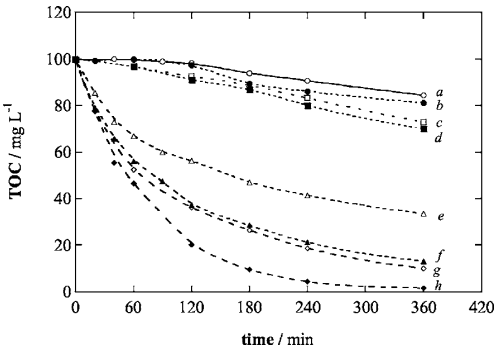

Figure 1. TOC decay vs electrolysis time for the degradation of 100 mL of 157 mg L^{-1} paracetamol solutions in 0.05 M Na_2SO_4 of pH 3.0 at 100 mA cm^{-2} and at 35°C, using a cell with a 3-cm^2 Pt anode and a 3-cm^2 O_2-diffusion cathode for H_2O_2 electrogeneration. Catalyst: (a, ○) None (anodic oxidation with H_2O_2 electrogeneration), (b, ●) UVA light with λ_{max} = 360 nm, (c, □) 1 mM Cu^{2+}, (d, ■) 1 mM Cu^{2+} + UVA light, (e, △) 1 mM Fe^{2+} (electro-Fenton process), (f, ▲) 1 mM Fe^{2+} + UVA light (photoelectro-Fenton process), (g, ◇) 1 mM Fe^{2+} + 1 mM Cu^{2+}, and (h, ◆) 1 mM Fe^{2+} + 1 mM Cu^{2+} + UVA light.

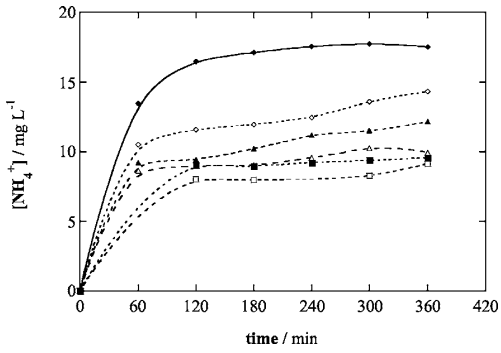

Figure 2. Concentration of ammonium ion accumulated during the treatment of 100 mL of 157 mg L^{-1} paracetamol solutions of pH 3.0 by the catalyzed experiments reported in Fig. 1. Catalyst: (□) 1 mM Cu^{2+}, (■) 1 mM Cu^{2+} + UVA light, (△) 1 mM Fe^{2+}, (▲) 1 mM Fe^{2+} + UVA light, (◇) 1 mM Fe^{2+} + 1 mM Cu^{2+}, and (◆) 1 mM Fe^{2+} + 1 mM Cu^{2+} + UVA light.

$$H_2O \rightarrow {}^{\bullet}OH_{ads} + H^+ + e^- \quad [4]$$

In addition, part of the electrogenerated H_2O_2 is also oxidized to O_2 at the anode via the hydroperoxyl radical ($HO_2^{\bullet}$), a weaker oxidant than $^{\bullet}OH$[9,17]

$$H_2O_2 \rightarrow HO_2^{\bullet} + H^+ + e^- \quad [5]$$

$$HO_2^{\bullet} \rightarrow O_2 + H^+ + e^- \quad [6]$$

The use of the electrolytic system without any catalyst corresponds to the method of anodic oxidation with H_2O_2 electrogeneration. As can be seen in curve a of Fig. 1, this treatment leads to a quite slow TOC decay, only attaining 15% of mineralization at 6 h. This can be explained by the low concentration of $^{\bullet}OH$ formed on the Pt anode surface from Reaction 4, which is the main oxidant of paracetamol and its products. When the solution is exposed to UVA light (see curve b of Fig. 1), the degradation process is slightly enhanced to give 19% of TOC removal. This behavior suggests a photodecomposition of several intermediates that accelerates the mineralization process, because UVA light does not photolyze H_2O_2 to $^{\bullet}OH$. Curve c of Fig. 1 shows that the presence of 1 mM Cu^{2+} causes a faster degradation rate to reach 28% of decontamination. This enhancement can be accounted for by (*i*) the oxidation of complexes of Cu^{2+} with intermediates[17] and (*ii*) the production of small amounts of $^{\bullet}OH$ in the medium from the Cu^{2+}/Cu^+ catalytic system,[36,37] involving the reduction of Cu^{2+} to Cu^+ with $HO_2^{\bullet}$ by Reaction 7 with $k_2 = 5 \times 10^7$ dm^3 mol^{-1} s^{-1}[38] and/or with organic radicals R$^{\bullet}$ by Reaction 8

$$Cu^{2+} + HO_2^{\bullet} \rightarrow Cu^+ + H^+ + O_2 \quad [7]$$

$$Cu^{2+} + R^{\bullet} \rightarrow Cu^+ + R^+ \quad [8]$$

followed by regeneration of Cu^{2+} by oxidation of Cu^+ with H_2O_2 from the Fenton-like Reaction 9 with $k_2 = 1 \times 10^4$ dm^3 mol^{-1} s^{-1}[39]

$$Cu^+ + H_2O_2 \rightarrow Cu^{2+} + {}^{\bullet}OH + OH^- \quad [9]$$

The slightly greater degradation observed in curve d of Fig. 1 under UVA illumination of the 1 mM Cu^{2+} solution also suggests additional photolysis of some oxidation products.

A much higher TOC removal is achieved when Fe^{2+} is added as catalyst. For the electro-Fenton process with 1 mM Fe^{2+} (see curve e of Fig. 1), TOC is rapidly reduced by 66% at 6 h, which can be related to the fast reaction of organics with the great amounts of $^{\bullet}OH$ produced from Fenton's Reaction 2. However, the electro-Fenton reaction does not yield total mineralization due to the formation of products that do not react with $^{\bullet}OH$, e.g., complexes of short carboxylic acids with Fe^{3+}.[9,14,15,17] Combination of UVA light with 1 mM Fe^{2+} in the photoelectro-Fenton process (see curve f of Fig. 1) already leads to 87% mineralization. This trend can be related to (*i*) the quick photodecomposition of some stable Fe^{3+} complexes under electro-Fenton conditions and/or (*ii*) the faster generation of $^{\bullet}OH$ from additional photoreduction of $Fe(OH)^{2+}$ from Reaction 3. Curve g of Fig. 1, obtained with 1 mM Fe^{2+} and 1 mM Cu^{2+} as catalysts, shows a similar TOC decay to that of the photoelectro-Fenton reaction, attaining 90% mineralization. This suggests that $^{\bullet}OH$ can easily oxidize some complexes of intermediates with Cu^{2+}, competitively formed with those of Fe^{3+}. As can be seen in curve h of Fig. 1, all complexes of Cu^{2+} and Fe^{3+} are completely destroyed when 1 mM Fe^{2+}, 1 mM Cu^{2+}, and UVA light are combined, since overall mineralization (>98% TOC decay) is reached at the end of electrolysis.

The above results indicate that the oxidation ability of the catalyzed methods increases in the order 1 mM Cu^{2+}<1 mM Cu^{2+}+UVA light≤1 mM Fe^{2+}+UVA light≤1 mM Fe^{2+}+1 mM Cu^{2+}<1 mM Fe^{2+}+1 mM Cu^{2+}+UVA light. However, only the last method is potent enough to destroy paracetamol completely.

Evolution of inorganic ions.— The possible loss of the initial nitrogen of paracetamol in the form of inorganic ions such as NH_4^+ and NO_3^- during its mineralization was investigated. No nitrite ions were detected in electrolyzed solutions. Figure 2 shows a rapid accumulation of NH_4^+ during the early stages of the above catalyzed treatments and a slow release of this ion from 2 h. The percentage of initial N converted into NH_4^+ is 48% for 1 mM Cu^{2+}, 51% for 1 mM Cu^{2+} + UVA light, 53% for 1 mM Fe^{2+}, 66% for 1 mM Fe^{2+} + UVA light, 75% for 1 mM Fe^{2+} + 1 mM Cu^{2+}, and 93% for 1 mM Fe^{2+} + 1 mM Cu^{2+} + UVA light. In contrast, quite low NO_3^- concentrations were found in the same final electrolyzed solutions: for example, 6.35 mg L^{-1} (10% of initial N) for 1 mM Fe^{2+} + 1 mM Cu^{2+} and a much lower value of 0.7 mg L^{-1} (1% of initial N) for the same catalysts under UVA irradiation. These results indicate that the nitrogen of paracetamol is mainly lost as NH_4^+, whereas only a minor portion of it is oxidized to NO_3^-. More NH_4^+ is formed with rising oxidation ability of the methods due to the faster mineralization of some nitrogen-containing intermediates produced at the early stages of treatments. UVA irradiation also favors the release of NH_4^+, instead of NO_3^-, probably by photolysis of such by-products.

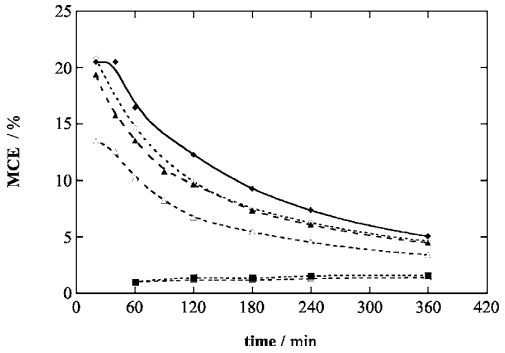

Figure 3. Dependence of mineralization current efficiency calculated from Eq. 11 on electrolysis time for the catalyzed experiments given in Fig. 1. Catalyst: (□) 1 mM Cu^{2+}, (■) 1 mM Cu^{2+} + UVA light, (△) 1 mM Fe^{2+}, (▲) 1 mM Fe^{2+} + UVA light, (◇) 1 mM Fe^{2+} + 1 mM Cu^{2+}, and (◆) 1 mM Fe^{2+} + 1 mM Cu^{2+} + UVA light.

Mineralization current efficiency.— The electrochemical destruction of paracetamol involves its transformation into CO_2 and mainly NH_4^+ as inorganic ion. The overall reaction can be written as follows

$$HO–C_6H_4–NH–CO–CH_3 + 14H_2O \rightarrow 8CO_2 + NH_4^+ + 33H^+ + 33e^- \quad [10]$$

Reaction 10 presupposes the consumption of 33 F per mole of compound. The mineralization current efficiency (MCE) for each experiment was then determined from the following expression

$$MCE = [\Delta(TOC)_{exper}/\Delta(TOC)_{theor}] \times 100 \quad [11]$$

where $\Delta(TOC)_{exper}$ is the experimental TOC removal in the solution at a given time and $\Delta(TOC)_{theor}$ is its theoretical TOC decay assuming that the applied electrical charge (=current × time) is only consumed to mineralize paracetamol by Reaction 10.

Figure 3 shows the evolution of the efficiency calculated from Eq. 11 for the catalyzed experiments depicted in Fig. 1. For 1 mM Cu^{2+} in the absence and presence of UVA light, this parameter is as low as 1.0–1.4%, slightly increasing at longer electrolysis times. In contrast, all the other methods involving the Fe^{3+}/Fe^{2+} system are much more efficient because they have much higher oxidation ability. The MCE values at 20 min are close to 13% for the electro-Fenton reaction, 19% for the photoelectron-Fenton reaction, and 21% for 1 mM Fe^{2+} + 1 mM Cu^{2+} with and without UVA light. At longer times, however, they undergo a dramatic drop toward the end of electrolysis, increasing in the order 1 mM Fe^{2+} < 1 mM Fe^{2+} + UVA light ≤ 1 mM Cu^{2+} + 1 mM Fe^{2+} < 1 mM Cu^{2+} +1 mM Fe^{2+} + UVA light. The gradual decay in efficiency with time can be related to the concomitant fall in pollutant content with formation of more stable by-products, thus favoring the loss of $^{\bullet}OH$ by parallel nonoxidizing reactions, e.g., its reaction with Fe^{2+} and/or Cu^{+} and its recombination into H_2O_2.[19,36] This trend is not so clear for 1 mM Cu^{2+} because organics are much more slowly degraded.

Effect of experimental parameters.— The influence of current on the oxidation ability of each catalyzed method was examined by electrolyzing 157 mg L^{-1} paracetamol solutions of pH 3.0 at 33, 100, and 150 mA cm^{-2}. Selected results after 1 and 4 h of such trials are collected in Table I. In all systems the percentage of TOC removal increases with increasing j. This enhancement in degradation power can be ascribed to a greater production of $^{\bullet}OH$ at the Pt anode from Reaction 4 and of H_2O_2 by the O_2-diffusion cathode from Reaction 1.[9,17] The larger accumulation of H_2O_2 causes the acceleration of Reactions 2 and/or 9, yielding more $^{\bullet}OH$ concentration that favors the oxidation of pollutants. Results of Table I indicate that even at 150 mA cm^{-2} the action of Cu^{2+} with and without UVA light is notably poor, leading to a maximum TOC removal of 21% at 4 h. Under these conditions, the electro-Fenton reaction with Fe^{2+} is much more effective with 60% TOC decay, because of the much faster generation of $^{\bullet}OH$ by Reaction 2 than by Reaction 9. The use of either Fe^{2+} + UVA light or Fe^{2+} + Cu^{2+} yields a similar TOC reduction of 80–81% after 4 h at 150 mA cm^{-2}, indicating that different stable species under electro-Fenton conditions are mineralized in each one of these systems. These products are totally destroyed by the combined action of Fe^{2+}, Cu^{2+}, and UVA light, reaching about 95–96% mineralization after 4 h at both 100 and 150 mA cm^{-2}. Table I also shows that at a given time the efficiency of each method always drops with increasing j, i.e., when more $^{\bullet}OH$ is produced, as stated above. This apparent contradictory behavior

Table I. Effect of applied current on the percentage of TOC removal and MCE for the degradation of 157 mg L^{-1} paracetamol solutions of pH 3.0 at 35°C by indirect electro-oxidation methods with H_2O_2 electrogeneration using different catalysts under selected experimental conditions.

		After 1 h of treatment		After 4 h of treatment	
Catalyst	j (mA cm^{-2})	% TOC removal	MCE	% TOC removal	MCE
1 mM Cu^{2+}	33	0.3	2.8	16	3.7
	100	3.2	0.9	17	1.3
	150	3.9	0.8	19	1.3
1 mM Cu^{2+} + UVA light	33	0.4	3.6	19	4.3
	100	3.4	0.9	20	1.5
	150	4.7	0.9	21	0.9
1 mM Fe^{2+}	33	24	22	55	12
(electro-Fenton process)	100	33	10	59	4.5
	150	39	8.0	60	3.0
1 mM Fe^{2+} + UVA light	33	39	36	75	17
(photoelectro-Fenton process)	100	44	13	79	6.0
	150	49	9.4	80	4.0
1 mM Fe^{2+} + 1 mM Cu^{2+}	33	21	19	53	12
	100	47	14	80	6.1
	150	48	9.4	81	4.4
1 mM Fe^{2+} + 1 mM Cu^{2+}	33	28	25	65	15
+UVA light	100	53	16	95	7.3
	150	61	12	96	4.9

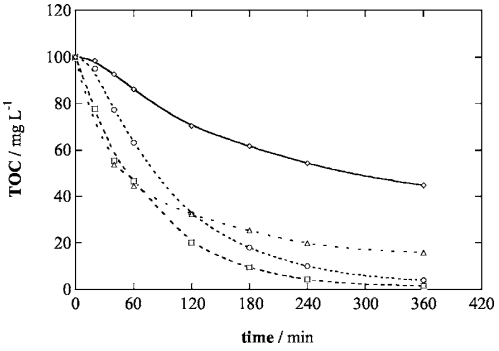

Figure 4. Effect of pH on TOC removal of 100 mL of 157 mg L^{-1} paracetamol solutions treated with 1 mM Fe^{2+} + 1 mM Cu^{2+} + UVA light at 100 mA cm^{-2} and at 35°C. Initial solution pH: (○) 2.0, (□) 3.0, (△) 4.0, and (◇) 6.0.

can be related to the oxidation of a larger proportion of this radical to O_2 at the anode and the acceleration of its nonoxidizing reactions in the medium.

The effect of pH was clarified by treating solutions containing 157 mg L^{-1} of drug and initial pH between 2.0 and 6.0 with 1 mM Fe^{2+} + 1 mM Cu^{2+} + UVA light. As an example, Fig. 4 shows the TOC–time plots obtained at 100 mA cm^{-2}, where the quickest TOC decay can be observed at pH 3.0. The same trend was found for this method at 33 and 150 mA cm^{-2}, as well as for similar treatments using the Fe^{2+}, Fe^{2+} + UVA light, and Fe^{2+} + Cu^{2+} systems. This behavior can be related to the highest generation rate of their main oxidant $^{\bullet}OH$ from Reaction 2, because its optimum pH is 2.8,[19] very close to pH 3.0 where paracetamol and its oxidation products are more rapidly destroyed.

The possible influence of Fe^{2+} and Cu^{2+} concentrations was tested by electrolyzing 157 mg L^{-1} drug solutions of pH 3.0 containing between 0.25 and 1 mM of both ions at 100 mA cm^{-2} under UVA illumination. As can be seen in Fig. 5, all solutions are mineralized with similar rate up to 95–98% of TOC reduction at 6 h, indicating that such ions act in catalytic amounts to destroy paracetamol.

The oxidation ability of the system with 1 mM Fe^{2+} + 1 mM Cu^{2+} + UVA light to degrade drug concentrations <1 g L^{-1} of pH 3.0 at 100 mA cm^{-2} was also examined. Figure 6a shows that total mineralization is attained for up to 313 mg L^{-1} of paracetamol,

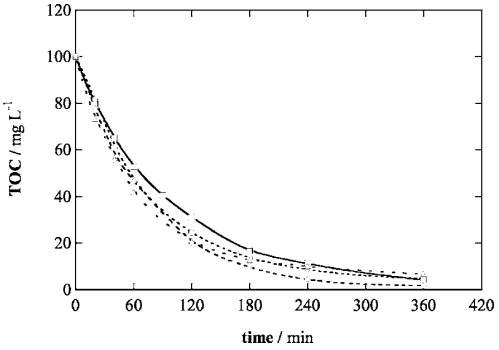

Figure 5. TOC removal with electrolysis time for the treatment of 100-mL solutions of pH 3.0 containing 157 mg L^{-1} paracetamol and different Fe^{2+} and Cu^{2+} concentrations under UVA irradiation, at 100 mA cm^{-2} and at 35°C: (○) 0.25 mM Fe^{2+} + 0.25 mM Cu^{2+}, (□) 1 mM Fe^{2+} + 0.25 mM Cu^{2+}, (△) 0.25 mM Fe^{2+} + 1 mM Cu^{2+}, and (◇) 1 mM Fe^{2+} + 1 mM Cu^{2+}.

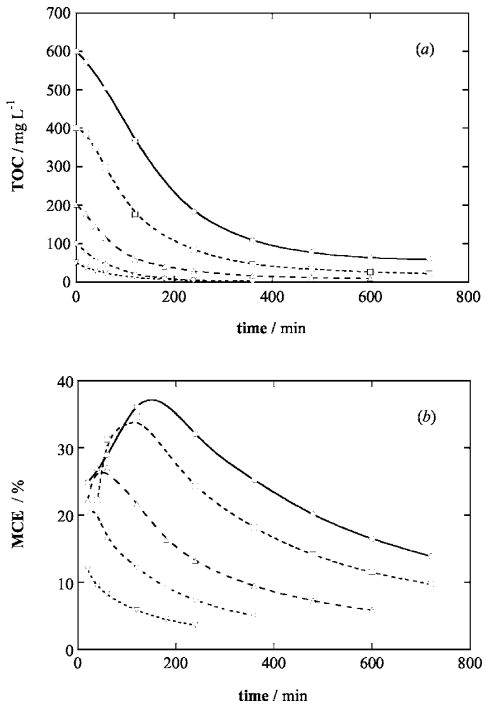

Figure 6. (a) TOC abatement with electrolysis time for the degradation of 100-mL solutions of pH 3.0 containing paracetamol concentrations of (○) 940, (□) 625, (△) 313, (◇) 157, and (▽) 78 mg L^{-1} using 1 mM Fe^{2+} + 1 mM Cu^{2+} + UVA light at 100 mA cm^{-2} and at 35°C. (b) Change of the mineralization current efficiency calculated from Eq. 11 with time for the same experiments.

whereas 6 and 10% TOC remain in solution from 625 and 940 mg L^{-1}, respectively, after prolonged electrolysis. The method is then able to destroy up to ca. 0.4 g L^{-1} of drug under the present experimental conditions. Figure 6b presents the MCE–time plots for the experiments of Fig. 6a. As can be seen, the efficiency increases with rising drug concentration, indicating a faster removal of larger amounts of organics. Because the same production of $^{\bullet}OH$ is expected from Reactions 2, 3, 4, and 9 in all trials, it seems plausible to consider that its competitive nonoxidizing reactions become slower and more $^{\bullet}OH$ concentration can then react with pollutants. From 313 mg L^{-1} of paracetamol, MCE progressively rises during longer times at early stages of the treatment, reaching a maximum value of 36% for 940 mg L^{-1} at 2 h. This suggests an increasing formation of products that react more easily with $^{\bullet}OH$ than the drug at early stages of electrolysis.

From the above findings, one can conclude that indirect electrooxidation methods with H_2O_2 electrogeneration using at least Fe^{2+} as catalyst are more effective for paracetamol degradation from water than classical ozonation and H_2O_2/UV.[25] For these electrochemical techniques, the optimum operative pH is 3.0. When Fe^{2+}, Cu^{2+}, and UVA light are combined, small quantities (up to 1 mM) of both ions are needed for achieving total mineralization of solutions containing up to about 0.4 g L^{-1} of drug at low current.

Identification of intermediates.— An attempt was made to identify the stable aromatic intermediates formed during paracetamol mineralization by means of GC-MS. To do this, solutions with 157 and 313 mg L^{-1} of this compound at pH 3.0 were electrolyzed at 100 mA cm^{-2} and at 35°C by anodic oxidation for 20 min and using 1 mM Fe^{2+} + 1 mM Cu^{2+} + UVA light for 5 min. All MS

spectra displayed the peak of the remaining paracetamol [m/z = 151 (21, M^+)] at t_r (retention time) = 22.5 min, along with two other peaks associated with the primary product hydroquinone [m/z = 110 (100, M^+)] at t_r = 15.2 min, and its oxidation product *p*-benzoquinone [*m/z* = 108 (51, M^+)] at t_r = 9.6 min. No other products were detected after derivatization of the organics contained in the same treated solutions with bis(trimethylsilyl)trifluoroacetamide.

Reversed-phase chromatograms of electrolyzed solutions with a 70:30 (v/v) acetonitrile/water mixture as mobile phase exhibited the peaks of paracetamol (t_r = 1.20 min) and *p*-benzoquinone (t_r = 1.49 min), whereas the use of a 95:5 (v/v) 0.1 M HCOOH + NaOH (pH 3.0)/acetonitrile mixture allowed the detection of hydroquinone (t_r = 3.50 min). These products were unequivocally identified from comparison of their t_r values and uv-visible (UV-vis) spectra, measured on the photodiode array detector, with those of pure compounds. The ion-exclusion chromatograms of treated solutions displayed peaks associated with generated carboxylic acids such as oxalic (t_r = 6.7 min), ketomalonic (t_r = 6.8 min), maleic (t_r = 8.1 min), oxamic (t_r = 9.4 min), and fumaric (t_r = 15.8 min) acids.

Ketomalonic, maleic, and fumaric acids come from the oxidation of the aryl moiety of paracetamol, as reported for other aromatics.[5,7,12,14,17,33-35] The treatment of solutions containing 50 mg L^{-1} of each one of these acids of pH 3.0 with 1 mM Fe^{2+} + 1 mM Cu^{2+} + UVA light showed that they are only oxidized to oxalic acid. Oxamic acid could be produced from $^{\bullet}OH$ attack on acetamide, released when paracetamol gives hydroquinone. This was confirmed by treating 50 mg L^{-1} of acetamide with the above system at pH 3 and at 100 mA cm^{-2}, because only oxamic acid was detected as product. Electrolyses of solutions with 50 mg L^{-1} of oxalic or oxamic acid of pH 3.0 at 100 mA cm^{-2} revealed that both acids remain stable in the presence of 1 mM Fe^{2+}, whereas they are slowly degraded using 1 mM Cu^{2+}. When such solutions were exposed to UVA light without applying current, it was found that both acids are not photolyzed with 1 mM Cu^{2+}, but the presence of 1 mM Fe^{2+} causes a quick and overall transformation of oxalic acid into CO_2 and a very slow mineralization of oxamic acid. It was also confirmed that only NH_4^+ is released when oxamic acid is mineralized.

Paracetamol decay and evolution of intermediates.— Once the identity of chromatographic peaks was made, a 157 mg L^{-1} paracetamol solution of pH 3.0 at 35°C was degraded by all treatments at 100 mA cm^{-2}, and the concentration of the drug and its products was determined as a function of electrolysis time via external calibration by using standard compounds.

Figure 7 shows that paracetamol undergoes a slow and similar decay for anodic oxidation and in the presence of Cu^{2+}, both with and without UVA irradiation, disappearing from the medium in 75 min. These findings indicate that the main oxidant in these methods is $^{\bullet}OH$ formed in small amount on the anode from Reaction 4. In contrast, the drug is rapidly removed in 6 min with a similar rate for the four treatments involving Fe^{2+}, alone or combined with Cu^{2+} and/or UVA light, thus confirming that it is mainly destroyed by the large amounts of $^{\bullet}OH$ generated from Fenton's Reaction 2, with little contribution of Reaction 4. Note that the decay of paracetamol does not follow kinetic equations related to simple reaction orders. This suggests the existence of a complex $^{\bullet}OH$ attack on this compound, leading to different primary products such as hydroquinone and 2-hydroxy-4-(*N*-acetyl)aminophenol, identified during its treatment with O_3 and H_2O_2/UV.[25] Under our experimental conditions, however, the second species is undetected, probably because it is rapidly destroyed by $^{\bullet}OH$.

The evolution of hydroquinone and *p*-benzoquinone for the catalyzed methods is shown in Fig. 8a and b, respectively. In all cases these products are present in the medium while the initial drug persists in it. A small concentration of about 0.6 mg L^{-1} is achieved as

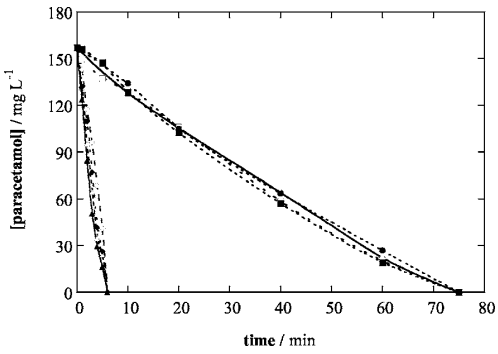

Figure 7. Paracetamol concentration decay for the experiments reported in Fig. 1. Catalyst: (○) none, (●) UVA light, (□) 1 mM Cu^{2+}, (■) 1 mM Cu^{2+} + UVA light, (△) 1 mM Fe^{2+}, (▲) 1 mM Fe^{2+} + UVA light, (◇) 1 mM Fe^{2+} + 1 mM Cu^{2+}, and (◆) 1 mM Fe^{2+} + 1 mM Cu^{2+} + UVA light.

maximum for hydroquinone using 1 mM Cu^{2+} in the presence and absence of UVA irradiation, as expected if it is rapidly oxidized to *p*-benzoquinone. In both procedures the latter species is more slowly degraded and can reach maximum concentrations of 19–23 mg L^{-1} at 20 min. However, both products are quickly formed and destroyed at a similar rate in the methods catalyzed at least with Fe^{2+}, attaining their maximum concentrations at 2–3 min. These results corroborate that these aromatic products are mainly oxidized by $^{\bullet}OH$, not being photodegraded by UVA light.

A very different behavior was found for generated carboxylic acids. As can be seen in Fig. 8c, ketomalonic acid is not completely removed after 6 h of electrolysis using both Cu^{2+} systems, but it is quickly oxidized to oxalic acid in 40 min by the other methods with Fe^{2+}. Figure 8d shows that maleic acid, similarly to its *trans*-isomer fumaric acid, is completely converted into oxalic acid in all cases. The slow accumulation of ketomalonic and maleic acids in the presence of Cu^{2+} can then be related to the slow oxidation of aromatic intermediates, whereas their fast degradation by the other methods with Fe^{2+} indicates that they are mainly oxidized by the action of $^{\bullet}OH$ formed from Fenton's Reaction 2. In contrast, Fig. 8e and f shows that the evolution of oxalic and oxamic acids depends on the catalyst used. For both Cu^{2+} systems, small concentrations between 2 and 4 mg L^{-1} of both acids remain in solution. When only Fe^{2+} is used, 90 mg L^{-1} of oxalic acid and 31 mg L^{-1} of oxamic acid are accumulated without practical destruction. The use of Fe^{2+} + UVA light causes a fast removal of oxalic acid up to a final value of 8 mg L^{-1}, while 42 mg L^{-1} of oxamic acid is reached at 2 h, further being slowly reduced to 29 mg L^{-1}. By combining Fe^{2+} and Cu^{2+}, 27 mg L^{-1} of oxalic acid and 2 mg L^{-1} of oxamic acid persist at 6 h. For the Fe^{2+} + Cu^{2+} + UVA light system, both acids are totally mineralized, in agreement with the total decontamination found for the paracetamol solution (see curve h of Fig. 1).

The degradation behavior of oxalic and oxamic acids can be related to the destruction of their complexes with Fe^{3+} and Cu^{2+}.[17,21] When paracetamol is treated with only Fe^{2+}, Fe^{3+}-oxalate and Fe^{3+}-oxamato complexes are competitively formed by the efficient generation of Fe^{3+} from Fenton's Reaction 2, but they cannot be mineralized by $^{\bullet}OH$ limiting the oxidation ability of the electro-Fenton reaction. The final solution of this treatment is composed of a mixture of stable Fe^{3+} complexes of both acids, because their concentrations in Fig. 8e and f are equivalent to 33 mg L^{-1} TOC, the same value attained by the paracetamol solution at 6 h (see curve e of Fig. 1). The remaining steady oxamic acid contains 33% initial nitrogen, indicating that NH_4^+ present in such a solution (see Fig. 2) is produced by the degradation of products different from acetamide. The efficient photodecomposition of Fe^{3+}-oxalato complexes, along with a slower photolysis of Fe^{3+}-oxamato complexes,

Journal of The Electrochemical Society, **153** (1) D1-D9 (2006)

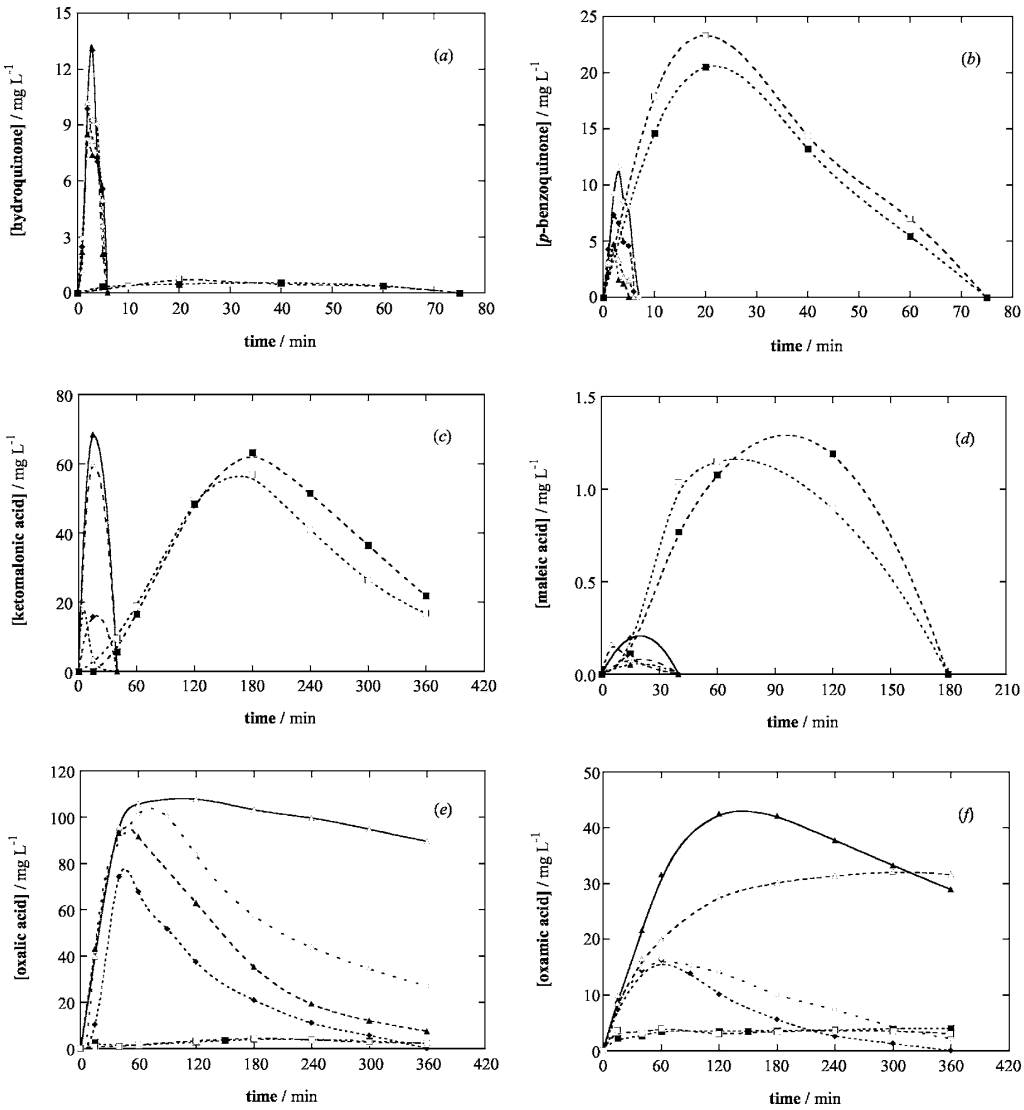

Figure 8. Time-course of the concentration of intermediates detected during the degradation of 157 mg L^{-1} paracetamol solutions of pH 3.0 at 100 mA cm^{-2} and at 35°C using the following catalysts: (□) 1 mM Cu^{2+}, (■) 1 mM Cu^{2+} + UVA light, (△) 1 mM Fe^{2+}, (▲) 1 mM Fe^{2+} + UVA light, (◇) 1 mM Fe^{2+} + 1 mM Cu^{2+}, and (◆) 1 mM Fe^{2+} + 1 mM Cu^{2+} + UVA light. Plot: (a) hydroquinone, (b) *p*-benzoquinone, (c) ketomalonic acid, (d) maleic acid, (e) oxalic acid, and (f) oxamic acid.

can account for the faster mineralization of the drug by the photoelectro-Fenton reaction (see curve f of Fig. 1). When only the Cu^{2+} system is used, Cu^{2+}-oxalato and Cu^{2+}-oxamato complexes are formed to a small extent in the medium, being destroyed by $^{\bullet}OH$ but not photolyzed by UVA light. The mineralization of these complexes can also explain the highest decontamination of paracetamol found in the presence of 1 mM Cu^{2+} than by anodic oxidation (see Fig. 1). By combining Fe^{2+} and Cu^{2+} as catalysts, Fe^{3+}-oxalato, Fe^{3+}-oxamato, Cu^{2+}-oxalato, and Cu^{2+}-oxamato complexes are produced, but only the Cu^{2+} complexes are destroyed, leading to a rapid TOC decay of paracetamol (see curve g of Fig. 1). The quickest and total mineralization of the drug with Fe^{2+} + Cu^{2+} + UVA light can thus be related to the oxidation of Cu^{2+}-oxalato and Cu^{2+}-oxamato complexes with $^{\bullet}OH$ in parallel with the photodecomposition of their Fe^{3+} complexes by UVA light.

Proposed degradation pathway.— A general reaction scheme for the mineralization of paracetamol in acid media by all indirect electro-oxidation methods with H_2O_2 electrogeneration under the action of Fe^{2+}, Cu^{2+}, and/or UVA light as catalysts is proposed in Fig. 9. The pathway involves all intermediates detected in this work and only shows the main oxidant $^{\bullet}OH$ for sake of simplicity, although parallel reactions with other weaker oxidizing agents (H_2O_2, $HO_2^{\bullet}$, Cu^{2+}, Fe^{3+}, etc.) are also possible. The process is initiated by $^{\bullet}OH$ attack at the C(4)-position of paracetamol, breaking its *N*-bond to yield hydroquinone and acetamide. Further oxidation of hydroquinone gives *p*-benzoquinone, which is degraded to a mixture of ketomalonic, maleic, and fumaric acids. These acids are subsequently transformed into oxalic acid. Parallel oxidation of acetamide leads to oxamic acid. Oxalic and oxamic acids are slowly converted

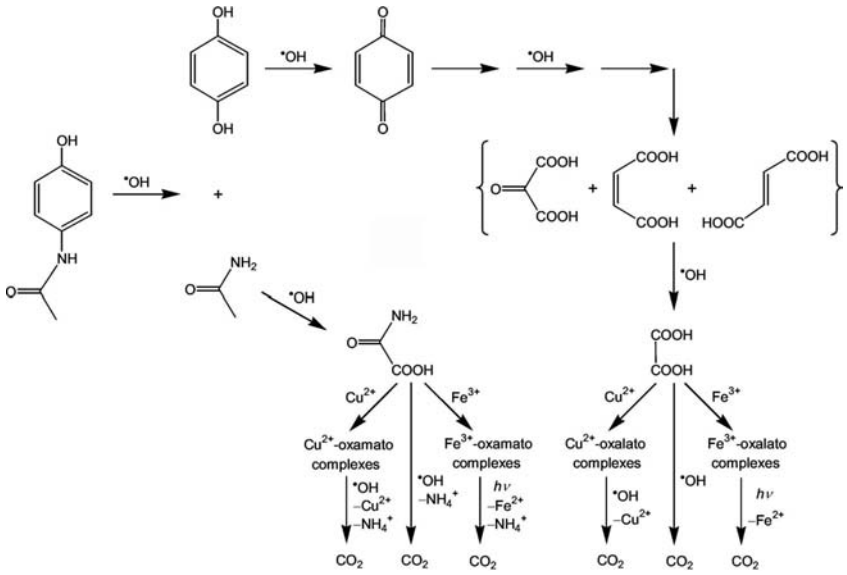

Figure 9. Proposed reaction sequence for paracetamol degradation in acid aqueous medium by the catalytic action of Fe^{2+}, Cu^{2+}, and/or UVA light on electrogenerated H_2O_2.

into CO_2 by $^{\bullet}OH$, although they form complexes with Fe^{3+} and/or Cu^{2+} when one or both ions are present in the medium. Although Cu^{2+}-oxalato and Cu^{2+}-oxamato complexes are mineralized with $^{\bullet}OH$, Fe^{3+}-oxalato and Fe^{3+}-oxamato complexes are very stable under electro-Fenton conditions. Both Fe^{3+} complexes can be photodecarboxylated with loss of Fe^{2+} under the action of UVA light, as proposed by Zuo and Hoigné.[21] The mineralization of oxamic acid is accompanied by the loss of NH_4^+. This inorganic ion, along with small amounts of NO_3^-, is also released during the degradation of undetected products, probably coming from unstable 2-hydroxy-4-(*N*-acetyl)aminophenol formed from direct hydroxylation at the C(2)-position of paracetamol.[25]

Conclusions

It has been demonstrated that acidic aqueous solutions of paracetamol can be rapidly degraded using an undivided electrolytic cell with a Pt anode and an O_2-diffusion cathode able to electrogenerate H_2O_2 under the combined catalytic action of 1 mM Fe^{2+}, 1 mM Cu^{2+}, and UVA light. This indirect electro-oxidation method allows complete mineralization for drug concentrations <0.4 g L^{-1}, because of the high amounts of $^{\bullet}OH$ produced from Fenton's reaction that oxidize the complexes of oxalic and oxamic acids with Cu^{2+}, along with the parallel photolysis of their complexes with Fe^{3+}. This treatment is more efficient than one involving 1 mM Fe^{2+} and 1 mM Cu^{2+}, or a photoelectro-Fenton system with 1 mM Fe^{2+} and UVA light, where the complexes of oxalic and oxamic acids with Fe^{3+} and/or Cu^{2+} are more slowly destroyed. For an electro-Fenton system with 1 mM Fe^{2+}, a lower decontamination is reached because Fe^{3+}-oxalato and Fe^{3+}-oxamato complexes are not destroyed by $^{\bullet}OH$. The optimum pH for all these electro-oxidation methods is 3.0. In contrast, the presence of 1 mM Cu^{2+} as catalyst or the use of direct anodic oxidation, both with and without UVA light, leads to slow destruction of pollutants due to the formation of small amounts of $^{\bullet}OH$ from water oxidation at the Pt anode, which are not significantly enhanced by reaction of Cu^{+} with H_2O_2. The percentage of TOC removal in all treatments increases with increasing applied current due to the greater production of $^{\bullet}OH$. The original nitrogen of the drug is mainly lost as NH_4^+ ion, along with a very small proportion of NO_3^- ion. In all cases, hydroquinone and *p*-benzoquinone are identified as aromatic products. The formation of hydroquinone is accompanied by the release of acetamide, which is further oxidized to oxamic acid. Degradation of *p*-benzoquinone leads to a mixture of ketomalonic, maleic, and fumaric acids, which are subsequently converted into oxalic acid.

Acknowledgments

The authors thank AGAUR (Agència de Gestió d'Ajuts Universitaris i de Recerca, Generalitat de Catalunya) for the grant given to I. Sirés to do this work, and MEC (Ministerio de Educación y Ciencia, Spain) for financial support under project CTQ2004-01954/BQU.

Universitat de Barcelona assisted in meeting the publication costs of this article.

References

1. Y. L. Hsiao and K. Nobe, *J. Appl. Electrochem.*, **23**, 943 (1993).
2. J. S. Do and C. P. Chen, *J. Electrochem. Soc.*, **140**, 1632 (1993).
3. C. Ponce de Leon and D. Pletcher, *J. Appl. Electrochem.*, **25**, 307 (1995).
4. E. Brillas, E. Mur, and J. Casado, *J. Electrochem. Soc.*, **143**, L49 (1996).
5. E. Brillas, R. Sauleda, and J. Casado, *J. Electrochem. Soc.*, **144**, 2374 (1997); E. Brillas, R. Sauleda, and J. Casado, *J. Electrochem. Soc.*, **145**, 759 (1998).
6. A. Alvarez-Gallegos and D. Pletcher, *Electrochim. Acta*, **44**, 2483 (1999).
7. T. Harrington and D. Pletcher, *J. Electrochem. Soc.*, **146**, 2983 (1999).
8. M. A. Oturan, J. Pinson, N. Oturan, and D. Deprez, *New J. Chem.*, **23**, 793 (1999).
9. E. Brillas, J. C. Calpe, and J. Casado, *Water Res.*, **34**, 2253 (2000).
10. M. A. Oturan, *J. Appl. Electrochem.*, **30**, 475 (2000).
11. J. J. Aaron and M. A. Oturan, *Turk. J. Chem.*, **25**, 509 (2001).
12. B. Boye, M. M. Dieng, and E. Brillas, *Environ. Sci. Technol.*, **36**, 3030 (2002).
13. A. Ventura, G. Jacquet, A. Bermond, and V. Camel, *Water Res.*, **36**, 3517 (2002).
14. E. Brillas, B. Boye, and M. M. Dieng, *J. Electrochem. Soc.*, **150**, E148 (2003).
15. B. Boye, E. Brillas, and M. M. Dieng, *J. Electroanal. Chem.*, **540**, 25 (2003).
16. B. Gözmen, M. A. Oturan, N. Oturan, and O. Erbatur, *Environ. Sci. Technol.*, **37**, 3716 (2003).
17. E. Brillas, M. A. Baños, S. Camps, C. Arias, P. L. Cabot, J. A. Garrido, and R. M. Rodríguez, *New J. Chem.*, **28**, 314 (2004).
18. A. Wang, J. Qu, J. Ru, H. Liu, and J. Ge, *Dyes Pigm.*, **65**, 225 (2005).
19. J. J. Pignatello, *Environ. Sci. Technol.*, **26**, 944 (1992).
20. Y. Sun and J. J. Pignatello, *Environ. Sci. Technol.*, **27**, 304 (1993).
21. Y. Zuo and J. Hoigné, *Environ. Sci. Technol.*, **26**, 1014 (1992).
22. C. Zwiener and F. H. Frimmel, *Water Res.*, **34**, 1881 (2000).
23. *Pharmaceuticals in the Environment: Sources, Fate and Risks*, K. Kümmerer, Editor, Springer, Berlin (2001).
24. D. W. Kolpin, E. T. Furlong, M. T. Meyer, E. M. Thurman, S. D. Zaugg, and L. B. Barber, *Environ. Sci. Technol.*, **36**, 1202 (2002).
25. R. Andreozzi, V. Caprio, R. Marotta, and D. Vogna, *Water Res.*, **37**, 992 (2003).
26. J. P. Bound and N. Vaulvaulis, *Chemosphere*, **56**, 1143 (2004).
27. M. Ravina, L. Campanella, and J. Kiwi, *Water Res.*, **36**, 3553 (2002).
28. T. A. Ternes, J. Stüber, N. Herrmann, D. McDowell, A. Ried, M. Kampmann, and B. Teiser, *Water Res.*, **37**, 1976 (2003).
29. M. M. Huber, S. Canonica, G. Y. Park, and U. Von Gunten, *Environ. Sci. Technol.*,

37, 1016 (2003).
30. D. Vogna, R. Marotta, A. Napolitano, R. Andreozzi and M. d'Ischia, *Water Res.*, **38**, 414 (2004).
31. E. Brillas, I. Sirés, C. Arias, P. L. Cabot, F. Centellas, R. M. Rodríguez, and J. A. Garrido, *Chemosphere*, **58**, 399 (2005).
32. C. Comninellis and A. De Battisti, *J. Chim. Phys. Phys.-Chim. Biol.*, **93**, 673 (1996).
33. M. A. Rodrigo, P. A. Michaud, I. Duo, M. Panizza, G. Cerisola, and C. Comninellis, *J. Electrochem. Soc.*, **148**, D60 (2001).
34. J. Iniesta, P. A. Michaud, M. Panizza, G. Cerisola, A. Aldaz, and C. Comninellis, *Electrochim. Acta*, **46**, 3573 (2001).
35. E. Brillas, B. Boye, I. Sirés, J. A. Garrido, R. M. Rodríguez, C. Arias, P. L. Cabot, and C. Comninellis, *Electrochim. Acta*, **49**, 4487 (2004).
36. H. Gallard, J. De Laat, and B. Legube, *Rev. Sci. Eau*, **12**, 715 (1999).
37. J. De Laat and H. Gallard, *Environ. Sci. Technol.*, **33**, 2726 (1999).
38. B. H. J. Bielski, D. E. Cabelli, R. L. Arudi, and A. B. Ross, *J. Phys. Chem. Ref. Data*, **14**, 1041 (1985).
39. V. K. Sharma and F. J. Millero, *Environ. Sci. Technol.*, **22**, 768 (1988).

7.2.2. Resultats i Discussió / *Results and Discussion*

The optimum catalysts concentrations are 1.0 mM Fe^{2+} and 1.0 mM Cu^{2+}, since they provide a slightly quicker mineralization by EF and PEF. According to TOC decay plots, the oxidation ability of the methods tested increases in the following order: AO < AO + UVA light < 1.0 mM Cu^{2+} < 1.0 mM Cu^{2+} + UVA light « 1.0 mM Fe^{2+} « 1.0 mM Fe^{2+} + UVA light < 1.0 mM Fe^{2+} + 1.0 mM Cu^{2+} < 1.0 mM Fe^{2+} + 1.0 mM Cu^{2+} + UVA light.

Uncatalyzed processes (AO) lead to a quite slow mineralization due to the low concentration of the main oxidant, $^{\bullet}OH_{ads}$, formed from H_2O oxidation at the anode. When Fe^{2+}, Cu^{2+} and UVA light catalysts are used separately an improved but partial mineralization is achieved due to the lack of enough $^{\bullet}OH$ in the medium and/or the stability of hardly oxidizable Fe^{3+} complexes and Cu^{2+} complexes. Finally, overall mineralization is reached after 5-6 h when 1.0 mM Fe^{2+}, 1.0 mM Cu^{2+} and UVA light are combined as catalysts (co-catalyzed PEF), even at low current densities. This fact can be explained by the oxidation of Cu^{2+}-oxalato and Cu^{2+}-oxamato complexes with $^{\bullet}OH$ in parallel with the photodecomposition of their Fe^{3+} complexes by UVA light (Reaction 5.-24). In addition, irradiation with UVA light causes photoreduction of uncomplexed Fe^{3+}, i.e. $Fe(OH)^{2+}$, thus regenerating Fe^{2+} (which can produce more $^{\bullet}OH$ from Fenton reaction) and enhancing the production of $^{\bullet}OH$ and hence, the mineralization of organics (Reaction 5.-23).

As apparent current density (j_{app}) increases, a higher TOC removal is achieved at a given time because the production of $^{\bullet}OH_{ads}$ at the Pt and the H_2O_2 electrogenerated at the cathode (and, consequently, the $^{\bullet}OH$ in the medium) is enhanced. At longer electrolysis time some hardly oxidizable intermediates, such as aliphatic carboxylic acids, are formed, so significant differences as a function of the current density tend to disappear. A current of 300 mA is selected as the most suitable current intensity,

since 100 mA leads to a significantly slower degradation of paracetamol.

Electrolyses at different initial pH values reveal that the quickest TOC decay is observed at pH 3.0, due to the highest generation rate of $^{\bullet}OH$. This fact completely agrees with the optimum pH for Fenton reaction (pH = 2.8).

Total mineralization is attained for up to 315 mg L^{-1} (200 mg L^{-1} TOC) of paracetamol, whereas 10% of TOC remains in solution when initial concentration is 940 mg L^{-1} (600 mg L^{-1} TOC). The method is then able to destroy up to ca. 0.4 g L^{-1} of drug.

No nitrite ions were detected in the electrolyzed solutions. NH_4^+ ion is quickly accumulated during the early stages of the described catalyzed treatments, and further it is slowly released. These results indicate that the initial N is mainly lost as NH_4^+: for the co-catalyzed PEF system, 93% of initial N is converted into NH_4^+, whereas only 1% is transformed into NO_3^-. Moreover, the accumulated NH_4^+ amount is higher as oxidation ability of the method rises, due to the faster mineralization of *N*-containing intermediates.

The overall mineralization reaction involves 34 F for each mol of paracetamol (Reaction 6.-2). Mineralization Current Efficiency (MCE) has been determined for the catalyzed systems by using Equation 6.-1, and the results show that the efficiency increases in the following order: 1.0 mM Cu^{2+} with or without UVA light « 1.0 mM Fe^{2+} « 1.0 mM Fe^{2+} + UVA light < 1.0 mM Fe^{2+} + 1.0 mM Cu^{2+} < 1.0 mM Fe^{2+} + 1.0 mM Cu^{2+} + UVA light. The efficiency for the latter process at 20 min is 21%, further undergoing a gradual decay with time due to the concomitant fall in pollutant content and the formation of hardly oxidizable intermediates, thus favoring the parasite nonoxidizing reactions of $^{\bullet}OH$. It must be noted that while the systems without Fe^{2+} exhibit MCE values about 1.5%, the methods involving the Fe^{3+}/Fe^{2+} system are much more efficient because they have much higher oxidation ability.

At a given time, the efficiency of each method always drops with increasing j_{app} due to a larger proportion of $^{\bullet}OH$ oxidized to O_2 at the anode, and the acceleration of its parasite reactions in the medium. In addition, MCE increases with rising drug concentration, indicating a faster removal of larger amount of organics because the parasite reactions in which $^{\bullet}OH$ is involved become slower and more amount of hydroxyl radicals can react with organic compounds. From 315 mg L^{-1} of paracetamol, MCE progressively rises during longer times at early stages of the treatment, reaching a maximum value of 36% for 940 mg L^{-1} at 2 h, thanks to the formation of more easily oxidizable intermediates at the beginning of the oxidation process.

Hydroquinone and *p*-benzoquinone are identified by GC-MS and reversed-phase chromatography, and then quantified by the latter technique. Acetamide coming from the attack of $^{\bullet}OH$ on the C-N bond has not been identified, but nevertheless its presence can be assumed as reported by Andreozzi et al. [356] and Skoumal et al. [194], and from interpretation of the surrounding data. By means of ion-exclusion chromatography several aliphatic carboxylic acids are identified and quantified: ketomalonic, maleic and fumaric acids (coming from the oxidation of the aryl moiety), oxalic acid (HOOC-COOH, coming from the oxidation of the former three acids), and oxamic acid ($HOOC-CONH_2$, probably generated from the attack of $^{\bullet}OH$ on acetamide).

Paracetamol is not photolyzed under UVA irradiation. This pharmaceutical undergoes a slow and similar decay for AO and in those processes with Cu^{2+} but without Fe^{2+}, disappearing from the medium after 75 min at 300 mA. In contrast, the drug is quickly removed in 6 min (25 min if applying 100 mA) with a similar rate for the four treatments involving Fe^{2+}, due to the great amount of $^{\bullet}OH$ in the medium. It is worth remarking that the decay of paracetamol does not follow kinetic equations related to simple reaction orders, just suggesting the existence of a complex $^{\bullet}OH$ attack on paracetamol.

Hydroquinone and *p*-benzoquinone are present in the medium while the initial drug persists in it. Both compounds are quickly formed and destroyed at similar rate in the methods catalyzed by Fe^{2+}, attaining their maximum concentrations at 2-3 min.

As for the carboxylic acids, ketomalonic acid is quickly oxidized to oxalic acid in 40 min by the methods with Fe^{2+}. Maleic acid, similarly to its *trans*-isomer fumaric acid, is removed in all cases and it is transformed into oxalic acid. On the contrary, the evolution of oxalic and oxamic acids depends on the catalyst used, and only the system with 1.0 mM Fe^{2+} + 1.0 mM Cu^{2+} + UVA light is able to reach their total removal. The degradation behaviour of both acids can be related to the destruction of their complexes with Fe^{3+} and Cu^{2+}: Fe^{3+}-oxalato, Fe^{3+}-oxamato, Cu^{2+}-oxalato and Cu^{2+}-oxamato complexes. Fe^{3+} complexes, which are formed by the efficient generation of Fe^{3+} from Fenton's reaction, can not be destroyed by $^{\bullet}OH$, thus limiting the oxidation ability of the EF reaction, for example. In contrast, since Fe^{3+}-oxalato complexes can be efficiently photodecomposed and Fe^{3+}-oxamato complexes are slowly photolyzed, PEF yield a higher TOC removal compared to EF. By combining Fe^{2+} with Cu^{2+} (co-catalyzed EF), all four complexes pointed out above are formed, but only Cu^{2+} complexes can be oxidized by $^{\bullet}OH$, so complete mineralization can not be achieved yet. It is necessary to combine Fe^{2+}, Cu^{2+} and UVA light to completely decontaminate the solutions, since a synergistic effect can be achieved: oxidation of Cu^{2+} complexes by $^{\bullet}OH$ and photodecomposition of Fe^{3+} complexes by UVA light.

Finally, the reaction pathway for the mineralization of paracetamol with $^{\bullet}OH$ involves all intermediates detected: $^{\bullet}OH$ firstly attacks at the C-N bond of paracetamol, yielding hydroquinone and acetamide. Further oxidation of hydroquinone gives *p*-benzoquinone, which is degraded to a mixture of ketomalonic, fumaric and maleic acids. These acids are subsequently transformed into oxalic. Parallel oxidation of acetamide leads to oxamic acid. Finally, the complexes of oxalic and oxamic acids with Fe^{3+} and Cu^{2+} are converted into CO_2, releasing Fe^{2+}, Cu^{2+} and

NH_4^+ ions. In contrast, Vogna et al. [355, 356] are able to identify a great deal of intermediates, mainly carboxylic acids (malonic, glyoxylic, glycolic, α-cetoglutaric and other ones), but two comments must be done: firstly, their work is based on less oxidizing methods (30-40% mineralization), so reactions take place slowlier and intermediates can have a longer residence time, and secondly, their analyses are mainly carried out by GC-MS and NMR instead of HPLC, so the importance of all of these intermediates in the reaction pathway is relative because identification of compounds does not imply their significant accumulation in the bulk solution.

7.3. TRACTAMENT MITJANÇANT OXIDACIÓ ANÒDICA / *TREATMENT BY ANODIC OXIDATION*

7.3.1. Finalitat del treball / *Aim of the work*

Once the effectivity of EAOPs in the Pt/O_2 diffusion cell to remove and mineralize paracetamol from aqueous solutions at acid pH was confirmed, the aim was comparing its oxidation ability with that of anodic oxidation (AO) processes, since among the electrochemical treatments for the destruction of organic pollutants in waters, AO is definitely the most usual technique. As previously explained (see section 5.3.3.2), AO treatments are based on the decontamination by direct reaction of pollutants with adsorbed hydroxyl radicals, $^{\bullet}OH_{ads}$, formed at the anode surface. Therefore, herein it is reported the study of the effectivity of a BDD anode to both degrade and mineralize paracetamol aqueous solutions in a wide range of experimental conditions. Comparative treatments using a Pt anode were made to underline the high oxidizing power of BDD. Graphite was used as cathode in all cases, and like Pt and BDD electrodes its area was 3 cm^2.

The first objective was comparing the oxidation ability of Pt and BDD anodes to degrade paracetamol. In this sense, 100-mL paracetamol solutions containing 157 mg L^{-1} paracetamol (i.e., 100 mg L^{-1} TOC) and 0.05 M Na_2SO_4, at pH 3.0 and at 35 ºC, were electrolyzed for 6 h at 300 mA using the Pt/graphite and BDD/graphite systems. This work was completed by carrying out the same experiments at pH 2.0, 4.0, 8.0, 10.0 and 12.0 to clarify if the observed behavior could be generalized to different aqueous media. TOC abatement analyses were done in all cases.

Once the great oxidizing power of BDD was confirmed, the possible effect of the variation of other experimental parameters on TOC decay was assessed in order to optimize the AO process for the BDD/graphite system at laboratory scale.

Firstly, paracetamol solutions of pH 3.0 up to 948 mg L^{-1} (i.e., 600 mg L^{-1} TOC) were electrolyzed at 300 mA and at 35 ºC. The Pt/graphite system was also studied under the same conditions. Secondly, TOC abatement analyses were carried out by varying the current applied to a 157 mg L^{-1} paracetamol solution of pH 3.0 at 35 ºC. A constant current of 100, 300 and 450 mA was applied. And lastly, temperature of the above solution treated at 100 mA was varied from 25 to 45 ºC (higher temperatures can not be used due to fast evaporation of water from the open cell used).

Following the experimental sequence reported for EF and PEF, after the detailed study of TOC decay under many experimental conditions, the evolution of inorganic ions was examined by ion chromatography to determine the possible loss of initial nitrogen of paracetamol. In this sense, a 157 mg L^{-1} paracetamol solution of pH 3.0 was electrolyzed with BDD at 300 mA and at 35 ºC. Moreover, to clarify the behavior of NH_4^+ ion in BDD systems, a 100-mL solution containing 100 mg L^{-1} of $(NH_4)_2SO_4$ at pH 3.0 was electrolyzed under similar conditions for 6 h.

Afterwards, the kinetics for the reaction between paracetamol and $^{\bullet}OH_{ads}$ was studied for both Pt and BDD systems. Several solutions of pH 3.0 and 12.0 were electrolyzed at 300 mA and at 35 ºC, and paracetamol decay was then followed by reversed-phase chromatography. Simultaneously, aromatic intermediates were identified and quantified, with the help of interpretation of mass spectra obtained by GC-MS. Finally, paracetamol solutions under the conditions previously referred were also electrolyzed by AO with BDD to obtain the ion-exclusion chromatograms reflecting the carboxylic acids accumulated.

The thorough results of this section are included in the following paper (Paper 3):

3. Brillas, E., **Sirés, I.**, Arias, C., Cabot, P.L., Centellas, F., Rodríguez, R.M., Garrido, J.A., Mineralization of paracetamol in aqueous medium by anodic oxidation with a boron-doped diamond electrode. *Chemosphere* **58** (2005) 399-406.

The following presentation in congress are related to this work:

C. Sirés, I., Skoumal, M., Arias, C., Cabot, P.L., Centellas, F., Garrido, J.A., Rodríguez, R.M., Brillas, E., Mineralización del paracetamol en medio ácido mediante procesos electroquímicos y químicos de oxidación avanzada, Vol. 1, page C47, XXVI Reunión del Grupo Especializado de Electroquímica de la RSEQ (VII Iberic Meeting of Electrochemistry), Córdoba, Spain, 12-15 April 2004. (Oral presentation)

UNIVERSITAT DE BARCELONA

ARTICLE 3 / *PAPER 3*

Mineralization of paracetamol in aqueous medium by anodic oxidation with a boron-doped diamond electrode

ELEC Mat MA

ELSEVIER

Chemosphere 58 (2005) 399–406

CHEMOSPHERE

www.elsevier.com/locate/chemosphere

Mineralization of paracetamol in aqueous medium by anodic oxidation with a boron-doped diamond electrode

Enric Brillas *, Ignasi Sirés, Conchita Arias, Pere Lluís Cabot, Francesc Centellas, Rosa María Rodríguez, José Antonio Garrido

Laboratori de Ciència i Tecnologia Electroquímica de Materials (LCTEM), Departament de Química Física, Facultat de Química, Universitat de Barcelona, Martí i Franquès 1-11, 08028 Barcelona, Spain

Received 30 March 2004; received in revised form 6 September 2004; accepted 20 September 2004

Abstract

The degradation of 100 ml of solutions with paracetamol (*N*-(4-hydroxyphenyl)acetamide) up to 1 g l^{-1} in the pH range 2.0–12.0 has been studied by anodic oxidation in a cell with a boron-doped diamond (BDD) anode and a graphite cathode, both of 3-cm^2 area, by applying a current of 100, 300 and 450 mA between 25 and 45 °C. Complete mineralization is always achieved due to the great concentration of hydroxyl radical (•OH) generated at the BDD surface, with release of NH_4^+ and NO_3^- ions. The mineralization rate is pH-independent, increases with increasing applied current and temperature, but decreases when drug concentration raises from 315 mg l^{-1}. Reversed-phase chromatography revealed a similar complex paracetamol decay in acid and alkaline media. Ion-exclusion chromatography allowed the detection of oxalic and oxamic acids as ultimate carboxylic acids. When the same solutions have been comparatively treated with a Pt anode, a quite poor mineralization is found because of the production of much lower •OH concentration. Under these conditions, the degradation rate is enhanced in alkaline medium and polymerization of intermediates is favored in concentrated solutions. Paracetamol can be completely destroyed with Pt and its kinetics follows a pseudo-first-order reaction with a constant rate independent of pH.

Keywords: Paracetamol; Anodic oxidation; Boron-doped diamond; Water treatment; Decay kinetics

1. Introduction

There is growing interest in the environmental relevance of pharmaceutical drugs in waters. This pollution can be due to emission from production sites, direct disposal of overplus drugs in households, excretion after drug administration to humans and animals and treatments throughout the water in fish farms (Zwiener and Frimmel, 2000). Since thousands of tons per year of drugs are consumed worldwide, a high number of anti-inflammatory, analgesics, betablockers, lipid regulators, antibiotics, antiepileptics and estrogens has been found as minor pollutants, usually with concentrations <10 μg l^{-1}, in sewage treatment plant (STP) effluents, surface and ground waters and even in drinking waters (Daughton and Jones-Lepp, 2001; Kümmerer, 2001; Ternes et al., 2002). For paracetamol (*N*-(4-hydroxyphenyl)acetamide), concentrations up to 6 μg l^{-1} have been

* Corresponding author. Tel.: +34 93 4021223; fax: +34 93 4021231.
E-mail addresses: brillas@ub.edu, ebrillas@qf.ub.es (E. Brillas).

0045-6535/$ - see front matter © 2004 Elsevier Ltd. All rights reserved.
doi:10.1016/j.chemosphere.2004.09.028

detected in STP effluents. Although there has been no proof that very low amounts of pharmaceuticals in natural waters have any adverse health effects, they can produce toxic effects to aquatic organisms and in the case of antimicrobials, the development of multi-resistant strains of bacteria (Balcioğlu and Ötker, 2003). To avoid the dangerous accumulation of drugs in the aquatic environment, research efforts are underway to develop more powerful oxidation methods than those currently applied in wastewater treatments for achieving their complete destruction.

Ozonation and some advanced oxidation processes (AOPs), such as O_3/H_2O_2, H_2O_2/UV and H_2O_2/Fe^{2+}/UV, have been successfully used to remove several common pharmaceuticals in aqueous media (Zwiener and Frimmel, 2000; Ravina et al., 2002; Ternes et al., 2002, 2003; Vogna et al., 2002; Andreozzi et al., 2003; Balcioğlu and Ötker, 2003; Huber et al., 2003). The great effectiveness of AOPs is due to the production of hydroxyl radical (•OH), which is a non-selective, very powerful oxidizing agent able to react with organics giving dehydrogenated or hydroxylated derivatives, up to their complete mineralization is reached (conversion into CO_2, water and inorganic ions). For paracetamol, however, only partial mineralization of 30% and 40% has been found from ozonation and H_2O_2/UV, respectively, in the pH range 2.0–5.5 (Andreozzi et al., 2003), indicating that more potent methods have to be applied to be completely mineralized.

In the last years, effective electrochemical treatments for the destruction of biorefractory organics in waters are being developed. The most usual technique is anodic oxidation, where solutions are decontaminated during electrolysis by the direct reaction of pollutants with adsorbed •OH formed at the anode surface from oxidation either of water in acid and neutral media or hydroxide ion at pH $\geqslant$ 10 (Brillas et al., 2003; Marselli et al., 2003; Torres et al., 2003):

$$H_2O \rightarrow {}^{\bullet}OH_{ads} + H^+ + e^- \quad (1)$$

$$OH^- \rightarrow {}^{\bullet}OH_{ads} + e^- \quad (2)$$

However, most aromatics in acid and alkaline media treated by anodic oxidation with conventional anodes such as Pt, PbO_2, doped PbO_2, doped SnO_2 and IrO_2, are slowly depolluted due to the generation of difficulty oxidizable carboxylic acids (Brillas et al., 1998, 2003; Bonfatti et al., 1999; Rodgers et al., 1999; Torres et al., 2003). The recent use of a boron-doped diamond (BDD) thin film anode has shown that it has much larger O_2 overvoltage than the above anodes, giving a much higher concentration of adsorbed •OH and a quicker oxidation of pollutants. Anodic oxidation with BDD then seems a suitable method for degrading organics up to their total mineralization, as found for $HClO_4$ aqueous solutions containing carboxylic acids such as acetic, malic, formic and oxalic (Gandini et al., 2000), 4-chlorophenol (Rodrigo et al., 2001), phenol (Iniesta et al., 2001) and herbicide 4-chlorophenoxyacetic acid (Boye et al., 2002), as well as for malic acid at pH 2.7 and ethylenediaminetetraacetic acid at pH 9.2 (Kraft et al., 2003) and for amarantha dyestuff in Na_2SO_4 solutions (Hattori et al., 2003).

This paper reports a study on the anodic oxidation with BDD of solutions containing paracetamol concentrations lower than 1 g l^{-1} and a low salt content of 0.05 M Na_2SO_4 to operate under similar conditions to those of aquatic environment. Higher drug concentrations than those found in STP and natural effluents were chosen to analyze better the oxidation ability of this method. The effect of pH in the range 2.0–12.0, applied current and temperature on the mineralization rate of this compound was examined. Comparative treatments using Pt as anode were made to confirm the high oxidizing power of BDD. The drug decay and the evolution of generated carboxylic acids were determined by chromatographic techniques.

2. Experimental

2.1. Chemicals

Paracetamol, oxalic acid and oxamic acids were reagent grade from Merck and Avocado. Anhydrous sodium sulfate used as background electrolyte was analytical grade from Fluka. All solutions were prepared with water from a Millipore Milli-Q system (conductivity $<6\times10^{-8}$ S cm^{-1}). The solution pH was adjusted with sulfuric acid or sodium hydroxide, both of analytical grade, from Merck. Organic solvents and the other chemicals used were either HPLC or analytical grade from Panreac and Aldrich.

2.2. Apparatus and analysis procedures

All electrolyses were performed with an Amel 2053 potentiostat-galvanostat. The solution pH was measured with a Crison 2000 pH-meter. Samples extracted from electrolyzed solutions were filtered with 0.45 μm PTFE filters from Whatman before analysis. The degradation of paracetamol solutions was monitored by the removal of their Total Organic Carbon (TOC), determined on a Shimadzu VCSN TOC analyzer. Reproducible TOC values were always obtained using the standard non-purgeable organic carbon method. The paracetamol decay was followed by reversed-phase chromatography with a Waters system composed of a Waters 600 HPLC liquid chromatograph fitted with a Spherisorb ODS2 5 μm, 150 × 4.6 mm, column at room temperature, and coupled with a Waters 996 photodiode array detector selected at 246 nm, controlled through a

Millennium-32® program. These analyses were made by injecting 20-μl aliquots into the chromatograph and circulating a 70:30 (v/v) acetonitrile/water mixture at 1.2 ml min^{-1} as mobile phase. Generated carboxylic acids were followed by ion-exclusion chromatography by injecting 20-μl samples into the above HPLC system with an Aminex HPX 87H, 300 × 7.8 mm column, at 35 °C from Bio-Rad. For these measurements, the photodiode detector was selected at 210 nm and the mobile phase was 4 mM H_2SO_4 at 0.6 ml min^{-1}. NH_4^+ concentration was determined following the standard colorimetric phenate method by flow injection analysis with an Alpkem Flow Solution IV system. NO_3^- concentration was obtained by ion chromatography, using a Kontron 600 HPLC fitted with a Waters IC-Pak anion column at 35 °C and coupled with a Waters spectrophotometric detector. These analyses were carried out with 100-μl aliquots after being ultramicrofiltrated by Ultrafree filters 10000 dalton cutoff and a borate-gluconate buffer of pH 8.5 as mobile phase.

2.3. Electrolytic system

All electrolyses were conducted in an open, one-compartment and thermostated cylindrical cell containing a 100-ml solution stirred with a magnetic bar. The anode was a 3-cm^2 BDD thin film deposited on a conductive Si sheet purchased from CSEM. For comparative purposes, a 3-cm^2 Pt sheet of 99.99% purity from SEMP was also employed as anode. The cathode was always a 3-cm^2 graphite bar from Sofacel. The interelectrode gap was about 3 cm.

Solutions containing less than 1 g l^{-1} of paracetamol and 0.05 M Na_2SO_4 of initial pH between 2.0 and 12.0 were comparatively degraded using a Pt or a BDD anode at constant current (I) of 100, 300 and 450 mA and at 35 °C. The effect of temperature (T) in the range 25–45 °C was also studied. During electrolyses for initial pH values ⩾4.0, the solution pH was continuously regulated within a range of ±0.03 units by adding small volumes of 0.5 M NaOH each 20 min.

3. Results and discussion

3.1. Comparative degradation behavior

A solution of 157 mg l^{-1} of paracetamol (corresponding to 100 mg l^{-1} of TOC) of pH 3.0 was initially electrolyzed at 300 mA and at 35 °C for 6 h to test its comparative degradation using a Pt or a BDD anode. In both cases, the solution pH remained practically constant up to final values of 2.8 or 3.3, respectively. Note that this parameter does not change when the same amounts of H^+ in the anode and OH^- in the cathode from water oxidation and reduction, respectively, are produced. The small pH decay for the Pt anode can then be related to the parallel oxidation of organic pollutants on its surface that releases an excess of H^+ from their hydrogen atoms (see, for example, Eq. (3)), thus slightly raising the medium acidity. The opposite trend found for the BDD anode can be due to the existence of a small proportion of oxidations of other species present in its surface without H^+ liberation, giving rise to the accumulation of an excess of OH^- in the medium that slightly increases its pH. The starting colorless solution always became clear yellow from 10–20 min of treatment due to the formation of some soluble aromatic products, although for the BDD anode, it was turned colorless again after 90 min because of the overall destruction of such species by ·OH adsorbed on its surface. The change in solution TOC with applied specific charge Q (in A h l^{-1}) for such trials is depicted in Fig. 1. A quite slow mineralization can be observed for Pt, only attaining 19% of TOC removal at 6 h (Q = 18 A h l^{-1}). In contrast, TOC very rapidly falls using BDD, so that paracetamol is completely mineralized (>98% of TOC decay) at the same time. These results indicate that anodic oxidation with BDD is a useful method for the fast and total destruction of paracetamol and its oxidation products, whereas the Pt anode has much smaller oxidizing power (with lower production of adsorbed ·OH) and leads to poor mineralization.

To clarify if the above behavior can be generalized to different aqueous media, comparative electrolyses at 300 mA were also carried out with 157 mg l^{-1} of paracetamol at pH 2.0 and in the pH range 4.0–12.0. While the solution pH did not vary along the experiments starting from pH 2.0, gradual pH decay with time was found at pH ⩾ 4.0, this being the reason why the solution pH was continuously regulated to its initial

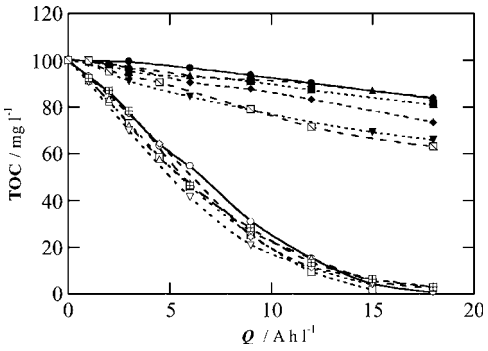

Fig. 1. TOC removal vs. specific charge for the anodic oxidation of 100 ml of a 157 mg l^{-1} paracetamol solution in 0.05 M Na_2SO_4 at 300 mA and at 35 °C using a cell with a (●,■,▲,◆,▼,▧) Pt or (○,□,△,◇,▽,⊞) BDD anode and a graphite cathode, all them of 3-cm^2 area. Initial pH: (●,○) 2.0, (■,□) 3.0; (▲,△) 4.0; (◆,◇) 8.0; (▼,▽) 10.0; and (▧,⊞) 12.0.

value. Under the latter conditions, the anode feature affected the color of treated solutions. For Pt, dark-orange solutions were always obtained at 1–2 h, becoming yellow at 6 h. This suggests the generation of soluble polyaromatic compounds on Pt, which are further slowly oxidized. A very different behavior was observed for anodic oxidation with BDD where clear yellow solutions were obtained for 2 h as maximum, being colorless at longer times, as expected if small amounts of soluble aromatic products are formed and quickly destroyed on this anode in all media. Fig. 1 also shows the TOC-Q plots obtained for these experiments. A very poor depollution can be seen for all pH values when Pt is used, since at 18 A $h\,l^{-1}$ TOC is only reduced by 17% at pH 2.0 and 4.0, 27% at pH 8.0 and about 35% at pH 10.0 and 12.0. From these data, one can conclude the existence of a larger mineralization of paracetamol in alkaline than in acid solutions. This tendency can be accounted for: (i) the generation of a greater concentration of oxidizing ·OH at the Pt surface by reaction (2) than by reaction (1); and/or (ii) the faster destruction of more easily oxidizable compounds present in alkaline medium, such as the anionic forms of possible phenolic derivatives (Torres et al., 2003). In contrast, a similar TOC decay can be observed in Fig. 1 in all media under treatment by anodic oxidation with BDD, reaching overall mineralization at Q values between 15 and 18 A $h\,l^{-1}$. This brings to consider that the concentration of generated ·OH at the BDD surface is always so high that all oxidation products have similar degradation rate within the pH range 2.0–12.0.

The above results confirm the great oxidizing power of BDD for an efficient and complete mineralization of paracetamol. The possible effect of other experimental parameters on TOC decay, as drug concentration, applied current and temperature, was then studied to know the best operative conditions for this method.

3.2. Effect of experimental parameters on paracetamol mineralization

A series of experiments was performed by electrolyzing solutions of paracetamol with concentration lower than 1 g l^{-1} of pH 3.0 at 300 mA and at 35 °C up to total mineralization by anodic oxidation with BDD. In all cases, the solution pH practically did not change with electrolysis time and a clear yellow color solution was observed for 90–120 min as maximum, as expected if soluble aromatic products are formed in low extent and rapidly oxidized. As can be seen in Fig. 2a, all solutions are completely mineralized, being required the consumption of a specific charge of about 36 A $h\,l^{-1}$ (12 h), 30 A $h\,l^{-1}$ (10 h), 24 A $h\,l^{-1}$ (8 h), 15 A $h\,l^{-1}$ (5 h) and 12 A $h\,l^{-1}$ (4 h) for 948, 677, 315, 157 and 78 mg l^{-1} of initial compound. The increase in Q with increasing drug concentration can be simply related to the existence

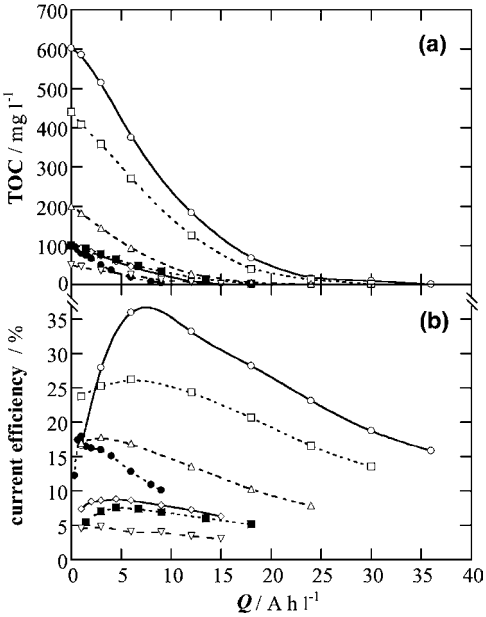

Fig. 2. (a) TOC abatement with specific charge and (b) current efficiency calculated from Eq. (4) vs. specific charge for the anodic oxidation with BDD of 100-ml paracetamol solutions in 0.05 M $Na_2SO_4 + H_2SO_4$ of pH 3.0 at 35 °C. Initial drug concentration: (○) 948; (□) 677; (△) 315; (◇,●,■) 157; and (▽) 78 mg l^{-1}. Applied current: (●) 100; (○,□,△,◇,▽) 300; and (■) 450 mA.

of more pollutants. This behavior can be better analyzed from the percentages of TOC removal after 1 and 4 h of treatment collected in Table 1. These data reveal a similar TOC decay of 27–30% at 1 h and 86–91% at 4 h up to 315 mg l^{-1}, whereas at higher concentration, the percentage of TOC removal undergoes a gradual fall attaining values of 15% at 1 h and 70% at 4 h for 948 mg l^{-1}. All these results allow establishing that the quickest mineralization rate for paracetamol by anodic oxidation with BDD is achieved working up to 315 mg l^{-1}, although the method is effective enough to depollute more concentrated solutions. Note that when the same experiments were comparatively made with Pt, a dark-orange precipitate was formed from 315 mg l^{-1} of paracetamol after 6 h, indicating the generation of insoluble polyaromatic compounds by slow reactions between products present in great concentration in solution. Anodic oxidation with Pt then favors polymerization of intermediates in concentrated solutions, thus limiting their mineralization process.

A more significant effect was found by varying the applied current. Fig. 2a shows that Q values of 9 A $h\,l^{-1}$ (9 h), 15 A $h\,l^{-1}$ (5 h) and 18 A $h\,l^{-1}$ (4 h) are needed to depollute a 157 mg l^{-1} paracetamol solution of pH 3.0

Table 1
Percentage of TOC removal and current efficiency obtained for selected degradations of 100-ml paracetamol solutions in 0.05 M Na_2SO_4 of pH 3.0 using anodic oxidation with a 3-cm^2 BDD electrode

c_0[a] ($mg\,l^{-1}$)	T (°C)	I (mA)	After 1 h of treatment		After 4 h of treatment	
			% TOC removal	CE[b]	% TOC removal	CE[b]
78	35	300	30	4.7	87	3.4
157	25	100	13	12	41	9.7
	35	100	20	18	64	15
	35	300	27	8.6	91	7.2
	35	450	36	7.6	98	5.2
	45	100	26	25	74	18
315	35	300	28	18	86	14
677	35	300	19	25	72	24
948	35	300	15	28	70	33

[a] Initial concentration.
[b] Current efficiency calculated from Eq. (4).

at 100, 300 and 450 mA, respectively, and at 35 °C. Since the specific charge increases as current rises, less electrolysis time is needed for total mineralization. This presupposes an increase in removed TOC with increasing I at constant time, as can be easily deduced from results given in Table 1, where at 1 h of treatment, for example, the percentage of TOC removal gradually raises from 20% to 36% between 100 and 450 mA. The fact that increasing current causes faster depollution can be related to the concomitant generation of more ·OH on the BDD surface. On the other hand, a similar behavior was found by varying the temperature from 25 to 45 °C. Note that higher temperatures cannot be used in our system due to fast evaporation of water. Results of Table 1 show that at 100 mA, the TOC of the above solution is reduced by 13%, 20% and 26% for 1 h and by 41%, 64% and 74% for 4 h at 25, 35 and 45 °C, respectively. The reaction of pollutants with ·OH is then accelerated with raising temperature, enhancing drug mineralization. Since the increase in temperature causes a greater mass transfer to the anode due to the decrease of medium viscosity, it can be inferred that the oxidation process under such experimental conditions is limited, at least partially, by the mass transfer of organics to the BDD surface.

The inorganic ions released after total mineralization of a 157 $mg\,l^{-1}$ paracetamol solution of pH 3.0 by anodic oxidation with BDD at 300 mA and at 35 °C were determined. Concentrations for NH_4^+ and NO_3^- of 12.2 and 22.0 $mg\,l^{-1}$, respectively, corresponding to 65% and 35% of initial nitrogen content, were found. No nitrite ions were detected by ion chromatography. To ascertain the nature of NO_3^- generation, a 100-ml solution with 100 $mg\,l^{-1}$ of ammonium ion (as $(NH_4)_2SO_4$) of pH 3.0 was electrolyzed under similar conditions for 6 h and 20 $mg\,l^{-1}$ of NO_3^-, due to the oxidation of 5.8% of initial NH_4^+, were determined in the final solution. These results indicate the main release of NH_4^+ during the ·OH attack on N-derivatives of paracetamol, with a small proportion of it transformed into NO_3^- at the BDD anode. However, the major part of NO_3^- accumulated in the mineralization process comes from the degradation of N-intermediates.

3.3. Current efficiency for the mineralization process

The above considerations allow concluding that mineralization of paracetamol involves its conversion into carbon dioxide and mainly NH_4^+. The overall reaction can be written as follows:

$$HO\text{–}C_6H_4\text{–}NH\text{–}CO\text{–}CH_3 + 14H_2O \rightarrow 8CO_2 + NH_4^+ + 33H^+ + 34e^- \quad (3)$$

The current efficiency (CE) at a given time t for the above solutions was then comparatively estimated from the following equation:

$$\text{current efficiency} = [\Delta(\text{TOC})_{\text{exper}}/\Delta(\text{TOC})_{\text{theor}}] \times 100 \quad (4)$$

where $\Delta(\text{TOC})_{\text{exper}}$ is the experimental solution TOC removal at time t and $\Delta(\text{TOC})_{\text{theor}}$ is the theoretically calculated TOC removal assuming that the applied electrical charge (=current × time) is only consumed to yield Eq. (3) as mineralization process.

Fig. 2b shows the efficiencies determined from Eq. (4) for the trials depicted in Fig. 2a. Several selected CE values are also collected in Table 1. As can be seen in Fig. 2b, in most cases the efficiency increases at the first treatment stages, up to 2 h for 677 and 948 $mg\,l^{-1}$ of paracetamol, suggesting the initial generation of more easily oxidizable products than the initial compound. Results of Fig. 2b and Table 1 show a continuous drop in CE with time once passed its maximum value, indicating a concomitant fall in oxidizing ability of the electrolytic system. This behavior can be ascribed to the gradual

decay in pollutant concentration favoring that ·OH can be wasted by other parallel non-oxidizing reactions, e.g. its recombination into H_2O_2; that is, the remaining products are more slowly degraded with decreasing ·OH concentration at the BDD surface. The drop in efficiency with decreasing drug concentration also supports this interpretation (see Fig. 2b and Table 1). For example, CE values of 33%, 24%, 14%, 7.2% and 3.4% for 948, 677, 315, 157 and 78 mg l^{-1} of this compound are found after 4 h of treatment at 300 mA and at 35 °C. This trend can be related again with a slower degradation of organics by an enhancement of parallel non-oxidizing reactions of generated ·OH. The same explanation can justify the decreasing efficiencies found with increasing I for 157 mg l^{-1} of paracetamol at 35 °C (see Fig. 2b and Table 1). Although the increase in current yields more TOC removal of this solution because of the generation of more ·OH at the BDD, a larger proportion of this radical is gradually wasted, making less efficient its reaction with organics. Results of Table 1 also confirm that the process becomes much more efficient as temperature raises, as expected if reactions of organics with ·OH are progressively enhanced in front of non-oxidizing reactions of this radical.

The above findings allow concluding that concentrated paracetamol solutions can be efficiently mineralized by anodic oxidation with BDD, even at low currents. This method can then be useful in practice, increasing its efficiency as temperature raises.

3.4. Paracetamol decay and time-course of products

The kinetics for the reaction between paracetamol and ·OH generated at the Pt or BDD anode was studied for several solutions of pH 3.0 and 12.0 at 300 mA and at 35 °C. The decay of its concentration was followed by reversed-phase chromatography, where it displayed a well-defined peak at a retention time t_r = 1.56 min.

As can be seen in Fig. 3a, the drug is slowly destroyed with similar rate at a given concentration for both pH values when Pt is used, disappearing from the medium in 300–360 min for 315 mg l^{-1} and ≈240 min for 157 and 78 mg l^{-1}. Kinetic analysis of these results only gave good linear plots, with regression coefficients >0.996, when they were fitted to a pseudo-first-order reaction. These correlations are presented in the inset of Fig. 3a, yielding the same pseudo-first-order rate constant of 0.013 ± 0.002 min^{-1}. This suggests that paracetamol reacts with a practically constant concentration of ·OH at the Pt surface, discarding its higher generation in alkaline medium by the participation of reaction (2), proposed above as a possibility to explain the greater TOC removal found under these conditions than in acid medium (see Fig. 1). The pH-independence of the pseudo-first-order rate constant for paracetamol (pK_a = 9.5) indicates the presence of the same electroactive species in all media, probably its neutral (not charged) form. It seems then plausible to associate the quicker mineralization of the drug in alkaline medium with the production of more easily oxidizable products than those formed in acid solutions, as also stated in Section 3.1.

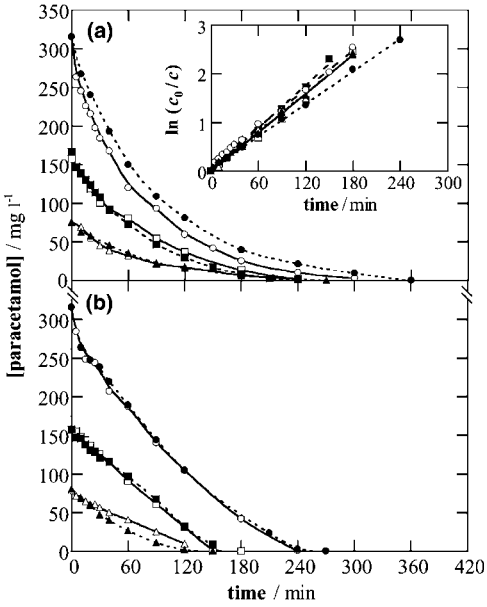

Fig. 3. Decay of paracetamol concentration with electrolysis time during the treatment of 100-ml solutions in 0.05 M Na_2SO_4 at 300 mA and at 35 °C by anodic oxidation. Plot (a): Pt anode. Plot (b): BDD anode. Initial drug concentration: (○,●) 315; (□,■) 157; and (△,▲) 78 mg l^{-1}. Initial pH: (○,□,△) 3.0; and (●, ■,▲) 12.0. The inset in plot (a) gives the kinetic analysis for the corresponding experiments assuming a pseudo-first-order reaction for paracetamol.

Fig. 3b shows a complex fall of paracetamol concentration with time using BDD, without following any kinetic equation related to simple reaction orders. A quite similar degradation rate for this drug can be observed for pH 3.0 and 12.0 at each initial concentration tested, as also obtained for Pt (see Fig. 3a), corroborating the oxidation of the same electroactive form of paracetamol in both media. However, comparison of Fig. 3a and b allows establishing that it is more rapidly destroyed with BDD, requiring lower times close to 240, 150 and 120 min for 315, 157 and 78 mg l^{-1}, respectively, to yield its complete removal, in agreement with the higher oxidizing power of this anode. The complex kinetics depicted in Fig. 3b can then be related to the competitive consumption of ·OH at the BDD surface by parallel fast reactions with products. This causes the attack of a variable ·OH concentration on the initial compound giving an undefined kinetics.

Reversed-phase chromatograms of solutions electrolyzed with Pt also exhibited two small peaks associated with primary product hydroquinone at $t_r = 1.62$ min and its oxidation derivative *p*-benzoquinone at $t_r = 1.95$ min. Note that both aromatic products have been detected during the oxidation of paracetamol by ozonation and H_2O_2/UV in the pH range 2.0–5.5 (Vogna et al., 2002; Andreozzi et al., 2003). Hydroquinone can be produced from ·OH attack on the C(1) position of aromatic ring of paracetamol, causing the breaking of the C(1)–N bond with the release of acetamide. However, the above aromatics were not detected in the reversed-phase chromatograms of solutions treated with BDD, as expected if they are so rapidly destroyed on the anode that are not accumulated in the medium. This supports the existence of competitive ·OH consumption by parallel oxidizing reactions of all pollutants leading to a complex kinetics for paracetamol, as shown in Fig. 3b.

The above solutions treated with BDD were also analyzed by ion-exclusion chromatography to try to detect generated carboxylic acids. In all cases, only two ultimate acids, oxalic (HOOC–COOH) at $t_r = 6.75$ min and oxamic (HOOC–$CONH_2$) at $t_r = 9.29$ min, were found. Oxalic acid come from the destruction of the benzenic ring of aromatic pollutants by ·OH (Brillas et al., 1998, 2003; Boye et al., 2002), while oxamic acid is expected to be produced from oxidation of acetamide released during the primary ·OH attack on the C(1) position of paracetamol. The evolution of such carboxylic acids during the treatments of solutions with 157 mg l^{-1} of this compound of pH 3.0 and 12.0 at 300 mA and at 35 °C is presented in Fig. 4. A small, but similar, accumulation of both acids can be observed in the two media, reaching their maximum concentrations between 60 and 90 min and disappearing in 240 min, a time lower than 300–360 min needed for total mineralization (see Fig. 1). These results, along with those found for paracetamol in Fig. 3b, corroborate the fast and similar destruction rate of all organics on BDD in acid and alkaline solutions, thus justifying the pH-independence for their TOC decay (see Fig. 1).

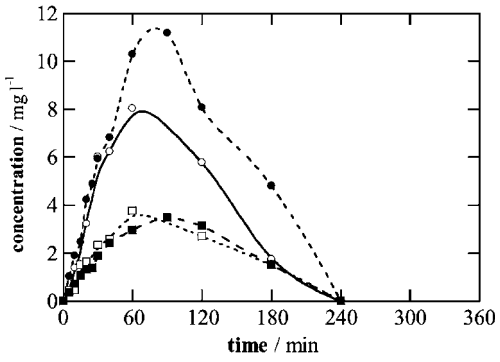

Fig. 4. Time-course of the concentration of (○,●) oxalic acid; and (□,■) oxamic acid, determined during the mineralization of 157 mg l^{-1} of paracetamol by anodic oxidation with BDD under the same conditions as in Fig. 3(b). Initial pH: (○,□) 3.0; and (●,■) 12.0.

4. Conclusions

It has been demonstrated that anodic oxidation with BDD is a very effective method for the complete mineralization of paracetamol up to 1 g l^{-1} in aqueous medium within the pH range 2.0–12.0. The TOC removal is pH-independent since the destruction of all organics by reaction with the great concentration of ·OH at the BDD surface has a similar rate in all media tested. This has been confirmed by the similar decay found for its concentration at pH 3.0 and 12.0 by reversed-phase chromatography, as well as by the analogous evolution of oxalic and oxamic acids detected as ultimate products in the same solutions by ion-exclusion chromatography. The mineralization process is accompanied by the release of NH_4^+ and NO_3^- ions. Its current efficiency increases with raising drug concentration and temperature, because of the gradual enhancement of ·OH concentration to oxidize pollutants in front its participation in non-oxidizing reactions. The increase in current causes generation of more ·OH, and hence, more TOC removal, but efficiency drops since a larger proportion of this radical is wasted. Paracetamol decay follows a complex kinetics, ascribed to its reaction with a variable ·OH concentration caused by the parallel consumption of this oxidant in fast reactions with products. In contrast, anodic oxidation with Pt has much lower oxidizing power and yields poor mineralization, although a higher TOC removal is reached in alkaline than in acid medium. This fact is related to the production of more easily oxidizable products in alkaline media. The treatment of concentrated solutions favors polymerization of intermediates, limiting the mineralization process. Paracetamol can be completely removed with Pt and its kinetics follows a pseudo-first-order reaction with a constant rate independent of pH, as expected if the same electroactive species of this compound is oxidized in all media tested.

Acknowledgments

Financial support received from MCYT (Ministerio de Ciencia y Tecnología, Spain) under project BQU2001-3712 is acknowledged. The authors also thank AGAUR (Agència de Gestió d'Ajuts Universitaris i de Recerca, Generalitat de Catalunya) for the grant awarded to I. S. to do this work.

References

Andreozzi, R., Caprio, V., Marotta, R., Vogna, D., 2003. Paracetamol oxidation from aqueous solution by means of ozonation and H_2O_2/UV system. Wat. Res. 37, 992–1004.

Balcioğlu, I.A., Ötker, M., 2003. Treatment of pharmaceutical wastewater containing antibiotics by O_3 and O_3/H_2O_2 processes. Chemosphere 50, 85–95.

Bonfatti, F., Ferro, S., Lavezzo, M., Malacarne, M., Lodi, G., De Battisti, A., 1999. Electrochemical incineration of glucose as a model organic substrate. I. Role of the electrode material. J. Electrochem. Soc. 146, 2175–2179.

Boye, B., Michaud, P.A., Marselli, B., Dieng, M.M., Brillas, E., Comninellis, C., 2002. Anodic oxidation of 4-chlorophenoxyacetic acid on synthetic boron-doped diamond electrodes. New Diamond Front. Carbon Technol. 12, 63–72.

Brillas, E., Sauleda, R., Casado, J., 1998. Degradation of 4-chlorophenol by anodic oxidation, electro-Fenton, photoelectro-Fenton and peroxi-coagulation processes. J. Electrochem. Soc. 145, 759–765.

Brillas, E., Cabot, P.L., Casado, J., 2003. Electrochemical methods for degradation of organic pollutants in aqueous media. In: Tarr, M. (Ed.), Chemical Degradation methods for Wastes and Pollutants. Environmental and Industrial Applications. Marcel Dekker, New York, USA, pp. 235–304.

Daughton, C.G., Jones-Lepp, T.L. (Eds.), 2001. Pharmaceuticals and Personal Care Products in the Environment. Scientific and Regulatory Issues. ACS Symposium Series, Washington, USA.

Gandini, D., Mahé, E., Michaud, P.A., Haenni, W., Perret, A., Comninellis, C., 2000. Oxidation of carboxylic acids at boron-doped diamond electrodes for wastewater treatment. J. Appl. Electrochem. 30, 1345–1350.

Hattori, S., Doi, M., Takahashi, E., Kurosu, T., Nara, M., Nakamatsu, S., Nishiki, Y., Furuta, T., Iida, M., 2003. Electrolytic decomposition of amarantha dyestuff using diamond electrodes. J. Appl. Electrochem. 33, 85–91.

Huber, M.M., Canonica, S., Park, G.Y., Von Gunten, U., 2003. Oxidation of pharmaceuticals during ozonation and advanced oxidation processes. Environ. Sci. Technol. 37, 1016–1024.

Iniesta, J., Michaud, P.A., Panizza, M., Cerisola, G., Aldaz, A., Comninellis, C., 2001. Electrochemical oxidation of phenol at boron-doped diamond electrode. Electrochim. Acta 46, 3573–3578.

Kraft, A., Stadelmann, M., Blaschke, M., 2003. Anodic oxidation with doped diamond electrodes: a new advanced oxidation process. J. Hazard. Mat. 103, 247–261.

Kümmerer, K. (Ed.), 2001. Pharmaceuticals in the Environment. Sources, Fate and Risks. Springer, Berlin, Germany.

Marselli, B., Garcia-Gomez, J., Michaud, P.A., Rodrigo, M.A., Comninellis, C., 2003. Electrogeneration of hydroxyl radicals on boron-doped diamond electrodes. J. Electrochem. Soc. 150, D79–D83.

Ravina, M., Campanella, L., Kiwi, J., 2002. Accelerated mineralization of the drug diclofenac via Fenton reactions in a concentric photo-reactor. Wat. Res. 36, 3553–3560.

Rodgers, J.D., Jedral, W., Bunce, N.J., 1999. Electrochemical oxidation of chlorinated phenols. Environ. Sci. Technol. 33, 1453–1457.

Rodrigo, M.A., Michaud, P.A., Duo, I., Panizza, M., Cerisola, G., Comninellis, C., 2001. Oxidation of 4-chlorophenol at boron-doped diamond electrode for wastewater treatment. J. Electrochem. Soc. 148, D60–D64.

Ternes, T.A., Meisenheimer, M., McDowell, D., Sacher, F., Brauch, H.J., Haist-Gulde, B., Preuss, G., Wilme, U., Zulei-Seibert, N., 2002. Removal of pharmaceuticals during drinking water treatment. Environ. Sci. Technol. 36, 3855–3863.

Ternes, T.A., Stüber, J., Herrmann, N., McDowell, D., Ried, A., Kampmann, M., Teiser, B., 2003. Ozonation: a tool for removal of pharmaceuticals, contrast media and musk fragrances from wastewater?. Wat. Res. 37, 1976–1982.

Torres, R.A., Torres, W., Peringer, P., Pulgarin, C., 2003. Electrochemical degradation of p-substituted phenols of industrial interest on Pt electrodes. Attempt of a structure–reactivity relationship assessment. Chemosphere 50, 97–104.

Vogna, D., Marotta, R., Napolitano, A., d'Ischia, M., 2002. Advanced oxidation chemistry of paracetamol. UV/H_2O_2-induced hydroxylation/degradation and ^{15}N-aided inventory of nitrogenous breakdown products. J. Org. Chem. 67, 6143–6151.

Zwiener, C., Frimmel, F.H., 2000. Oxidative treatment of pharmaceuticals in waters. Wat. Res. 34, 1881–1885.

7.3.2. Resultats i Discussió / *Results and Discussion*

TOC decay as function of applied specific charge Q (in A h L^{-1}) clearly shows that a slow mineralization is achieved with Pt in comparison with BDD: after 6 h (Q = 18 A h L^{-1}) at 300 mA, 19% of TOC removal is attained at pH 3.0 and 35% at pH 10.0 and 12.0 using Pt, whereas complete mineralization for all pH values even at 5 h (Q = 15 A h L^{-1}) is reached using BDD. The enhanced mineralization of paracetamol in alkaline media using Pt can not be accounted for by the generation of a greater amount of $^{\bullet}OH_{ads}$ (Reaction 5.-46), because kinetic analyses suggest a constant $^{\bullet}OH_{ads}$ concentration in all media, so the observed trend must be attributed to the faster destruction of more easily oxidizable anionic forms of possible phenolic intermediates present in alkaline media (it can not be attributed to differences in paracetamol electroactivity, since the same rate constant is obtained in all media). In contrast, the amount of effective $^{\bullet}OH_{ads}$ generated at the BDD surface is always so high that all oxidation products have a similar degradation rate within the pH range 2.0-12.0, so AO with BDD is an effective pH-independent mineralization process. At this point it is interesting to establish a comparison with PEF with 1.0 mM Fe^{2+} + 1.0 mM Cu^{2+} + UVA light, because this is the process that allows completes mineralization using the O_2-diffusion cathode. Figure 7.-3 shown below indicates that: (i) AO with Pt leads to a very low TOC removal, and (ii) AO with BDD and PEF with 1.0 mM Fe^{2+} + 1.0 mM Cu^{2+} + UVA light lead to complete mineralization after 5-6 h, but PEF exhibits a greater mineralization rate at nearly all of the stages due to the high amount of $^{\bullet}OH$ generated in the medium from Fenton's reaction.

All solutions of pH 3.0 up to 948 mg L^{-1} paracetamol are completely mineralized at 300 mA and at 35 ºC with BDD, requiring between 4 h (Q = 12 A h L^{-1}) and 12 h (Q = 36 A h L^{-1}) for 78 and 948 mg L^{-1}, respectively. The increase in Q with increasing initial drug concentration can be explained by the presence of more pollutants in the medium. A relevant trend can be detected from the percentages of TOC removal

after 1 h and 4 h of treatment: 86-91% of TOC removal is attained up to 315 mg L^{-1} paracetamol at 4 h, whereas 70% is reached for 948 mg L^{-1}. In conclusion, the quickest mineralization rate is achieved up to 315 mg L^{-1} paracetamol. It is worth reminding that Paper 2 shows that PEF with 1.0 mM Fe^{2+} + 1.0 mM Cu^{2+} + UVA light is able to destroy uniquely up to ca. 0.4 g L^{-1} of drug. On the other hand, the Pt/graphite system favors polymerization of intermediates in concentrated solutions, thus limiting the mineralization process.

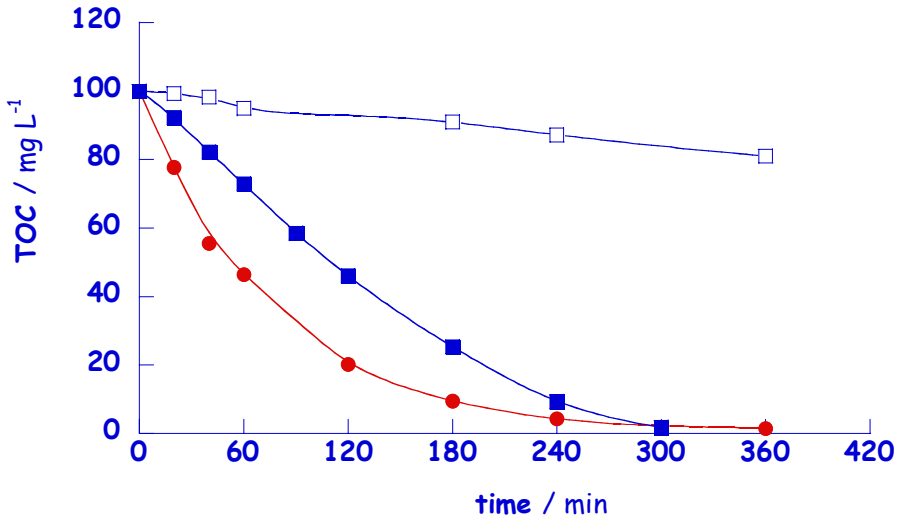

Figure 7.-3 TOC decay vs. electrolysis time for the degradation of 100 mL of 157 mg L^{-1} paracetamol solutions in 0.05 M Na_2SO_4 of pH 3.0 at 300 mA and at 35 °C. Process: (●) PEF with 1.0 mM Fe^{2+} + 1.0 mM Cu^{2+} + UVA light (co-catalyzed PEF), using a 3-cm^2 Pt anode and a 3-cm^2 O_2-diffusion cathode, (■) AO with a 3-cm^2 BDD anode and a 3-cm^2 graphite cathode, and (□) AO with a 3-cm^2 Pt anode and a 3-cm^2 graphite cathode.

Q values of 9, 15 and 18 A h L^{-1} (9, 5 and 4 h, respectively) are needed to depollute a 157 mg L^{-1} paracetamol solution of pH 3.0 at 35 °C when 100, 300 and 450 mA are applied, respectively. That is to say, as current intensity (*I*) increases the time required to reach a certain TOC value decreases because a higher amount of $^{\bullet}OH_{ads}$ are formed at the anode surface, but simultaneously a proportionally greater amount of $^{\bullet}OH_{ads}$ is also destroyed, thus requiring a greater *Q* (i.e., higher electrical consumption). In other words, a similar conclusion to that of EF and PEF processes can be obtained: as *I* increases, a higher TOC removal is achieved at a given time.

In the case of EF and PEF this trend is attributed to the enhanced production of $^{\bullet}OH$ in the medium, whereas here it is due to the higher amount of $^{\bullet}OH_{ads}$. To tell the truth, the situation is a bit more complex, since the production of weak oxidants such as O_3, H_2O_2 and $S_2O_8^{2-}$ ions is also enhanced with increasing *I*, thus indicating the existence of a mass-transport controlled process: a gradual accumulation of these species can be observed, attaining a quasi-steady concentration from 4 h of electrolysis, just when they are generated and destroyed at the same rate. When Pt is used as anode, no weak oxidants are detected, so the low amount of effective $^{\bullet}OH_{ads}$ is the unique source of oxidizing species to remove the pollutants. In addition, as *T* increases from 25 to 45 °C, a part of the aforementioned oxidizing agents ($^{\bullet}OH_{ads}$, O_3, H_2O_2 and $S_2O_8^{2-}$) is consumed due to their decomposition and/or their reaction with greater amount of organics. The effect of temperature variation can then be summarized in the following way: the reaction of pollutants is accelerated when *T* raises, thus enhancing drug mineralization. Moreover, since the increase in temperature causes a greater mass transfer to the anode due to the decrease of medium viscosity, it can be concluded again that the oxidation process is limited by the mass transfer of organics towards the BDD surface.

As pointed out for EF and PEF, the determination of *N*-containing inorganic ions reveals that the initial N is mainly lost as NH_4^+. Nevertheless, for such an oxidizing method as the PEF process with 1.0 mM Fe^{2+} + 1.0 mM Cu^{2+} + UVA light, 93% of initial N is converted into NH_4^+ and only 1% is transformed into NO_3^-, whereas in AO with BDD 65% of initial N content is converted into NH_4^+ and 35% into NO_3^-. After electrolyzing an ammonium salt with the same BDD system, it can be said that only a small proportion of NO_3^- comes from NH_4^+ oxidation at the BDD surface. Then, NO_3^- should mainly come from the oxidation of *N*-intermediates at the BDD. Some of these intermediates could resemble to the ones proposed by Vogna et al. [355, 356] thanks to ^{15}N-labeling: *N*-acetylaminocatechol and *N*-acetylaminoresorcinol coming from paracetamol hydroxylation, and some *N*-containing carboxylic acids.

In section 7.2.2 it has been commented that the overall mineralization reaction involves 34 F for each mol of paracetamol (Reaction 6.-2). MCE values for several intensities and initial paracetamol concentrations can be calculated by using Equation 6.-1. As in section 7.2, results show a continuous drop in efficiency with time (i.e., with *Q*) after going through the maximum value, thus indicating a concomitant decrease in the oxidizing ability of the electrolytic system. This trend can be ascribed again to the larger proportion of $^{\bullet}OH_{ads}$ oxidized to O_2 at the anode, and its recombination to H_2O_2. Similarly, higher MCE values are obtained as initial concentration of pollutant rises. Moreover, decreasing efficiencies can be observed when *I* increases, as could be inferred from the aforementioned comment: as *I* increases, a greater electrical consumption (i.e., a greater *Q*) is required to mineralize because a larger proportion of hydroxyl radical is wasted in parasite reactions. Finally, the process is more efficient with rising *T*, as is expected if reactions between organics and all the oxidizing agents ($^{\bullet}OH_{ads}$, O_3, H_2O_2 and $S_2O_8^{2-}$) are enhanced due to the increase in mass transfer of pollutants. A really forceful conclusion can then be presented after comparing the data in Paper 2 and Paper 3: at low paracetamol concentrations, PEF with 1.0 mM Fe^{2+} + 1.0 mM Cu^{2+} + UVA light is much more efficient than AO with BDD at nearly all of the stages, whereas at high concentrations both processes exhibit similar efficiencies. This explanation can be quantified at 300 mA, pH 3.0 and 35 ºC: 53% of TOC removal (16% MCE) and 95% (7%) is achieved at 1 and 4 h by PEF with 1.0 mM Fe^{2+} + 1.0 mM Cu^{2+} + UVA light, whereas 27% (9%) and 91% (7%) is reached by AO with BDD. In contrast, when 948 mg L^{-1} of paracetamol are electrolyzed, the TOC removal at 4 h is around 70% (32% MCE) for both processes. These values corroborate the idea given before and confirmed by several authors, that AO with BDD is a mass-transfer controlled process, therefore increasing its efficiency as pollutant concentration rises. Figure 7.-4 given below gathers these tendencies in a very clear way.

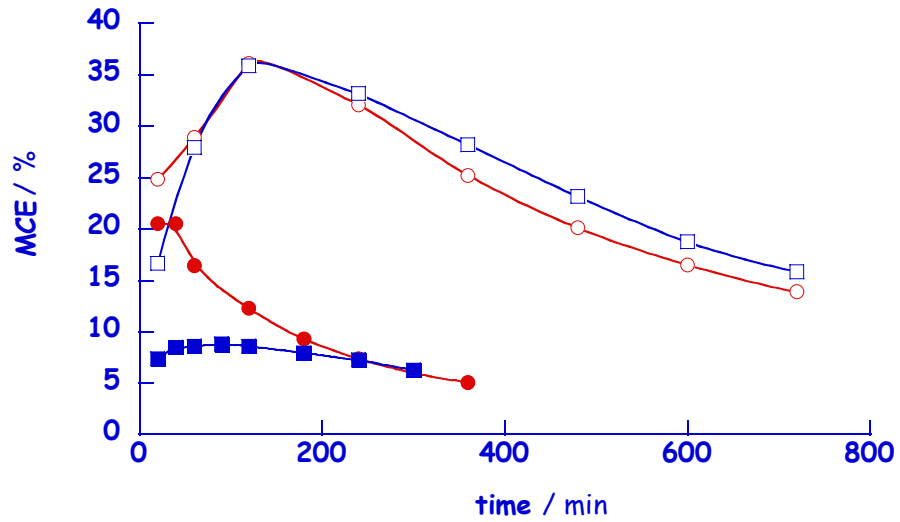

Figure 7.-4 Change of MCE with electrolysis time for the degradation of 100 mL of paracetamol solutions in 0.05 M Na_2SO_4 of pH 3.0 at 300 mA and at 35 °C. Initial drug concentration: (●,■) 157 mg L^{-1}, (○,□) 948 mg L^{-1}. Process: (●,○) PEF with 1.0 mM Fe^{2+} + 1.0 mM Cu^{2+} + UVA light (co-catalyzed PEF), using a 3-cm^2 Pt anode and a 3-cm^2 O_2-diffusion cathode, (■,□) AO with a 3-cm^2 BDD anode and a 3-cm^2 graphite cathode.

Reversed-phase chromatograms for solutions electrolyzed at 300 mA show a slow degradation of paracetamol in comparison with EF and PEF processes, where paracetamol can be degraded in 6 min. When AO with Pt is used, paracetamol disappears after nearly 240 min for 157 mg L^{-1}, and the degradation is pH-independent for all the initial concentrations tested. Kinetic analyses give good linear plots when fitted to a pseudo-first-order reaction, yielding the same pseudo-first-order rate constant of k_1 = 0.013±0.002 min^{-1} up to 315 mg L^{-1}. This suggests that $^{\bullet}OH_{ads}$ at Pt surface is practically constant. On the other hand, a complex decay of paracetamol with time is observed in AO with BDD, without following any kinetic equation related to simple reaction orders, similarly to what is observed in EF and PEF processes. This complex kinetics can be related to the competitive consumption of $^{\bullet}OH_{ads}$ by parallel fast reactions with some products, yielding an undefined kinetics due to a variable $^{\bullet}OH_{ads}$ concentration attacking paracetamol. A pH-independent decay is observed for AO with BDD as well. Nevertheless, the higher oxidizing power of BDD in comparison with Pt is evident

because paracetamol is destroyed in 150 min (still really slow in comparison to EF and PEF). Figure 7.-5 compares paracetamol degradation curves for PEF with 1.0 mM Fe^{2+} + 1.0 mM Cu^{2+} + UVA light, AO with Pt and AO with BDD, and the obvious differences can be observed at first sight:

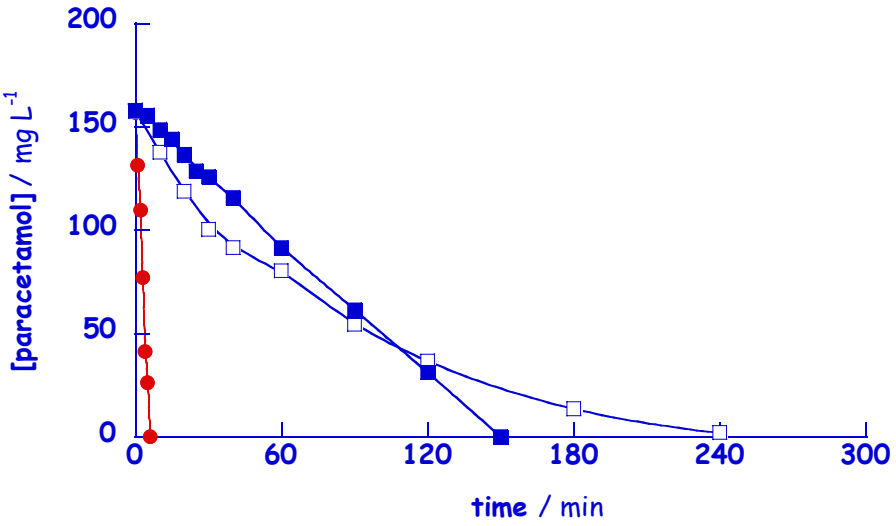

Figure 7.-5 Decay of paracetamol concentration with electrolysis time for the degradation of 100 mL of 157 mg L^{-1} paracetamol solutions in 0.05 M Na_2SO_4 of pH 3.0 at 300 mA and at 35 °C. Process: (●) PEF with 1.0 mM Fe^{2+} + 1.0 mM Cu^{2+} + UVA light (co-catalyzed PEF), using a 3-cm^2 Pt anode and a 3-cm^2 O_2-diffusion cathode, (■) AO with a 3-cm^2 BDD anode and a 3-cm^2 graphite cathode, and (□) AO with a 3-cm^2 Pt anode and a 3-cm^2 graphite cathode.

Reversed-phase chromatograms from electrolyses with Pt exhibit the peaks of hydroquinone and *p*-benzoquinone as aromatic intermediates. These products are also observed by EF and PEF. However, they are not detected in AO with BDD, as expected if they can not be accumulated in the medium because paracetamol and its intermediates are simultaneously destroyed with $^{\bullet}OH_{ads}$ (and other weak oxidants reported elsewhere), thus yielding a complex kinetics.

Finally, ion-exclusion chromatograms for AO with BDD show the accumulation of oxalic and oxamic acids as the ultimate intermediates. Not ketomalonic nor maleic or fumaric acids are accumulated. The evolution of oxalic and oxamic acids shows no significant differences at pH 3.0 and 12.0. It must be highlighted that maximum

concentrations of oxalic and oxamic acids are about 10 and 4 mg L^{-1}, respectively, and they disappear after 240 min, whereas in PEF with 1.0 mM Fe^{2+} + 1.0 mM Cu^{2+} + UVA light up to 80 and 15 mg L^{-1} are accumulated, and they remain in the solution during all the mineralization process (i.e., 360 min). In other words, both paracetamol and its intermediates are oxidized at fast and similar destruction rate on BDD in acidic and alkaline media, thus justifying the low accumulation of the products and the pH-independence for their TOC decay, and yielding a complex kinetics.

After the analyses carried out in order to establish the intermediates involved in the reaction pathway, it can be concluded that the scheme proposed in section 7.2.2 is definitely a good electrochemical sequence for paracetamol, since no other by-products have been identified by AO compared to EF and PEF. Hydroquinone and acetamide are the primary products, being subsequently oxidized to *p*-benzoquinone and oxamic acid, respectively. Ring opening leads to oxalic acid, while oxamic acid oxidation releases NH_4^+ ions. At the end, all the organic C content can be transformed into CO_2 using BDD, whereas with Pt the mineralization is very poor.

When BDD is used the solutions are turned colorless because of the overall destruction of soluble aromatic products, responsible for the coloration observed in Pt systems. It must be noted that in the previously commented EF and PEF processes the initial solutions turned into dark yellow due to the complexes between Fe^{3+} and H_2O_2. The solution pH always remains practically constant when the initial pH is 3.0, as in the case of EF and PEF systems. On the contrary, a gradual pH decay is found at pH ≥ 4.0 due to the formation of carboxylic acids.

8. DESTRUCCIÓ D'UN METABÒLIT ACTIU DE FÀRMACS REGULADORS DE LÍPIDS EN SANG: ÀCID CLOFÍBRIC / *DESTRUCTION OF A BLOOD LIPID REGULATOR AGENT: CLOFIBRIC ACID*

This chapter is devoted to the study of the degradation of the blood lipid regulator agent clofibric acid. It is divided into three main parts: (i) an introduction giving an overview on the characteristics of clofibric acid, its environmental data and some results published in literature on its destruction, (ii) the results obtained for the treatment of this drug by anodic oxidation, and (iii) the results obtained by electro-Fenton and photoelectro-Fenton processes.

8.1. CARACTERÍSTIQUES DE L'ÀCID CLOFÍBRIC / *CHARACTERISTICS OF CLOFIBRIC ACID*

Clofibric acid (2-(4-chlorophenoxy)-2-methylpropionic acid, Figure 8.-1) is the active metabolite of the drugs clofibrate, etofibrate and etofyllineclofibrate, widely used as blood lipid regulators at high therapeutical doses (up to 1-2 grams per day and person). These substances are used to decrease the plasmatic concentration of cholesterol and triglycerides. Moreover, clofibric acid is a structural isomer of the phenoxyalkanoic acid herbicide mecoprop (2-(4-chloro-2-methylphenoxy)propionic acid).

Fibrates, a group of drugs marketed since 1963, are classified as peroxisomal proliferators (PPs) because they have demonstrated affinity for the activated receptors, then increasing the number and size of cellular peroxisomes not only in the liver but also in many other tissues. Peroxisomes are single membrane bound organelles found in most plant and animal cells performing various metabolic functions, and segregate harmful products, such as H_2O_2, from the rest of the cell while carrying on β-oxidation of very long-chain fatty acids. Effects on fish such as rainbow trouts or Atlantic salmon have been reported by Trudeau et al. [359]. Clofibric acid toxicity has been recently assessed using three estuarine organisms (an alga, a crustacean and a fish) [360]: no adverse effects on the basis of parameters examined are expected to occur at clofibric acid environmental levels, but the potential for longer term effects can not be ruled out. In addition, possible mixture toxicity, bioaccumulation, and trophic transfer of this contaminant should be considered.

Moreover, clofibric acid is known to possess antiauxin activity. Auxin is one of major plant hormones which affect numerous plant growth processes functions including cell division and elongation, autumnal loss of leaves, and the formation of buds,

roots, flowers and fruits. Auxins usually have a ring system with an attached side-chain that terminates in a carboxyl group, so it can be consequently understood that clofibric acid affects several plant hormonal functions. In fact, this acid has been used as an efficient antiauxin for more than five decades.

Clofibric acid is usually found as pale yellow crystals, with a very characteristic odour. Some of its most remarkable properties are summarized in Table 8.-1.

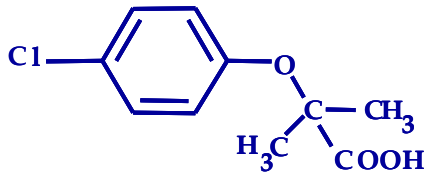

Figure 8.-1 Clofibric acid.

Table 8.-1 Clofibric acid data (several sources).

CAS number	882-09-7
Parent lipid-lowering agents	Clofibrate Etofibrate Etofyllineclofibrate
Trade names	Atromid-S (clofibrate)
Molecular formula	$C_{10}H_{11}ClO_3$
Molecular mass (g mol^{-1})	214.66
Melting point (°C)	118-119
Boiling point (°C)	-
Solubility in H_2O (mg L^{-1})$_{20\ °C}$	582.5 [360]
Density (g cm^{-3})$_{21\ °C}$	-
pK_a	3.18

Clofibric acid is a high volume chemical with an estimated annual production in the low kiloton range. It is mainly used in the form of the ethyl ester (clofibrate) in human medical care.

Two main characteristics can define clofibric acid: ubiquity and persistence. Precisely, its environmental interest is due to its widespread occurrence as well as its long-time exposure (its estimated environmental persistence is about 21 days) [361]. Heberer et al. showed no removal rate in different STPs of Berlin [362], but the results of Stumpf et al. point out a relatively high removal rate of 15% (biological filtration), 34% (activated sludge) and 51% (activated sludge and $FeCl_3$) [363]. In other words, clofibric acid is generally not eliminated from wastewater, but a removal can appear in some sewage treatment plants. Since its logK_{OW} is 3.1, clofibric acid is liable to persist in the aquatic environment. Provided that it is not biotransformed into a more hydrophilic derivative, it is not likely to bioaccumulate [361].

Clofibric acid was one of the first drugs/metabolites ever reported in sewage influent/effluent. In 1976 it was detected in raw sewage and activated sludge effluent with values from 0.8 to 2.0 μg L^{-1} [44]. In 1977 it was measured in Missouri STP effluents with an average concentration equal to 2.1 kg/day [364]. Later, in 1992, researchers looking for phenoxyalkanoic herbicides in water found clofibric acid around the city of Berlin. Since then, clofibric acid has been widely reported as occurring in STPs influents and effluents, in German rivers, in Swiss lakes, ground waters and even drinking water in studies carried out across Europe and USA [365, 366]. It has also been described as an ubiquitous contaminant in the marine environment, present at concentrations between 0.03 and 19 ng L^{-1} in samples collected from the North Sea [367, 368]. Researchers estimate that the North Sea contains 48 to 96 tons of clofibric acid, with 50 to 100 tons entering the Sea each year. The Danube in Germany, and the Po in Italy, also contain mesurable quantities of clofibric acid. Two of the samples collected from UK estuaries contained concentrations of approximately 100 ng L^{-1} [369]. Influent concentration of 1 μg L^{-1} has been found in *STPs* in Brazil [370]. Finally, a more immediate concern to humans is the finding that up to 270 ng L^{-1} have been measured in German tap water [366]. These findings suggest this contamination to be not only a local problem from

improper waste disposal but also likely to be a general environmental problem.

Several works describe that clofibric acid is easily degraded but poorly mineralized by ozone [32, 371], sunlight and UV photolysis using Xe-arc lamp solar simulators [372, 373], and AOPs such as H_2O_2/UV [371]. Oturan et al. [286] have also shown the complete degradation of clofibric acid, by means of electro-Fenton process using a mercury pool as the working electrode, but this can not be considered as an environmentally friendly procedure in water remediation.

Zwiener et al. [374] have reported the poor mineralization of clofibric acid by application of biological treatments. The compound reached a level of approximately 95% of its initial concentration, so it is defined as non-biodegradable under the experimental conditions applied.

Up to the present thesis only TiO_2/UV [375] has been presented as an effective method for clofibric acid mineralization. This latter paper proposes a multi-step scheme for the degradation of clofibric acid by photocatalysis. Moreover, a reaction mechanism is discussed. In a recent paper, Canterino et al. [376] pay attention to the presence of clofibric acid in slurries, rather than in the aquatic environment. Ozonation then seems to be a particularly suited process for the treatment of recalcitrant soil contaminants such as clofibric acid.

In conclusion, more potent oxidation procedures are needed to be applied to destroy this compound in wastewaters.

In this thesis, clofibric acid degradation and mineralization have been studied under different EAOPs applied: anodic oxidation with both Pt and BDD anodes, as well as electro-Fenton and photoelectro-Fenton processes with both anodes and an O_2-diffusion cathode.

8.2. TRACTAMENT MITJANÇANT OXIDACIÓ ANÒDICA / *TREATMENT BY ANODIC OXIDATION*

8.2.1. Finalitat del treball / *Aim of the work*

In section 7.3 the effectivity of AO process using a BDD anode for the removal and mineralization of paracetamol in waters under several experimental conditions at laboratory scale has been shown. In order to verify all the conclusions drawn for that process, mainly as for the relevance of the oxidizing species pointed out before ($^{\bullet}OH_{ads}$, O_3, H_2O_2 and $S_2O_8^{2-}$), the destruction of the blood lipid regulators bioactive metabolite called clofibric acid has been thoroughly studied. Nextly the results obtained with BDD are reported, as well as the ones using Pt because its comparatively lower oxidizing power allows a greater and larger accumulation of intermediates, thus making it easier to propose a possible electrochemical degradation pathway for this pharmaceutical. A stainless steel sheet was used as cathode in all cases, and like Pt and BDD electrodes its area was 3 cm^2.

First of all, the anodic oxidation of 100 mL of 179 mg L^{-1} clofibric acid solutions (i.e., 100 mg L^{-1} TOC) containing 0.05 M Na_2SO_4 was performed by carrying out a series of electrolyses in the pH range 2.0-12.0 at 100 mA cm^{-2} and at 35 ºC. The oxidation ability of both Pt/steel and BDD/steel systems to mineralize clofibric acid was studied for 7 h. TOC decay was analyzed in all cases.

Once the great oxidizing power of BDD was confirmed within a wide pH range, the possible effect of the variation of apparent current density (j_{app} = 33, 100 and 150 mA cm^{-2}) and temperature (25, 35 and 45 ºC) on TOC decay and MCE was assessed in order to optimize the AO process with BDD at laboratory scale. With this aim, several electrolyses of 179 mg L^{-1} clofibric acid solutions were performed at pH 3.0 and 12.0. In addition, to know the influence of electrogenerated species

($^{\bullet}OH_{ads}$, O_3, H_2O_2 and $S_2O_8^{2-}$ ions) on the mineralization of clofibric acid, the concentrations of H_2O_2 and total oxidizing agents were determined during the treatment of 100 mL of 179 mg L^{-1} clofibric acid solutions of pH 3.0 at several j_{app} and temperatures. As reported in section 6.3, H_2O_2 was analyzed spectrophotometrically at λ = 408 nm (Reaction 6.-6) [339, 340], and the amount of total oxidizing species was determined by iodometric titration [341].

The great oxidizing power of AO with BDD anode was then studied by electrolyzing solutions of pH 12.0 with metabolite contents up to close to saturation (45, 89, 179, 268, 358, 447 and 557 mg L^{-1} clofibric acid, corresponding to 25, 50, 100, 150, 200, 250 and 313 mg L^{-1} TOC, respectively) at 100 mA cm^{-2} and at 35 ºC.

After the detailed study of TOC abatement under many experimental conditions, the evolution of inorganic ions released from initial chlorine of the metabolite was examined by ion chromatography. In this sense, 100 mL of 179 mg L^{-1} clofibric acid solutions of pH 3.0 and 12.0 were electrolyzed using a BDD anode at 100 mA cm^{-2} and at 35 ºC. Several electrolyses using a Pt anode were comparatively done.

Afterwards, the kinetics for the reaction between clofibric acid and $^{\bullet}OH_{ads}$ was studied for both Pt and BDD systems. Firstly, it was necessary to clarify whether clofibric acid can also be oxidized with H_2O_2 and/or $S_2O_8^{2-}$, two of the weak oxidants having notorious role in AO with a BDD anode. Chemical tests were carried out by preparing 100 mL solutions of pH 3.0 and 12.0 containing 179 mg L^{-1} of the pharmaceutical, 20 mM of both oxidizing species and 0.05 M Na_2SO_4. Several solutions of 179 mg L^{-1} clofibric acid of pH 3.0 and 12.0, at 35 ºC and at different j_{app} values were further electrolyzed. In all cases, clofibric acid decay was followed by reversed-phase chromatography. The possible influence of clofibric acid concentration on its decay kinetics was clarified from electrolyses of different solutions of pH 12.0 at 100 mA cm^{-2} and at 35 ºC.

Simultaneously, aromatic intermediates were unequivocally identified and quantified by reversed-phase chromatography of aliquots withdrawn from electrolyzed 179 mg L^{-1} clofibric acid solutions of pH 3.0 and pH 12.0 at 100 mA cm^{-2} and at 35 ºC using Pt and BDD. Clofibric acid solutions under the conditions referred were electrolyzed by AO with Pt and BDD to obtain the ion-exclusion chromatograms reflecting the carboxylic acids accumulated. Due to the formation of 2-hydroxyisobutyric acid, a particular carboxylic acid not deeply studied by other authors, during the degradation of the pharmaceutical, an electrolysis of this acid with BDD was carried out at pH 3.0, at 100 mA cm^{-2} and at 35 ºC to clarify its oxidation pathway.

To help product identification, several 179 mg L^{-1} clofibric acid solutions of pH 3.0 and 12.0 were electrolyzed with a Pt anode at 100 mA cm^{-2} and at 35 ºC for 60 and 40 min, respectively, and after some preparatives (see section 6.3) the remaining intermediates were analyzed by GC-MS.

Finally, considering all the intermediates that were identified, a plausible reaction sequence for the anodic oxidation of clofibric acid in aqueous medium could be proposed.

The thorough results of this section are included in the following paper (Paper 4):

4. Sirés, I., Cabot, P.L., Centellas, F., Garrido, J.A., Rodríguez, R.M., Arias, C., Brillas, E., Electrochemical degradation of clofibric acid in water by anodic oxidation. Comparative study with platinum and boron-doped diamond electrodes. *Electrochim. Acta* **52** (2006) 75-85.

The following presentations in a congress are related to this work:

D. Sirés, I., Cabot, P.L., Centellas, J.A., Garrido, J.A., Rodríguez, R.M., Arias, C., Brillas, E., Destruction of clofibric acid in aqueous medium using both platinum and boron-doped diamond electrodes, Vol. 1, page 59, 7th Electrochemistry Days (7. Elektrokimiya Günleri), Hacettepe Üniversitesi, Ankara, Turkey, 28-30 June 2006. (Poster presentation)

E. Sirés, I., Cabot, P.L., Centellas, F., Garrido, J.A., Rodríguez, R.M., Arias, C., Brillas, E., Un esquema degradativo para la mineralización completa del ácido clofíbrico mediante oxidación anódica, Vol. 1, page 55, XXVIII Reunión del Grupo Especializado de Electroquímica de la RSEQ (IX Iberic Meeting of Electrochemistry), A Coruña, Spain, 10-13 July 2006. (Oral presentation)

UNIVERSITAT DE BARCELONA

ARTICLE 4 / *PAPER 4*

Electrochemical degradation of clofibric acid in water by anodic oxidation: Comparative study with platinum and boron-doped diamond electrodes

Available online at www.sciencedirect.com
ScienceDirect
Electrochimica Acta 52 (2006) 75–85
ELECTROCHIMICA Acta
www.elsevier.com/locate/electacta

Electrochemical degradation of clofibric acid in water by anodic oxidation Comparative study with platinum and boron-doped diamond electrodes

Ignasi Sirés, Pere Lluís Cabot [1], Francesc Centellas, José Antonio Garrido, Rosa María Rodríguez, Conchita Arias, Enric Brillas [*,1]

Laboratori de Ciència i Tecnologia Electroquímica de Materials, Departament de Química Física, Facultat de Química, Universitat de Barcelona, Martí i Franquès 1-11, 08028 Barcelona, Spain

Received 10 February 2006; received in revised form 27 March 2006; accepted 28 March 2006
Available online 27 April 2006

Abstract

Aqueous solutions containing the metabolite clofibric acid (2-(4-chlorophenoxy)-2-methylpropionic acid) up to close to saturation in the pH range 2.0–12.0 have been degraded by anodic oxidation with Pt and boron-doped diamond (BDD) as anodes. The use of BDD leads to total mineralization in all media due to the efficient production of oxidant hydroxyl radical (•OH). This procedure is then viable for the treatment of wastewaters containing this compound. The effect of pH, apparent current density, temperature and metabolite concentration on the degradation rate, consumed specific charge and mineralization current efficiency has been investigated. Comparative treatment with Pt yields poor decontamination with complete release of stable chloride ion. When BDD is used, this ion is oxidized to Cl_2. Clofibric acid is more rapidly destroyed on Pt than on BDD, indicating that it is more strongly adsorbed on the Pt surface enhancing its reaction with •OH. Its decay kinetics always follows a pseudo-first-order reaction and the rate constant for each anode increases with increasing apparent current density, being practically independent of pH and metabolite concentration. Aromatic products such as 4-chlorophenol, 4-chlorocatechol, 4-chlororesorcinol, hydroquinone, *p*-benzoquinone and 1,2,4-benzenetriol are detected by gas chromatography–mass spectrometry (GC–MS) and reversed-phase chromatography. Tartronic, maleic, fumaric, formic, 2-hydroxyisobutyric, pyruvic and oxalic acids are identified as generated carboxylic acids by ion-exclusion chromatography. These acids remain stable in solution using Pt, but they are completely converted into CO_2 with BDD. A reaction pathway for clofibric acid degradation involving all these intermediates is proposed.

Keywords: Clofibric acid; Anodic oxidation; Platinum anode; Boron-doped diamond anode; Oxidation products

1. Introduction

The presence of drugs and their metabolites as emerging pollutants in the aquatic environment has been recently documented [1–13]. A fairly large number of these compounds such as anti-inflammatories, analgesics, betablockers, lipid regulators, antibiotics, antiepileptics and estrogens has been detected in sewage treatment plant effluents, surface and ground waters and even in drinking water at concentration usually ranging from nanograms to micrograms per liter. This pollution can be due to different sources involving emission from production sites, direct disposal of overplus drugs in households, excretion after drug administration to humans and animals, treatments throughout the water in fish and other animal farms and inadequate treatment of manufacturing waste [10]. Widespread contamination is produced when drugs are recalcitrant towards degradation and can only be partially removed in sewage treatment plants. Powerful oxidation methods are then needed to be applied to ensure the complete degradation of drugs and their metabolites in waters to avoid their potential adverse health effects on both, humans and animals.

Anodic oxidation is one of the most promising electrochemical technologies for the treatment of wastewaters with low contents of organic pollutants. In this method contaminants are destroyed by reaction with adsorbed hydroxyl radical (•OH) generated at the surface of a high O_2-overvoltage anode from oxidation of water in acid and neutral media [14–18]:

$$H_2O \rightarrow {}^{\bullet}OH_{ads} + H^+ + e^- \quad (1)$$

* Corresponding author. Tel.: +34 93 4021223; fax: +34 93 4021231.
E-mail address: brillas@ub.edu (E. Brillas).
[1] ISE member.

0013-4686/$ – see front matter © 2006 Elsevier Ltd. All rights reserved.
doi:10.1016/j.electacta.2006.03.075

or hydroxide ion at pH ≥ 10:

$$OH^- \rightarrow {}^{\bullet}OH_{ads} + e^- \quad (2)$$

Hydroxyl radical is a non-selective, very powerful oxidizing agent able to react with organics giving dehydrogenated or hydroxylated by-products until their total mineralization, i.e., their overall transformation into CO_2, water and inorganic ions.

The recent use of a boron-doped diamond (BDD) thin-film electrode in anodic oxidation has shown that it possesses technologically important characteristics such as an inert surface with low adsorption properties, remarkable corrosion stability and an extremely wide potential window in aqueous medium [17]. This electrode has much greater O_2-overvoltage than a Pt anode, yielding quicker oxidation of most organics. This has been confirmed from recent studies showing the total mineralization of several aromatics and short carboxylic acids in waters from electrolysis with a BDD anode [15–36]. The use of anodic oxidation with BDD then seems an adequate technique for the treatment of wastewaters containing toxic and biorefractory organic pollutants.

In previous work we have reported that anodic oxidation with BDD can destroy toxic chlorophenoxy acids such as 4-chlorophenoxyacetic [23] and 4-chloro-2-methylphenoxyacetic, 2-(4-chloro-2-methylphenoxy)propionic and 2-(4-chlorophenoxy)-2-methylpropionic (clofibric acid) [36] in 1 M $HClO_4$. The degradation of 4-chlorophenoxyacetic, 2,4-dichlorophenoxyacetic and 2,4,6-trichlorophenoxyacetic acids in acid aqueous solutions of pH 2.0–6.0 using this technique has also been investigated [28]. Among these compounds, clofibric acid has relevant environmental interest due to its significant accumulation and large persistence in waters. It is the active metabolite of clofibrate, etofibrate and etofyllineclofibrate, which are drugs widely used as blood lipid regulators with therapeutic doses of about 1–2 g day^{-1} per person, since they decrease the plasmatic concentration of cholesterol and triglycerides [3,37]. Clofibric acid concentrations up to 10 μg l^{-1} have been detected in sewage treatment plant influents and effluents and in rivers, lakes, North Sea, ground and drinking waters [1–3,9]. Several papers have described that this compound is poorly mineralized in aqueous medium by different oxidation methods such as electrogenerated Fenton's reagent [38], ozone [8,39], H_2O_2/UV [39], sunlight and UV photolysis [40] and TiO_2/UV [41], as well as after application of different biological and physico-chemical methods in sewage treatment plants [37,42].

This paper reports a detailed study on the electrochemical degradation of aqueous solutions of clofibric acid, as a model of chlorophenoxy compounds, in the pH range 2.0–12.0 to know the characteristics of its anodic oxidation with BDD for the possible application of this method to the treatment of wastewaters containing such kind of compounds. The effect of pH, apparent current density, temperature and clofibric acid concentration up to close to saturation on the degradation rate, consumed specific charge and mineralization current efficiency was examined. The metabolite decay and the evolution of its by-products were followed by chromatographic techniques. Comparative experiments with a Pt anode were also made, since the metabolite is mineralized in smaller extent than with the BDD one, allowing a better interpretation of its kinetic behavior and a clearer detection of by-products produced during its degradation.

2. Experimental

2.1. Chemicals

Clofibric acid, 4-chlorophenol, 4-chlororesorcinol, hydroquinone, *p*-benzoquinone and 1,2,4-benzenetriol were reagent grade, with purity >97%, supplied by Sigma–Aldrich, Merck, Panreac and Avocado. 4-Chlorocatechol was synthesized by chlorination of pyrocatechol with SO_2Cl_2 at room temperature following a standard method reported in the literature [43]. 2-Hydroxyisobutyric, maleic, fumaric, pyruvic, tartronic, formic and oxalic acids were either reagent or analytical grade from Sigma–Aldrich, Panreac and Avocado. Anhydrous sodium sulfate used as background electrolyte was analytical grade from Fluka. All solutions were prepared with high-purity water obtained from a Millipore Milli-Q system with resistivity >18 MΩ cm at 25 °C. The initial solution pH was adjusted with sulfuric acid or sodium hydroxide, both of analytical grade, purchased from Merck or Fluka, respectively. Organic solvents and the other chemicals utilized were either HPLC or analytical grade from Merck and Fluka.

2.2. Instruments

Electrolyses were carried out with an Amel 2053 potentiostat-galvanostat. The solution pH was measured with a Crison 2000 pH-meter. Aromatic intermediates were identified by gas chromatography–mass spectrometry (GC–MS) with a Hewlett-Packard system composed of a HP 5890 Series II gas chromatograph fitted with a HP-5 0.25 μm, 30 m × 0.25 mm, column and coupled with a HP 5989A mass spectrometer operating in EI mode at 70 eV. The temperature ramp was 35 °C for 2 min, 10 °C min^{-1} up to 320 °C and hold time 5 min, and the temperatures of the inlet, transfer line and detector were 250, 250 and 290 °C, respectively. The degradation of clofibric acid solutions was monitored by the removal of their total organic carbon (TOC), determined on a Shimadzu VCSN TOC analyzer. The metabolite decay and the evolution of its aromatic intermediates were followed by reversed-phase chromatography using a Waters 600 HPLC liquid chromatograph fitted with a Spherisorb ODS2 5 μm, 15 cm × 4.6 mm, column at room temperature, coupled with a Waters 996 photodiode array detector and controlled through a Millennium-32® program. For each compound, this detector was selected at the maximum wavelength of its UV-absorption band. Generated carboxylic acids were followed by ion-exclusion chromatography with the above chromatograph fitted with a Bio-Rad Aminex HPX 87H, 30 cm × 7.8 mm, column at 35 °C and with the photodiode detector selected at λ = 210 nm. Cl^- concentration in treated solutions was determined by ion chromatography using a Shimadzu 10Avp HPLC chromatograph fitted with a Shim-Pack IC-A1S, 10 cm × 4.6 mm, anion column at

40 °C and coupled with a Shimadzu CDD 10Avp conductivity detector.

2.3. Electrolytic system

All electrolyses were conducted in a one-compartment and thermostated cylindrical cell of 100 ml capacity. The anode was either a Pt sheet of 99.99% purity from SEMP or a BDD thin-film deposited on conductive single crystal p-type Si (1 0 0) wafers from CSEM, both of 3 cm^2 of apparent area. The cathode was always a 3 cm^2 stainless steel (AISI 304) sheet. The interelectrode gap was about 1 cm.

Solutions of 100 ml containing up to 0.56 g l^{-1} of clofibric acid (close to saturation) and 0.05 M Na_2SO_4 in the pH range 2.0–12.0 were comparatively degraded using a Pt or a BDD anode at a constant apparent current density (j_{app}) of 33, 100 and 150 mA cm^{-2} and at 35.0 °C. The effect of temperature between 25.0 and 45.0 °C was also studied. All solutions were vigorously stirred with a magnetic bar during treatment. The pH value of solutions starting from initial pH between 3.0 and 10.0 decreased with electrolysis time and then, it was continuously regulated within a range of ±0.03 units by adding small volumes of 0.1 M NaOH.

2.4. Analytical procedures

To identify the aromatic products, several 179 mg l^{-1} clofibric acid solutions of pH 3.0 and 12.0 were electrolyzed with a Pt anode at 100 mA cm^{-2} and at 35.0 °C for 60 and 40 min, respectively, and their organic components were extracted with 45 ml of CH_2Cl_2 in three times. Each collected organic solution was then dried with anhydrous Na_2SO_4, filtered and its volume reduced to about 5 ml to concentrate the remaining products for further analysis by GC–MS.

Before TOC and chromatographic analyses, all samples withdrawn from electrolyzed solutions were filtered with 0.45 μm Whatman PTFE filters. Reproducible TOC values were always obtained by injecting 100 μl aliquots into the TOC analyzer, using the standard non-purgeable organic carbon method. From these data, the mineralization current efficiency (MCE) for treated solutions at a given time t was calculated from the following equation:

$$\mathrm{MCE} = \frac{\Delta(\mathrm{TOC})_{\mathrm{exp}}}{\Delta(\mathrm{TOC})_{\mathrm{theor}}} \times 100 \quad (3)$$

where $\Delta(\mathrm{TOC})_{\mathrm{exp}}$ is the experimental solution TOC removal at time t and $\Delta(\mathrm{TOC})_{\mathrm{theor}}$ is the theoretically calculated TOC decay considering that the applied electrical charge (=current × time) is only consumed in the mineralization process of clofibric acid.

Reversed-phase chromatography of initial and treated solutions was made by injecting 20 μl samples into the HPLC chromatograph under circulation of a 50:47:3 (v/v/v) methanol/0.01 M phosphate buffer (pH 2.5)/pentanol mixture at 1.0 ml min^{-1} as mobile phase. For ion-exclusion chromatography, 20 μl samples were also injected into the HPLC chromatograph and the mobile phase was 4 mM H_2SO_4 at 0.6 ml min^{-1}. Cl^- measurements were carried out with a 2.5 mM phtalic acid and 2.4 mM tris(hydroxymethyl)aminomethane solution of pH 4.0 as mobile phase at 1.5 ml min^{-1}. The concentration of H_2O_2 accumulated in electrolyzed solutions was obtained from the light absorption of the titanic-hydrogen peroxide colored complex at λ = 408 nm [44], measured with a Unicam UV4 Prisma double-beam spectrometer thermostated at 25.0 °C. The concentration of total oxidants generated in the same solutions was determined by iodometric titration [21].

3. Results and discussion

3.1. TOC removal using a BDD or Pt anode

A series of electrolyses was carried out with 179 mg l^{-1} clofibric acid solutions (corresponding to 100 mg l^{-1} of TOC) in the pH range 2.0–12.0 at 100 mA cm^{-2} and at 35.0 °C for 7 h to test their comparative degradation by anodic oxidation with Pt and BDD. In the experiments performed with initial pH between 3.0 and 10.0, the solution pH underwent a progressive decay to lower values with time due to the formation of acidic products and hence, it was continuously regulated to its initial pH with 0.1 M NaOH. All solutions treated with the BDD anode always remained colorless, but their degradation with the Pt one caused a change in color, being pale pink at 5 min, orange at about 1 h, dark-brown at ca. 2 h and yellow at approximately 4 h, further being slowly decolorized up to become colorless again after 6 h of treatment. The coloration of solutions degraded with Pt can be related to the generation of soluble polyaromatics in large extent, which can be totally destroyed by oxidant •OH produced by reaction (1) or (2). These colored products are not accumulated in the medium using BDD, probably due to the faster destruction of aromatic intermediates.

The variation of solution TOC with applied specific charge (Q, in A h l^{-1}) for the above trials is depicted in Fig. 1. A continuous and quick TOC abatement can be observed for all solutions treated with BDD, being reduced by more than 91% at 7 h

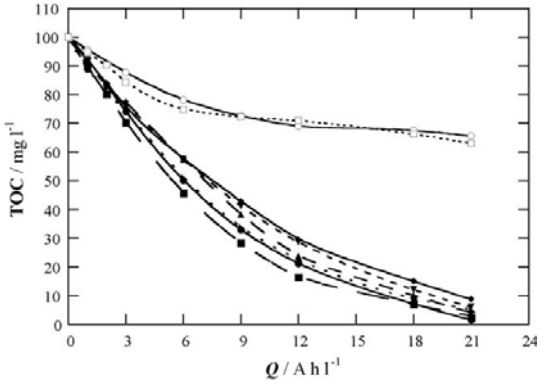

Fig. 1. TOC removal versus specific charge for the anodic oxidation of 100 ml of 179 mg l^{-1} clofibric acid solutions in 0.05 M Na_2SO_4 at 100 mA cm^{-2} and at 35.0 °C using a one-compartment cell with a (◯,□) Pt, (♦,●,▲,▼,◣,■) BDD anode and a stainless steel cathode, all them of 3 cm^2 area. Initial pH: (♦) 2.0, (◯,●) 3.0, (▲) 6.0, (▼) 8.0, (◣) 10.0, and (□,■) 12.0.

($Q = 21$ A h l^{-1}) in all cases. These results indicate that clofibric acid and its by-products are destroyed at similar rate in the pH range 2.0–12.0 by anodic oxidation with BDD. This behavior can be explained by the generation of similar concentration of •OH from reaction (1) or (2). Note that overall mineralization (>97% TOC decay) is achieved starting from pH 3.0 and from pH 12.0, where the degradation rate is slightly faster. In contrast, Fig. 1 also shows that both solutions are slowly degraded with Pt up to reach near 30% of mineralization at 4 h, whereas at longer time they are not practically decontaminated. Consequently, under comparable conditions the use of a Pt anode yields quite poor mineralization of clofibric acid solutions. That means that Pt is unable to destroy some products that are hardly oxidizable with •OH, as short carboxylic acids, as will be discussed below.

The possible effect of apparent current density and temperature on the degradation rate of the above clofibric acid solutions taking place in anodic oxidation with BDD was studied to clarify the oxidation ability of this anode. As an example, Fig. 2 presents the TOC–Q plots obtained for pH 3.0 and 12.0 at 33, 100 and 150 mA cm^{-2} and at 35.0 °C. The TOC of both solutions decays at similar rate for each j_{app}, confirming that the degradation of the metabolite and its by-products is practically pH-independent. However, increasing j_{app} causes faster TOC removal with time and more consumption of specific charge for total mineralization, which varies from 10 A h l^{-1} at 33 mA cm^{-2} to 27 A h l^{-1} at 150 mA cm^{-2}. This corresponds to a drop in time required for overall decontamination from 10 to 5.5 h since TOC is more rapidly removed with time. Fig. 2 also shows that an increase in temperature from 25.0 to 45.0 °C working at pH 12.0 and at 100 mA cm^{-2} also accelerates the degradation process, decreasing the time for total mineralization from 10 to 6 h, with a concomitant fall in Q from 30 to 18 A h l^{-1}.

The change in TOC abatement with varying j_{app} and temperature can be explained taking into account that in Na_2SO_4

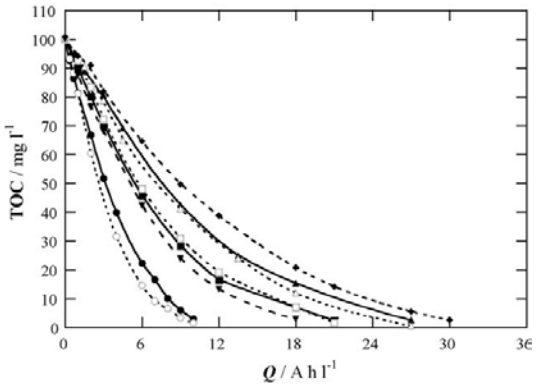

Fig. 2. Effect of experimental parameters on the variation of TOC with specific charge for the treatment of 100 ml of 179 mg l^{-1} clofibric acid solutions by anodic oxidation with BDD electrode. Initial pH: (◯,□,△) 3.0 and (●,■,▲,♦,▼) 12.0. Apparent current density: (◯,●) 33 mA cm^{-2}, (□,■,♦,▼) 100 mA cm^{-2}, and (△,▲) 150 mA cm^{-2}. Temperature: (♦) 25.0 °C, (◯,□,△,●,■,▲) 35.0 °C, and (▼) 45.0 °C.

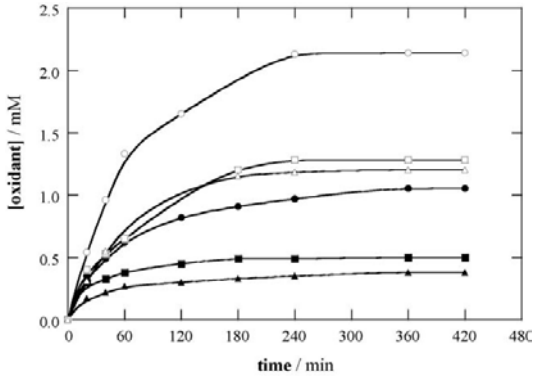

Fig. 3. Time-course of the concentration of: (◯,□,△) total oxidants, (●,■,▲) hydrogen peroxide generated during the anodic oxidation of 100 ml of 179 mg l^{-1} clofibric acid solutions of pH 3.0 using a BDD electrode. Apparent current density: (□,△,■,▲) 33 mA cm^{-2} and (◯,●) 100 mA cm^{-2}. Temperature: (◯,□,●,■) 25.0 °C and (△,▲) 45.0 °C.

medium other weaker oxidants such as ozone, peroxodisulfate ion and H_2O_2 can be competitively formed with •OH at the BDD anode from the following reactions [17]:

$$3H_2O \rightarrow O_3 + 6H^+ + 6e^- \quad (4)$$

$$2HSO_4^- \rightarrow S_2O_8^{2-} + 2H^+ + 2e^- \quad (5)$$

$$2H_2O \rightarrow H_2O_2 + 2H^+ + 2e^- \quad (6)$$

where H_2O_2 generation in reaction (6) can proceed via •OH recombination. To know the influence of such electrogenerated species on the mineralization of clofibric acid, the concentrations of H_2O_2 and total oxidants (ozone, $S_2O_8^{2-}$ and H_2O_2) were determined during the treatment of 100 ml of 179 mg l^{-1} clofibric acid solutions of pH 3.0 at several apparent current densities and temperatures. The results obtained are shown in Fig. 3, where the difference between the concentration of total oxidants and H_2O_2 mainly corresponds to that of $S_2O_8^{2-}$. A gradual accumulation of all species can be always observed, attaining a quasi-steady concentration usually from 4 h of electrolysis, just when they are generated and destroyed at the same rate. An increase in j_{app} from 33 to 100 mA cm^{-2} at 25.0 °C leads to the formation of more weak oxidants due to the acceleration of reactions (4)–(6), indicating the existence of a mass-transport controlled process. However, part of these species is consumed when the temperature increases to 45.0 °C at 33 mA cm^{-2}, indicating that increasing temperature enhances their decomposition and/or their reaction with greater amount of organics accelerating their oxidation. Note that no electrogenerated oxidants were detected when comparable solutions were degraded with Pt.

From the above findings, the fact that TOC is more rapidly removed with time when j_{app} raises for the 179 mg l^{-1} clofibric acid solutions of pH 3.0 and 12.0 can be ascribed to the higher production of •OH from reaction (1) or (2) and weaker oxidants (ozone, $S_2O_8^{2-}$ and H_2O_2) from reactions (4)–(6), thus favoring the degradation of organics. The increase in Q for total mineralization under these conditions is indicative of a lower relative generation of the main oxidant •OH due to its quicker oxida-

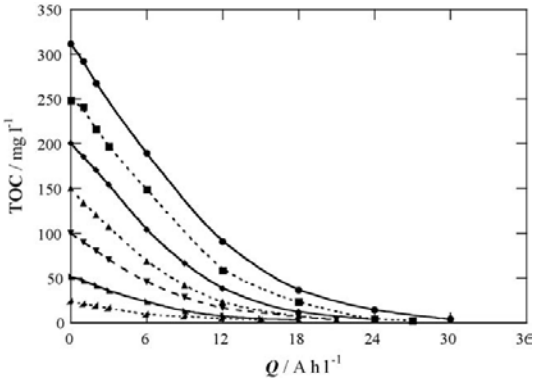

Fig. 4. TOC abatement with specific charge for the degradation of 100 ml of solutions with: (●) 557 mg l^{-1} (close to saturation), (■) 447 mg l^{-1}, (♦) 358 mg l^{-1}, (▲) 268 mg l^{-1}, (▼) 179 mg l^{-1}, (◣) 89 mg l^{-1}, and (◢) 45 mg l^{-1} of clofibric acid at pH 12.0, at 100 mA cm^{-2} and at 35.0 °C by anodic oxidation with BDD.

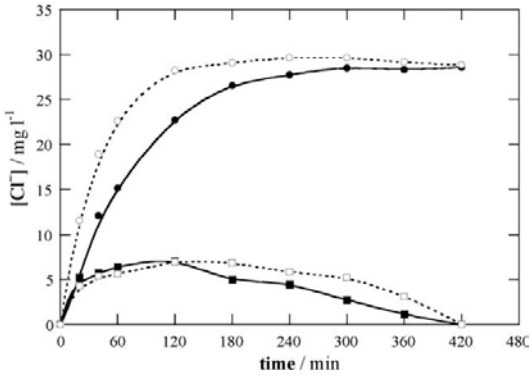

Fig. 5. Concentration of chloride ion accumulated during the treatment of 100 ml of 179 mg l^{-1} clofibric acid solutions of pH: (●,■) 3.0 and (○,□) 12.0, at 100 mA cm^{-2} and at 35.0 °C by anodic oxidation with a: (●,○) Pt and (■,□) BDD electrode.

tion to O_2. On the other hand, the faster TOC decay found when temperature increases, as exemplified in Fig. 2 for the metabolite solution of pH 12.0 at 100 mA cm^{-2}, can be explained by the concomitant increase in mass transfer of pollutants towards the BDD anode due to the decrease of medium viscosity. This causes the acceleration of their reaction with •OH and weaker oxidants such as ozone, $S_2O_8^{2-}$ and H_2O_2, enhancing metabolite mineralization. It can then be inferred that the oxidation process is limited, at least partially, by the mass transfer of organics to BDD surface.

These results indicate that anodic oxidation with BDD is potent enough to decontaminate wastewaters of clofibric acid in a large variety of experimental conditions. The great oxidizing power of this method was confirmed by electrolyzing solutions with metabolite contents up to close to saturation at 100 mA cm^{-2} and at 35.0 °C. Fig. 4 illustrates the fast and total TOC abatement found for 45, 89, 179, 268, 358, 447 and 557 mg l^{-1} of this compound at pH 12.0. Similar TOC–Q plots were obtained for the same solutions at pH 3.0. As can be seen, the specific charge consumed for overall mineralization gradually increases from 15 to 30 A h l^{-1} as initial concentration rises. This trend can be, in principle, related to the existence of more organic matter in solution. However, increasing metabolite concentration causes a quicker TOC abatement. For example, at 2 h of electrolysis (Q = 6 A h l^{-1}) 15, 28, 56, 81, 95, 101 and 121 mg l^{-1} of TOC are removed starting from 45, 89, 179, 268, 358, 447 and 557 mg l^{-1} of clofibric acid, respectively. This gradual enhancement in oxidizing power of the BDD anode can be accounted for by the reaction of more •OH with greater amount of pollutants, and hence, this radical is wasted in smaller extent by other nonoxidizing reactions such as its decomposition to O_2 and its recombination to H_2O_2.

3.2. Mineralization current efficiency

Generation of inorganic ions from the initial chlorine of the metabolite is expected during its mineralization process. Ionic chromatographic analysis of all electrolyzed solutions revealed the formation of chloride ion. However, the presence of other chlorine–oxygen ions such as chlorite, chlorate and perchlorate in treated solutions was not detected by this technique. As can be seen in Fig. 5, Cl^- is rapidly accumulated for 180–240 min of anodic oxidation with Pt of 179 mg l^{-1} clofibric acid solutions at both pH 3.0 and 12.0, operating at 100 mA cm^{-2} and at 35.0 °C. At longer time than 360 min, this ion reaches a quasi-steady concentration of about 29 mg l^{-1} in both media, a value practically equal to 29.5 mg l^{-1} corresponding to the initial chlorine contained in solution. All chloro-organics are then mainly destroyed for 5–6 h of electrolysis, with the release of chloride ion. A very different behavior can be observed in Fig. 5 for the evolution of Cl^- in the same solutions comparatively degraded with BDD. In both media this ion attains a maximum concentration of ca. 7 mg l^{-1} at 120 min and further, it is slowly destroyed until disappearing at 420 min. The instability of Cl^- under these conditions can be explained by its oxidation to Cl_2 gas on BDD, as reported for the electrolysis of NaCl aqueous solutions with this anode [45].

These findings allow establishing that the mineralization of clofibric acid by anodic oxidation with BDD involves its conversion into CO_2 and chloride ion as primary inorganic ion. This overall reaction can be written as follows:

$$C_{10}H_{11}ClO_3 + 17H_2O \rightarrow 10CO_2 + Cl^- + 45H^+ + 44e^- \quad (7)$$

where the destruction of each mole of the metabolite needs the consumption of 44 F.

Taking into account reaction (7), the mineralization current efficiency of solutions treated with BDD was determined from Eq. (3). This parameter was found to be practically pH-independent, although it strongly increased with increasing initial metabolite concentration and temperature, as well as with decreasing apparent current density. To illustrate these trends, Fig. 6 presents the MCE–Q plots found for different clofibric

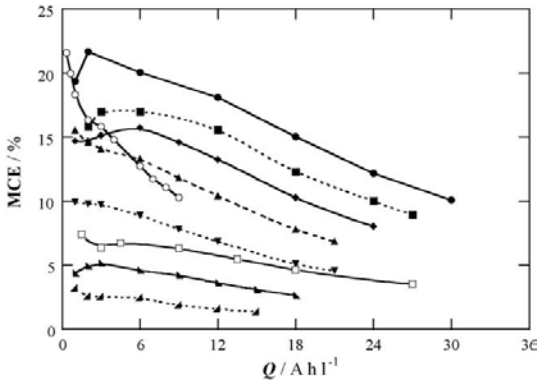

Fig. 6. Dependence of mineralization current efficiency calculated from Eq. (3) on specific charge for the anodic oxidation with BDD of 100 ml of clofibric acid solutions of pH 12.0 at 35.0 °C. Initial metabolite concentration: (●) 557 mg l^{-1} (close to saturation), (■) 447 mg l^{-1}, (♦) 358 mg l^{-1}, (▲) 268 mg l^{-1}, (○,□,▼) 179 mg l^{-1}, (◣) 89 mg l^{-1}, and (◢) 45 mg l^{-1}. Apparent current density: (○) 33 mA cm^{-2}, (●,■,♦,▲,▼,◣,◢) 100 mA cm^{-2}, and (□) 150 mA cm^{-2}.

acid solutions of pH 12.0 at several j_{app} values and at 35.0 °C. A slight increase in efficiency can be observed at the early stages of most treatments, as expected if a higher amount of pollutants is converted more quickly into CO_2. This enhancement in MCE can be accounted for by the faster degradation of some products that are able to react simultaneously with •OH and with weaker oxidants as ozone, $S_2O_8^{2-}$ and H_2O_2 produced from reactions (4)–(6). When electrolyses are prolonged, the efficiency always undergoes a slow, but continuous, decay, as expected if products that are more difficultly oxidizable with •OH than the initial compound, such as short carboxylic acids, are progressively formed. The slower production of such hardly oxidizable species with raising initial metabolite content can then justify the concomitant increase in efficiency at constant j_{app}. This behavior can be easily deduced from results of Fig. 6, where, for example, after 2 h (Q = 6 A h l^{-1}) of electrolysis at 100 mA cm^{-2}, increasing MCE values of 2.5, 4.5, 8.9, 13, 16, 17 and 20% are obtained for increasing clofibric acid concentrations of 45, 89, 179, 268, 358, 447 and 557 mg l^{-1}, respectively. This tendency also confirms the gradual reaction of higher amount of •OH with more pollutants, indicating that this radical is lost in smaller extent in other nonoxidizing reactions. Fig. 6 also shows a dramatic fall in efficiency as higher j_{app} is applied, confirming the existence of a mass-transport controlled process. For example, the MCE values at 1 h of treatment of 179 mg l^{-1} of the metabolite are 18, 9.7 and 6.7% at 33, 100 and 150 mA cm^{-2}, respectively. This trend corroborates the progressive faster production of O_2 and other weak oxidants (ozone, $S_2O_8^{2-}$ and H_2O_2), to the detriment of the main oxidant •OH with increasing apparent current density.

All these results allow concluding that concentrated clofibric acid solutions can be efficiently and totally mineralized by anodic oxidation with BDD, even at low current, increasing its efficiency as temperature rises. This method is then viable for treating wastewaters containing this metabolite.

3.3. Kinetics of clofibric acid decay

To clarify whether clofibric acid can be oxidized with H_2O_2 and $S_2O_8^{2-}$, chemical tests were carried out by preparing 100 ml solutions with 179 mg l^{-1} of this metabolite, 20 mM of each one of these oxidants and 0.05 M Na_2SO_4 at pH 3.0 and 12.0. The concentration of clofibric acid in these experiments was determined by reversed-phase chromatography, where it exhibits a well-defined absorption peak with a retention time (t_r) of 7.6 min. However, no change in the metabolite content of solutions was found for 3 h at 35.0 °C, indicating that it does not react with such weak oxidants. That means that in anodic oxidation this compound can only react with •OH.

The kinetics for the reaction between clofibric acid and •OH formed from reaction (1) or (2) at the Pt and BDD anodes was comparatively studied with 179 mg l^{-1} metabolite solutions of pH 3.0 and 12.0 at different j_{app} values and at 35.0 °C. The change of its concentration with time is presented in Fig. 7(a) and (b). As can be seen in Fig. 7(a), it disappears from the medium at pH 12.0 after 420, 360 and 240 min of anodic oxidation with Pt at 33, 100 and 150 mA cm^{-2}, respectively. However, longer

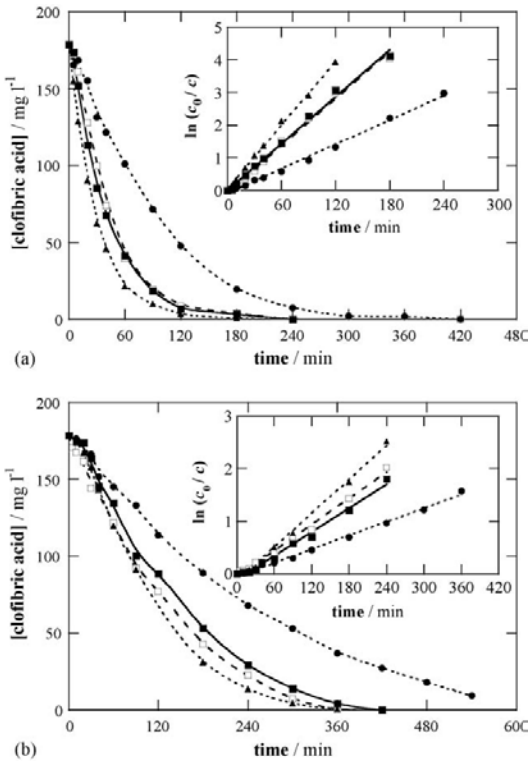

Fig. 7. Clofibric acid concentration decay with electrolysis time for the treatment of 100 ml of 179 mg l^{-1} metabolite solutions at 35.0 °C by anodic oxidation with a: (a) Pt and (b) BDD electrode. Initial pH: (□) 3.0 and (●,■,▲) 12.0. Apparent current density: (●) 33 mA cm^{-2}, (□,■) 100 mA cm^{-2}, and (▲) 150 mA cm^{-2}. The inset panel presents the kinetic analysis assuming a pseudo-first-order reaction for clofibric acid.

electrolyses time of about 540, 420 and 360 min is needed to be removed under comparable conditions using BDD, as it is shown in Fig. 7(b). This is surprising if one takes into account that the BDD anode produces much more reactive •OH able to mineralize the metabolite and all intermediates, while the Pt one is unable to destroy some by-products giving poor mineralization (see Fig. 1). The greater oxidation ability of clofibric acid on Pt can then be ascribed to its higher adsorption on its surface favoring its reaction with more amount of •OH. Note that the time required for total destruction of this compound on BDD at each applied j_{app} is practically equal to that needed for its overall mineralization (see Figs. 2 and 7(b)), indicating that it persists up to the end of its degradation process. Results of Fig. 7(a) and (b) also show a similar destruction rate for the metabolite at pH 3.0 and 12.0 and at 100 mA cm^{-2} on each electrode. This brings to consider that the same electroactive species of the metabolite is oxidized in the pH range tested, probably its anionic (unprotonated) form since its pK_a = 3.18 [40].

The above clofibric acid concentration decays were well fitted to a pseudo-first-order kinetic equation. The excellent linear correlations obtained are depicted in the panel inset of Fig. 7(a) and (b). This behavior suggests the production of a constant concentration of •OH from reaction (1) or (2) at each anode during electrolysis, which is much greater than that of the metabolite adsorbed on its surface. From this analysis, an increasing pseudo-first-order rate constant (k) of 2.4×10^{-4} s^{-1} (square regression coefficient, $R^2 = 0.994$), 4.0×10^{-4} s^{-1} ($R^2 = 0.993$) and 5.4×10^{-4} s^{-1} ($R^2 = 0.998$) for Pt and of 7.2×10^{-5} s^{-1} ($R^2 = 0.995$), 1.3×10^{-4} s^{-1} ($R^2 = 0.991$) and 1.8×10^{-4} s^{-1} ($R^2 = 0.994$) for BDD is found at increasing j_{app} of 33, 100 and 150 mA cm^{-2}, respectively. Note that k does not vary proportionally with j_{app}, confirming that a smaller proportion of this oxidant reacts with pollutants when apparent current density rises, since it is more quickly oxidized to O_2 in both anodes.

The possible influence of clofibric acid concentration on its decay kinetics was clarified from electrolyses of different solutions of pH 12.0 at 100 mA cm^{-2} and at 35.0 °C. The concentration–time plots obtained with Pt and BDD are shown in Fig. 8(a) and (b), respectively. Comparison of these data allows concluding that the metabolite is always more quickly removed with Pt, confirming the existence of a greater adsorption of this compound on this anode that accelerates its reaction with •OH. Note that for all solutions treated with BDD, a similar time is required for clofibric acid disappearance and for its overall mineralization (see Figs. 4 and 8(b)). This evidences the existence of simultaneous degradation of the initial pollutant and its intermediates under such conditions. Assuming a pseudo-first-order reaction kinetics for clofibric acid, good straight lines with $R^2 > 0.991$ were found in all cases, as can be seen in the inset of Fig. 8(a) and (b). This analysis shows a rather similar constant rate for all initial concentrations tested, corresponding to an average k-value of $(4.0 \pm 0.6) \times 10^{-4}$ s^{-1} for Pt and $(1.3 \pm 0.1) \times 10^{-4}$ s^{-1} for BDD. This behavior corroborates the existence of a much greater amount of •OH than metabolite adsorbed on each electrode surface, even operating with a concentration close to saturation.

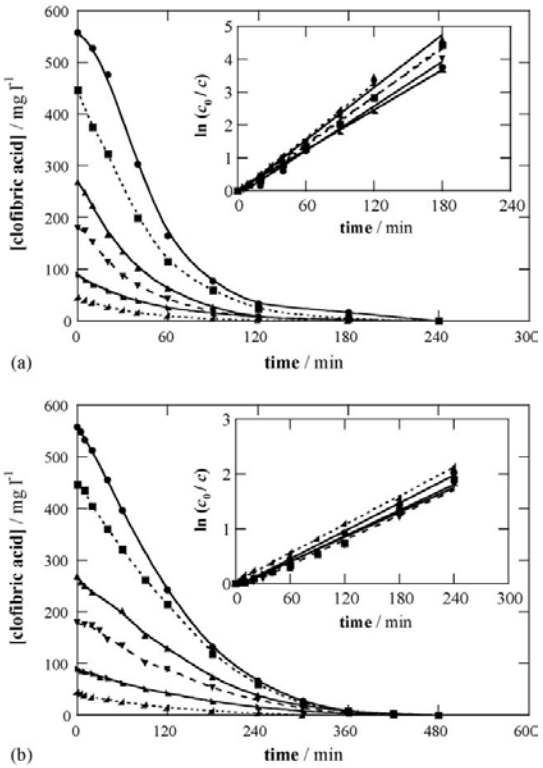

Fig. 8. Time-course of clofibric acid concentration for the anodic oxidation of 100 ml of: (●) 557 mg l^{-1} (close to saturation), (■) 447 mg l^{-1}, (▲) 268 mg l^{-1}, (▼) 179 mg l^{-1}, (◣) 89 mg l^{-1}, and (◢) 45 mg l^{-1} metabolite solutions of pH 12.0 at 100 mA cm^{-2} and at 35.0 °C using a: (a) Pt and (b) BDD electrode. The corresponding kinetic analysis assuming a pseudo-first-order reaction for the metabolite is shown in the inset panel.

3.4. Identification and time-course of intermediates

The MS spectra obtained in the GC–MS analyses of organics extracted after short-time electrolyses of 179 mg l^{-1} metabolite solutions of pH 3.0 and 12.0 with Pt at 100 mA cm^{-2} and at 35.0 °C, displayed three peaks associated with stable aromatic products such as 4-chlorophenol (m/z = 128 (100, M^+), 130 (33 $(M+2)^+$)) at t_r = 11.5 min, hydroquinone (m/z = 108 (100, M^+)) at t_r = 13.2 min and p-benzoquinone (m/z = 110 (45, M^+)) at t_r = 6.5 min. Reversed-phase chromatograms of the same degraded solutions exhibited peaks related to these compounds at retention time of 5.0, 1.7 and 2.0 min, respectively, along with other additional peaks ascribed to 4-chlorocatechol at t_r = 3.1 min, 4-chlororesorcinol at t_r = 2.3 min and 1,2,4-benzenetriol at t_r = 1.8 min. All these compounds were unequivocally identified by comparing their retention times and UV–vis spectra, measured on the photodiode array, with those of pure products.

The evolution of aromatic intermediates in the above solutions treated with Pt is shown in Fig. 9(a). A much greater accumulation of these products can be observed at pH 3.0 than at pH 12.0, where only 1,2,4-benzenetriol and 4-chlorophenol

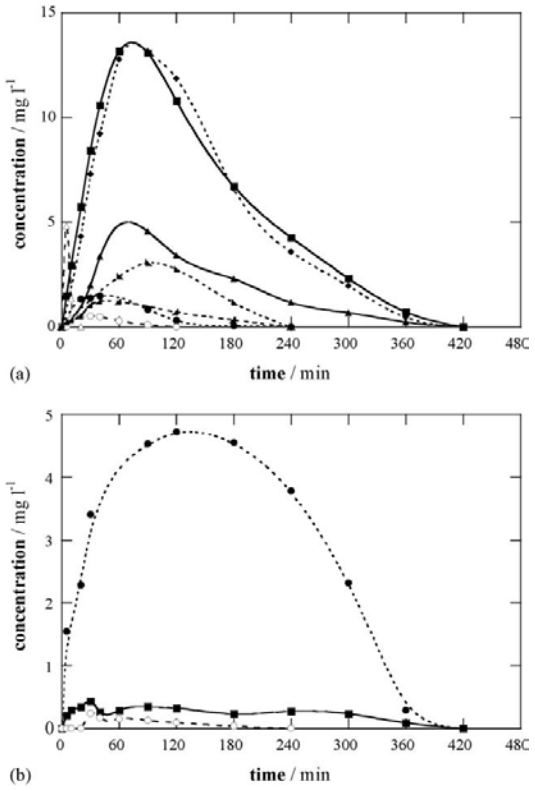

Fig. 9. Evolution of the concentration of aromatic intermediates detected during the degradation of 100 ml of 179 mg l^{-1} clofibric acid solutions at 100 mA cm^{-2} and at 35.0 °C by anodic oxidation with a: (a) Pt and (b) BDD electrode. Initial pH: (●,♦,◣ ,◢ ,■,▲) 3.0, and (◯,△) 12.0. Compound: (●,◯) 4-chlorophenol, (♦) 4-chlorocatechol, (◣) 4-chlororesorcinol, (◢) hydroquinone, (■) *p*-benzoquinone, and (▲,△) 1,2,4-benzenetriol.

are detected up to 20 and 120 min, respectively. At pH 3.0, 1,2,4-benzenetriol, 4-chlorocatechol and *p*-benzoquinone persist to 420 min after reaching maximum contents of 4.5, 13.0 and 13.2 mg l^{-1} at about 60 min, whereas 4-chlorophenol, 4-chlororesorcinol and hydroquinone are more quickly destroyed, disappearing in 240 min. In contrast, reversed-phase chromatograms of the same solutions degraded under the same conditions with BDD only allowed the detection of 4-chlorophenol and *p*-benzoquinone. As can be seen in Fig. 9(b), both compounds are present in the medium of pH 3.0 up to 420 min, i.e., a time similar to that of clofibric acid disappearance (see Fig. 7(b)), but only the first product is accumulated up to 240 min at pH 12.0. These findings indicate that the degradation of all aromatics, except the initial pollutant, is more rapid on BDD, although they are completely degraded with both anodes.

Ion-exclusion chromatography of the above electrolyzed solutions revealed the generation of carboxylic acids such as oxalic at $t_r = 6.6$ min, tartronic at $t_r = 7.7$ min, maleic at $t_r = 8.1$ min, pyruvic at $t_r = 9.2$ min, 2-hydroxyisobutyric at $t_r = 12.6$ min, formic at $t_r = 14.0$ min and fumaric at $t_r = 16.1$ min. Tartronic, maleic, fumaric and formic acids can be produced from the oxidative breaking of the benzenic moiety of aromatic intermediates [16–18,25,28], while 2-hydroxyisobutyric acid is expected to be released when 4-chlorophenol is formed from clofibric acid. The pathway of the last product was clarified from the anodic oxidation with BDD of a solution with 50 mg l^{-1} of 2-hydroxyisobutyric acid of pH 3.0 at 100 mA cm^{-2} and at 35.0 °C. Under these conditions, this compound gives pyruvic acid, which is further oxidized to oxalic acid. This acid can also be generated from the independent degradation of longer chain acids as tartronic, maleic and fumaric [16,18,28]. Oxalic [30] and formic acids are finally converted into CO_2.

The production and destruction rate of generated carboxylic acids depends on both, pH and anode tested. Fig. 10(a) shows that large amounts of these products are slowly accumulated using Pt, without apparent degradation, as expected from the quite low mineralization achieved in these conditions (see Fig. 1). At pH 3.0 tartronic, 2-hydroxyisobutyric and oxalic acids are the main products, whereas the two latter acids are also largely formed in the solution of pH 12.0. A different behavior can be seen in Fig. 10(b) for BDD, where all carboxylic acids are destroyed at 420 min when total mineralization of starting

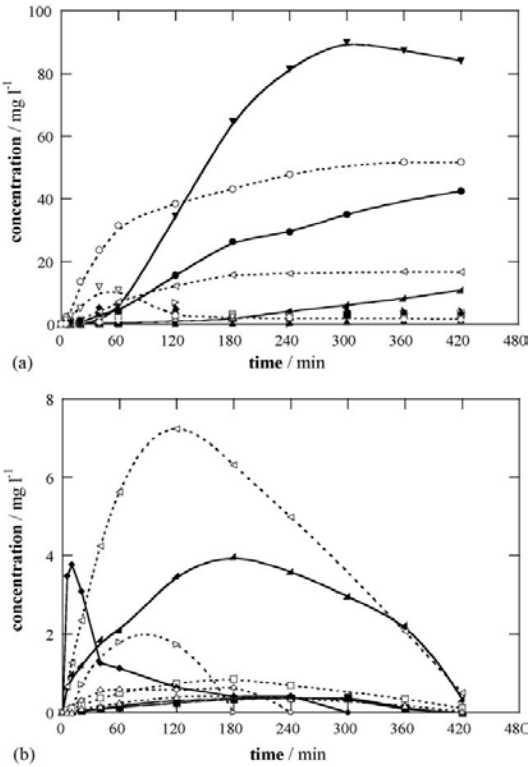

Fig. 10. Time-course of the concentration of carboxylic acids generated during the anodic oxidation of 179 mg l^{-1} clofibric acid solutions under the same conditions as in Fig. 9. Anode: (a) Pt and (b) BDD. Initial pH: (●,■,♦,▲,▼,◣,◢) 3.0 and (◯,□,△,◇,▽,▷,◁) 12.0. Compound: (●,◯) 2-hydroxyisobutyric acid, (■,□) maleic acid, (▲,△) fumaric acid, (♦,◇) pyruvic acid, (▼,▽) tartronic acid, (◣,▷) formic acid, and (◢,◁) oxalic acid.

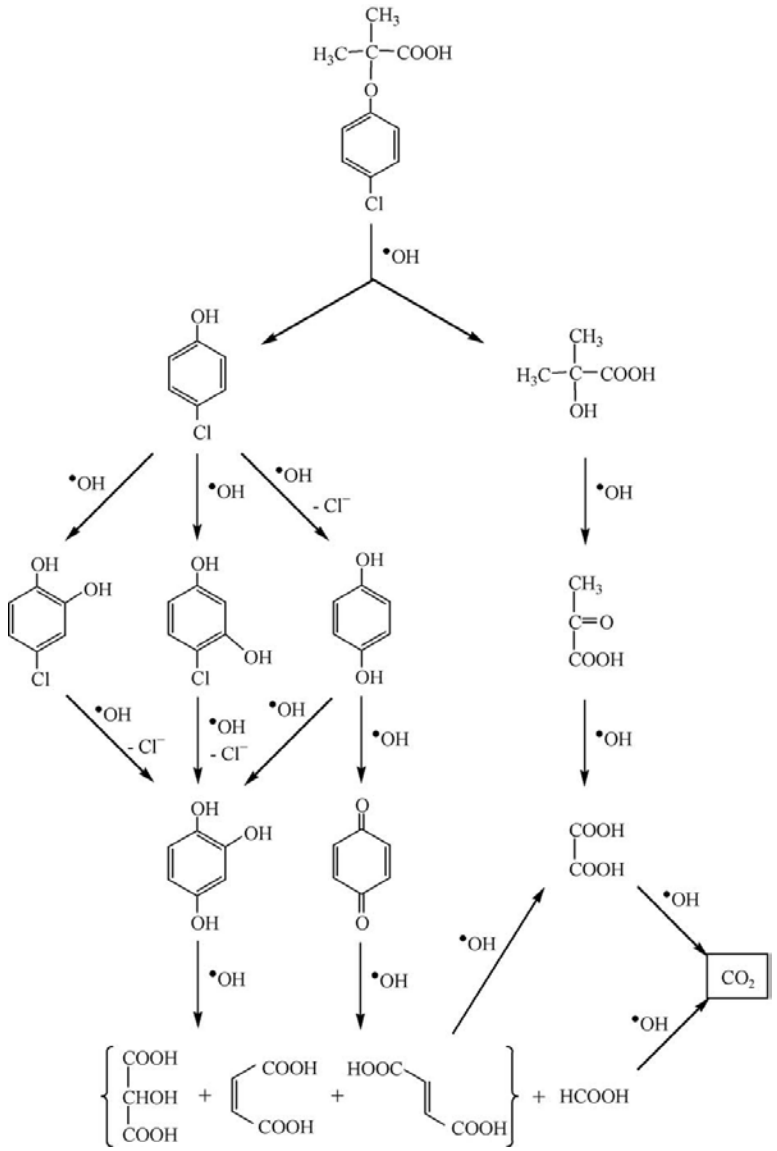

Fig. 11. Proposed reaction sequence for clofibric acid degradation in aqueous medium by anodic oxidation with a Pt or BDD electrode.

solutions is reached (see Fig. 2). Oxalic acid is the most largely accumulated product in both media, although great amounts of pyruvic acid at pH 3.0 and formic and maleic acids at pH 12.0 are also produced.

The balance of carbon content from detected pollutants shown in Figs. 7, 9 and 10 was analyzed and compared with TOC data given in Fig. 1 for 179 mg l^{-1} metabolite solutions of pH 3.0 and 12.0 at 100 mA cm^{-2}. This study allows concluding that the carbon content of solutions degraded with the BDD anode practically corresponds to the remaining initial compound. For example, after 60 min of both treatments, the resulting solutions contain about 73 mg l^{-1} of TOC (see Fig. 1), which can be ascribed to the main presence of ca. 70 mg l^{-1} of carbon coming from clofibric acid, along with minor contribution of 2 and 0.1 mg l^{-1} from 4-chlorophenol and 0.6 and 1.5 mg l^{-1} from oxalic acid at pH 3.0 and 12.0, respectively. A different behavior is found for the Pt anode, where detected aromatics and carboxylic acids lead to high carbon contents while clofibric acid persists. Thus, after 60 min of degradation, the solution TOC is close to 86 mg l^{-1} for both pH 3.0 and 12.0 (see Fig. 1), but only ca. 23 mg l^{-1} of carbon come from clofibric acid and some products significantly contribute to the carbon content,

for example, 4-chlorocatechol (7 mg l^{-1}) and *p*-benzoquinone (11 mg l^{-1}) at pH 3.0 and 2-hydroxyisobutyric acid (15 mg l^{-1}) at pH 12.0. When clofibric acid disappears, 2-hydroxyisobutyric, tartronic and oxalic acids always remain in both media, but at 420 min all carboxylic acids only yield 48 and 25 mg l^{-1} of total carbon at pH 3.0 and 12.0, respectively, values much lower than about 63 mg l^{-1} of TOC found for the resulting solutions (see Fig. 1), thus indicating the formation of large amounts of other undetected products, mainly at pH 12.0.

The above results evidence that different carboxylic acids, mainly oxalic acid (see Fig. 10(b)), and some aromatic intermediates (see Fig. 9(b)) are oxidized on BDD while clofibric acid is destroyed (see Fig. 7(b)). These species are then present in the medium during the degradation process of this metabolite. In contrast, generated carboxylic acids cannot be removed with Pt (see Fig. 10(a)) and then, they remain in the final treated solutions.

3.5. Proposed mineralization pathway

A plausible reaction sequence for the anodic oxidation of clofibric acid in aqueous medium is proposed in Fig. 11. This pathway includes all products detected using Pt and BDD as anodes, but carboxylic acids can only be destroyed on the last electrode, as pointed out above. Electrogenerated $^{\bullet}OH$ is stated as the main oxidant, although the reaction of some organics with other weaker oxidants (ozone, $S_2O_8^{2-}$ and H_2O_2) on BDD is also possible.

The process starts with the breaking of the C(1)–O bond of the metabolite to yield 4-chlorophenol and 2-hydroxyisobutyric acid. 4-Chlorophenol can then undergo a parallel attack of $^{\bullet}OH$ on its C(2)-, C(3)- and C(4)-positions giving 4-chlorocatechol, 4-chlororesorcinol and hydroquinone with loss of chloride ion, respectively. The subsequent hydroxylation with dechlorination of 4-chlorocatechol and 4-chlororesorcinol leads to 1,2,4-benzenetriol. The last product can also be formed from $^{\bullet}OH$ attack on hydroquinone, which is oxidized in parallel to *p*-benzoquinone. Further degradation of 1,2,4-benzenetriol and *p*-benzoquinone yields a mixture of tartronic, maleic, fumaric and formic acids. The three former acids are independently transformed into oxalic acid, which is also generated from the oxidation of the initially electrogenerated 2-hydroxyisobutyric acid via pyruvic acid. The ultimate carboxylic acids, oxalic and formic, are finally converted into CO_2.

4. Conclusions

It has been demonstrated that aqueous solutions of clofibric acid up to close to saturation can be completely mineralized in the pH range 2.0–12.0 by anodic oxidation with BDD in a large variety of experimental conditions due to the efficient production of oxidant $^{\bullet}OH$ by reaction (1) or (2). The removal of solution TOC is practically pH-independent and becomes faster with increasing *j*, although with consumption of more specific charge, because of the higher production of this radical and other weaker oxidants such as ozone, $S_2O_8^{2-}$ and H_2O_2. The increase in temperature favors the degradation rate, indicating that the process is limited, at least partially, by the mass transfer of organics to the BDD surface. Increasing metabolite concentration also enhances the oxidizing power of this anode, since more $^{\bullet}OH$ is able to react with greater amount of pollutants, decreasing the rate of other nonoxidizing reactions of this oxidant. The mineralization current efficiency increases with decreasing j_{app} and with increasing initial metabolite concentration and temperature. Comparative treatment of the same solutions with a Pt anode leads to poor mineralization, although all chloro-organics are destroyed with release of chloride ion, which remains stable in solution. In contrast, this ion is completely oxidized to Cl_2 on BDD. The clofibric acid decay always follows a pseudo-first-order kinetics, being quicker for Pt than for BDD. This evidences a stronger adsorption of the metabolite on the Pt surface that enhances its reaction with electrogenerated $^{\bullet}OH$. The pseudo-rate constant calculated for each anode increases with increasing j_{app} and it is practically independent of pH and initial metabolite concentration. Aromatic products such as 4-chlorophenol, 4-chlorocatechol, 4-chlororesorcinol, hydroquinone, *p*-benzoquinone and 1,2,4-benzenetriol are detected by GC–MS and reversed-phase chromatography. All these intermediates are destroyed with both anodes, although they are more rapidly degraded on BDD. Generated carboxylic acids such as tartronic, maleic, fumaric, formic, 2-hydroxyisobutyric, pyruvic and oxalic are identified by ion-exclusion chromatography. While these acids remain stable in solution using a Pt anode, they are completely mineralized with the BDD one. Most of these species and some aromatic intermediates are simultaneously oxidized with clofibric acid on BDD up to the end of its degradation process.

Acknowledgments

Financial support from MEC (Ministerio de Educación y Ciencia, Spain) under project CTQ2004-01954/BQU is acknowledged. The authors thank DURSI (Departament d'Universitats, Recerca i Societat de la Informació, Generalitat de Catalunya) for the grant given to I. Sirés to do this work.

References

[1] Th. Heberer, H.J. Stan, Int. J. Environ. Anal. Chem. 77 (1997) 113.
[2] T.A. Ternes, Water Res. 32 (1998) 3245.
[3] H.R. Buser, M.D. Muller, N. Theobald, Environ. Sci. Technol. 32 (1998) 188.
[4] C. Zwiener, F.H. Frimmel, Water Res. 34 (2000) 1881.
[5] C.G. Daughton, T.L. Jones-Lepp (Eds.), Pharmaceuticals and Personal Care Products in the Environment, Scientific and Regulatory Issues, Symposium Series 791, American Chemical Society, Washington, 2001.
[6] K. Kümmerer (Ed.), Pharmaceuticals in the Environment. Sources, Fate and Risks, Springer, Berlin, 2001.
[7] D.W. Kolpin, E.T. Furlong, M.T. Meyer, E.M. Thurman, S.D. Zaugg, L.B. Barber, Environ. Sci. Technol. 36 (2002) 1202.
[8] T.A. Ternes, M. Meisenheimer, D. McDowell, F. Sacher, H.J. Brauch, B. Haist-Gulde, G. Preuss, U. Wilme, N. Zulei-Seibert, Environ. Sci. Technol. 36 (2002) 3855.
[9] C. Tixier, H.P. Singer, S. Oellers, S.R. Müller, Environ. Sci. Technol. 37 (2003) 1061.
[10] I.A. Balcioglu, M. Ötker, Chemosphere 50 (2003) 85.

[11] P.E. Stackelberg, E.T. Furlong, M.T. Meyer, S.D. Zaugg, A.K. Henderson, D.B. Reissman, Sci. Total Environ. 329 (2004) 99.
[12] J.P. Bound, N. Vaulvaulis, Chemosphere 56 (2004) 1143.
[13] M. Carballa, F. Omil, J.M. Lema, M. Llompart, C. Garcia-Jares, I. Rodriguez, M. Gomez, T. Ternes, Water Res. 38 (2004) 2918.
[14] B. Marselli, J. García-Gomez, P.A. Michaud, M.A. Rodrigo, Ch. Comninellis, J. Electrochem. Soc. 150 (2003) D79.
[15] A. Kraft, M. Stadelmann, M. Blaschke, J. Hazard. Mater. B 103 (2003) 247.
[16] E. Brillas, I. Sirés, C. Arias, P.L. Cabot, F. Centellas, R.M. Rodríguez, J.A. Garrido, Chemosphere 58 (2005) 399.
[17] M. Panizza, G. Cerisola, Electrochim. Acta 51 (2005) 191.
[18] C. Flox, J.A. Garrido, R.M. Rodríguez, F. Centellas, P.L. Cabot, C. Arias, E. Brillas, Electrochim. Acta 50 (2005) 3685.
[19] M.A. Rodrigo, P.A. Michaud, I. Duo, M. Panizza, G. Cerisola, Ch. Comninellis, J. Electrochem. Soc. 148 (2001) D60.
[20] J. Iniesta, P.A. Michaud, M. Panizza, G. Cerisola, A. Aldaz, Ch. Comninellis, Electrochim. Acta 46 (2001) 3573.
[21] M. Panizza, P.A. Michaud, G. Cerisola, Ch. Comninellis, J. Electroanal. Chem. 507 (2001) 206.
[22] F. Montilla, P.A. Michaud, E. Morallón, J.L. Vázquez, Ch. Comninellis, Electrochim. Acta 47 (2002) 3509.
[23] B. Boye, P.A. Michaud, B. Marselli, M.M. Dieng, E. Brillas, Ch. Comninellis, New Diamond Front. Carbon Technol. 12 (2002) 63.
[24] S. Hattori, M. Doi, E. Takahashi, T. Kurosu, M. Nara, S. Nakamatsu, Y. Nishiki, T. Furuta, M. Iida, J. Appl. Electrochem. 33 (2003) 85.
[25] P. Cañizares, J. García-Gómez, C. Sáez, M.A. Rodrigo, Ind. Eng. Chem. Res. 42 (2003) 956.
[26] G. Lissens, J. Peters, M. Verhaege, L. Pinoy, W. Verstraete, Electrochim. Acta 48 (2003) 1655.
[27] M. Panizza, G. Cerisola, Electrochim. Acta 49 (2004) 3221.
[28] E. Brillas, B. Boye, I. Sirés, J.A. Garrido, R.M. Rodríguez, C. Arias, P.L. Cabot, Ch. Comninellis, Electrochim. Acta 49 (2004) 4487.
[29] P. Cañizares, C. Sáez, J. Lobato, M.A. Rodrigo, Ind. Eng. Chem. Res. 43 (2004) 1944.
[30] C.A. Martinez-Huitle, S. Ferro, A. De Battisti, Electrochim. Acta 49 (2004) 4027.
[31] P. Cañizares, C. Sáez, J. Lobato, M.A. Rodrigo, Electrochim. Acta 49 (2004) 4641.
[32] M. Mitadera, N. Spataru, A. Fujishima, J. Appl. Electrochem. 34 (2004) 249.
[33] P. Cañizares, J. Lobato, R. Paz, M.A. Rodrigo, C. Sáez, Water Res. 39 (2005) 2687.
[34] B. Nasr, G. Abdellatif, P. Cañizares, C. Sáez, J. Lobato, M.A. Rodrigo, Environ. Sci. Technol. 39 (2005) 7234.
[35] X. Chen, G. Chen, Sep. Purif. Technol. 48 (2006) 45.
[36] B. Boye, E. Brillas, B. Marselli, P.A. Michaud, Ch. Comninellis, G. Farnia, G. Sandonà, Electrochim. Acta 51 (2006) 2872.
[37] A. Tauxe-Wuersch, L.F. De Alencastro, D. Grandjean, J. Tarradellas, Water Res. 39 (2005) 1761.
[38] M.A. Oturan, J.J. Aaron, N. Oturan, J. Pinson, Pestic. Sci. 55 (1999) 558.
[39] R. Andreozzi, V. Caprio, R. Marotta, A. Radovnikovic, J. Hazard. Mater. B 103 (2003) 233.
[40] J.L. Packer, J.J. Werner, D.E. Latch, K. McNeill, W.A. Arnold, Aquat. Sci. 65 (2003) 342.
[41] T. Doll, F.H. Frimmel, Water Res. 38 (2004) 955.
[42] C. Zwiener, F.H. Frimmel, Sci. Total Environ. 309 (2003) 201.
[43] J. Frejka, B. Sefránek, J. Zika, Collect. Czech. Chem. Commun. 9 (1937) 238.
[44] F.J. Welcher (Ed.), Standard Methods of Chemical Analysis, vol. 2, 6th ed., RE Krieger Publ. Co., Huntington, New York, 1975, p. 1827 (Part B).
[45] S. Ferro, A. De Battisti, I. Duo, Ch. Comninellis, W. Haenni, A. Perret, J. Electrochem. Soc. 147 (2000) 2614.

8.2.2. Resultats i Discussió / *Results and Discussion*

The variation of TOC with applied specific charge (Q) for the AO treatment of 100 mL of 179 mg L^{-1} clofibric acid solutions in the pH range 2.0-12.0 at 100 mA cm^{-2} and at 35 ºC is analogous to the one described in section 7.3.2 for paracetamol: a quick and continuous TOC decay can be observed for all experiments using BDD, achieving a reduction > 97% at 7 h (i.e., 21 A h L^{-1}) in most media, whereas a slow degradation yielding a maximum mineralization of 30% at 4 h is observed using Pt due to the formation of hardly oxidizable intermediates. Again, the almost pH-independence can be explained by the generation of similar $^{\bullet}OH_{ads}$ concentration from Reactions 5.-44 and 5.-46. It is worth noting that TOC abatement is slightly faster at pH 12.0, and that is the reason why the possible influence of other experimental parameters has been studied at this initial pH value.

The electrolyses of several 100-mL clofibric acid solutions of pH 3.0 and 12.0 containing 100 mg L^{-1} initial TOC, at 33, 100 and 150 mA cm^{-2} and at 35 ºC, show a similar TOC abatement rate for both pH values, thus confirming the aforementioned trend that the degradation of this pharmaceutical and its by-products is practically pH-independent using a BDD anode. However, as described in section 7.3.2, increasing j_{app} causes faster TOC removal with time and more consumption of specific charge for total mineralization, varying from 10 A h L^{-1} (i.e., 10 h) at 33 mA cm^{-2} to 27 A h L^{-1} (i.e., 6 h) at 150 mA cm^{-2}. In addition, an increase in temperature from 25 to 45 ºC, working at pH 12.0 and at 100 mA cm^{-2}, enhances the degradation process, thus decreasing the time required for total mineralization from 10 to 6 h (that is to say, the consumption of specific charge falls from 30 to 18 A h L^{-1}). This trend agrees with the data summarized for paracetamol in section 7.3.

The change in TOC abatement when varying j_{app} and temperature can be explained in terms of the multiple oxidizing agents electrogenerated in these systems, taking

into account that in Na_2SO_4 medium several weak oxidant species such as O_3, $S_2O_8^{2-}$ ions and H_2O_2 can be competitively formed (reactions 4, 5 and 6 in page 218). Reminding the explanation introduced in section 7.3.2, it has been demonstrated that the amount of O_3, H_2O_2 and $S_2O_8^{2-}$ ions is higher as j_{app} increases, attaining a quasi-steady concentration from 4 h of electrolysis. In this study, the difference between the concentration of total oxidizing agents and the concentration of H_2O_2 mainly corresponds to that of $S_2O_8^{2-}$ ions, because O_3 is really unstable and $^{\bullet}OH$ are adsorbed on the BDD surface and are highly reactive too. The faster TOC removal when increasing j_{app} is then due to the greater amount of $^{\bullet}OH_{ads}$ (from Reactions 5.-44 and 5.-46), O_3, H_2O_2 and $S_2O_8^{2-}$ ions generated in the BDD system. When Pt is used as anode no weak oxidizing agents are detected, so the low amount of effective $^{\bullet}OH_{ads}$ is the unique source of oxidant species to remove the pollutants, thus yielding the poor mineralization already discussed. In addition, when T increases from 25 to 45 ºC, a part of the aforementioned agents ($^{\bullet}OH_{ads}$, O_3, H_2O_2 and $S_2O_8^{2-}$ ions) is consumed due to their decomposition and/or their reaction with greater amount of organics. This fact can be related to the improved mineralization process with rising temperature from 25 to 45 ºC. It must be highlighted that the oxidation process is limited, at least partially, by the mass transfer of organics to the BDD surface (see section 7.3.2).

Clofibric acid solutions of pH 12.0 up to close to saturation can be completely mineralized with a BDD anode at 100 mA cm^{-2} and at 35 ºC. A quick and total abatement is reached working in the concentration range 45-557 mg L^{-1} clofibric acid (i.e., 25-313 mg L^{-1} TOC). The Q consumed for overall mineralization gradually increases from 15 to 30 A h L^{-1} (i.e., from 5 to 10 h) as initial TOC rises from 25 to 313 mg L^{-1}. This trend can be related to the existence of more organic matter in solution. It is worth remarking that increasing metabolite concentration causes a quicker TOC abatement: for example, after 2 h of electrolysis (6 A h L^{-1}) 15, 28, 56, 81, 95, 101 and 121 mg L^{-1} of TOC can be removed starting from 25, 50, 100, 150, 200, 250 and 313 mg L^{-1} of TOC, respectively. This gradual enhancement in the oxidizing power of the

BDD anode can be basically accounted for by the reaction of more $^{\bullet}OH_{ads}$ with a greater amount of pollutants, decreasing the amount of this radical wasted in nonoxidizing reactions, such as its decomposition to O_2 and/or its recombination to H_2O_2. Similar TOC-*Q* plots are obtained for the same solutions at pH 3.0.

The generation of inorganic ions studied by ion chromatography reveals the formation of chloride ion, while other chlorine-oxygen ions such as chlorite, chlorate and perchlorate in treated solutions were not detected. Chloride ion evolution for the electrolyses of 100 mL of 179 mg L^{-1} clofibric acid solutions of pH 3.0 and 12.0, at 100 mA cm^{-2} and at 35 ºC, allows concluding that in AO with a Pt anode Cl^- is quickly accumulated at both pH values for 180-240 min, further reaching a quasi-steady concentration of about 29 mg L^{-1}, which is a value practically equal to 29.5 mg L^{-1} corresponding to the chlorine contained in the initial solution. This means that all chloro-organics are definitely destroyed after 5-6 h of electrolysis with Pt, with the release of chloride ion. In contrast, in AO with a BDD anode a maximum concentration of 7 mg L^{-1} at 120 min is attained in both media, further being slowly destroyed to disappear at 420 min. This lack of stability of Cl^- can be explained by its oxidation to Cl_2 gas on BDD, as reported for the electrolysis of NaCl aqueous solutions with this anode [377].

All those previous findings allow establishing that the overall mineralization reaction by AO with a BDD anode involves the consumption of 44 F for each mol of clofibric acid, with chloride ion as primary inorganic ion (Reaction 6.-3). From these considerations, Equation 6.-1 can be applied to determine the MCE values. The efficiency is almost pH-independent (this fact agrees with the pH-indepenence observed in the TOC-*Q* plots previously commented), but it strongly increases when initial clofibric acid and temperature rise, as well as when j_{app} decreases. In fact, MCE-*Q* trends are similar to the ones of paracetamol, although the maximum MCE value for clofibric acid is 22% whereas for paracetamol it is 35%. This difference

clearly explains the interest of studying several molecules to correctly assess the oxidizing ability of BDD anodes, because the nature of each compound and its intermediates modifies the activity of the electrode towards the total mineralization, and this is undoubtedly an interesting factor regarding a possible future scaling-up of the process. Results show a slight increase in efficiency at the early stages of most treatments, which means that a higher amount of pollutants is more easily converted into CO_2. This enhancement in MCE is due to the faster degradation of some by-products that are able to react simultaneously with $^{\bullet}OH_{ads}$, O_3, H_2O_2 and $S_2O_8^{2-}$ ions. A continuous drop in the efficiency with time (i.e., with *Q*) after going through the maximum value is observed, indicating a concomitant decrease in oxidizing ability of the electrolytic system. This trend can be ascribed to the larger proportion of $^{\bullet}OH_{ads}$ oxidized to O_2 at the anode and/or its recombination to H_2O_2, as well as to the continuous formation of more difficultly oxidizable intermediates. Similarly, at constant j_{app} higher efficiencies are obtained as initial concentration of pollutant rises, because of the slower production of such hardly oxidizable intermediates. For example, after 2 h (6 A h L^{-1}) of electrolysis at 100 mA cm^{-2}, increasing MCE values of 2.5%, 4.5%, 8.9%, 13.0%, 16.0%, 17.0% and 20.0% are obtained for 45, 89, 179, 268, 358, 447 and 557 mg L^{-1} clofibric acid, respectively. This tendency also confirms the gradual reaction of higher amount of $^{\bullet}OH_{ads}$ with more pollutants, indicating that this hydroxyl radical is wasted to a smaller extent. Finally, decreasing efficiencies can be observed as j_{app} increases. That means that the mineralization requires a greater electrical consumption (i.e., greater *Q*) because a larger proportion of hydroxyl radical is wasted and furthermore, other weak agents (O_3, H_2O_2 and $S_2O_8^{2-}$ ions) are formed to the detriment of the main oxidant agent $^{\bullet}OH_{ads}$ thus corroborating the idea that AO with BDD is a mass-trasport controlled process, as explained in section 7.3.2. For example, the MCE values at 1 h are 18%, 9.7% and 6.7% at 33, 100 and 150 mA cm^{-2}, respectively.

Regarding the kinetics of clofibric acid decay, the role of the weak oxidizing species has been assessed. Reversed-phase chromatograms for solutions of pH 3.0 and pH 12.0 containing clofibric acid, Na_2SO_4, H_2O_2 and $S_2O_8^{2-}$ show no change in the pharmaceutical content at 35 ºC after 3 h, indicating that this compound does not react with H_2O_2 and $S_2O_8^{2-}$ (they could play a relevant role in the oxidation of some intermediates), so the kinetics can be established on the basis of the reaction between clofibric acid and $^{\bullet}OH_{ads}$. This reaction has been studied by AO with Pt and BDD anodes, by electrolyzing 179 mg L^{-1} clofibric acid solutions of pH 3.0 and 12.0 at different j_{app} values and at 35 ºC. At pH 12.0 clofibric acid disappears from the medium after 420, 360 and 240 min in AO with Pt at 33, 100 and 150 mA cm^{-2}, respectively. However, 540, 420 and 360 min are needed to remove clofibric acid in AO with BDD under comparable experimental conditions. This means that despite the fact that clofibric acid is more slowly mineralized with Pt than with BDD, it is more quickly destroyed and transformed into its intermediates. This is surprising taking into account that BDD anode produces much more reactive $^{\bullet}OH_{ads}$. Then, the greater oxidation ability of clofibric acid on Pt can be ascribed to its higher adsorption on its surface, favoring its reaction with a greater amount of $^{\bullet}OH_{ads}$. These results are opposite to the ones obtained for paracetamol (see Figure 7.-5 in section 7.3.2), which is more quickly destroyed using a BDD anode. These differences reflect the importance of the particularities of each compound and its interactions with the electrode surface. It can be noted that the time required for total destruction of clofibric acid on BDD at each j_{app} is very similar to the time needed for its overall mineralization (10, 7 and 6 h at 33, 100 and 150 mA cm^{-2}), confirming the trend already observed for paracetamol that the initial contaminant persists in the solution up to the end of the degradation process when a BDD anode is used. This is due to a simultaneous degradation of initial compound and its intermediates. AO with Pt and BDD also show a similar destruction rate at both pH values, and this brings to consider that the same electroactive clofibric acid species is oxidized in the pH range tested, probably its unprotonated form since it has a pK_a = 3.18. The concentration

decays are well fitted to a pseudo-first order kinetic equation, exhibiting excellent linear correlations. This suggests that a constant $^{\bullet}OH_{ads}$ concentration, which is much greater than that of the pharmaceutical adsorbed on their surface, is produced at each anode during the electrolysis. From this analysis, an increasing pseudo-first order rate constant (k_1) of 2.4 x 10^{-4}, 4.0 x 10^{-4} and 5.4 x 10^{-4} s^{-1} for Pt, and of 7.2 x 10^{-5}, 1.3 x 10^{-4} and 1.8 x 10^{-4} s^{-1} for BDD is found at 33, 100 and 150 mA cm^{-2}, respectively. These values do not vary proportionally with j_{app}, indicating that a smaller proportion of hydroxyl radical reacts with pollutants when j_{app} rises, since it is progressively more quickly wasted. And finally, the possible influence of initial clofibric acid concentration on its decay kinetics was clarified from electrolyses of clofibric acid solutions of pH 12.0 up to close to saturation, at 35 ºC and 100 mA cm^{-2}, using Pt and BDD. Again, the pharmaceutical is more quickly removed with Pt in all cases, confirming the existence of a greater adsorption on Pt. In addition, the time required for clofibric acid disappearance in AO with BDD is quite close to the time needed for total mineralization. Good linear correlations are obtained for all initial concentrations tested, assuming a pseudo-first order reaction kinetics, and giving average k_1-values of (4.0±0.6) x 10^{-4} s^{-1} for Pt and (1.3±0.1) x 10^{-4} s^{-1} for BDD. This kinetic behavior corroborates the existence of a much greater amount of $^{\bullet}OH_{ads}$ in comparison with the amount of clofibric acid adsorbed on each electrode surface, even working close to saturation.

GC-MS spectra obtained from electrolyses described in section 8.2.1 display three peaks associated with stable aromatic intermediates such as 4-chlorophenol, hydroquinone and *p*-benzoquinone. Reversed-phase chromatograms of the same electrolyzed solutions, using Pt and BDD, allow defining the evolution of these three compounds, as well as the evolution of 4-chlorocatechol, 4-chlororesorcinol and 1,2,4-benzenetriol. For AO with a Pt anode, a much greater accumulation of aromatic intermediates can be observed at pH 3.0 (at pH 12.0 only a reduced number of intermediates are detected, exhibiting lower amounts and shorter times).

1,2,4-Benzenetriol, 4-chlorocatechol and *p*-benzoquinone persist for 420 min after reaching maximum contents equal to 4.5, 13.0 and 13.2 mg L^{-1} at about 60 min, and 4-chlorophenol, 4-chlororesorcinol and hydroquinone disappear after 240 min. The results for AO with a BDD anode show that only 4-chlorophenol and *p*-benzoquinone are accumulated to a certain extent, being present in the medium up to 420 min at pH 3.0 (a time similar to that of clofibric acid disappearance), and up to 240 min at pH 12.0, but they reach lower concentrations than using Pt. In conclusion, all the aromatics generated during the electrolysis can be destroyed using both anodes, although they are more quickly transformed using a BDD anode, thus confirming the 'simultaneous degradation' ability of this anode towards all the compounds present in the treated solution, as pointed out in section 7.3.2.

Ion-exclusion chromatograms of the above electrolyzed solutions reveal the accumulation of several carboxylic acids: tartronic, maleic, fumaric and formic acids, that can be formed from the oxidative breaking of the benzenic moiety of aromatic intermediates, along with 2-hydroxyisobutyric and oxalic acids. 2-hydroxyisobutyric acid is expected to be released when 4-chlorophenol is generated from clofibric acid, and an electrolysis with BDD at 100 mA cm^{-2} shows that it is degraded to oxalic acid. This latter acid can also be formed from the degradation of tartronic, maleic and fumaric acids previously identified. Oxalic and formic acids are finally converted into CO_2. The evolution curves of carboxylic acids depend on both pH and anode tested. Large amounts of carboxylics are slowly accumulated using Pt, without apparent degradation, as expected from the quite low mineralization achieved with such an anode. Tartronic, 2-hydroxyisobutyric and oxalic acids are the main carboxylic acids in both media for AO with a Pt anode. In contrast, all the carboxylic acids have disappeared after 420 min when BDD is used, according to the time needed for the overall mineralization with this anode. Oxalic acid is the main carboxylic acid in both media.

Once the product analysis has been finished, it is interesting to check the balance of carbon content from initial compound and detected intermediates, and compare it with TOC values at pH 3.0 and 12.0. It is obvious that the TOC measured during electrolyses with BDD mainly corresponds to the remaining clofibric acid, because very small amounts of aromatic and carboxylic intermediates are found using this anode. Only minor contribution of 4-chlorophenol and oxalic acid are worth mentioning, and they are present uniquely during the degradation process of the pharmaceutical. Pt shows a different behavior, because intermediates lead to high carbon contents while clofibric acid persists, and further on. For example, after 60 min the solution TOC is close to 86 mg L^{-1} in both media, but only ca. 23 mg L^{-1} carbon come from clofibric acid because 4-chlorocatechol and *p*-benzoquinone amounts are equivalent to 7 mg L^{-1} and 11 mg L^{-1} carbon at pH 3.0, respectively, and 2-hydroxyisobutyric acid is equivalent to 15 mg L^{-1} at pH 12.0. However, at 420 min all carboxylic acids in the solution only yield 48 and 25 mg L^{-1} of total carbon at pH 3.0 and 12.0, respectively, values much lower than 63 mg L^{-1} of TOC given in TOC-*Q* plots, meaning that large amounts of other products are formed, mainly at pH 12.0.

Considering all the intermediates reported above, a plausible reaction scheme for the AO of clofibric acid in aqueous medium is proposed, reminding that carboxylic acids can only be destroyed using BDD, and accepting $^{\bullet}OH_{ads}$ as the main oxidizing agent. This radical firstly breaks the C(1)-O bond of clofibric acid, yielding 4-chlorophenol and 2-hydroxyisobutyric acid. Subsequent attack of $^{\bullet}OH_{ads}$ on *orto-*, *meta-* and *para-*position of 4-chlorophenol (regarding –OH) releases 4-chlorocatechol, 4-chlororesorcinol and hydroquinone, respectively. Hydroquinone formation is simultaneous to chloride ion release. Hydroxylation of 4-chlorocatechol and 4-chlororesorcinol gives 1,2,4-benzenetriol with loss of chloride ion, whereas hydroquinone can be hydroxylated to form 1,2,4-benzenetriol too, or can be oxidized to *p*-benzoquinone. Further degradation of the latter two compounds yields a mixture of tartronic, maleic, fumaric and formic acids. The former three acids are

transformed into oxalic acid, which is also generated from the oxidation of the initially electrogenerated 2-hydroxyisobutyric acid. In AO with BDD anode, the ultimate carboxylic acids, oxalic and formic acids, are finally converted into CO_2, and Cl^- is oxidized to Cl_2.

The coloration observed for Pt/steel and BDD/steel systems is analogous to the one commented in section 7.3.2 for the AO of paracetamol. All solutions treated with BDD anode always remain colorless because of the overall destruction of soluble polyaromatic products. In contrast, the degradation with Pt causes a change in color, being pale pink after 5 min, orange at about 1 h, dark-brown at ca. 2 h and yellow at approximately 4 h, further being slowly decolorized up to become colorless after 6 h of treatment. A gradual pH decay with electrolysis time is found for solutions starting at pH ≥ 4.0 due to the formation of carboxylic acids, so continuous regulation within a range of ±0.03 units is carried out by adding small volumes of 0.1 M NaOH.

8.3. TRACTAMENT MITJANÇANT ELECTRO-FENTON I FOTOELECTRO-FENTON / *TREATMENT BY ELECTRO-FENTON AND PHOTOELECTRO-FENTON*

8.3.1. Finalitat del treball / *Aim of the work*

The complete mineralization of aqueous solutions of clofibric acid up to close to saturation in the pH range 2.0-12.0 has been just described by AO with BDD in a large variety of experimental conditions, so this is certainly an interesting option to be taken into account regarding wastewaters where the presence of such a pharmaceutical is described. Immediately, a question can be posed: would EF and PEF processes be a feasible alternative compared to AO with BDD? Could coupling between BDD anode and O_2-diffusion cathode even enhance the oxidizing ability of AO with BDD and PEF with Pt? In order to analyze critically the situation on the basis of well verified data, EF and PEF processes were applied using an O_2-diffusion cathode and Pt or BDD as anode, all of them with an area of 3 cm^2. Both EF and PEF treatments were always performed by adding 1.0 mM Fe^{2+} (chosen as the optimal concentration, as pointed out in section 7.2.2) and 0.05 M Na_2SO_4 to the solution at the beginning of the electrolyses. All trials were carried out at 35 ºC, which is the maximum temperature allowed without significant water evaporation from solution. Similarly, treatments by AO with electrogenerated H_2O_2 but in the absence of Fe^{2+} were carried out to underline the effectivity of the $^{\bullet}OH$ produced from Fenton's reaction in EF and PEF.

Comparative electrolyses were initially made for 100-mL solutions of pH 3.0 containing 179 mg L^{-1} clofibric acid (i.e., 100 mg L^{-1} TOC) at 100 mA cm^{-2}, using Pt or BDD as anode. Note that the electrolytic system continuously produces H_2O_2 from bielectronic reduction of O_2 at the O_2-diffusion cathode. The use of this system without catalyst corresponds to the method of AO with electrogenerated H_2O_2. Then, the same experiments were done with UVA irradiation. Later, 1.0 mM Fe^{2+} was used

as catalyst without (EF) or with (PEF) UVA illumination to test the oxidation ability of all these processes.

Ion chromatograms for the above treated solutions by AO without H_2O_2 electrogeneration, EF and PEF were recorded to study the evolution of inorganic ions released from initial chlorine of the pharmaceutical.

Afterwards, the effect of pH, current density and metabolite concentration on the oxidizing power of PEF with Pt and EF with BDD was investigated from TOC decay and MCE calculation in order to clarify the optimum operative conditions. These two processes were selected because they provide overall mineralization, and EF with BDD in particular was considered to be more suitable than PEF because its slower TOC abatement allows a better understanding and critical analysis of the differences observed. Firstly, the influence of pH was studied in the pH range 2.0-6.0 under the experimental conditions pointed out above. Secondly, several solutions of pH 3.0 with 179 mg L^{-1} of the metabolite were electrolyzed at 33, 100 and 150 mA cm^{-2} to assess the effect of current density. And finally, the great oxidizing power of these two methods was studied by degrading solutions containing 89, 179, 358 and 557 (close to saturation) mg L^{-1} of clofibric acid at pH 3.0 and at 100 mA cm^{-2}.

The decay of the pharmaceutical in the four electrochemical methods (AO without and with UVA irradiation, EF and PEF) was followed by reversed-phase HPLC chromatography using a Pt anode or a BDD anode. As stated in section 8.2.1, first of all it was necessary to clarify whether clofibric acid can be oxidized with other weaker oxidizing species generated along the electrolysis. A previous chemical test was carried out by adding 20 mM H_2O_2 and 0.05 M Na_2SO_4 to a 100-mL solution of pH 3.0 containing 179 mg L^{-1} clofibric acid, because H_2O_2 is certainly the most concentrated of the weaker oxidizing agents formed due to the notorious accumulation already discussed in section 7.2.1 (see Figure 7.-2). After this, the

comparative kinetics of clofibric acid decay by its reaction with $^{\bullet}OH$ in the bulk solution and $^{\bullet}OH_{ads}$ in the electrode surface was determined by electrolyzing 179 mg L^{-1} of the pharmaceutical with 1.0 mM Fe^{2+} at pH 3.0 and at 100 mA cm^{-2} for the four processes mentioned using each anode. The influence of j_{app} on clofibric acid decay was further studied for PEF with Pt and EF with BDD, by electrolyzing 100-mL solutions of pH 3.0 with 179 mg L^{-1} clofibric acid, at 33, 100 and 150 mA cm^{-2}. Lastly, the role of initial clofibric acid concentration on its decay kinetics was clarified for PEF with Pt alone from electrolyses of different solutions of pH 3.0 containing 89, 179, 358 and 557 mg L^{-1} of pharmaceutical at 100 mA cm^{-2}.

To help identifying aromatic intermediates, a 100-mL solution of pH 3.0 containing 179 mg L^{-1} of clofibric acid was electrolyzed by EF using Pt and BDD with 1.0 mM Fe^{2+} at 100 mA cm^{-2} and at 35 °C for 2 min, and after some preparatives (see section 6.3) the remaining intermediates were analyzed by GC-MS. Similarly, to identify the final carboxylic acids, the above solution was treated under the same EF conditions for 6 h, further evaporating it at low pressure and dissolving the remaining solid in ethanol to characterize the esterified acids by GC-MS. Reversed-phase chromatograms and ion-exclusion chromatograms were obtained to follow the evolution of the corresponding aromatic and carboxylic acid intermediates by AO, EF and PEF with Pt or BDD under the conditions already described above for GC-MS.

Considering all the intermediates that were identified, plausible reaction sequences for the degradation of clofibric acid by EF and PEF with 1.0 mM Fe^{2+} and/or UVA light as catalysts were proposed.

The thorough results of this section are included in the following papers (Paper 5-6):

5. Sirés, I., Arias, C., Cabot, P.L., Centellas, F., Garrido, J.A., Rodríguez, R.M., Brillas, E., Degradation of clofibric acid in acidic aqueous medium by electro-Fenton and photoelectro-Fenton. *Chemosphere*, doi:10.1016/j.chemosphere.2006.07.039.

6. Sirés, I., Garrido, J.A., Centellas, F., Rodríguez, R.M., Cabot, P.L., Arias, C., Brillas, E., Mineralization of clofibric acid by electrochemical advanced oxidation processes using a boron-doped diamond anode and Fe^{2+} and UVA light as catalysts. *Appl. Catal. B: Environ.* (submitted)

The following presentation in a congress is related to this work:

F. Sirés, I., Garrido, J.A., Centellas, F., Rodríguez, R.M., Cabot, P.L., Arias, C., Brillas, E., Clofibric acid mineralization by electrochemical advanced oxidation processes using a boron-doped diamond anode and cathodically generated H_2O_2 with Fe^{2+} and UVA light as catalysts, Vol. 1, page 152, EAAOP-1: Environmental Applications of Advanced Oxidation Processes. Technical University of Crete and Aristotle University of Thessaloniki, Chania, Greece, 7-9 September 2006. (Poster presentation)

UNIVERSITAT DE BARCELONA

ARTICLE 5 / *PAPER 5*

Degradation of clofibric acid in acidic aqueous medium by electro-Fenton and photoelectro-Fenton

ARTICLE IN PRESS

ELSEVIER

Chemosphere xxx (2006) xxx–xxx

CHEMOSPHERE

www.elsevier.com/locate/chemosphere

Degradation of clofibric acid in acidic aqueous medium by electro-Fenton and photoelectro-Fenton

Ignasi Sirés, Conchita Arias, Pere Lluís Cabot, Francesc Centellas, José Antonio Garrido, Rosa María Rodríguez, Enric Brillas *

Laboratori d'Electroquímica dels Materials i del Medi Ambient, Departament de Química Física, Facultat de Química, Universitat de Barcelona, Martí i Franquès 1-11, 08028 Barcelona, Spain

Received 28 April 2006; received in revised form 17 July 2006; accepted 18 July 2006

Abstract

Acidic aqueous solutions of clofibric acid (2-(4-chlorophenoxy)-2-methylpropionic acid), the bioactive metabolite of various lipid-regulating drugs, have been degraded by indirect electrooxidation methods such as electro-Fenton and photoelectro-Fenton with Fe^{2+} as catalyst using an undivided electrolytic cell with a Pt anode and an O_2-diffusion cathode able to electrogenerate H_2O_2. At pH 3.0 about 80% of mineralization is achieved with the electro-Fenton method due to the efficient production of oxidant hydroxyl radical from Fenton's reaction between Fe^{2+} and H_2O_2, but stable Fe^{3+} complexes are formed. The photoelectro-Fenton method favors the photodecomposition of these species under UVA irradiation, reaching more than 96% of decontamination. The mineralization current efficiency increases with rising metabolite concentration up to saturation and with decreasing current density. The photoelectro-Fenton method is then viable for treating acidic wastewaters containing this pollutant. Comparative degradation by anodic oxidation (without Fe^{2+}) yields poor decontamination. Chloride ion is released during all degradation processes. The decay kinetics of clofibric acid always follows a pseudo-first-order reaction, with a similar rate constant in electro-Fenton and photoelectro-Fenton that increases with rising current density, but decreases at greater metabolite concentration. 4-Chlorophenol, 4-chlorocatechol, 4-chlororesorcinol, hydroquinone, *p*-benzoquinone and 1,2,4-benzenetriol, along with carboxylic acids such as 2-hydroxyisobutyric, tartronic, maleic, fumaric, formic and oxalic, are detected as intermediates. The ultimate product is oxalic acid, which forms very stable Fe^{3+}-oxalato complexes under electro-Fenton conditions. These complexes are efficiently photodecarboxylated in photoelectro-Fenton under the action of UVA light.

Keywords: Drug mineralization; Electro-Fenton; Photoelectro-Fenton; Catalysis; Water treatment

1. Introduction

There is great interest in the environmental relevance of pharmaceutical drugs and their metabolites as emerging pollutants in waters (Daughton and Jones-Lepp, 2001; Kümmerer, 2001; Heberer, 2002; Kolpin et al., 2002; Heberer and Adam, 2004; Weigel et al., 2004; Tauxe-Wuersch et al., 2005). Different anti-inflammatories, analgesics, betablockers, lipid regulators, antimicrobials, antiepileptics and estrogens have been detected in sewage treatment plant effluents, surface and ground waters and even in drinking water at concentrations usually ranging from ng l^{-1} to μg l^{-1}. The sources of this pollution involve emission from production sites, direct disposal of overplus drugs in households, excretion after drug administration to humans and animals, treatments throughout the water in fish and other animal farms and inadequate treatment of manufacturing waste. Among these compounds, clofibric acid (2-(4-chlorophenoxy)-2-methylpropionic acid, **1**) has long term persistence in the environment. It is the bioactive metabolite of clofibrate, etofibrate and etofyllineclofibrate, which are drugs widely used as blood lipid regulators with therapeutic doses of about 1–2 g d^{-1} per person, since they decrease the

* Corresponding author. Tel.: +34 93 4021223; fax: +34 93 4021231.
E-mail address: brillas@ub.edu (E. Brillas).

0045-6535/$ - see front matter © 2006 Elsevier Ltd. All rights reserved.
doi:10.1016/j.chemosphere.2006.07.039

Please cite this article as: Ignasi Sirés et al., Degradation of clofibric acid in acidic aqueous medium ..., Chemosphere (2006), doi:10.1016/j.chemosphere.2006.07.039.

plasmatic concentration of cholesterol and triglycerides (Buser et al., 1998; Tauxe-Wuersch et al., 2005). Concentrations of **1** up to 10 μg l^{-1} have been detected in sewage treatment plant influents and effluents and in rivers, lakes, North Sea, ground and drinking waters (Heberer and Stan, 1997; Buser et al., 1998; Ternes, 1998; Tixier et al., 2003).

To avoid the potential adverse health effects of drugs and their metabolites as water pollutants on both humans and animals, research efforts are underway to develop efficient techniques for achieving their total destruction (Zwiener and Frimmel, 2000; Doll and Frimmel, 2004). However, **1** is poorly degraded by oxidation methods such as ozonolysis (Ternes et al., 2002; Andreozzi et al., 2003), H_2O_2/UV (Andreozzi et al., 2003), sunlight and UV photolysis (Packer et al., 2003) and TiO_2/UV (Doll and Frimmel, 2004), as well as after application of different biological and physico-chemical methods in sewage treatment plants (Tauxe-Wuersch et al., 2005). More potent oxidation procedures are then needed to be applied to destroy this compound in wastewaters.

Recently, indirect electrooxidation methods such as electro-Fenton and photoelectro-Fenton are being developed for wastewater remediation. In these environmentally clean electrochemical techniques, hydrogen peroxide is continuously generated in an acidic contaminated solution from the two-electron reduction of O_2 at reticulated vitreous carbon (Xie and Li, 2006), mercury pool (Ventura et al., 2002), carbon-felt (Oturan et al., 1999; Gözmen et al., 2003; Hanna et al., 2005; Irmak et al., 2006) and O_2-diffusion (Boye et al., 2002; Brillas et al., 2004a,b; Sirés et al., 2006) cathodes:

$$O_2 + 2H^+ + 2e^- \rightarrow H_2O_2 \quad (1)$$

The oxidizing power of H_2O_2 is enhanced in the electro-Fenton method by adding small amounts of Fe^{2+} as catalyst to the acidic solution. Hydroxyl radical (·OH) and Fe^{3+} are then generated from the classical Fenton's reaction between Fe^{2+} and H_2O_2 (Sun and Pignatello, 1993):

$$Fe^{2+} + H_2O_2 \rightarrow Fe^{3+} + {}^{\cdot}OH + OH^- \quad (2)$$

Reaction (2) is propagated from Fe^{2+} regeneration, which mainly occurs by reduction of Fe^{3+} species at the cathode (Oturan et al., 1999). ·OH acts as a non-selective, strong oxidant, with ability to react with organics yielding dehydrogenated or hydroxylated derivatives until their overall mineralization (conversion into CO_2, water and inorganic ions). In the photoelectro-Fenton process the solution is irradiated with UVA light to favor: (i) the photodecomposition of complexes of Fe^{3+} with generated carboxylic acids (Zuo and Hoigné, 1992; Brillas et al., 2004a,b; Sirés et al., 2006) and (ii) the regeneration of Fe^{2+} from additional photoreduction of $Fe(OH)^{2+}$, which is the predominant Fe^{3+} species in acid medium (Sun and Pignatello, 1993):

$$Fe(OH)^{2+} + h\nu \rightarrow Fe^{2+} + {}^{\cdot}OH \quad (3)$$

Reaction (3) also enhances the production of ·OH and hence, the mineralization of organics.

The electro-Fenton treatment of 100-ml solutions with 1 mM of **1** and 2 mM Fe^{2+} in 0.01 M HCl has been previously reported by Oturan et al. (1999), but these authors only described its decay kinetics and the detection of some initial aromatic products. To show the possible viability of the electro-Fenton and photoelectro-Fenton methods to remove this metabolite in wastewaters, we have carried out a detailed study on the degradation of acidic aqueous solutions of **1** in the pH range 2.0–6.0 using 1.0 mM Fe^{2+} in both procedures. Comparative treatments in the absence of this catalyst were also made to demonstrate the positive oxidation action of ·OH formed from reaction (2). The effect of current density and clofibric acid concentration on the degradation process and current efficiency was explored. Aromatic products were identified by gas chromatography–mass spectrometry (GC–MS). The decay of **1** and the evolution of its by-products were followed by chromatographic techniques. The results obtained in this study are reported herein.

2. Experimental

2.1. Chemicals

Clofibric acid (**1**), 4-chlorophenol (**2**), hydroquinone (**3**), 4-chlororesorcinol (**4**), *p*-benzoquinone (**6**), 1,2,4-benzenetriol (**7**), 2-hydroxyisobutyric acid (**9**), tartronic acid (**10**), maleic acid (**11**), fumaric acid (**12**), formic acid (**13**) and oxalic acid (**14**) were either reagent or analytical grade from Sigma-Aldrich, Merck, Panreac and Avocado. 4-Chlorocatechol (**5**) was synthesized by chlorination of pyrocatechol with SO_2Cl_2 at room temperature, as reported elsewhere (Boye et al., 2002). Analytical grade sulfuric acid was purchased from Merck. Anhydrous sodium sulfate and heptahydrated ferrous sulfate were analytical grade from Fluka. All solutions were prepared with pure water obtained from a Millipore Milli-Q system with resistivity >18 MΩ cm at 25 °C. Organic solvents and other chemicals employed were either HPLC or analytical grade from Panreac.

2.2. Apparatus and analysis procedures

The solution pH was measured with a Crison 2000 pH-meter. Electrolyses were carried out at a constant current density (*j*) of 33, 100 and 150 mA cm^{-2} with an Amel 2053 potentiostat–galvanostat. All samples withdrawn from treated solutions were filtered with Whatman 0.45 μm PTFE filters before analysis. The mineralization of each solution of **1** was monitored by the abatement of its total organic carbon (TOC), determined on a Shimadzu VCSN TOC analyzer. Reproducible TOC values were obtained from analysis of 100-μl aliquots using the standard non-purgeable organic carbon method. From these data, the mineralization current efficiency (MCE) for elec-

Please cite this article as: Ignasi Sirés et al., Degradation of clofibric acid in acidic aqueous medium ..., Chemosphere (2006), doi:10.1016/j.chemosphere.2006.07.039.

trolyzed solutions at a given time t was calculated as follows:

$$\mathrm{MCE} = \frac{\Delta(\mathrm{TOC})_{\mathrm{exp}}}{\Delta(\mathrm{TOC})_{\mathrm{theor}}} \times 100 \quad (4)$$

where $\Delta(\mathrm{TOC})_{\mathrm{exp}}$ is the experimental TOC removal and $\Delta(\mathrm{TOC})_{\mathrm{theor}}$ is the theoretically calculated TOC decay assuming that the applied electrical charge (=current × time) is only consumed in the mineralization process of **1**.

The decay of **1** and the evolution of aromatic intermediates were followed by reversed-phase chromatography using a Waters 600 HPLC liquid chromatograph fitted with a Spherisorb ODS2 5 μm, 150 × 4.6 mm (i.d.), column at room temperature, and coupled with a Waters 996 photodiode array detector, controlled through a Millennium-32® program. For each compound, this detector was selected at the maximum wavelength of its UV-absorption band. These analyses were made by injecting 20-μl aliquots into the chromatograph and circulating a 50:47:3 (v/v/v) methanol/phosphate buffer (pH = 2.5)/pentanol mixture at 1.0 ml min^{-1} as mobile phase. Generated carboxylic acids were followed by ion-exclusion chromatography by injecting 20-μl samples into the above HPLC chromatograph fitted with a Bio-Rad Aminex HPX 87 H, 300 × 7.8 mm (i.d.), column at 35 °C. For these measurements, the photodiode detector was selected at 210 nm and the mobile phase was 4 mM H_2SO_4 at 0.6 ml min^{-1}. Cl^- concentration in electrolyzed solutions was determined by ion chromatography using a Shimadzu 10Avp HPLC chromatograph fitted with a Shim-Pack IC-A1S, 100 × 4.6 mm (i.d.), anion column at 40 °C and coupled with a Shimadzu CDD 10Avp conductivity detector. These measurements were carried out with a 2.5 mM phtalic acid and 2.4 mM *tris*(hydroxymethyl)aminomethane solution of pH 4.0 as mobile phase at 1.5 ml min^{-1}.

A 100 ml-solution with 179 mg l^{-1} of **1** of pH 3.0 was electrolyzed at 100 mA cm^{-2} and at 35.0 °C by electro-Fenton with 1.0 mM Fe^{2+} for 2 min. The resulting organics were extracted with 45 ml of CH_2Cl_2 in three times. The collected organic solution was dried with anhydrous Na_2SO_4, filtered and evaporated to about 2 ml. The remaining products were separated and identified by GC–MS using a Hewlett-Packard 5890 Series II gas chromatograph fitted with a HP-5 0.25 μm, 30 m × 0.25 mm (i.d.), column, and a Hewlett-Packard 5989 A mass spectrophotometer operating in EI mode at 70 eV. The temperature ramp for this column was 35 °C for 2 min, 10 °C min^{-1} up to 320 °C and hold time 5 min, and the temperature of the inlet, transfer line and detector was 250 °C, 250 °C and 290 °C, respectively. To identify the final carboxylic acids, the above solution was treated under the same electro-Fenton conditions for 6 h. The resulting solution was evaporated at low pressure and the remaining solid was dissolved in 2 ml of ethanol. The esterified acids were further analyzed by GC–MS using the gas chromatograph fitted with a HP-INNOWax 0.25 μm, 30 m × 0.25 mm (i.d.), column. In this case the temperature ramp was 35 °C for 2 min, 10 °C min^{-1} up to 250 °C and hold time 15 min, and the temperature of the inlet, transfer line and detector was always 250 °C.

2.3. Electrolytic system

All electrolyses were conducted in an open, undivided and thermostated cylindrical cell containing 100 ml of solution stirred with a magnetic bar. The anode was a 3-cm^2 Pt sheet of 99.99% purity from SEMPSA and the cathode was a 3-cm^2 carbon-PTFE electrode from E-TEK, which was fed with pure O_2 at 12 ml min^{-1} to generate continuously H_2O_2 from reaction (1). The electrolytic setup and the preparation of the O_2-diffusion cathode have been described (Boye et al., 2002). For the experiments with UVA irradiation, a Philips 6 W fluorescent black light blue tube was placed at 7 cm above the solution. The tube emitted UVA light in the wavelength region between 300 and 420 nm, with $\lambda_{\mathrm{max}} = 360$ nm, supplying a photoionization energy input to the solution of 140 μW cm^{-2}, detected with a NRC 820 laser power meter working at 514 nm. Both electro-Fenton and photoelectro-Fenton treatments were performed after addition of 1.0 mM Fe^{2+} to the solution. All trials were carried out at 35.0 °C, which is the maximum temperature to work with the open electrolytic cell without significant water evaporation from solution (Boye et al., 2002).

3. Results and discussion

3.1. Comparative degradation

Comparative electrolyses at 100 mA cm^{-2} for 6 h were initially made for solutions containing 179 mg l^{-1} of **1** (equivalent to 100 mg l^{-1} of TOC) and 0.05 M Na_2SO_4 regulated with H_2SO_4 at pH 3.0 and at 35.0 °C. In these experiments the solution pH remained practically constant, reaching final values between 2.8 and 3.0. The change in solution TOC with consumed specific charge (Q, in A h l^{-1}) for such trials is depicted in Fig. 1a. Note that the electrolytic system produces continuously hydrogen peroxide from reaction (1), whereas adsorbed ·OH is formed at the Pt anode from water oxidation (Boye et al., 2002; Brillas et al., 2004a,b; Sirés et al., 2006):

$$H_2O \rightarrow {\cdot}OH_{ads} + H^+ + e^- \quad (5)$$

The use of this system without catalyst corresponds to the method of anodic oxidation with electrogenerated H_2O_2. Fig. 1a shows that this procedure gives a quite slow TOC removal, attaining 41% of mineralization at 6 h (Q = 18 A h l^{-1}). This behavior can be accounted for by the low concentration of ·OH formed at the Pt surface from reaction (5), which is the main oxidant of **1** and its by-products. A similar degradation rate can be seen in Fig. 1a when the solution without catalyst is illuminated with UVA light, yielding 39% of TOC decay at the end of electrolysis. This brings to consider that organics are not directly photode-

Please cite this article as: Ignasi Sirés et al., Degradation of clofibric acid in acidic aqueous medium ..., Chemosphere (2006), doi:10.1016/j.chemosphere.2006.07.039.

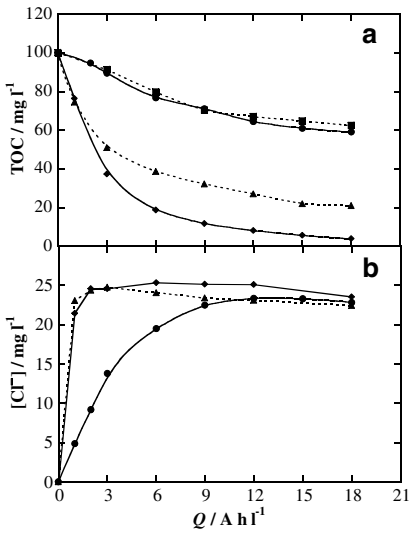

Fig. 1. (a) Total organic carbon and (b) concentration of accumulated chloride ion vs. specific charge for the degradation of 100-ml solutions with 179 mg l^{-1} clofibric acid (**1**) and 0.05 M Na_2SO_4 of pH 3.0 at 100 mA cm^{-2} and at 35.0 °C using an undivided cell with a 3-cm^2 Pt anode and a 3-cm^2 carbon-PTFE O_2-diffusion cathode. Method: (●) anodic oxidation with electrogenerated H_2O_2; (■) anodic oxidation with electrogenerated H_2O_2 under a 6-W UVA irradiation with $\lambda_{max} = 360$ nm; (▲) electro-Fenton with 1.0 mM Fe^{2+} in the solution; (♦) photoelectro-Fenton with 1.0 mM Fe^{2+} and UVA light.

composed by UVA light. A different behavior can be observed in Fig. 1a when 1.0 mM Fe^{2+} is added as catalyst. For the electro-Fenton process, TOC is rapidly reduced by 79% at 6 h due to the fast reaction of organics with the great amounts of ·OH produced from Fenton's reaction (2). In contrast, the photoelectro-Fenton process leads to quicker TOC decay with almost overall mineralization (>96% TOC removal) at the end of electrolysis. This trend can be related to: (i) the rapid photolysis of some stable complexes of Fe^{3+} with generated carboxylic acids under electro-Fenton conditions (Zuo and Hoigné, 1992; Brillas et al., 2004a; Sirés et al., 2006) and/or (ii) the enhanced generation of ·OH from additional photoreduction of $Fe(OH)^{2+}$ from reaction (3). Note that the starting pale yellow solution changed to pale orange color at the end of both electro-Fenton and photoelectro-Fenton degradations. This is indicative of the formation of soluble colored polyaromatics in small extent, which can be not be destroyed by oxidant ·OH produced by reactions (2), (3) and (5).

Mineralization of **1** is accompanied by its overall dechlorination. Ion chromatograms for the above treated solutions only displayed a defined peak related to Cl^- ion. No other chlorine–oxygen ions such as ClO_3^- and ClO_4^- were detected by this technique. Fig. 1b shows a gradual accumulation of Cl^- up to 23 mg l^{-1} for 4 h ($Q = 12$ A h l^{-1}) by anodic oxidation with electrogenerated H_2O_2, whereas for electro-Fenton and photoelectro-Fenton, a Cl^- concentration of about 25 mg l^{-1} is already attained at 40 min ($Q = 2$ A h l^{-1}), whereupon it undergoes a slight drop due to its oxidation to Cl_2 at the Pt anode. These findings indicate that chloro-organics are always degraded with release of Cl^-, although they are much more rapidly destroyed in the two last methods. However, all procedures only lead to the release of 78–85% of the initial chlorine content of **1** (29.5 mg l^{-1}), suggesting that stable colored polyaromatics formed during degradation contain the remaining chlorine.

These results indicate that electro-Fenton only yields partial decontamination of **1**, whereas this pollutant can be almost completely mineralized by photoelectro-Fenton. For this last technique, the effect of pH, current density and metabolite concentration on its oxidizing power was investigated to clarify its optimum operative conditions.

3.2. Effect of experimental parameters on the photoelectro-Fenton process

The TOC–Q plots obtained for solutions of 179 mg l^{-1} of **1** in the pH range 2.0–6.0 degraded by photoelectro-Fenton at 100 mA cm^{-2} are depicted in Fig. 2a. The pH of solutions with initial pH 4.0 and 6.0 underwent a progressive decrease with time, mainly during the first hour of electrolysis, due to the generation of acid products and for this reason, it was continuously regulated within a range of ±0.3 units by adding 1 M NaOH. Fig. 2a shows that the quickest TOC decay takes place starting from pH 3.0, whereas for the other solutions, the degradation rate falls in the order pH 2.0 > pH 4.0 ≫ pH 6.0. This behavior can be associated with the highest generation rate of the main oxidant ·OH from Fenton's reaction (2), since its optimum pH is 2.8 (Sun and Pignatello, 1993), very close to pH 3.0 where **1** and its by-products are more rapidly destroyed.

The influence of current density on the oxidation ability of this method was examined by electrolyzing solutions with 179 mg l^{-1} of **1** of pH 3.0 at 33, 100 and 150 mA cm^{-2}. As can be seen in Fig. 2b, a progressive increase in Q from 7 to 27 A h l^{-1} for achieving total decontamination takes place when j increases. However, the time needed for overall mineralization drops from 7 h at 33 mA cm^{-2} to 5.5 h at 150 mA cm^{-2}. The faster mineralization rate with time when j raises can be ascribed to a greater production of ·OH at the Pt anode from reaction (5) and in the medium from reaction (2) due to the electrogeneration of more H_2O_2 by the O_2-diffusion cathode from reaction (1) (Brillas et al., 2004a). The increase in Q for total decontamination under these conditions is indicative of a slower relative generation of oxidant ·OH due to the acceleration of non-oxidizing reactions of this radical, for example, its oxidation to O_2 at the Pt anode and its recombination into H_2O_2.

The great oxidizing power of the photoelectro-Fenton method was confirmed by degrading up to 0.56 g l^{-1} (close to saturation) of **1** at pH 3.0 and at 100 mA cm^{-2}. The TOC–Q plots thus obtained are shown in Fig. 2c. As can be seen, more than 96% of mineralization is achieved after

Please cite this article as: Ignasi Sirés et al., Degradation of clofibric acid in acidic aqueous medium ..., Chemosphere (2006), doi:10.1016/j.chemosphere.2006.07.039.

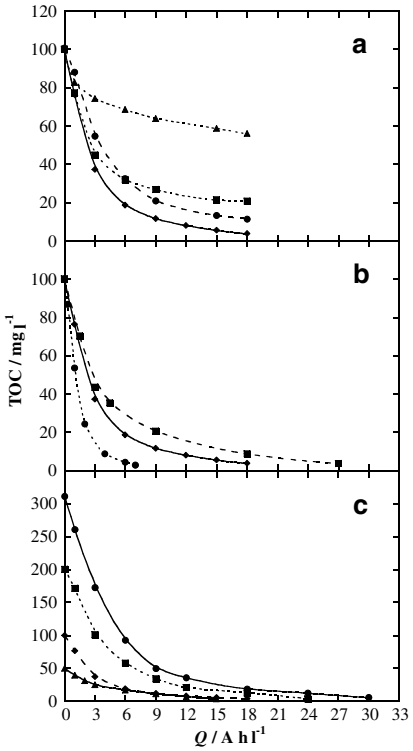

Fig. 2. Effect of experimental parameters on TOC abatement vs. specific charge for the treatment of 100 ml of different clofibric acid (**1**) solutions with 1.0 mM Fe^{2+} at 35.0 °C by photoelectro-Fenton. In plot (a), concentration of **1**: 179 mg l^{-1}; initial solution pH: (●) 2.0; (♦) 3.0; (■) 4.0; (▲) 6.0; current density: 100 mA cm^{-2}. In plot (b), concentration of **1**: 179 mg l^{-1}; solution pH: 3.0; current density: (●) 33; (♦) 100; (■) 150 mA cm^{-2}. In plot (c), initial concentration of **1**: (●) 557 (close to saturation); (■) 358; (♦) 179; (▲) 89 mg l^{-1}; solution pH: 3.0; current density: 100 mA cm^{-2}.

consumption of 30 A h l^{-1} (10 h), 24 A h l^{-1} (8 h), 18 A h l^{-1} (6 h) and 15 A h l^{-1} (5 h) for 557, 358, 179 and 89 mg l^{-1} of **1**, respectively. The drop in Q with decreasing clofibric acid concentration could be simply associated with the presence of lower amount of organics. However, results of Fig. 2c evidence the removal of more TOC at a given time with increasing initial pollutant content. For example, after 2 h of electrolysis, TOC is reduced by 33, 81, 143 and 218 mg l^{-1} starting from 89, 179, 358 and 557 mg l^{-1} of **1**, respectively. Since the same production of ·OH is expected from reactions (2), (3) and (5) in these trials, it seems plausible to consider that its competitive non-oxidizing reactions become slower and more ·OH concentration can then react with pollutants.

3.3. Mineralization current efficiency

The mineralization of **1** yields carbon dioxide and Cl^- as final products. The overall reaction can be written as follows:

$$C_{10}H_{11}ClO_3 + 17H_2O \rightarrow 10CO_2 + Cl^- + 45H^+ + 44e^- \quad (6)$$

Taking into account reaction (6) to calculate the theoretical TOC removal, the mineralization current efficiency of electrolyzed solutions was determined from Eq. (4). The MCE values thus obtained for the different treatments reported in Fig. 1a are depicted in Fig. 3a. The efficiency for both anodic oxidation procedures is very small, reaching a maximum value of 3.3–3.8% at 2 h (Q = 6 A h l^{-1}), as expected from their low oxidation ability. In contrast, this parameter attains a value of 25% and 23% at the early stages (20 min) of electro-Fenton and photoelectro-Fenton processes, respectively. When electrolysis is prolonged, a dramatic drop in MCE can be observed in Fig. 3a for such treatments, indicating the generation of products that are more difficultly oxidized with ·OH than the initial pollutant. The efficiency for the photoelectro-Fenton method is clearly higher from 1 h of electrolysis (Q = 3 A h l^{-1}), because it is able to destroy most products, including complexes of Fe^{3+} with generated carboxylic acids that are stable under electro-Fenton conditions.

For the photoelectro-Fenton treatment at the optimum pH 3.0, the MCE value always decays with rising current density, as can be seen in Fig. 3b. For example, after 1 h of electrolysis of 179 mg l^{-1} of **1**, decreasing efficiencies of 46% (Q = 1 A h l^{-1}), 20% (Q = 3 A h l^{-1}) and 14% (Q = 4.5 A h l^{-1}) are found at increasing j values of 33, 100 and 150 mA cm^{-2}, respectively. This tendency corroborates the enhancement of parallel non-oxidizing reactions of ·OH (e.g., its anodic oxidation to O_2 and its recombina-

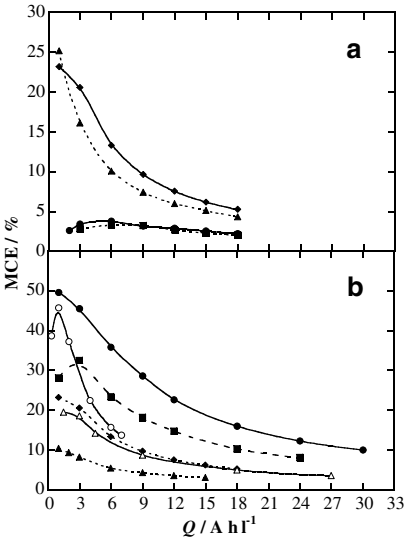

Fig. 3. Dependence of mineralization current efficiency calculated from Eq. (4) on specific charge for the degradation of 100 ml of clofibric acid (**1**) solutions of pH 3.0 at 35.0 °C. Plot (a) corresponds to the different treatments shown in Fig. 1a at 100 mA cm^{-2}. Plot (b) corresponds to the photoelectro-Fenton treatment of: (●) 557; (■) 358; (○, ♦, △) 179; (▲) 89 mg l^{-1} of **1** with 1.0 mM Fe^{2+} at (○) 33; (●, ■, ♦, ▲) 100; (△) 150 mA cm^{-2}.

Please cite this article as: Ignasi Sirés et al., Degradation of clofibric acid in acidic aqueous medium ..., Chemosphere (2006), doi:10.1016/j.chemosphere.2006.07.039.

tion into H_2O_2) when j raises, yielding a smaller proportion of this oxidant with ability to destroy pollutants. Fig. 3b also illustrates that the efficiency for the photoelectro-Fenton degradation at pH 3.0 and at 100 mA cm^{-2} undergoes a progressive increase with rising metabolite concentration, indicating the removal of larger amounts of organics with ·OH because its non-oxidizing reactions become slower. Thus, the MCE values at 1 h ($Q = 3$ A h l^{-1}) are 8.2%, 20%, 32% and 45% for 89, 179, 358 and 557 mg l^{-1} of **1**, respectively. Under these conditions, the highest efficiency of 50% is obtained at the beginning (20 min) of the degradation of the more concentrated solution.

The above results allow concluding that the photoelectro-Fenton method is viable for treating acidic wastewaters containing clofibric acid up to close saturation at optimum pH 3.0. This technique becomes more efficient when the content of this pollutant increases and current density decreases.

3.4. Clofibric acid decay and kinetic analysis

The kinetics of the reaction between **1** and ·OH generated in the different methods tested was comparatively studied by electrolyzing 179 mg l^{-1} of this compound at pH 3.0, at 100 mA cm^{-2} and at 35.0 °C. Its concentration was determined by reversed-phase chromatography, where it exhibits a well-defined absorption peak with a retention time (t_r) of 7.9 min. As can be seen in Fig. 4a, the concentration of **1** undergoes a similar fall by anodic oxidation without and with UVA irradiation, disappearing from the medium in 240 min in both cases. This confirms that **1** is not directly photolyzed by UVA light. Good straight lines were obtained when the above concentration decays were fitted to a pseudo-first-order kinetic equation, as depicted in the inset of Fig. 4a. From this analysis, an average pseudo-first-order rate constant (k) of $(4.7 \pm 0.1) \times 10^{-4}$ s^{-1} (square regression coefficient, $R^2 = 0.991$) is found for both anodic oxidation treatments. This behavior suggests the production of a constant concentration of ·OH from reaction (5) at the Pt anode during electrolysis.

Fig. 4b shows a much quicker decay of **1** under comparable electro-Fenton and photoelectro-Fenton treatments of 179 mg l^{-1} of **1** at 100 mA cm^{-2}, as expected if the production of oxidant ·OH from Fenton's reaction (2) is much greater than that of reaction (5) at the Pt anode. In both cases **1** is destroyed at a similar rate, being completely removed in approximately 7 min. Kinetic analysis of these data also agrees with a pseudo-first-order reaction of the metabolite (see inset of Fig. 4b), leading to an average k-value of $(1.35 \pm 0.10) \times 10^{-2}$ s^{-1} ($R^2 = 0.996$). This behavior indicates a very low generation of ·OH by reaction (3) under the action of UVA light.

The concentration–time plots obtained for the photoelectro-Fenton treatment of different metabolite contents and current densities at pH 3.0 are also presented in Fig. 4b. As can be seen, the complete removal of **1** at

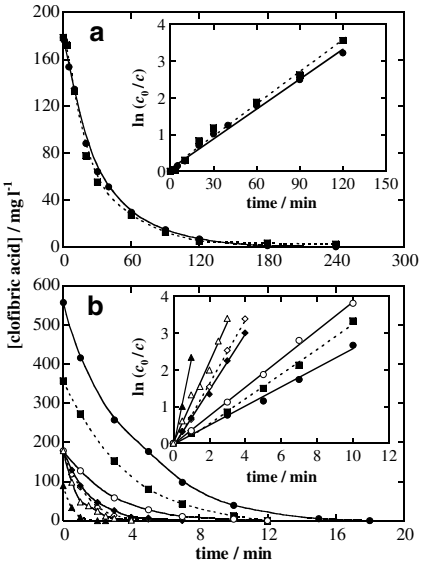

Fig. 4. Clofibric acid (**1**) decay with electrolysis time at pH 3.0 and at 35.0 °C. Plot (a) presents the degradation of 100 ml of a solution with 179 mg l^{-1} of **1** at 100 mA cm^{-2} by (●) anodic oxidation with electrogenerated H_2O_2; (■) anodic oxidation with electrogenerated H_2O_2 and UVA light. Plot (b) shows the treatments by: (◊) electro-Fenton of the same solution with 1.0 mM Fe^{2+} at 100 mA cm^{-2}; photoelectro-Fenton of: (●) 557; (■) 358; (○, ♦, △) 179; (▲) 89 mg l^{-1} of **1** with 1.0 mM Fe^{2+} at (○) 33; (●, ■, ♦, ▲) 100; (△) 150 mA cm^{-2}. The corresponding kinetic analysis assuming a pseudo-first-order reaction for **1** is given in the inset panels.

100 mA cm^{-2} is achieved at longer time when its initial concentration rises. Thus, it disappears after 3, 7, 12 and 18 min for 89, 179, 358 and 557 mg l^{-1}, respectively. Their kinetics analysis (see the inset of Fig. 4b) gives decreasing k-values of 3.88×10^{-2} s^{-1} ($R^2 = 0.992$), 1.26×10^{-2} s^{-1} ($R^2 = 0.997$), 5.6×10^{-3} s^{-1} ($R^2 = 0.996$) and 4.3×10^{-3} s^{-1} ($R^2 = 0.995$). The decay in k with raising the content of **1** indicates the gradual acceleration of competitive reactions between ·OH and by-products, thus enhancing TOC removal and MEC values as experimentally found (see Figs. 2c and 3b). Fig. 4b evidences a more rapid decay of 179 mg l^{-1} of **1** with rising j and their kinetic analysis shows greater k-values of 6.5×10^{-3} s^{-1} ($R^2 = 0.9996$), 1.26×10^{-2} s^{-1} ($R^2 = 0.997$) and 1.81×10^{-2} s^{-1} ($R^2 = 0.990$) at higher current densities of 33, 100 and 150 mA cm^{-2}, respectively. Note that k does not vary proportionally with j, confirming the reaction of a smaller proportion of ·OH with pollutants when j rises, since it is more quickly wasted by parallel non-oxidizing reactions.

3.5. Identification and evolution of intermediates

A solution of 179 mg l^{-1} of **1** of pH 3.0 was treated by electro-Fenton at 100 mA cm^{-2} and at 35.0 °C for 2 min

Please cite this article as: Ignasi Sirés et al., Degradation of clofibric acid in acidic aqueous medium ..., Chemosphere (2006), doi:10.1016/j.chemosphere.2006.07.039.

ARTICLE IN PRESS

and the remaining organics were extracted and analyzed by GC–MS. The MS spectrum displayed peaks related to stable aromatics such as 4-chlorophenol (**2**) ($m/z = 128$ (100, M^+), 130 (33, $(M+2)^+$)) at $t_r = 17.0$ min, hydroquinone (**3**) ($m/z = 108$ (100, M^+)) at $t_r = 21.5$ min, 4-chlorocatechol (**5**) ($m/z = 144$ (100, M^+), 146 (33, $(M+2)^+$)) at $t_r = 18.2$ min and *p*-benzoquinone (**6**) ($m/z = 110$ (53, M^+)) at $t_r = 4.1$ min. In addition, an intense peak ascribed to a chloro-derivative, with $m/z = 214$ (12, $(M+2)^+$), 212 (36, M^+), 184 (22), 169 (100) and 144 (49) as main fragmentation, was detected at $t_r = 14.2$ min. Although this product was not identified by pure standards, it can be reasonably assigned to a dehydrated species of 2-(4-chloro-2-hydroxyphenoxy)-2-methylpropionic acid (**8**), a hydroxylated product of **1** that can be transformed into **5** (molecular peak = 144). The silylated derivatives of **2**, **3**, **5** and **8** were also detected by GC–MS after derivatization with *N*,*O*-*bis*-(trimetylsilyl)acetamide.

Reversed-phase chromatograms of treated solutions exhibited peaks related to the products **2** at $t_r = 5.0$ min, **5** at $t_r = 3.1$ min and **6** at $t_r = 2.0$ min, along with other additional peaks associated with 4-chlororesorcinol (**4**) at $t_r = 2.8$ min and 1,2,4-benzenetriol (**7**) at $t_r = 1.8$ min. All these aromatics were unequivocally identified by comparing their t_r-values and UV–vis spectra, measured on the photodiode detector, with those of pure products. Note that only **2**, **5** and **6** have been previously reported as products of **1** during its electro-Fenton degradation in 0.01 M HCl (Oturan et al., 1999).

The evolution of aromatic intermediates during the treatment of 179 mg l^{-1} of **1** at pH 3.0 and at 100 mA cm^{-2} by anodic oxidation with electrogenerated H_2O_2 is shown in Fig. 5a. Under these conditions, all products are poorly accumulated and persist during long time, as expected from the slow removal of **1** in 240 min (see Fig. 4a). Compounds **5**, **6** and **7** are detected up to 300, 360 and 240 min, respectively, after reaching 4.2, 2.1 and 2.8 mg l^{-1} as maximum at 30–40 min, whereas **2** and **4** attain ca. 2.5 mg l^{-1} at 30 min and disappear after 180 min. In contrast, the same products are much more quickly formed and destroyed under comparable electro-Fenton and photoelectro-Fenton degradations due to the greater generation of ·OH from reaction (2). Fig. 5b shows that in both cases the product **2** is accumulated up to 7.3 mg l^{-1} at 1 min and persists to 10–12 min, whereas **5** and **6** are formed in smaller extent and destroyed in 7 and 10 min, respectively. The fact that all products show a similar evolution in both electro-Fenton and photoelectro-Fenton processes confirms that they are not photolyzed under UVA illumination.

Ion-exclusion chromatograms of electrolyzed solutions showed well-defined peaks ascribed to carboxylic acids such as 2-hydroxyisobutyric (**9**) at $t_r = 12.6$ min, tartronic (**10**) at $t_r = 7.7$ min, maleic (**11**) at $t_r = 8.1$ min, fumaric (**12**) at $t_r = 16.1$ min, formic (**13**) at $t_r = 14.0$ min and oxalic (**14**) at $t_r = 6.6$ min. Acids **10**–**13** come from the oxidation of the aryl moiety of aromatics (Boye et al., 2002; Brillas et al., 2004a; Sirés et al., 2006), whereas **9** is expected to be released in the first degradation stages of **1**. This was confirmed from the GC–MS analysis of organics produced after 2 min of the electro-Fenton treatment of 179 mg l^{-1} of **1** at pH 3.0 and at 100 mA cm^{-2}, since the MS spectrum after derivatization exhibited a peak of the disylilated derivative of **9** ($m/z = 248$ (10, M^+)) at $t_r = 10.2$ min. The photoelectro-Fenton treatment of 50 mg l^{-1} of **9** at pH 3.0, at 100 mA cm^{-2} and at 35.0 °C corroborated its oxidation to acid **14**. This acid can also be generated from the independent degradation of **10**–**12** (Sirés et al., 2006). The production of **13** and **14** as ultimate carboxylic acids was confirmed by electrolyzing 179 mg l^{-1} of **1** at pH 3.0 and at 100 mA cm^{-2} under electro-Fenton conditions for 6 h. The GC–MS analysis after esterification of the remaining acids with ethanol revealed the presence of an intense peak corresponding to diethyl oxalate ($m/z = 146$ (2, M^+)) at $t_r = 7.9$ min, and a very weak peak related to ethyl formate ($m/z = 74$ (10, M^+)) at $t_r = 10.5$ min.

As can be seen in Fig. 6a for the anodic oxidation treatment with electrogenerated H_2O_2 of 179 mg l^{-1} of **1** at pH 3.0 and at 100 mA cm^{-2}, large amounts of acids **9**–**14** are slowly accumulated without apparent degradation, except for acid **10** that reaches a maximum content of 57 mg l^{-1} at 180 min. After 360 min of electrolysis, 23.8, 25.1, 3.5, 1.7, 11.0 and 14.1 mg l^{-1} of **9**, **10**, **11**, **12**, **13** and **14**,

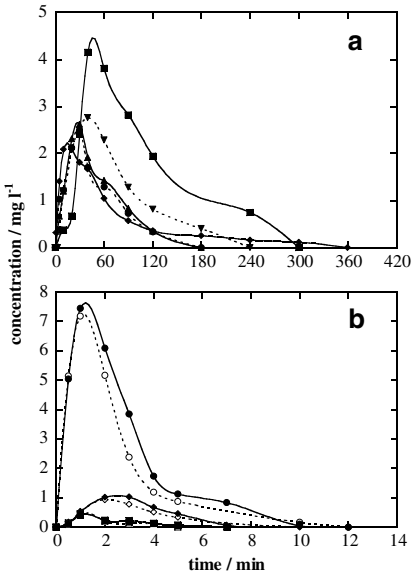

Fig. 5. Evolution of the concentration of aromatic intermediates detected during the degradation of 100 ml of 179 mg l^{-1} clofibric acid (**1**) solutions of pH 3.0 at 100 mA cm^{-2} and at 35.0 °C. In plot (a), anodic oxidation with electrogenerated H_2O_2. In plot (b), electro-Fenton (hollow symbols) and photoelectro-Fenton (solid symbols), both with 1.0 mM Fe^{2+}. Compound: (●, ○) 4-chlorophenol (**2**); (▲) 4-chlororesorcinol (**4**); (■, □) 4-chlorocatechol (**5**); (♦, ◊) *p*-benzoquinone (**6**); (▼) 1,2,4-benzenetriol (**7**).

Please cite this article as: Ignasi Sirés et al., Degradation of clofibric acid in acidic aqueous medium ..., Chemosphere (2006), doi:10.1016/j.chemosphere.2006.07.039.

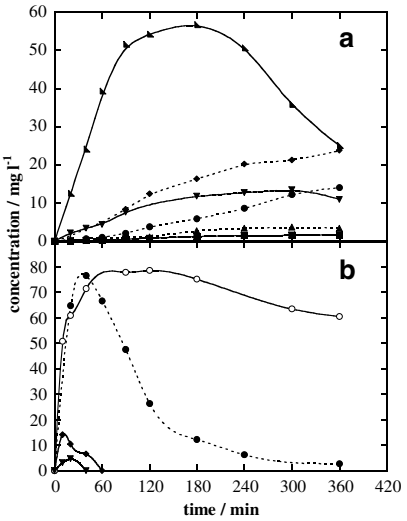

Fig. 6. Time-course of the concentration of carboxylic acids detected under the same conditions as in Fig. 5. In plot (a), anodic oxidation with electrogenerated H_2O_2. In plot (b), electro-Fenton (hollow symbols) and photoelectro-Fenton (solid symbols), both with 1.0 mM Fe^{2+}. Compound: (♦) 2-hydroxyisobutyric acid (**9**); (◣) tartronic acid (**10**); (▲) maleic acid (**11**); (■) fumaric acid (**12**); (▼) formic acid (**13**); (●, ○) oxalic acid (**14**). Concentrations of **9** and **13** in photoelectro-Fenton were determined at 33 mA cm^{-2}.

respectively, corresponding to 11.0, 7.5, 1.5, 0.7, 2.9 and 3.8 mg l^{-1} of TOC, are found. This balance indicates that all detected carboxylic acids give 27 mg l^{-1} of soluble TOC, a value much lower than 59 mg l^{-1} determined for the final degraded solution (see Fig. 1a). That means that this solution contains high contents of undetected products, probably hardly oxidizable aromatics.

A very different behavior is found for carboxylic acids in the electro-Fenton and photoelectro-Fenton processes of the above solution of **1**. These products are rapidly degraded by both treatments at 100 mA cm^{-2}, so that only the ultimate acid **14** is largely accumulated (see Fig. 6b), although less than 0.1 mg l^{-1} of acid **13** is also detected at the end of electro-Fenton. Fig. 6b illustrates that **9** and **13** persist in large extent to ca. 60 min when smaller amount of ·OH is produced by photoelectro-Fenton at 33 mA cm^{-2}. In both methods complexes of acid **14** with Fe^{3+} generated from reaction (2) are expected to be formed (Zuo and Hoigné, 1992). These Fe^{3+}-oxalato complexes are difficulty oxidized with ·OH in electro-Fenton, remaining ca. 60 mg l^{-1} of **14**, corresponding to 16 mg l^{-1} of TOC, at 360 min (see Fig. 6b). Since the resulting solution contains 21 mg l^{-1} of TOC (see Fig. 1a), one can conclude that the stable colored chlorinated polyaromatics formed yield about 5 mg l^{-1} of TOC. In contrast, Fig. 6b shows the complete mineralization of acid **14** in photoelectro-Fenton, because Fe^{3+}-oxalato complexes are efficiently photodecarboxylated under the action of UVA light (Zuo and Hoigné, 1992). The remaining solution TOC (<4 mg l^{-1}, Fig. 1a) can then be ascribed to the stable colored chlorinated polyaromatics generated during degradation of **1**.

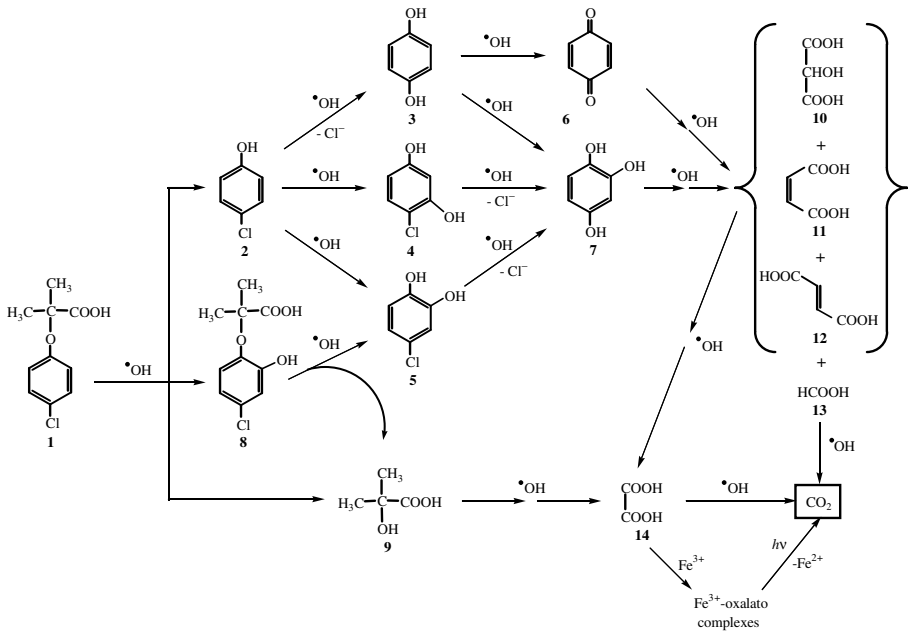

Fig. 7. Proposed reaction pathway for clofibric acid (**1**) degradation in acidic aqueous medium by electro-Fenton and photoelectro-Fenton processes with Fe^{2+} as catalyst.

Please cite this article as: Ignasi Sirés et al., Degradation of clofibric acid in acidic aqueous medium ..., Chemosphere (2006), doi:10.1016/j.chemosphere.2006.07.039.

3.6. Proposed degradation pathway

Fig. 7 presents a plausible pathway for the degradation of **1** by the electro-Fenton and photoelectro-Fenton processes with Fe^{2+} as catalyst. The sequence involves all intermediates detected in this work, including those that are only identified in anodic oxidation with electrogenerated H_2O_2 since they are quickly destroyed, without accumulation, in the above methods. Electrogenerated $^{\bullet}OH$ is stated as the main oxidant and the possible parallel oxidation of complexes of Fe^{3+} with other products containing OH groups, different from acid **14**, is not indicated for sake of simplicity.

The process is initiated either by the breaking of the C(1)–O bond of clofibric acid to form the phenol **2** with loss of acid **9**, or the direct hydroxylation on its C(2)-position to give **8**. Further parallel attack of $^{\bullet}OH$ on the C(4)-, C(3)- and C(2)-positions of **2** yields the benzenediols **3**, with release of Cl^- ion, **4** and **5**, respectively. Product **5** is also formed from the oxidation of **8** with loss of acid **9**. The subsequent hydroxylation with dechlorination of **4** and **5** leads to the benzenetriol **7**. This product is also formed from $^{\bullet}OH$ attack on **3**, which is oxidized in parallel to **6**. Further degradation of **6** and **7** leads to a mixture of acids **10**, **11**, **12** and **13**. The latter acid is directly mineralized to CO_2, whereas the three former ones are independently transformed into acid **14**, which is also generated from the oxidation of **9**. The ultimate carboxylic acid **14** is very slowly converted into CO_2 by $^{\bullet}OH$ since it forms very stable Fe^{3+}-oxalato complexes under electro-Fenton conditions. These species can be photodecarboxylated with loss of Fe^{2+} under the action of UVA light (Zuo and Hoigné, 1992).

4. Conclusions

It has been demonstrated that the photoelectro-Fenton method with Fe^{2+} and UVA light as catalysts is able to mineralize more than 96% of **1** in aqueous medium of pH 3.0. Its efficiency rises with increasing metabolite content and with decreasing *j*. This procedure is then viable for treating acidic wastewaters containing this pollutant. In contrast, the electro-Fenton method only yields about 80% of decontamination due to the formation of products hardly oxidizable with $^{\bullet}OH$, which is mainly formed from reaction (2). Comparative treatment by anodic oxidation with electrogenerated H_2O_2 confirms that $^{\bullet}OH$ is produced in much smaller extent at the Pt anode from water oxidation. Cl^- ion is released during mineralization. The decay of **1** always follows a pseudo-first-order kinetics with similar rate constant for electro-Fenton and photoelectro-Fenton. Aromatic products and generated carboxylic acids have been identified by GC–MS. From their quantification by HPLC chromatography, the different oxidation ability of both methods can be explained from the behavior of acid **14**. This acid forms very stable Fe^{3+}-oxalato complexes under electro-Fenton conditions, which can be efficiently photolyzed to CO_2 in photoelectro-Fenton under the action of UVA light.

Acknowledgements

The authors thank the financial support from MEC (Ministerio de Educación y Ciencia, Spain) under project CTQ2004-01954/BQU and the grant given to I. Sirés by DURSI (Departament d'Universitats, Recerca i Societat de la Informació, Generalitat de Catalunya) to do this work.

References

Andreozzi, R., Caprio, V., Marotta, R., Radovnikovic, A., 2003. Ozonation and H_2O_2/UV treatment of clofibric acid in water: a kinetic investigation. J. Hazard. Mater. B 103, 233–246.

Boye, B., Dieng, M.M., Brillas, E., 2002. Degradation of herbicide 4-chlorophenoxyacetic acid by advanced electrochemical oxidation methods. Environ. Sci. Technol. 36, 3030–3035.

Brillas, E., Baños, M.A., Camps, S., Arias, C., Cabot, P.L., Garrido, J.A., Rodríguez, R.M., 2004a. Catalytic effect of Fe^{2+}, Cu^{2+} and UVA light on the electrochemical degradation of nitrobenzene using an oxygen-diffusion cathode. New J. Chem. 28, 314–322.

Brillas, E., Boye, B., Sirés, I., Garrido, J.A., Rodríguez, R.M., Arias, C., Cabot, P.L., Comninellis, C., 2004b. Electrochemical destruction of chlorophenoxy herbicides by anodic oxidation and electro-Fenton using a boron-doped diamond electrode. Electrochim. Acta 49, 4487–4496.

Buser, H.R., Muller, M.D., Theobald, N., 1998. Occurrence of the pharmaceutical drug clofibric acid and the herbicide mecoprop in various Swiss lakes and in the North Sea. Environ. Sci. Technol. 32, 188–192.

Daughton, C.G., Jones-Lepp, T.L., (Eds.), 2001. Pharmaceuticals and Personal Care Products in the Environment. Scientific and Regulatory Issues. ACS Symposium Series, Washington.

Doll, T., Frimmel, F.H., 2004. Kinetic study of photocatalytic degradation of carbamazepine, clofibric acid, iomeprol and iopromide assisted by different TiO_2 materials—determination of intermediates and reaction pathways. Water Res. 38, 955–964.

Gözmen, B., Oturan, M.A., Oturan, N., Erbatur, O., 2003. Indirect electrochemical treatment of bisphenol A in water via electrochemically generated Fenton's reagent. Environ. Sci. Technol. 37, 3716–3723.

Hanna, K., Chiron, S., Oturan, M.A., 2005. Coupling enhanced water solubilization with cyclodextrin to indirect electrochemical treatment for pentachlorophenol contaminated soil remediation. Water Res. 39, 2763–2773.

Heberer, T., 2002. Tracking persistent pharmaceutical residues from municipal sewage to drinking water. J. Hydrol. 266, 175–189.

Heberer, T., Adam, M., 2004. Transport and attenuation of pharmaceutical residues during artificial groundwater replenishment. Environ. Chem. 1, 22–25.

Heberer, T., Stan, H.J., 1997. Determination of clofibric acid and *N*-(phenylsulfonyl)-sarcosine in sewage, river, and drinking water. Int. J. Environ. Anal. Chem. 67, 113–124.

Irmak, S., Yavuz, H.I., Erbatur, O., 2006. Degradation of 4-chloro-2-methylphenol in aqueous solution by electro-Fenton and photoelectro-Fenton processes. Appl. Catal. B: Environ. 63, 243–248.

Kolpin, D.W., Furlong, E.T., Meyer, M.T., Thurman, E.M., Zaugg, S.D., Barber, L.B., 2002. Pharmaceuticals, hormones, and other organic wastewater contaminants in U.S. Streams, 1999–2000: A national reconnaissance. Environ. Sci. Technol. 36, 1202–1211.

Kümmerer, K. (Ed.), 2001. Pharmaceuticals in the Environment. Sources, Fate and Risks. Springer, Berlin.

Please cite this article as: Ignasi Sirés et al., Degradation of clofibric acid in acidic aqueous medium ..., Chemosphere (2006), doi:10.1016/j.chemosphere.2006.07.039.

Oturan, M.A., Aaron, J.J., Oturan, N., Pinson, J., 1999. Degradation of chlorophenoxyacid herbicides in aqueous media, using a novel electrochemical method. Pestic. Sci. 55, 558–562.

Packer, J.L., Werner, J.J., Latch, D.E., McNeill, K., Arnold, W.A., 2003. Photochemical fate of pharmaceuticals in the environment: Naproxen, diclofenac, clofibric acid, and ibuprofen. Aquat. Sci. 65, 342–351.

Sirés, I., Garrido, J.A., Rodríguez, R.M., Cabot, P.L., Centellas, F., Arias, C., Brillas, E., 2006. Electrochemical degradation of paracetamol from water by catalytic action of Fe^{2+}, Cu^{2+}, and UVA light on electrogenerated hydrogen peroxide. J. Electrochem. Soc. 153, D1–D9.

Sun, Y., Pignatello, J.J., 1993. Photochemical reactions involved in the total mineralization of 2,4-D by iron(3+)/hydrogen peroxide/UV. Environ. Sci. Technol. 27, 304–310.

Tauxe-Wuersch, A., De Alencastro, L.F., Grandjean, D., Tarradellas, J., 2005. Occurrence of several acidic drugs in sewage treatment plants in Switzerland and risk assessment. Water Res. 39, 1761–1772.

Ternes, T.A., 1998. Occurrence of drugs in German sewage treatment plants and rivers. Water Res. 32, 3245–3260.

Ternes, T.A., Meisenheimer, M., McDowell, D., Sacher, F., Brauch, H.J., Haist-Gulde, B., Preuss, G., Wilme, U., Zulei-Seibert, N., 2002. Removal of pharmaceuticals during drinking water treatment. Environ. Sci. Technol. 36, 3855–3863.

Tixier, C., Singer, H.P., Oellers, S., Müller, S.R., 2003. Occurrence and fate of carbamazepine, clofibric acid, diclofenac, ibuprofen, ketoprofen, and naproxen in surface waters. Environ. Sci. Technol. 37, 1061–1068.

Ventura, A., Jacquet, G., Bermond, A., Camel, V., 2002. Electrochemical generation of the Fenton's reagent: application to atrazine degradation. Water Res. 36, 3517–3522.

Weigel, S., Berger, U., Jensen, E., Kallenborn, R., Thoresen, H., Hühnerfuss, H., 2004. Determination of selected pharmaceuticals and caffeine in sewage and seawater from Tromsø/Norway with emphasis on ibuprofen and its metabolites. Chemosphere 56, 583–592.

Xie, Y.B., Li, X.Z., 2006. Interactive oxidation of photoelectrocatalysis and electro-Fenton for azo dye degradation using TiO_2–Ti mesh and reticulated vitreous carbon electrodes. Mater. Chem. Phys. 95, 39–50.

Zuo, Y., Hoigné, J., 1992. Formation of hydrogen peroxide and depletion of oxalic acid in atmospheric water by photolysis of iron(III)-oxalato complexes. Environ. Sci. Technol. 26, 1014–1022.

Zwiener, C., Frimmel, F.H., 2000. Oxidative treatment of pharmaceuticals in water. Water Res. 34, 1881–1885.

Please cite this article as: Ignasi Sirés et al., Degradation of clofibric acid in acidic aqueous medium ..., Chemosphere (2006), doi:10.1016/j.chemosphere.2006.07.039.

UNIVERSITAT DE BARCELONA

ARTICLE 6 / *PAPER 6*

Mineralization of clofibric acid by electrochemical advanced oxidation processes using a boron-doped diamond anode and Fe^{2+} and UVA light as catalysts

ELEC Mat MA

Elsevier Editorial System(tm) for Applied Catalysis B: Environmental

Manuscript Draft

Manuscript Number:

Title: Mineralization of clofibric acid by electrochemical advanced oxidation processes using a boron-doped diamond anode and Fe2+ and UVA light as catalysts

Article Type: Full Length Article

Keywords: Boron-doped diamond anode; Catalysis; Electro-Fenton; Photoelectro-Fenton; Drug mineralization

Corresponding Author: Prof. Enric Brillas, PhD

Corresponding Author's Institution: Universitat de Barcelona

First Author: Enric Brillas

Order of Authors: Enric Brillas; Ignasi Sirés, PhD; Fancesc Centellas, PhD; Jose A Garrido, PhD; Rosa M Rodriguez, PhD; Conchita Arias, PhD; Pere L Cabot, PhD

Cover Letter

Dear Prof. X. Verykios,

I am sending you our paper entitled: "Mineralization of clofibric acid by electrochemical advanced oxidation processes using a boron-doped diamond anode and Fe^{2+} and UVA light as catalysts", co-authored by E. Brillas, I. Sirés, F. Centellas, J.A. Garrido, R.M. Rodríguez, C. Arias and P.L. Cabot, for its publication in Applied Catalysis B: Environmental.

This original paper deals with the degradation of a widely used drug as clofibric acid, a well-known pollutant of the aquatic environment, by electrochemical advanced oxidation processes (EAOPs) such as electro-Fenton and photoelectro-Fenton. In these environmentally friendly techniques hydrogen peroxide is electrogenerated from an oxygen-diffusion cathode and its reaction with catalytic Fe^{2+} produces hydroxyl radical ($^{\bullet}OH$) as strong oxidant of organic pollutants. The degradation is made using an undivided electrolytic cell with a boron-doped diamond (BDD) anode that also yields adsorbed hydroxyl radical (BDD($^{\bullet}OH$)). In the work the oxidizing ability of both kinds of hydroxyl radicals ($^{\bullet}OH$ and (BDD($^{\bullet}OH$)) are compared. Thus, electro-Fenton with 1.0 mM Fe^{2+} as catalyst is found as a very efficient method to mineralize rapidly and completely this compound. Nevertheless, the overall mineralization is strongly enhanced in the photoelectro-Fenton method with UVA irradiation since it photodecomposes Fe^{3+} complexes of some products. It should be noted that the use of photoelectro-Fenton with a BDD anode and Fe^{2+} and UVA light as catalysts has not been reported previously in the literature. The effect of applied current and clofibric acid concentration on the degradation rate and mineralization current efficiency of such EAOPs is examined to clarify their oxidation power. The kinetics of clofibric acid decay is followed by reversed-phase HPLC chromatography. Aromatic products are detected by GC-MS and also followed by this technique to discuss the initial reaction pathway of this compound. The quantification of final generated carboxylic acids by ion-exclusion chromatography shows that in photoelectro-Fenton UVA light enhances the photodegradation of Fe^{3+}-oxalato complexes, which are also oxidized with BDD($^{\bullet}OH$), but not by $^{\bullet}OH$. Our results show clearly that the photoelectro-Fenton method is the most adequate EAOP for the remediation of wastewaters containing clofibric acid. From these considerations, we believe that this paper is of general and great interest for researchers in catalytic chemistry and electrochemical treatment of organic pollutants in waters and consequently, it can be published in Applied Catalysis B: Environmental.

Sincerely yours,

Prof. E. Brillas

*** List of Three (3) Potential Reviewers**

Three potential reviewers, excellent specialists in the electrochemical treatment of wastewaters, are:

- Prof. Cesar Pulgarin, Ecole Polytechnique Fédérale de Lausanne (EPFL), Institute of Chemical Science and Engineering, GGEC, Station 6, CH-1015 Lausanne, Switzerland, e-mail: cesar.pulgarin@epfl.ch
- Prof. Oktay Erbatur, Department of Chemistry, Çukurova University, 01330 Balcalı, Adana, Turkey, e-mail: erbatur@cu.edu.tr
- Dr. Birame Boye, Istituto di Chimica Fisica ed Elettrochimica, Università degli Study di Padova, Via Marzolo 14, 35131 Padova, Italy, e-mail: b.boye@mbi-consultin.com

*** Manuscript**

Mineralization of clofibric acid by electrochemical advanced oxidation processes using a boron-doped diamond anode and Fe^{2+} and UVA light as catalysts

Enric Brillas*, Ignasi Sirés, Francesc Centellas, José Antonio Garrido, Rosa María Rodríguez, Conchita Arias, Pere-Lluís Cabot

Laboratori d'Electroquímica dels Materials i del Medi Ambient, Departament de Química Física, Facultat de Química, Universitat de Barcelona, Martí I Franquès 1-11, 08028 Barcelona (Spain)

Paper submitted to be published in Applied Catalysis B: Environmental

*Corresponding author: Tel.: +34 93 4021223; Fax: +34 93 4021231; e-mail: brillas@ub.edu

Abstract

This work shows that aqueous solutions of clofibric acid (2-(4-chlorophenoxy)-2-methylpropionic acid), the bioactive metabolite of various lipid-regulating drugs, up to saturation at pH 3.0 are efficiently and completely degraded by electrochemical advanced oxidation processes such as electro-Fenton and photoelectro-Fenton with Fe^{2+} and UVA as catalysts using an undivided electrolytic cell with a boron-doped diamond (BDD) anode and an O_2-diffusion cathode able to electrogenerate H_2O_2. This is feasible in these environmentally friendly methods by the production of oxidant hydroxyl radical at the BDD surface from water oxidation and in the medium from Fenton's reaction between Fe^{2+} and electrogenerated H_2O_2. The degradation process is accelerated in photoelectro-Fenton by additional photolysis of Fe^{3+} complexes under UVA irradiation. Comparative treatments by anodic oxidation with electrogenerated H_2O_2, but without Fe^{2+}, yield much slower decontamination. Chloride ion is released and totally oxidized to chlorine at the BDD surface in all treatments. The decay kinetics of clofibric acid always follows a pseudo-first-order reaction. 4-Chlorophenol, 4-chlorocatechol, hydroquinone, *p*-benzoquinone and 2-hydroxyisobutyric, tartronic, maleic, fumaric, formic and oxalic acids, are detected as intermediates. The ultimate product is oxalic acid, which is slowly but progressively oxidized on BDD in anodic oxidation. In electro-Fenton this acid forms Fe^{3+}-oxalato complexes that can also be totally destroyed at the BDD anode, whereas in photoelectro-Fenton the mineralization rate of these complexes is enhanced by its parallel photodecarboxylation with UVA light.

Keywords: Boron-doped diamond anode; Catalysis; Electro-Fenton; Photoelectro-Fenton; Drug mineralization

1. Introduction

The detection of a large variety of pharmaceutical drugs and metabolites including analgesics, anti-inflammatories, antimicrobials, antiepileptics, beta-blockers, estrogens and lipid regulators as emerging pollutants in waters at concentrations from nanograms to micrograms per litre has been recently documented [1-10]. The main sources of this contamination include emission from production sites, direct disposal of overplus drugs in households, excretion after drug administration to humans and animals, treatments throughout the water in fish and other animal farms and inadequate treatment of manufacturing waste [8]. To avoid the potential adverse health effects of these pollutants on living beings, research efforts are underway to develop efficient oxidation techniques for achieving their total mineralization, i.e. their complete conversion into CO_2.

Clofibric acid (2-(4-chlorophenoxy)-2-methylpropionic acid) is the bioactive metabolite of drugs such as clofibrate, etofibrate and etofyllineclofibrate, widely used as blood lipid regulators because they decrease the plasmatic content of cholesterol and triglycerides [9]. This compound has an estimated environmental persistence of 21 days [10] and has been found up to 10 μg l^{-1} in sewage treatment plant effluents, rivers, lakes, North Sea, ground waters and drinking waters [1,2,6]. However, it is poorly degraded by ozonation [5,11], H_2O_2/UV [11], sunlight and UV photolysis [7] and TiO_2/UV [12], as well as after application of biological and physico-chemical methods in sewage treatment plants [9]. In previous work [13] we have explored the electrochemical degradation of clofibric acid solutions in the pH range 2.0-12.0 by means of the classical method of anodic oxidation with a cell containing either a Pt or boron-doped diamond (BDD) anode and a stainless steel cathode. Under these conditions, the metabolite solutions were poorly decontaminated with a Pt anode, whereas the alternative use of BDD yielded their complete mineralization, but with very low degradation rate and current efficiency. The greater oxidizing power of BDD compared to Pt is ascribed to its higher O_2-overpotential, which allows the

generation of more amount of the strong oxidant hydroxyl radical (BDD(•OH)) adsorbed on its surface from water oxidation [14-18]:

$$BDD(H_2O) \rightarrow BDD(^{\bullet}OH) + H^+ + e^- \quad (1)$$

Under these conditions, other weaker oxidants such as peroxodisulfate ion, H_2O_2 and O_3 at the BDD anode are also produced [18]. Anodic oxidation with a BDD anode seems a viable technique to mineralize clofibric acid, but its very low oxidation power prevents its possible application to the treatment of industrial wastewaters containing this compound. This makes necessary the search of other potent technologies with higher ability to remove this pollutant from waters.

Recently, powerful indirect electrooxidation methods such as electro-Fenton and photoelectro-Fenton are being developed for water remediation [19-31]. These electrochemical advanced oxidation processes (EAOPs) are environmentally friendly technologies based on the continuous supply of H_2O_2 to an acidic contaminated solution from the two-electron reduction of injected O_2:

$$O_2 + 2\,H^+ + 2\,e^- \rightarrow H_2O_2 \quad (2)$$

Reticulated vitreous carbon [19,20], carbon-felt [21,22,24,27,30], activated carbon fibre [28] and O_2-diffusion [23,25,26,29,31] cathodes are usually employed to reduce efficiently O_2 from reaction (2). In the electro-Fenton process the oxidizing ability of electrogenerated H_2O_2 is strongly enhanced by adding to the solution a small quantity of Fe^{2+} to produce hydroxyl radical (•OH) and Fe^{3+} from the classical Fenton's reaction [32]:

$$Fe^{2+} + H_2O_2 \rightarrow Fe^{3+} + {}^{\bullet}OH + OH^- \quad (3)$$

An advantage of this method is that the Fe^{3+}/Fe^{2+} system is catalytic and reaction (3) is propagated from Fe^{2+} regeneration, mainly by reduction of Fe^{3+} at the cathode [21]. However, a part of

generated $^{\bullet}OH$ is wasted by non-oxidizing reactions, for example, with Fe^{2+} and H_2O_2 or its direct recombination to hydrogen peroxide [32,33]:

$$Fe^{2+} + {}^{\bullet}OH \rightarrow Fe^{3+} + OH^{-} \quad (4)$$

$$H_2O_2 + {}^{\bullet}OH \rightarrow HO_2^{\bullet} + H_2O \quad (5)$$

$$2\,{}^{\bullet}OH \rightarrow H_2O_2 \quad (6)$$

In the photoelectro-Fenton process, the treated solution is illuminated with UV light, which can also act as catalyst to favor: (i) the photodecomposition of complexes of Fe^{3+} with generated carboxylic acids [23,25,30,34] and/or (ii) the regeneration of more Fe^{2+} with additional production of $^{\bullet}OH$ from photoreduction of $Fe(OH)^{2+}$, the predominant Fe^{3+} species in acid medium [32]:

$$Fe(OH)^{2+} + h\nu \rightarrow Fe^{2+} + {}^{\bullet}OH \quad (7)$$

This paper reports a comparative study on the degradation of clofibric acid by electro-Fenton and photoelectro-Fenton using an undivided electrolytic cell with a BDD anode and an O_2-diffusion cathode to electrogenerate continuously H_2O_2 from reaction (2). Both EAOPs were tested with metabolite solutions containing a low content of 0.05 M Na_2SO_4 as background electrolyte and 1.0 mM Fe^{2+} as catalyst at pH 3.0, near the optimum pH of 2.8 for Fenton's reaction (3) [32]. For these methods, organic pollutants are expected to be mainly oxidized by BDD($^{\bullet}OH$) and $^{\bullet}OH$ formed from reactions (1) and (3), respectively, although parallel reactions with weaker oxidants such as electrogenerated H_2O_2, as well as peroxodisulfate ion [18], ozone [18] and ferrate ion [35] also produced at the BDD anode, are possible in much less extent. Photoelectro-Fenton was performed by irradiating the solution with UVA light. Comparative treatments by anodic oxidation without and with UVA irradiation were also made to assess the higher oxidation power of electro-Fenton and photoelectro-Fenton. The influence of current density and metabolite concentration on the

degradation rate and mineralization current efficiency of these EAOPs was investigated. The decay kinetics of clofibric acid in each method was determined. The evolution of identified aromatic products and carboxylic acids was followed by chromatographic techniques to clarify their pathways in the different oxidation processes.

2. Experimental

Clofibric acid, 4-chlorophenol, hydroquinone, *p*-benzoquinone, 2-hydroxyisobutyric acid, tartronic acid, maleic acid, fumaric acid, formic acid and oxalic acid were either reagent or analytical grade from Sigma-Aldrich, Merck, Panreac and Avocado. 4-Chlorocatechol was synthesized by chlorination of pyrocatechol with SO_2Cl_2 [23]. Anhydrous sodium sulfate and heptahydrated ferrous sulfate were analytical grade from Fluka. Solutions were prepared with high-purity water obtained from a Millipore Milli-Q system (resistivity > 18 MΩ cm at 25 ºC) and their pH was adjusted to 3.0 with analytical grade sulfuric acid from Merck. Other chemicals and organic solvents were either HPLC or analytical grade from Panreac.

The solution pH was determined with a Crison 2000 pH-meter. Aliquots withdrawn from treated solutions were filtered with Whatman 0.45 µm PTFE filters before analysis. The degradation of clofibric acid solutions was monitored from the removal of their total organic carbon (TOC), measured on a Shimadzu VCSN TOC analyzer. Reproducible values were obtained using the standard non-purgeable organic carbon method. From these results, the mineralization current efficiency (MCE) for each treated solution at a given electrolysis time was calculated from the following equation:

$$MCE = \frac{\Delta(TOC)_{exp}}{\Delta(TOC)_{theor}} \times 100 \qquad (8)$$

where $\Delta(TOC)_{exp}$ is the experimental TOC decay and $\Delta(TOC)_{theor}$ is the theoretically calculated TOC removal assuming that the applied electrical charge (= current x time) is only consumed in the mineralization process of clofibric acid.

The concentration of chloride ion in treated solutions was determined by ion chromatography with a Shimadzu 10Avp HPLC chromatograph fitted with a Shim-Pack IC-A1S, 100 mm x 4.6 mm (i. d.), anion column at 40 °C and coupled with a Shimadzu CDD 10Avp conductivity detector. A mixture of 2.5 mM phtalic acid and 2.4 mM tris(hydroxymethyl)aminomethane) of pH 4.0 at 1.5 ml min^{-1} was used as mobile phase for this analysis. Aromatic products were identified by gas chromatography-mass spectrometry (GC-MS) using a Hewlett-Packard 5890 Series II gas chromatograph fitted with a HP-5 0.25 µm, 30 m x 0.25 mm (i. d.), column, and a Hewlett-Packard 5989A mass spectrophotometer operating in EI mode at 70 eV and 290 °C. The metabolite decay and the time-course of its aromatic products were followed by reversed-phase HPLC chromatography using a Waters 600 high-performance liquid chromatograph fitted with a Spherisorb ODS2 5 µm, 150 mm x 4.6 mm (i. d.), column at room temperature, coupled with a Waters 996 photodiode array detector, and circulating a 50:47:3 (v/v/v) methanol/phosphate buffer (pH = 2.5)/pentanol mixture at 1.0 ml min^{-1} as mobile phase. For each product, this detector was selected at the maximum wavelength of its UV-absorption band. Carboxylic acids were identified by ion-exclusion chromatography using the above HPLC chromatograph fitted with a Bio-Rad Aminex HPX 87H, 300 mm x 7.8 mm (i. d.), column at 35 °C. For these measurements, the photodiode detector was selected at 210 nm and the mobile phase was 4 mM H_2SO_4 at 0.6 ml min^{-1}.

All electrolyses were conducted in an open, cylindrical, undivided and thermostated cell containing 100 ml of solution vigorously stirred with a magnetic bar. The anode was a 3-cm^2 BDD thin-film deposited on conductive single crystal *p*-type Si (100) wafers from CSEM and the cathode was a 3-cm^2 carbon-PTFE electrode from E-TEK, which was fed with pure O_2 at 12 ml min^{-1} to generate continuously H_2O_2 from reaction (2). The setup of the electrolytic system and the

characteristics of the O_2-diffusion cathode have been described elsewhere [23,25]. Experiments were made at a constant current density (j) of 33, 100 and 150 mA cm^{-2}, supplied by an Amel 2053 potentiostat-galvanostat. Electro-Fenton and photoelectro-Fenton treatments were carried out with solutions containing 0.05 M Na_2SO_4 as background electrolyte and 1.0 mM Fe^{2+} as catalyst of pH 3.0 at 35.0 ºC, which were found as optimum conditions for the degradation of other aromatics in the cell used [23,25]. The latter method became operative when the solution was irradiated with UVA light of λ_{max} = 360 nm emitted by a Philips 6-W fluorescent black light blue tube, yielding a photoionization energy input to the solution of 140 μW cm^{-2}, as detected with a NRC 820 laser power meter working at 514 nm. Comparative anodic oxidation treatments without catalyst Fe^{2+} were performed in the absence and presence of UVA irradiation at 100 mA cm^{-2}.

3. Results and discussion

3.1. Comparative degradation of clofibric acid

Comparative treatments were made for solutions containing 179 mg l^{-1} clofibric acid (equivalent to 100 mg l^{-1} TOC) of pH 3.0 at 100 mA cm^{-2}. In these trials the solution pH did not practically vary, reaching final values of 2.8-2.9. The change in solution TOC with applied specific charge (Q, in A h l^{-1}) for anodic oxidation without and with UVA irradiation, electro-Fenton and photoelectro-Fenton is depicted in Fig. 1. As can be seen, total degradation (> 97% TOC removal) is attained in all cases, although the time required for overall mineralization depends on the method tested. Both anodic oxidation methods lead to a slow, but similar, TOC decay up to yield total mineralization at Q = 18 A h l^{-1}, i.e., after 6 h of both treatments. This behavior indicates that all organics are destroyed by the oxidant BDD($^{\bullet}$OH) formed at the anode surface from reaction (1), without significant photodecomposition by UVA light, at least of final products. Fig. 1 evidences that the degradation rate (the change of TOC with time) is strongly enhanced using both EAOPs due to the

catalytic action of the Fe^{3+}/Fe^{2+} system combined with UVA light when the solution is simultaneously irradiated. The significant acceleration of the destruction of organic pollutants in the early stages of the electro-Fenton process can be explained by their quicker reaction with the great amount of $^{\bullet}OH$ formed from Fenton's reaction (3). For this EAOP, however, the rate in TOC decay gradually falls at longer electrolysis time, probably due to the formation of complexes of Fe^{3+} with final carboxylic acids that are hardly oxidized, and the solution is decontaminated after about 6 h of electrolysis, that is, at similar time to that needed for both anodic oxidation treatments. In contrast, TOC is much more rapidly removed by photoelectro-Fenton, where total mineralization is achieved at Q = 12 A h l^{-1} (4 h). The increase in mineralization rate in photoelectro-Fenton can be related to: (i) the parallel photodegradation of complexes of Fe^{3+} with final carboxylic acids and/or (ii) the enhanced generation of $^{\bullet}OH$ due to additional photoreduction of $Fe(OH)^{2+}$ from reaction (7).

The above comparative study shows that photoelectro-Fenton is the method with highest oxidation power, then being the best EAOP for the treatment of wastewaters containing clofibric acid. Electro-Fenton also yields much faster degradation than anodic oxidation, but its oxidation power drops significantly at the end of electrolysis due to the very slow destruction of final products, which is strongly enhanced by UVA light in photoelectro-Fenton.

The influence of current density and clofibric acid concentration on the oxidizing ability of the above electro-Fenton and photoelectro-Fenton processes was explored. It was found that these experimental parameters showed the same trends in both EAOPs, as expected if they mainly affect the behavior of the electrolytic system. These effects are depicted in Figs. 2a and 2b for electro-Fenton in which they were more clearly observed due to its lower oxidation power. Thus, Fig. 2a shows that when j increases from 33 to 150 mA cm^{-2}, the specific charge for total decontamination of 179 mg l^{-1} of clofibric acid rises from 12 to 22 A h l^{-1}, but the time needed for overall mineralization drops from 12 to about 5 h since the degradation rate is strongly enhanced. This latter tendency can be accounted for by the faster destruction of all pollutants due to the greater

production of BDD(•OH) from reaction (1) and of •OH from Fenton's reaction (3) as *j* increases, because more H_2O_2 is generated at the O_2-diffusion cathode from reaction (1) [25] and then, its reaction with Fe^{2+} becomes faster. However, the increase in *Q* for total decontamination when *j* rises suggests a lower amount of reactive BDD(•OH) and •OH. That means that a higher proportion of both oxidants is progressively wasted by their non-oxidizing reactions since they take place in larger extent. These reactions involve, for example, the anodic oxidation of BDD(•OH) to O_2 and reactions (4)-(6) for •OH. Moreover, increasing *j* can accelerate the formation of weaker oxidants such as peroxodisulfate ion and ozone [18] that also reduces the relative proportion of BDD(•OH) adsorbed at the anode. On the other hand, Fig. 2b shows that at 100 mA cm^{-2} overall mineralization is achieved with decreasing consumption of 24 A h l^{-1} (8 h), 21 A h l^{-1} (7 h), 18 A h l^{-1} (6 h) and 12 A h l^{-1} (4 h) starting from 557 (close to saturation), 358, 179 and 89 mg l^{-1} of the metabolite, respectively, as expected if lower amount of organic matter is destroyed in solution. These results also evidence the removal of more TOC at a given time with rising initial pollutant content. As an example, at 2 h of electrolysis (*Q* = 6 A h l^{-1}) the TOC of the above solutions is reduced by 231, 150, 70 and 39 mg l^{-1}. Since the same quantity of BDD(•OH) and •OH is expected to be produced from reactions (1) and (3) in these trials carried out at 100 mA cm^{-2}, it can be assumed that their parallel non-oxidizing reactions occur in less proportion with rising metabolite concentration. This favors the reaction of more amounts of both kinds of hydroxyl radicals with organics, thus raising the degradation rate of the process. All these findings allow establishing that the oxidation power of EAOPs, corresponding to their degradation rate, increases with increasing current density and initial substrate concentration.

3.2. Mineralization current efficiency

It is well-known that reaction of chloroaromatics with hydroxyl radical leads to the release of chloride ion [16,23,26]. This point was confirmed for clofibric acid by recording the ion chromatograms of all treated solutions, which only displayed a defined peak at a retention time (t_r)

of 2.3 min related to Cl^- ion. The formation of ClO_3^- and ClO_4^- ions was discarded since they were not detected in these chromatograms. The evolution of Cl^- concentration during the degradation of 179 mg l^{-1} of metabolite by anodic oxidation with electrogenerated H_2O_2 and the two EAOPs at 100 mA cm^{-2} is presented in Fig. 3. As can be seen, this ion is accumulated and completely removed in 300-360 min in all cases, after reaching a maximum concentration of about 8 mg l^{-1} at 180 min of anodic oxidation, 23 mg l^{-1} at 20 min of electro-Fenton and 19 mg l^{-1} at 40 min of photoelectro-Fenton, corresponding to 27%, 78% and 64% of the initial chlorine content in solution (29.5 mg l^{-1}). The slow accumulation of Cl^- in the former method confirms the slow reaction of chloro-organics with BDD(•OH), whereas its much faster release at the early stages of both EAOPs corroborates the quick destruction of these pollutants with •OH. The gradual destruction of this ion when electrolysis is prolonged can be explained by its slow oxidation to Cl_2 on BDD, as reported by Kraft et al. [16].

The above findings allow concluding that the mineralization of clofibric acid involves its conversion into CO_2 and Cl^- as primary ion. This reaction can be written as follows:

$$C_{10}H_{11}ClO_3 + 17\ H_2O \rightarrow 10\ CO_2 + Cl^- + 45\ H^+ + 44\ e^- \quad (9)$$

Reaction (9) was then used to calculate the value of $\Delta(TOC)_{theor}$ for each treated solution at chosen electrolysis times and from these data, the corresponding efficiency by means of Eq. 8.

Fig. 4a presents the MCE values determined for the trials reported in Fig. 1. An increase in efficiency with increasing the oxidation power of the method can be observed. Thus, the two less potent anodic oxidation processes possess a similar, small and practically constant MCE value of about 7%, suggesting that most organics are mineralized at the same rate by BDD(•OH) along electrolysis without significant role of UVA light. In contrast, this parameter attains a much higher value for electro-Fenton and photoelectro-Fenton, although the latter procedure with highest oxidation power is the most efficient because of the parallel photodecomposition of some final products. Note that 33% and 35% efficiencies are found after 20 min of these EAOPs, respectively,

confirming that organics are more quickly mineralized with •OH than with BDD(•OH). At longer time, a dramatic drop in MCE takes place in both cases due to the generation of final products such as complexes of Fe^{3+} with carboxylic acids that are more difficultly destroyed by both oxidants and/or UVA light.

Fig. 4b illustrates the effect of current density and clofibric acid concentration reported in Figs. 2a and 2b on the efficiency of EAOPs as a function of specific charge. A gradual drop in MCE, at least up to 6 A h l^{-1}, can be observed when *j* increases from 33 to 150 mA cm^{-2}. This trend could seem contradictory to the fact that rising *j* causes the increase in degradation rate due to the production of more amounts of reactive BDD(•OH) and •OH, as pointed out above. The concomitant loss in efficiency under these conditions can be associated with the larger waste of both oxidants in faster parallel non-oxidizing reactions giving rise to lower amounts of them with ability to destroy organics and hence, favoring the consumption of more ineffective specific charge. Fig. 4b also evidences a gradual increase in efficiency of EAOPs with rising metabolite concentration, in agreement with the higher degradation rate found in these trials. This confirms the removal of greater amounts of pollutants with BDD(•OH) and •OH, because their competitive non-oxidizing reactions become less significant.

3.3. Kinetics of clofibric acid decay

The decay of the metabolite in the different electrochemical methods was followed by reversed-phase HPLC chromatography, where it exhibited a well-defined peak at t_r = 7.9 min. A previous experiment carried out by adding 20 mM H_2O_2 to a 179 mg l^{-1} clofibric acid solution of pH 3.0 showed that the content of this compound remained unchanged, indicating that it can not react directly with electrogenerated H_2O_2 in the electrolytic systems.

The comparative kinetics of the removal of clofibric acid with generated strong oxidizing agents (mainly BDD(•OH) and/or •OH) was determined from the treatment of 179 mg l^{-1} metabolite

solutions at 100 mA cm^{-2}. Fig. 5a shows that clofibric acid concentration undergoes a similar fall by anodic oxidation without and with UVA illumination, disappearing in 360 min in both cases, a time similar to that needed for its total mineralization (see Fig. 1). This confirms that this compound is mainly oxidized by BDD(•OH) from reaction (1), without direct photolysis by UVA light. The above concentration decays were well-fitted to a pseudo-first-order equation, as can be seen in the inset panel of Fig. 5a. From this kinetic analysis, an average pseudo-first-order rate constant (k) of $(1.70\pm0.13)\text{x}10^{-4}$ s^{-1} (square regression coefficient (R^2) = 0.992) is found for both anodic oxidation treatments. This behavior suggests that a steady BDD(•OH) concentration reacts with the metabolite along electrolysis.

On the other hand, Fig. 5b evidences a much quicker and similar abatement of the metabolite under comparable electro-Fenton and photoelectro-Fenton treatments, being completely removed in 7 min, as expected if it reacts with a much greater amount of oxidant •OH formed from Fenton's reaction (3). The inset panel of Fig. 5b shows that the kinetic analysis of these data also agrees with a pseudo-first-order reaction, giving the same k-value of $1.35\text{x}10^{-2}$ s^{-1} (R^2 = 0.993). This allows concluding that •OH is produced in insignificant quantity by reaction (7) under UVA irradiation.

The effect of current density on the decay kinetics of this compound was further explored for the electro-Fenton treatment. As can be seen in Fig. 5b, increasing k-values of $5.10\text{x}10^{-3}$ s^{-1} (R^2 = 0.991), $1.35\text{x}10^{-2}$ s^{-1} (R^2 = 0.993) and $2.04\text{x}10^{-2}$ s^{-1} (R^2 = 0.992) are found for j values of 33, 100 and 150 mA cm^{-2}, respectively. This trend confirms a higher •OH production in the medium from Fenton's reaction (3) when j rises, due to the concomitant accumulation of more electrogenerated H_2O_2 from reaction (2) [25].

3.4. Identification and evolution of intermediates

A 179 mg l^{-1} clofibric acid solution of pH 3.0 was treated by electro-Fenton at 100 mA cm^{-2} for 2 min and its organic components were extracted with 45 ml of CH_2Cl_2 in three times. The collected

organic solution was dried with Na_2SO_4, filtered and its volume reduced to 2 ml to concentrate the remaining aromatics to be analyzed by GC-MS. The MS spectrum showed peaks related to stable aromatics such as 4-chlorophenol (m/z = 128 (100, M^+), 130 (33, $(M+2)^+$)) at t_r = 17.0 min, hydroquinone (m/z = 108 (100, M^+)) at t_r = 21.5 min, 4-chlorocatechol (m/z = 144 (100, M^+), 146 (33, $(M+2)^+$)) at t_r = 18.2 min and *p*-benzoquinone (m/z = 110 (53, M^+)) at t_r = 4.1 min. These products were confirmed in the reversed-phase HPLC chromatograms of electrolyzed solutions, which exhibited well-defined peaks corresponding to 4-chlorophenol at t_r = 5.0 min, 4-chlorocatecol at t_r = 3.1 min and *p*-benzoquinone at t_r = 2.0 min. These peaks were unequivocally identified by comparing their t_r-values and UV-Vis spectra, measured on the photodiode detector, with those of pure compounds. However, only traces of hydroquinone were detected by this technique in all cases, as expected if it is very quickly converted into *p*-benzoquinone by all oxidizing agents.

The evolution of aromatic intermediates during the different treatments of 179 mg l^{-1} metabolite solutions at 100 mA cm^{-2} is presented in Fig. 6. As can be seen in Fig. 6a, 4-chlorophenol is largely produced in all cases and persists long time, up to 360 min, in both anodic oxidation processes, but it is removed very rapidly, for 7-8 min, in electro-Fenton and photoelectro-Fenton. Comparison of results of Figs. 6a and 5 evidences that in each method this primary product disappears at the same time as the initial pollutant. In contrast, Fig. 6b shows that 4-chlorocatechol is accumulated in much smaller extent in the two latter EAOPs, disappearing in 7 min. The same removal time is found for *p*-benzoquinone in electro-Fenton and photoelectro-Fenton, although it persists for 60 and 360 min in anodic oxidation with and without UVA irradiation, respectively (see Fig. 6c). These findings suggest the parallel quick photolysis of *p*-benzoquinone by UVA light, which it is not observed in photoelectro-Fenton because it reacts much more quickly with $^{\bullet}OH$.

From the above results, a general reaction sequence for the initial degradation of clofibric acid is proposed in Fig. 7, where pollutants can react with BDD($^{\bullet}OH$) formed at the anode surface from

reaction (1) and/or with •OH produced from Fenton's reaction (3) in the medium. The process is initiated by the breaking of the C(1)-O bond of clofibric acid by both oxidants to yield 4-chlorophenol and 2-hydroxyisobutyric acid as primary products. Further attack of BDD(•OH) and •OH on the C(4)-position of 4-chlorophenol gives hydroquinone, with loss of Cl^- ion, which is then oxidized to *p*-benzoquinone. Parallel hydroxylation of 4-chlorophenol only by attack of •OH on its C(2)-position leads to 4-chlorocatechol. The subsequent oxidation of the latter product, with release of Cl^-, and *p*-benzoquinone (not shown in Fig. 7) can cause the opening of their benzenic rings to yield different carboxylic acids. The formation of such products was confirmed from analysis of degraded solutions by ion-exclusion HPLC chromatography.

Ion-exclusion chromatograms of solutions treated by the two anodic oxidation methods displayed peaks ascribed to small contents of generated carboxylic acids such as 2-hydroxyisobutyric at t_r = 12.6 min, tartronic at t_r = 7.7 min, maleic at t_r = 8.1 min, fumaric at t_r = 16.1 min, formic at t_r = 14.0 min and oxalic at t_r = 6.6 min. Tartronic, maleic, fumaric and formic acids come from the oxidation of the aryl moiety of aromatics [26,29,31], whereas 2-hydroxyisobutyric acid is expected to be released in the early stages of the degradation process when 4-chlorophenol is formed (see Fig. 7). All these acids, except oxalic acid, were undetected or detected as traces for short time in electro-Fenton and photoelectro-Fenton. Oxalic acid was accumulated in large extent and persisted up to the end of the mineralization in both processes. This ultimate acid formed from the independent oxidation of the precedent longer-chain carboxylic acids, as well as formic acid, are directly converted into CO_2 [17,29,31].

Fig. 6d presents the time-course of oxalic acid concentration during all treatments. In both anodic oxidation methods this acid is formed and destroyed at similar rate, reaching 5-6 mg l^{-1} as maximum at 180 min and disappearing in 360 min, just when the initial substrate is completely removed (see Fig. 5a) and the solution is totally decontaminated (see Fig. 1). This confirms the simultaneous destruction of clofibric acid and most of its products with BDD(•OH) in these

processes, in agreement with the constant efficiency found during degradation (see Fig. 4a). In contrast, oxalic acid reaches high contents of 68 and 59 mg l^{-1} after 40 min of electro-Fenton and photoelectro-Fenton, respectively, due to the very quick oxidation of precedent organics with $^{\bullet}OH$ formed from Fenton's reaction (3). Nevertheless, it is completely removed in 240 min by photoelectro-Fenton, just when the solution is totally decontaminated (see Fig. 1), still remaining about 6 mg l^{-1} (less than 1.5 mg l^{-1} of TOC) in solution after 360 min of electro-Fenton. Since in these EAOPs a large amount of Fe^{3+} is formed in the medium from reactions (3) and (4), oxalic acid is really expected to be present in the form of Fe^{3+}-oxalato complexes, which can not be oxidized by $^{\bullet}OH$ in the medium [23,29,33]. Our results indicate that these complexes are slowly mineralized in electro-Fenton with a BDD anode and even more quickly photodecomposed by UVA irradiation in photoelectro-Fenton.

According to these considerations, Fig. 8 shows a proposed degradation pathway for oxalic acid under the present experimental conditions. This acid is oxidized to CO_2 with BDD($^{\bullet}OH$) at the anode surface either directly in both anodic oxidation treatments or as Fe^{3+}-oxalato complexes in electro-Fenton. The latter complexes also undergo a parallel quick photodecarboxylation under the action of UVA light in photoelectro-Fenton, with regeneration of Fe^{2+} as proposed by Zuo and Hoigné [34]. This photolytic reaction explains the fastest degradation rate and highest efficiency of photoelectro-Fenton. The fact that oxalic acid is still detected after 6 h of electro-Fenton, while it is removed at the same time for anodic oxidation, suggests a slower reaction of BDD($^{\bullet}OH$) with its Fe^{3+} complexes that causes the decay in oxidation power of this EAOP at long electrolysis time.

4. Conclusions

It is demonstrated that EAOPs such as electro-Fenton with Fe^{2+} and photoelectro-Fenton with Fe^{2+} and UVA light, both with a BDD anode, yield an efficient and complete degradation of

aqueous solutions of clofibric acid up to saturation at pH 3.0. The efficiency of both methods increases with rising metabolite concentration and with decreasing current density. Comparative treatments by anodic oxidation are much slower, confirming the high production of $^{\bullet}OH$ from Fenton's reaction (3) in the above EAOPs. In all methods Cl^- is released and totally oxidized to Cl_2 on BDD. The clofibric acid decay always follows a pseudo-first-order kinetics. This compound is hydroxylated to yield 4-chlorophenol, which is further oxidized either to *p*-benzoquinone via hydroquinone or to 4-chlorocatechol. These products are subsequently degraded to tartronic, maleic and fumaric acids, which are quickly converted into oxalic acid. The latter acid is also obtained from the oxidation of 2-hydroxyisobutyric acid, initially generated when 4-chlorophenol is formed. Formic acid also generated in the degradation path is rapidly converted into CO_2. The ultimate product oxalic acid is then transformed into CO_2 on BDD either directly in anodic oxidation or as Fe^{3+}-oxalato complexes in electro-Fenton. The parallel quick photolysis of these complexes by UVA light in photoelectro-Fenton explains the fastest degradation rate and highest efficiency of this method, which appears to be the best EAOP for the treatment of wastewaters containing clofibric acid.

Acknowledgements

Financial support from MEC (Ministerio de Educación y Ciencia, Spain) under project CTQ2004-01954/BQU and the grant awarded to I. Sirés from DURSI (Departament d'Universitats, Recerca i Societat de la Informació, Generalitat de Catalunya) to do this work are acknowledged.

References

[1] T. Heberer, H.J. Stan, Int. J. Environ. Anal. Chem. 67 (1997) 113-124.

[2] H.R. Buser, M.D. Muller, N. Theobald, Environ. Sci. Technol. 32 (1998) 188-192.

[3] K.Kümmerer, (Ed.), Pharmaceuticals in the Environment. Sources, Fate and Risks, Springer, Berlin, 2001.

[4] D.W. Kolpin, E.T. Furlong, M.T. Meyer, E.M. Thurman, S.D. Zaugg, L.B. Barber, Environ. Sci. Technol. 36 (2002) 1202-1211.

[5] T.A. Ternes, M. Meisenheimer, D. McDowell, F. Sacher, H.J. Brauch, B. Haist-Gulde, G. Preuss, U. Wilme, N. Zulei-Seibert, Environ. Sci. Technol. 36 (2002) 3855-3863.

[6] C. Tixier, H.P. Singer, S. Oellers, S.R. Müller, Environ. Sci. Technol. 37 (2003) 1061-1068.

[7] J.L. Packer, J.J. Werner, D.E. Latch, K. McNeill, W.A. Arnold, Aq. Sci. 65 (2003) 342-351.

[8] J.P. Bound, N. Vaulvaulis, Chemosphere 56 (2004) 1143-1155.

[9] A. Tauxe-Wuersch, L.F. De Alencastro, D. Grandjean, J. Tarradellas, Water Res. 39 (2005) 1761-1772.

[10] J.P. Emblidge, M.E. DeLorenzo, Environ. Res. 100 (2006) 216-226.

[11] R. Andreozzi, V. Caprio, R. Marotta, A. Radovnikovic, J. Hazard. Mat. B103 (2003) 233-246.

[12] T. Doll, F.H. Frimmel, Water Res. 38 (2004) 955-964.

[13] I. Sirés, P.L. Cabot, F. Centellas, J.A. Garrido, R.M. Rodríguez, C. Arias, E. Brillas, Electrochim. Acta 52 (2006) 75-85.

[14] M. Panizza, P.A. Michaud, G. Cerisola, Ch. Comninellis, J. Electroanal. Chem. 507 (2001) 206-214.

[15] B. Marselli, J. García-Gomez, P.A. Michaud, M.A. Rodrigo, Ch. Comninellis, J. Electrochem. Soc. 150 (2003) D79-D83.

[16] A. Kraft, M. Stadelmann, M. Blaschke, J. Hazard. Mat. B 103 (2003) 247-261.

[17] C.A. Martinez-Huitle, S. Ferro, A. De Battisti, Electrochim. Acta 49 (2004) 4027-4034.

[18] M. Panizza, G. Cerisola, Electrochim. Acta 51 (2005) 191-199.

[19] A. Alverez-Gallegos, D. Pletcher, Electrochim. Acta 44 (1999) 2483-2492.

[20] T. Harrington, D. Pletcher, J. Electrochem. Soc. 146 (1999) 2983-2989.

[21] M.A. Oturan, J.J. Aaron, N. Oturan, J. Pinson, Pestic. Sci. 55 (1999) 558-562.

[22] M. A. Oturan, J. Appl. Electrochem. 30 (2000) 475-482.

[23] B. Boye, M.M. Dieng, E. Brillas, Environ. Sci. Technol. 36 (2002) 3030-3035.

[24] B. Gözmen, M.A. Oturan, N. Oturan, O. Erbatur, Environ. Sci. Technol. 37 (2003) 3716-3723.

[25] E. Brillas, M.A. Baños, S. Camps, C. Arias, P.L. Cabot, J.A. Garrido, R.M. Rodríguez, New J. Chem. 28 (2004) 314-322.

[26] E. Brillas, B. Boye, I. Sirés, J.A. Garrido, R.M. Rodríguez, C. Arias, P.L. Cabot, Ch. Comninellis, Electrochim. Acta 49 (2004) 4487-4496.

[27] K. Hanna, S. Chiron, M.A. Oturan, Water Res. 39 (2005) 2763-2773.

[28] A. Wang, J. Qu, J. Ru, H. Liu, J. Ge, Dyes Pigments 65 (2005) 227-233.

[29] I. Sirés, J.A. Garrido, R.M. Rodríguez, P.L. Cabot, F. Centellas, C. Arias, E. Brillas, J. Electrochem. Soc. 153 (2006) D1-D9.

[30] S. Irmak, H.I. Yavuz, O. Erbatur, Appl. Catal. B: Environ. 63 (2006) 243-248.

[31] C. Flox, S. Ammar, C. Arias, E. Brillas, A.V. Vargas-Zavala, R. Abdelhedi, Appl. Catal. B: Environ. 67 (2006) 93-104.

[32] Y. Sun, J.J. Pignatello, Environ. Sci. Technol. 27 (1993) 304-310.

[33] G.U. Buxton, C.L. Greenstock, W.P. Helman, A.B. Ross, J. Phys. Chem. Data Ref. 17 (1988) 513-886.

[34] Y. Zuo, J. Hoigné, Environ. Sci. Technol. 26 (1992) 1014-1022.

[35] J. Lee, D.A. Tryk, A. Fujishima, S.M. Park, Chem. Commun. (2002) 486-487.

Figure captions

Fig. 1. TOC removal with specific charge for the degradation of 100-ml solutions containing 179 mg l^{-1} clofibric acid and 0.05 M Na_2SO_4 of pH 3.0 at 100 mA cm^{-2} and at 35.0 ºC using an undivided cell with a 3-cm^2 BDD anode and a 3-cm^2 carbon-PTFE cathode fed with pure O_2 at 12 ml min^{-1}. Method: (○) anodic oxidation with electrogenerated H_2O_2, (●) anodic oxidation with electrogenerated H_2O_2 under a 6-W UVA irradiation with λ_{max} = 360 nm, (■) electro-Fenton with 1.0 mM Fe^{2+} and (▲) photoelectro-Fenton with 1.0 mM Fe^{2+} and UVA light.

Fig. 2. Effect of experimental parameters on TOC abatement vs. specific charge for the treatment of 100 ml of clofibric acid solutions of pH 3.0 at 35.0 ºC by electro-Fenton with a BDD anode and 1.0 mM Fe^{2+}. In plot (a), metabolite concentration: 179 mg l^{-1}; current density: (◆) 33, (■) 100 and (▼) 150 mA cm^{-2}. In plot (b), metabolite concentration: (□) 557 (close to saturation), (◇) 358, (■) 179 and (Δ) 89 mg l^{-1}; current density: 100 mA cm^{-2}.

Fig. 3. Concentration of chloride ion accumulated during the treatment of 100 ml of 179 mg l^{-1} clofibric acid solutions of pH 3.0 at 100 mA cm^{-2} and at 35.0 ºC using a BDD anode and electrogenerated H_2O_2 by: (○) anodic oxidation, (■) electro-Fenton and (▲) photoelectro-Fenton.

Fig. 4. Mineralization current efficiency calculated from Eq. 8 vs. specific charge. Plot(a) corresponds to the experiments shown in Fig. 1 and plot (b) to those reported in Figs. 2a and 2b.

Fig. 5. Time-course of clofibric acid concentration during the degradation of 100 ml of 179 mg l^{-1} metabolite solutions of pH 3.0 at 35.0 ºC with a BDD anode and electrogenerated H_2O_2. Plot (a): (○) anodic oxidation and (●) anodic oxidation with UVA light at 100 mA cm^{-2}. Plot (b): electro-Fenton at (◆) 33, (■) 100 and (▼) 150 mA cm^{-2} and (▲) photoelectro-Fenton at 100 mA cm^{-2}. The

inset panels show the corresponding kinetic analysis assuming a pseudo first-order reaction for clofibric acid.

Fig. 6. Evolution of the concentration of selected intermediates during the mineralization of 100 ml of 179 mg l^{-1} clofibric acid solutions of pH 3.0 at 100 mA cm^{-2} and at 35.0 °C with a BDD anode and electrogenerated H_2O_2. Plots correspond to: (a) 4-chlorophenol, (b) 4-chlorocatechol, (c) *p*-benzoquinone and (d) oxalic acid. Method: (○) anodic oxidation, (●) anodic oxidation with UVA light, (■) electro-Fenton and (▲) photoelectro-Fenton.

Fig. 7. Proposed reaction sequence for the initial degradation of clofibric acid with a BDD anode and electrogenerated H_2O_2 by anodic oxidation, electro-Fenton with Fe^{2+} and photoelectro-Fenton with Fe^{2+} and UVA light. The oxidant hydroxyl radical is denoted as BDD($^{\bullet}$OH) or $^{\bullet}$OH when it is formed at the BDD anode surface or from Fenton's reaction, respectively.

Fig. 8. Proposed reaction pathways for oxalic acid mineralization with a BDD anode and electrogenerated H_2O_2 by anodic oxidation, electro-Fenton with Fe^{2+} and photoelectro-Fenton with Fe^{2+} and UVA light.

Figure(s)

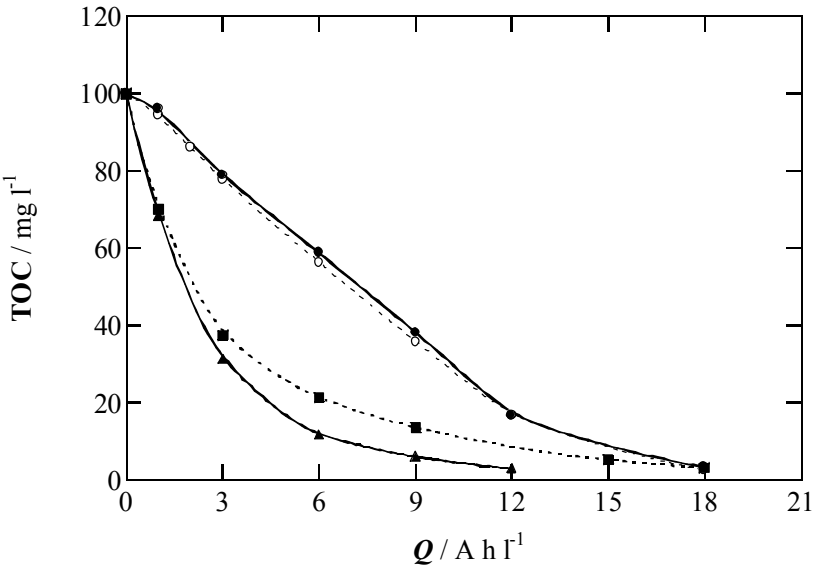

Fig. 1

Figure(s)

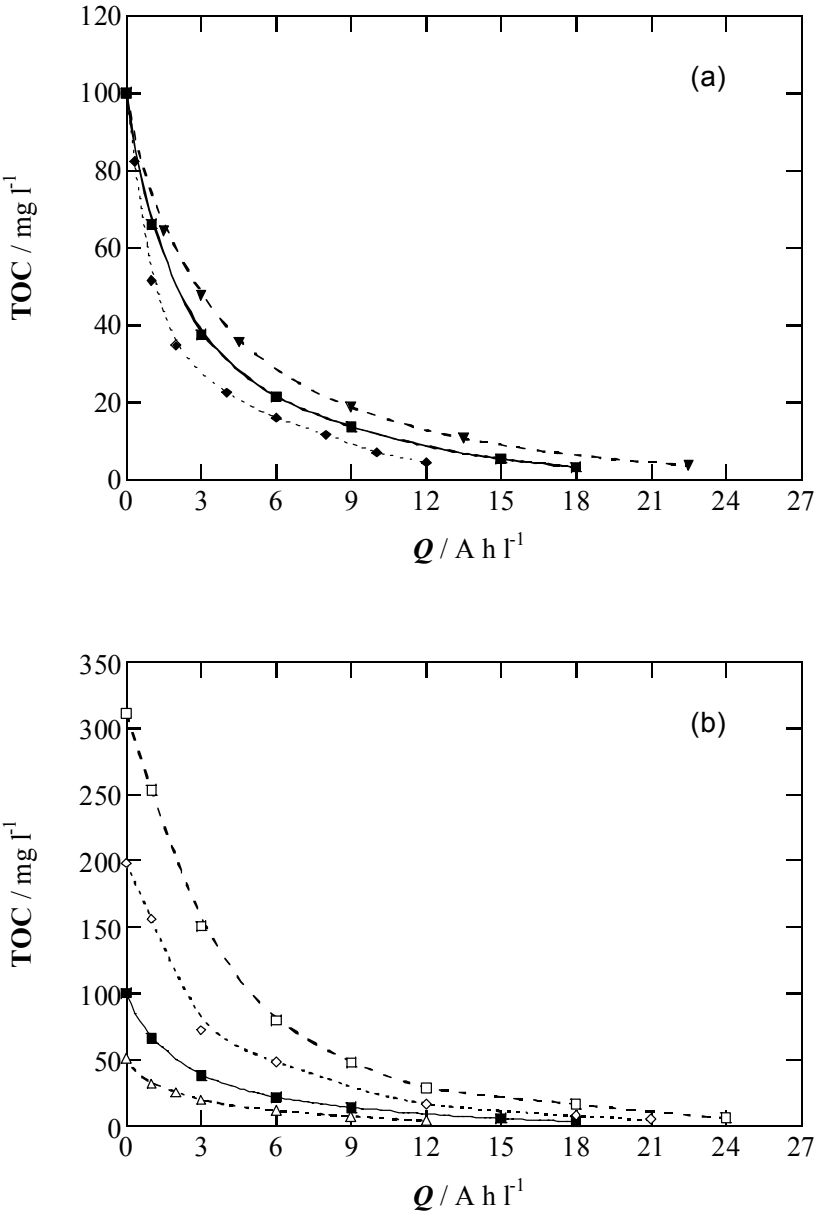

Fig. 2

Figure(s)

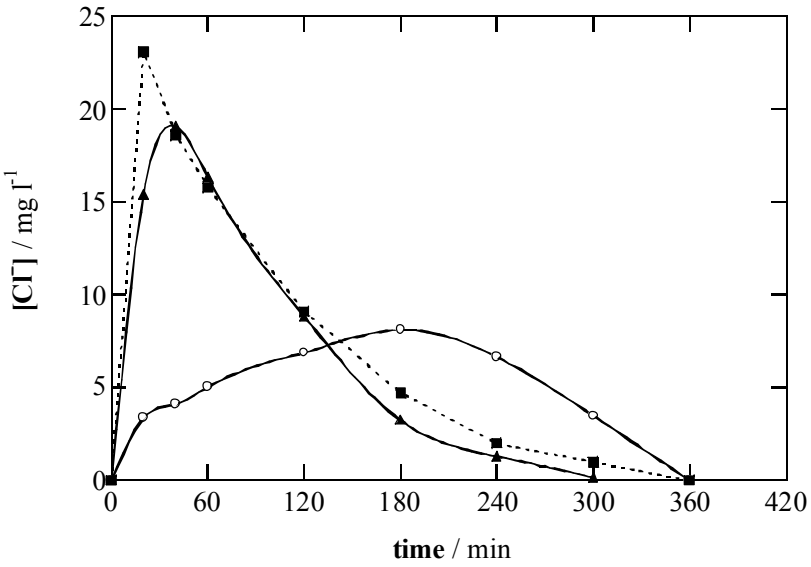

Fig. 3

Figure(s)

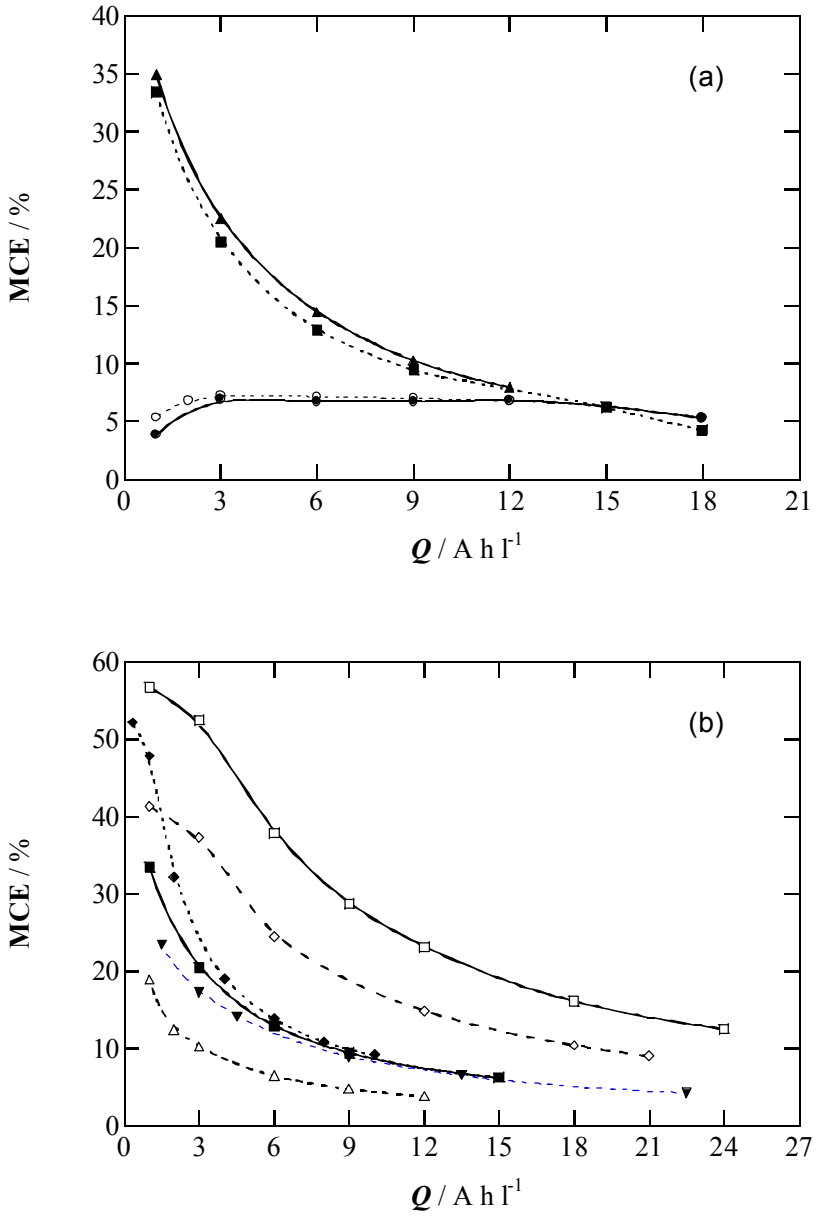

Fig. 4

Figure(s)

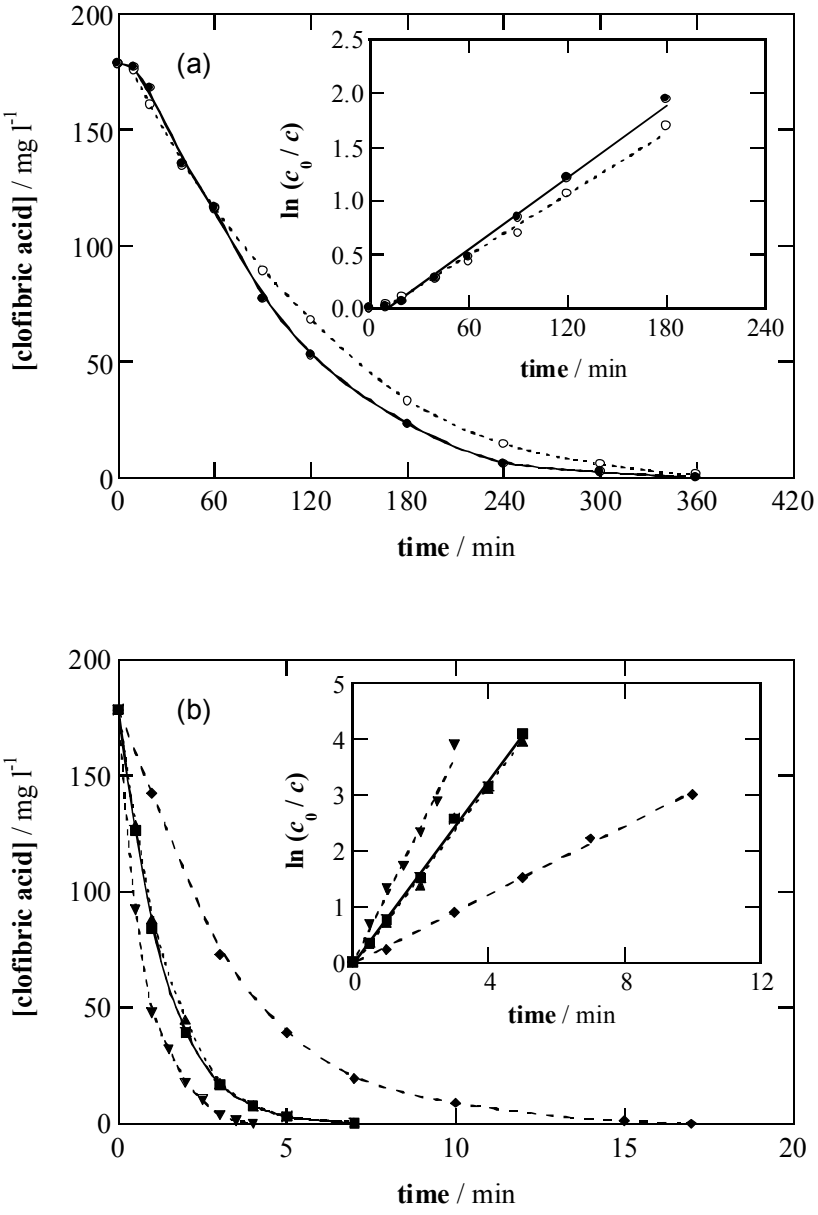

Fig. 5

Figure(s)

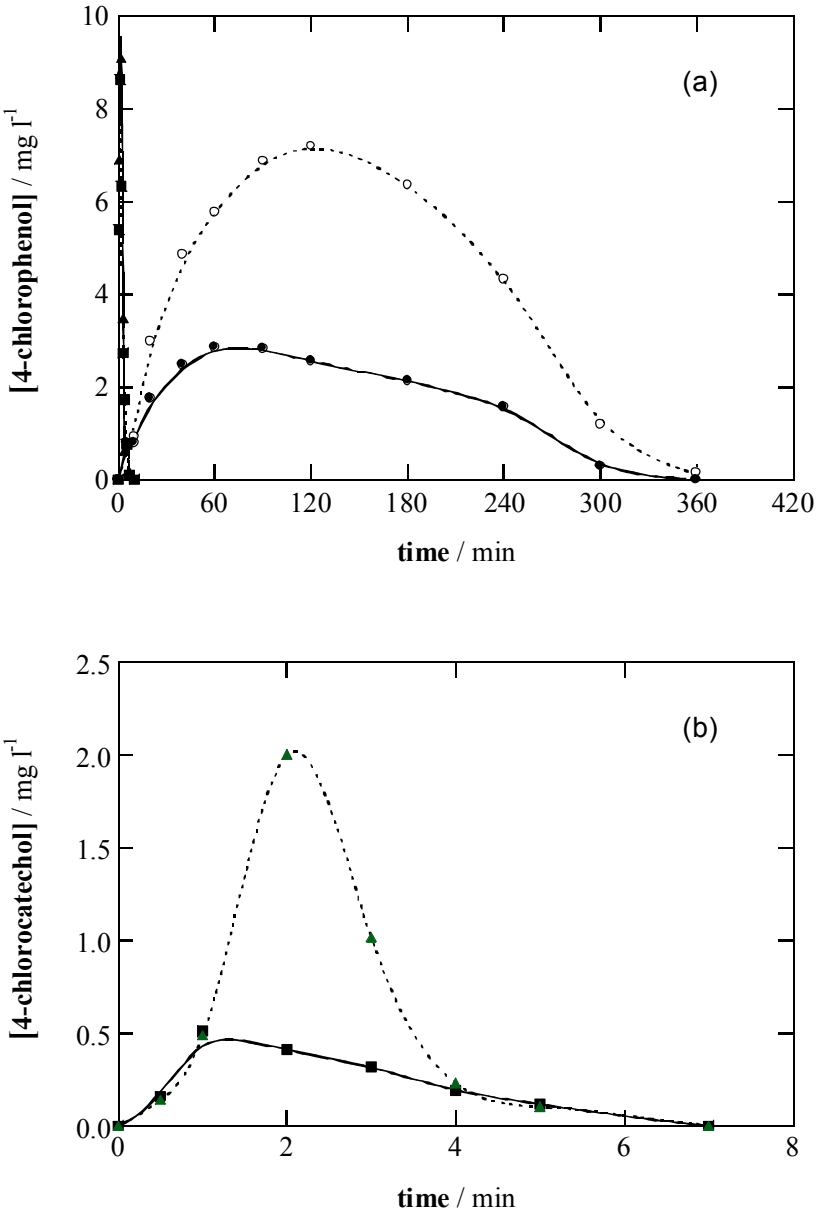

Fig. 6

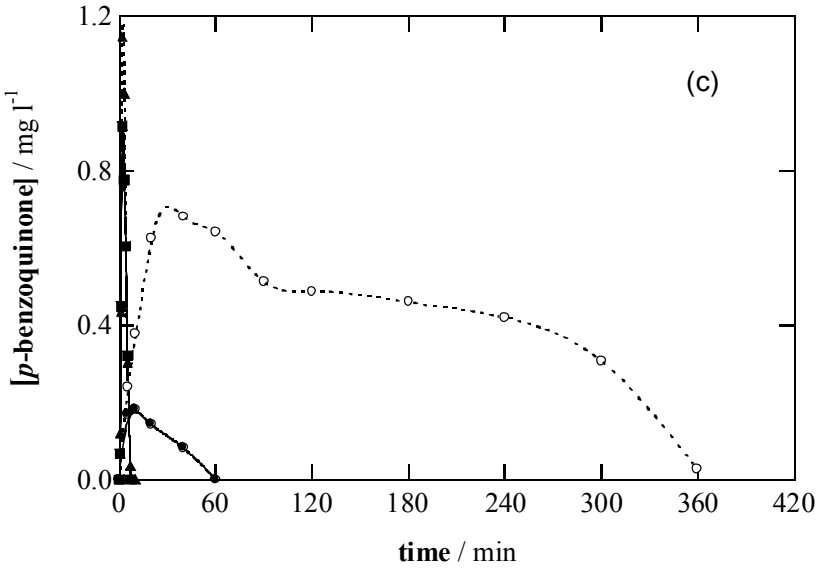
1.2
0.8
0.4
0.0
(c)
[p-benzoquinone] / mg l-1
0
60
120
180
240
300
360
420
time / min

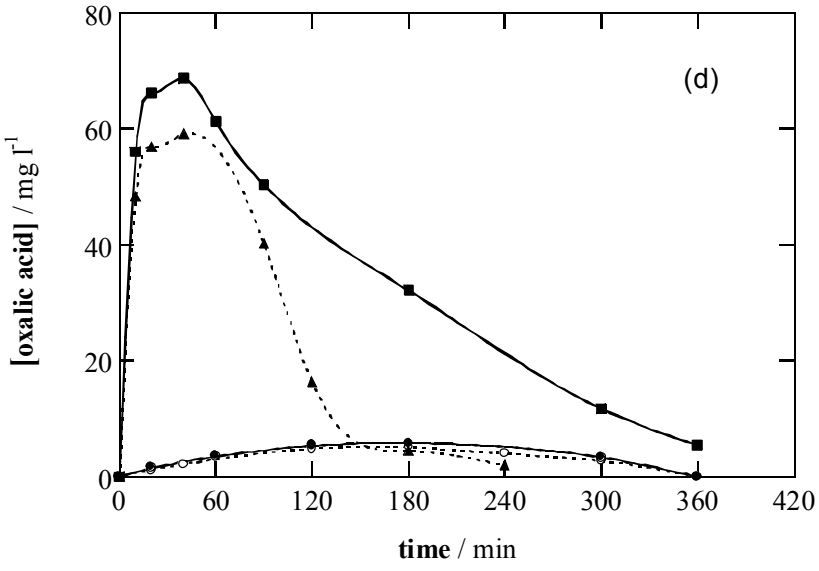
80
60
40
20
0
(d)
[oxalic acid] / mg l-1
0
60
120
180
240
300
360
420
time / min

Fig. 6

Figure(s)

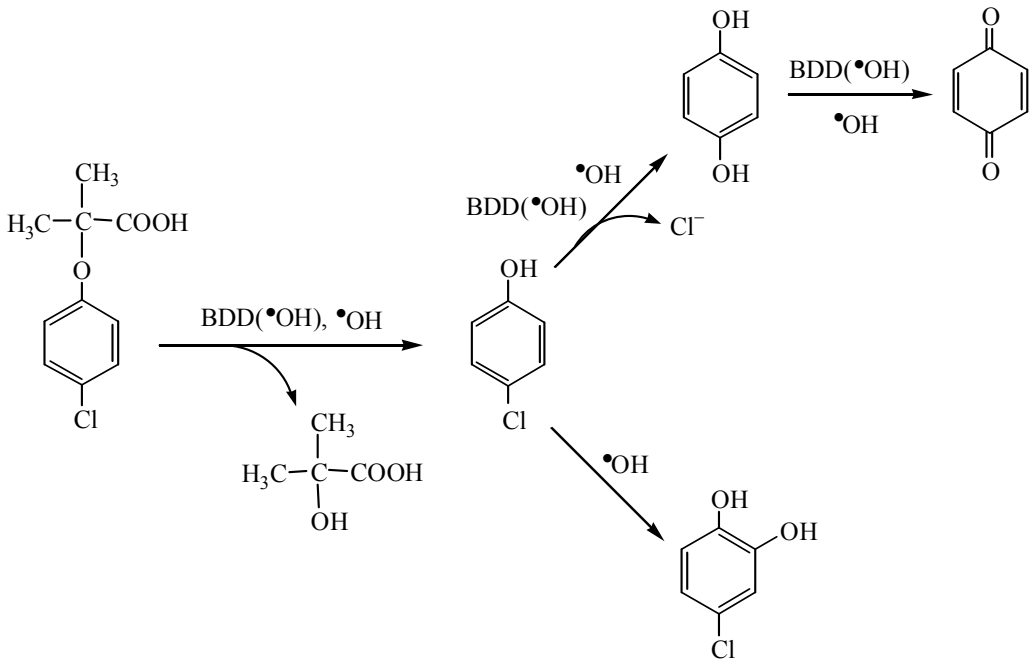

Fig. 7

Figure(s)

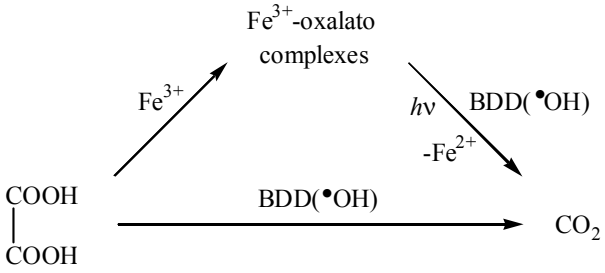

Fig. 8

8.3.2. Resultats i Discussió / *Results and Discussion*

The oxidizing ability of the AO, EF and PEF processes has been asessed through the variation of TOC with specific charge (Q, in A h L^{-1}) for the treatment of 100 mL of 179 mg L^{-1} clofibric acid solutions at pH 3.0 and at 100 mA cm^{-2} using a Pt anode. As expected, AO with electrogenerated H_2O_2 gives a quite slow TOC removal, attaining 41% of mineralization at 18 A h L^{-1} (6 h). This behavior can be accounted for by the low concentration of effective $^{\bullet}OH_{ads}$ formed at the Pt surface from Reaction 5.-44. An analogous degradation rate is observed by AO with UVA irradiation, yielding 39% of TOC abatement at 18 A h L^{-1}. That means that clofibric acid and its intermediates are not directly photodegraded by UVA light. When 1.0 mM Fe^{2+} is present in the solution, TOC decay at 6 h is 79% due to the fast reaction of organics with the great amount of $^{\bullet}OH$ produced from Fenton's reaction (Reaction 5.-3), but some hardly oxidizable products remain still stable. PEF leads to quicker TOC decay and almost overall mineralization (> 96%) at the end of electrolysis. This can be reached because UVA illumination favors: (i) the photodecomposition of complexes of Fe^{3+} with generated carboxylic acids (Reaction 5.-24), and (ii) the regeneration of Fe^{2+} from additional photoreduction of $Fe(OH)^{2+}$, with a simultanous production of additional $^{\bullet}OH$ (Reaction 5.-23).

In contrast, a continuous TOC decay until attaining total mineralization can be observed for all experiments using BDD. This peculiar behavior has been previously shown for AO with BDD in the treatment of paracetamol (section 7.3) and clofibric acid (section 8.2), and again it is an evidence of the great oxidizing power of this anode. But in this case, the time required for total mineralization depends on the method tested. Thus, AO without or with UVA illumination leads to a similar slow TOC abatement up to complete mineralization for 18 A h L^{-1} (6 h), indicating that all organics are destroyed by the high amount of BDD($^{\bullet}OH$), i.e. $^{\bullet}OH_{ads}$, formed at the BDD surface. The degradation rate is strongly enhanced in the EF process due to $^{\bullet}OH$

formed from Fenton's reaction (Reaction 5.-3), but complexes of Fe^{3+} with carboxylic acids can only be oxidized by BDD($^{\bullet}OH$), so total mineralization is slowly attained for 15-18 A h L^{-1} (5-6 h). However, TOC is quickly removed by PEF as pointed out above (Reactions 5.-23 and 5.-24), and overall mineralization is attained for 12 A h L^{-1} (4 h).

In Figure 8.-2 a compendium of all the electrochemical processes proposed in this thesis for the overall mineralization of clofibric acid is presented. Six methods are able to degrade totally 100-mL solutions of pH 3.0 containing 179 mg L^{-1} clofibric acid at 100 mA cm^{-2}. AO with a BDD anode and a stainless steel cathode leads to complete mineralization after the consumption of 21 A h L^{-1} (7 h). AO with a BDD anode and H_2O_2 electrogeneration slightly accelerates the process (6 h) due to the contribution of H_2O_2, but TOC evolution is practically analogous because it can be considered that the same amount of effective BDD($^{\bullet}OH$) is formed at the BDD surface. It is clear that UVA irradiation does not affect significantly to clofibric acid and its intermediates. A great enhancement of the mineralization rate is achieved with 1.0 mM Fe^{2+} as catalyst due to the generation of high amounts of $^{\bullet}OH$ in the bulk solution. TOC abatement is quite similar in EF with BDD and PEF with Pt, but anyway total mineralization is attained at the same time as that described for AO because Fe^{3+} complexes with carboxylic acids are very slowly oxidized by BDD($^{\bullet}OH$) in EF with BDD and by UVA light in PEF with Pt. PEF with a BDD anode combines the oxidizing power of $^{\bullet}OH$, BDD($^{\bullet}OH$) and UVA light, and as a result TOC is completely removed at 4 h.

At this point, it is worth mentioning that parallel oxidation of organics with weaker oxidizing species formed in the bulk solution, such as $HO_2^{\bullet}$, H_2O_2, $SO_4^{\bullet-}$ [182], ferrate ions [92] and other hypervalent iron species [148], as well as at the BDD surface, as for example O_3, H_2O_2 and $S_2O_8^{2-}$ ions, is also possible. In addition, whenever BDD anode is used and chlorinated compounds are treated, the oxidizing substance Cl_2 is formed in the medium [377]. There is no doubt about the fact that all these species

can play a significant role regarding the destruction of pollutants in the solution, but at the same time it is necessary to realize that considering hydroxyl radicals as the main oxidizing agents constitutes more than an acceptable approach that helps simplifying these systems and the reactions involved, so the conclusions can be presented on the basis of this prevailing oxidizing agent.

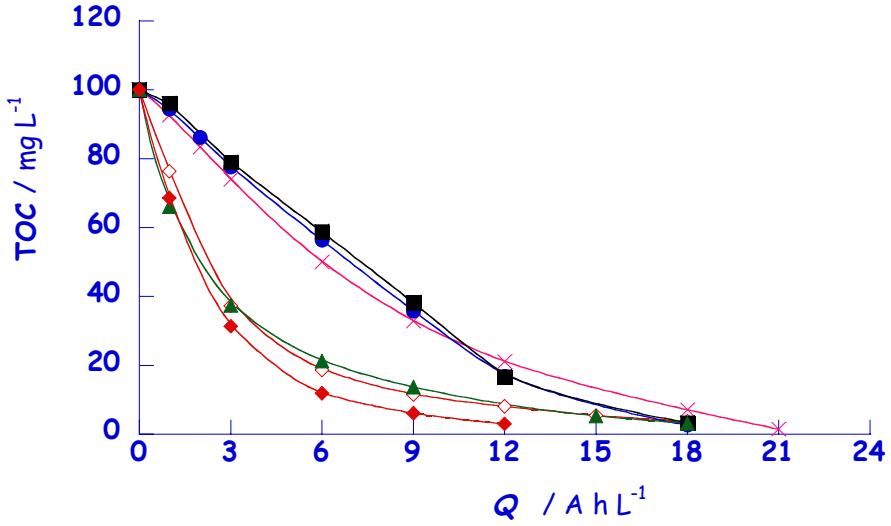

Figure 8.-2 TOC vs. specific charge for the degradation of 100 mL of 179 mg L^{-1} clofibric acid solutions in 0.05 M Na_2SO_4 of pH 3.0 at 100 mA cm^{-2} and at 35 °C, using an undivided cell with 3-cm^2 electrodes.
Processes without an O_2-diffusion cathode: (×) AO with a BDD anode and a stainless steel cathode. Processes with an O_2-diffusion cathode: (◊) PEF with a Pt anode and 1.0 mM Fe^{2+} + UVA light, (●) AO with a BDD anode and electrogenerated H_2O_2, (■) latter AO under UVA irradiation, (▲) EF with a BDD anode and 1.0 mM Fe^{2+}, (♦) PEF with a BDD anode and 1.0 mM Fe^{2+}.

Mineralization of clofibric acid is accompanied by its overall dechlorination. Ion chromatograms only display a defined peak related to Cl^- ion. No other chlorine-oxygen ions such as ClO_2^-, ClO_3^- and ClO_4^- were detected by this technique. Chloride ion evolution for the electrolyses of 179 mg L^{-1} clofibric acid solutions of pH 3.0 at 100 mA cm^{-2} using a Pt anode shows that in AO with electrogenerated H_2O_2, Cl^- is gradually accumulated up to 23 mg L^{-1} for 12 A h L^{-1} (4 h) and further on it keeps stable, whereas in EF and PEF a quasi-steady concentration of about 25 mg L^{-1} is already attained at 2 A h L^{-1} (40 min), just undergoing a slight drop due to its

oxidation to Cl_2 at the Pt anode. These findings allow concluding that chloro-organics are always degraded with release of Cl^-, being much more quickly destroyed by EF and PEF. These three methods only lead to the release of 78-85% of the chlorine contained in the initial solution of 179 mg L^{-1} clofibric acid (29.5 mg L^{-1}), suggesting that stable colored polyaromatics formed during the degradation process contain the remaining chlorine. On the other hand, the results for the same processes using a BDD anode show that Cl^- is acumulated and completely removed after 300-360 min in all cases, after reaching a maximum concentration of about 8 mg L^{-1} at 180 min in AO, 23 mg L^{-1} at 20 min in EF and 19 mg L^{-1} at 40 min in PEF, corresponding to 27%, 78% and 64% of the initial chlorine content. The slow accumulation in AO confirms the slow reaction of chloro-organics with BDD($^{\bullet}OH$), whereas its much faster release at early stages of EF and PEF corroborates the quick destruction of pollutants with $^{\bullet}OH$ in the bulk solution. The progressive destruction of Cl^- when electrolysis is prolonged can be explained by its slow oxidation to Cl_2 on BDD. In comparison with the chloride ion evolution depicted in section 8.2, the AO behavior is very similar, but EF and PEF exhibit such an oxidizing ability that a fast great accumulation of Cl^- can be attained at their early stages, further being quasi-stabilized when Pt is used and gradually oxidized when BDD is used.

The study of the influence of initial pH in PEF with Pt and EF with BDD, at 100 mA cm^{-2}, confirms in both cases that the quickest TOC decay takes place for initial pH 3.0, as can be seen for example in Figure 8.-3 given below. For the rest of electrolyses tested, the mineralization rate falls in the order pH 2.0 > pH 4.0 >> pH 6.0. This fact can be easily associated to the highest generation rate of $^{\bullet}OH$ from Fenton's reaction. It is interesting to note that in PEF with Pt the total mineralization can be attained uniquely at pH 3.0, whereas in EF with BDD it can be achieved at all pH values studied. This is coherent because the systems with Pt are based on Fenton's reaction with $^{\bullet}OH$ formation, and thus an increase in pH is related to a total loss of the oxidizing ability, whereas in the systems with BDD a significant parallel

oxidizing route with BDD(•OH) and other weaker species continues acting at high pH values, making these processes viable in a wider variety of conditions.

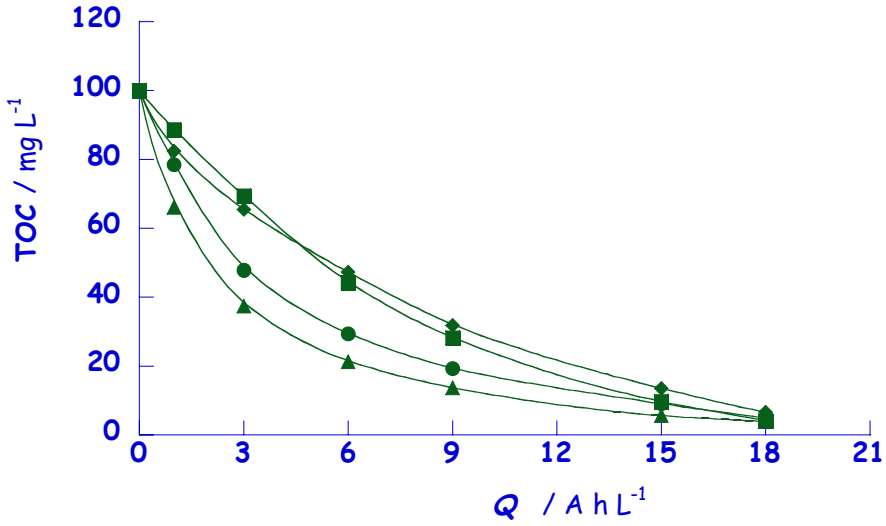

Figure 8.-3 Effect of pH on TOC removal vs. specific charge for the degradation of 100 mL of 179 mg L^{-1} clofibric acid solutions by EF with 1.0 mM Fe^{2+} in 0.05 M Na_2SO_4 of pH 3.0 at 100 mA cm^{-2} and at 35 °C, using an undivided cell with a 3-cm^2 BDD anode and a 3-cm^2 O_2-diffusion cathode.
Initial solution pH: (●) 2.0, (▲) 3.0, (■) 4.0, (♦) 6.0.

The effect of current density on the oxidation ability of the two processes aforementioned has been studied for 100-mL solutions with 179 mg L^{-1} clofibric acid at pH 3.0 and at 33, 100 and 150 mA cm^{-2}. A progressive increase in Q from 7 to 27 A h L^{-1} (i.e., a decrease in time from 7 to 5.5 h) and from 12 to 22 A h L^{-1} (12 to 5 h) for PEF with Pt and EF with BDD, respectively, is required for overall mineralization when j_{app} increases from 33 to 150 mA cm^{-2}. This increase is indicative of an acceleration of parallel non-oxidizing reactions involving •OH as well as a higher production of other weaker oxidants described elsewhere, whereas the decrease in time required can be mainly ascribed to a greater production of $^{\bullet}OH_{ads}$ at the anode surface due to larger H_2O oxidation, and •OH in the medium because of the greater electrogeneration of H_2O_2 at the cathode (and, to a certain extent, the action of the weaker oxidizing species mentioned).

The great oxidizing power of these two methods has been confirmed by degrading up to 0.56 g L^{-1} (close to saturation) of clofibric acid at pH 3.0 and at 100 mA cm^{-2}. TOC-*Q* plots for PEF with Pt show that overall mineralization is achieved after consumption of 30, 24 and 18 A h L^{-1} (10, 8 and 6 h) for 557, 358 and 179 mg L^{-1} of clofibric acid, respectively. The same initial concentrations of clofibric acid require 24, 21 and 15 A h L^{-1} (8, 7 and 5 h), respectively, for EF with BDD. It is clear that systems using an anode such as BDD, which has a greater oxidizing ability, require less energy consumption to attain overall mineralization (i.e., BDD systems can attain overall mineralization more quickly than Pt systems). In both cases, as initial pollutant concentration decreases, a lower *Q* is required due to the presence of lower amount of organics. Moreover, a higher TOC removal is attained at a given time with increasing initial pollutant content, because the competitive non-oxidizing reactions of $^{\bullet}OH$ and $^{\bullet}OH_{ads}$ become slower and these radicals can react with pollutants to a larger extent.

All these findings, along with the results discussed in section 8.2.2, allow concluding that overall mineralization reaction for clofibric acid involves 44 F for each mol of pharmaceutical, with chloride ion as primary inorganic ion (Reaction 6.-3). The efficiency can then be determined from Equation 6.-1 for the four processes tested at the beginning of this section using Pt and BDD. It can be observed that in the systems with Pt the efficiency for both AO procedures is very small, reaching a maximum value of 3.3%-3.8% at 6 A h L^{-1} (2 h), as expected from their low oxidation ability. In contrast, MCE reaches a value of 25% and 23% at the early stages in EF and PEF, respectively, but the efficiency of PEF is clearly higher from 3 A h L^{-1} (1 h) because it is able to destroy all products. On the other hand, in the systems with BDD a constant efficiency of about 7% is found for both AO methods, suggesting a constant slow mineralization rate of all organics with BDD($^{\bullet}OH$). MCE values are much higher in EF and PEF, attaining 33% and 31% at 20 min, and again PEF is the most efficient method from 3 A h L^{-1} (1 h). In Figure 8.-4 given below the MCE-*Q* plots for

the six experiments leading to total mineralization shown in the above Figure 8.-2 are represented. All AO processes have a low constant MCE along the electrolysis, whereas EF and PEF exhibit much higher MCE values at their early stages thanks to the great production of •OH from Fenton's reaction. Systems with BDD in particular show the highest efficiencies because of the action of additional weaker oxidizing species. In EF and PEF, MCE always undergoes a dramatic drop with time (i.e., with *Q*), due to the hardly oxidizable products generated and/or the increase of parallel non-oxidizing reactions because lower amounts of organics are present in the medium.

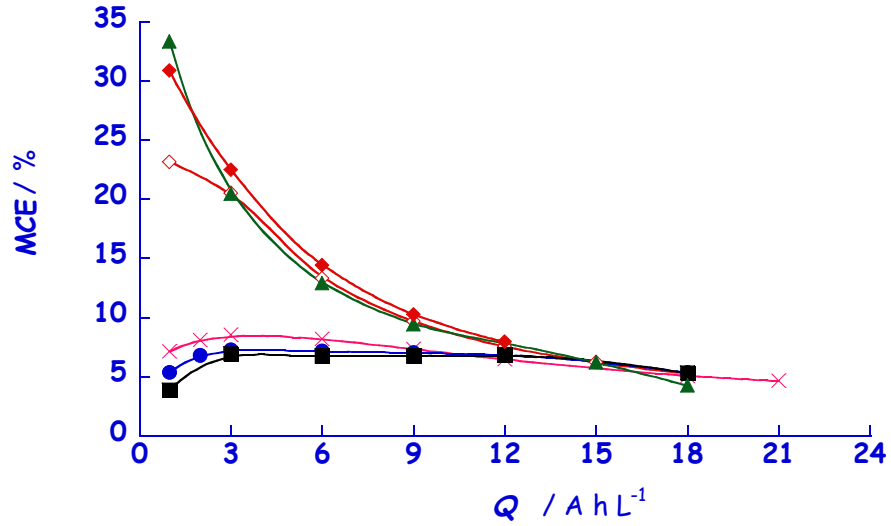

Figure 8.-4 Change of MCE with specific charge for the experiments shown in Fig.8.-2.

On the other hand, from the MCE values at the different j_{app} and initial concentrations for PEF with Pt and EF with BDD, it can be concluded that the efficiency strongly increases with rising initial clofibric acid and decreasing j_{app}. Results show a slight increase in the efficiency at the early stages of most treatments, as expected if higher amount of pollutants is more easily converted into CO_2. Afterwards, a continuous drop in MCE is observed in all treatments. Electrolyses of 179 mg L^{-1} clofibric acid at pH 3.0 show decreasing efficiencies as j_{app} increases. This tendency could seem contradictory to the fact that rising j_{app} causes the increase in degradation rate due to the production of more amounts of •OH and $•OH_{ads}$ in the

medium and at the anode surface, respectively. But certainly, a greater electrical consumption (i.e., a greater *Q*) is required to mineralize because a larger proportion of both kind of hydroxyl radicals is wasted in parasite reactions, yielding a smaller proportion of this oxidizing agent with enough ability to destroy organics. For example, after 1 h of PEF with Pt decreasing MCE values of 46% (1 A h L^{-1}), 20% (3 A h L^{-1}) and 14% (4.5 A h L^{-1}) are found at increasing j_{app} values of 33, 100 and 150 mA cm^{-2}, respectively. At constant j_{app} of 100 mA cm^{-2} and at pH 3.0 higher MCE values are obtained when initial concentration of pollutant rises, because of the slower production of hardly oxidizable intermediates. For example, at 1 h (3 A h L^{-1}) of PEF with Pt, increasing MCE values of 8.2%, 20%, 32% and 45% are obtained for 89, 179, 358 and 557 mg L^{-1} clofibric acid, respectively. This tendency also confirms the gradual reaction of higher amount of $^{\bullet}OH$ and $^{\bullet}OH_{ads}$ with more pollutants, indicating that this hydroxyl radical is wasted to a smaller extent. Overall mineralization is achieved by PEF with Pt and by both, EF and PEF with BDD. It must be noted that the greatest maximum MCE values among the different studies carried out in this thesis are found for EF and PEF of clofibric acid. Thus, efficiencies of 50% and 57% are obtained at 20 min when saturated solutions of this compound at pH 3.0 are electrolyzed at 100 mA cm^{-2} by PEF with Pt and EF with BDD, respectively.

Regarding the kinetics of clofibric acid decay, first of all the role of weak oxidants has been assessed. Reversed-phase chromatograms for 100-mL solutions of pH 3.0 containing 179 mg L^{-1} clofibric acid, 20 mM H_2O_2 and 0.05 M Na_2SO_4 show no alteration in the pharmaceutical content, thus assuring that it can not react with electrogenerated H_2O_2. In addition, it must be reminded that in section 8.2.2 it was also demonstrated that the concentration of clofibric acid remains unaltered towards chemical oxidation by $S_2O_8^{2-}$, one of the oxidizing species produced in the systems with BDD. As a whole, it means that the comparative kinetics of the removal of clofibric acid can be discussed on the basis of its reaction with generated strong oxidizing agents such as $^{\bullet}OH$ and $^{\bullet}OH_{ads}$. Therefore, the kinetics of clofibric acid

destruction by both kind of hydroxyl radicals has been studied for the four methods pointed out above using Pt and BDD, by electrolyzing 179 mg L^{-1} clofibric acid solutions of pH 3.0 at 100 mA cm^{-2}. On the one hand, clofibric acid decays with time by AO with electrogenerated H_2O_2 using Pt and BDD have been studied. For a better comparison between all the AO processes applied to the clofibric acid destruction, the decays for these four AO processes with electrogenerated H_2O_2, along with the decays for the two AO processes using a stainless steel cathode in section 8.2, are gathered in Figure 8.-5 shown below. From these results, it is possible to come to three main conclusions: (i) clofibric acid concentration undergoes a similar fall without and with UVA illumination, thus confirming that this pharmaceutical is not directly photolyzed by UVA light, (ii) in all cases clofibric acid is more quickly destroyed and transformed into its intermediates using Pt, despite the fact that clofibric acid is more slowly mineralized with this anode than with BDD, and then, a higher adsorption of clofibric acid on Pt surface, favoring its reaction with the main oxidizing agent in AO (i.e., $^{\bullet}OH_{ads}$), can be hypothesized, and (iii) when BDD is used, clofibric acid disappears at a time similar to that needed for its total mineralization, thus confirming that the initial pollutant persists in the solution up to the end of the degradation process due to its simultaneous degradation along with all intermediates. As an example to corroborate these three trends, it can be noted in Figure 8.-5 that clofibric acid disappears after 240 min by AO processes with Pt, and after 360 min by AO with BDD. The latter data is similar to the one observed for total mineralization with BDD depicted in Figure 8.-2. Good straight lines are obtained when the concentrations decays in Figure 8.-5 are fitted to a pseudo-first-order kinetic equation, as shown in the respective inset panel. This behaviour suggests that a steady $^{\bullet}OH_{ads}$ concentration reacts with the drug along the electrolysis, giving an average pseudo-first-order rate constant (k_1) of (4.70±0.10) x 10^{-4} s^{-1} and (1.70±0.13) x 10^{-4} s^{-1} for AO with H_2O_2 electrogeneration using Pt and BDD, respectively. These values are very close to 4.0 x 10^{-4} and 1.3 x 10^{-4} s^{-1} for Pt and BDD, respectively, found in AO with a stainless steel cathode.

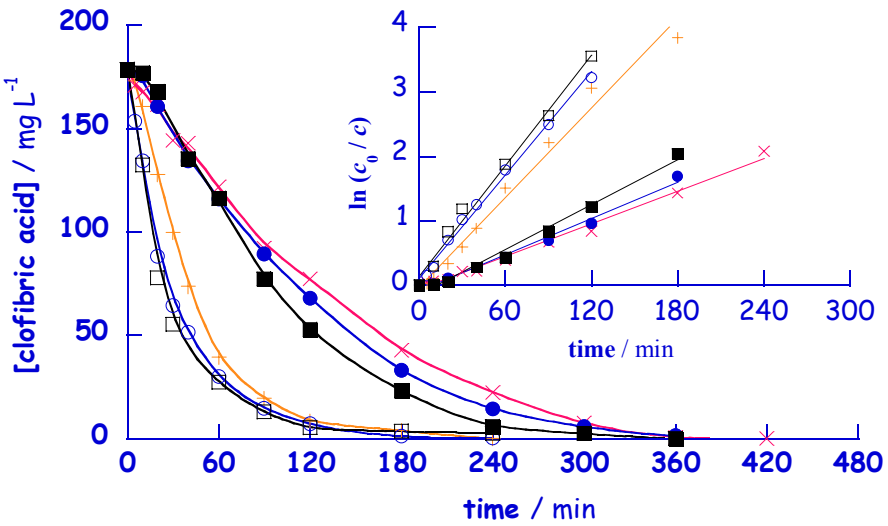

Figure 8.-5 Clofibric acid decay with electrolysis time for the AO process of 100 mL of 179 mg L^{-1} clofibric acid solutions in 0.05 M Na_2SO_4 of pH 3.0 at 100 mA cm^{-2} and at 35 °C, using an undivided cell with 3-cm^2 electrodes.
Process: (+) AO with a Pt anode and a stainless steel cathode, (×) AO with a BDD anode and a stainless steel cathode, (○) AO with a Pt anode and electrogenerated H_2O_2, (□) Latter AO under UVA irradiation, (●) AO with a BDD anode and electrogenerated H_2O_2, (■) Latter AO under UVA irradiation.
The corresponding kinetic analysis assuming a pseudo-first-order reaction for clofibric acid is given in the inset panel.

Similarly, clofibric acid decays with time by both EF and PEF with Pt and BDD can be compared. A comparison between the decays for these four processes during the electrolysis of 179 mg L^{-1} clofibric acid at pH 3.0 and at 100 mA cm^{-2} is depicted in Figure 8.-6 shown below. A much quicker and similar decay of clofibric acid is achieved compared to AO treatments pointed out above, as expected from the great production of $^{\bullet}OH$ from Fenton's reaction. In all cases this pollutant is destroyed at a similar rate, being completely removed after ca. 7 min. Again, kinetic analysis in the inset panel in Figure 8.-6 agrees with a pseudo-first-order reaction, leading to an average k_1-value of (1.35±0.10) x 10^{-2} s^{-1} for the four experiments, thus confirming the prevailing role of $^{\bullet}OH$ compared to $^{\bullet}OH_{ads}$. Moreover, the almost coincidence between EF and PEF indicates a very low generation of $^{\bullet}OH$ from Reaction 5.-23 with UVA irradiation.

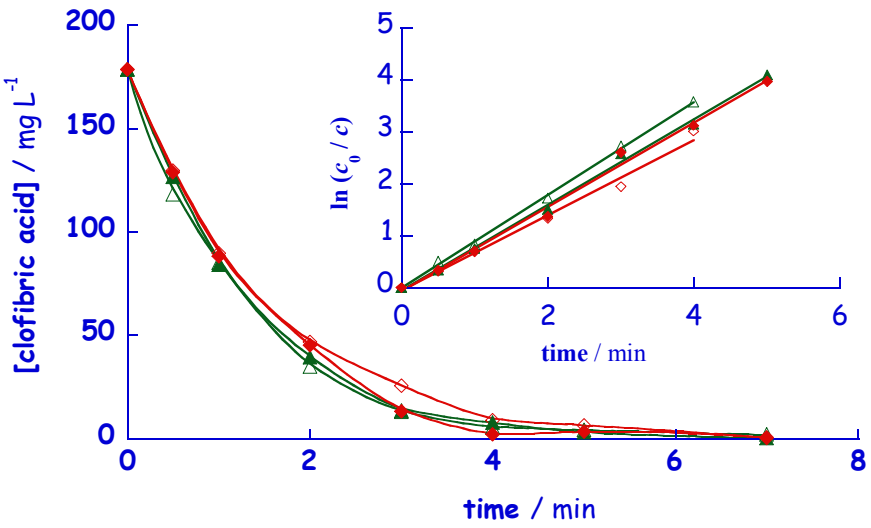

Figure 8.-6 Clofibric acid decay with electrolysis time for the degradation of 100 mL of 179 mg L^{-1} clofibric acid solutions in 0.05 M Na_2SO_4 with 1.0 mM Fe^{2+} of pH 3.0 at 100 mA cm^{-2} and at 35 °C, using an undivided cell with a 3-cm^2 anode and a 3-cm^2 O_2-diffusion cathode.
Process: (Δ) EF with a Pt anode, (◊) PEF with a Pt anode, (▲) EF with a BDD anode, (♦) PEF with a BDD anode.
The corresponding kinetic analysis assuming a pseudo-first-order reaction for clofibric acid is given in the inset panel.

The concentration-time plots obtained for the treatments of 179 mg L^{-1} clofibric acid at different current densities and at pH 3.0 for PEF with Pt and EF with BDD, show that a more rapid decay of clofibric acid is achieved when j_{app} rises, with increasing k_1-values of 6.50 x 10^{-3}, 1.26 x 10^{-2} and 1.81 x 10^{-2} s^{-1} for PEF with Pt, and 5.10 x 10^{-3}, 1.35 x 10^{-2} and 2,04 x 10^{-2} s^{-1} for EF with BDD at higher j_{app} of 33, 100 and 150 mA cm^{-2}, respectively. This trend confirms a larger $^{\bullet}OH$ and $^{\bullet}OH_{ads}$ production when j_{app} increases. It is interesting to say that k_1 does not vary proportionally with this parameter, indicating a progressive rising waste of hydroxyl radicals by parasite reactions. Finally, the possible influence of initial pollutant concentration in PEF with Pt has been clarified from electrolyses of clofibric acid solutions of pH 3.0 up to close to saturation at 100 mA cm^{-2}. A complete removal of the pharmaceutical is reached in all cases. Thus, it disappears after 3, 7, 12 and 18 min for 89, 179, 358 and 557 mg L^{-1}, respectively. Good linear correlations are obtained for all concentrations tested,

assuming a pseudo-first order reaction kinetics, and thus decreasing k_1-values of 3.88 x 10^{-2}, 1.26 x 10^{-2}, 5.60 x 10^{-3} and 4.30 x 10^{-3} s^{-1} are found. This kinetic behavior confirms again the existence of a much greater and constant amount of reactant $^{\bullet}OH$ in comparison with the amount of clofibric acid, even working close to saturation. In addition, the decay in k_1 with rising pollutant concentration indicates the gradual acceleration of competitive reactions between hydroxyl radicals and intermediates, thus enhancing the TOC removal and the MCE values, as previously discussed in this section.

Simultaneously to the clofibric acid decay study, the evolution of aromatic intermediates has been carried out. GC-MS spectra for the experiments reported in section 8.3.1 show peaks related to stable aromatics such as 4-chlorophenol, 4-chlorocatechol, hydroquinone and *p*-benzoquinone. In addition, in the electrolyses with a Pt anode an intense peak ascribed to a chloro-derivative is detected. Although this product can not be identified by pure standards, it can be reasonably assigned to a dehydrated species of 2-(4-chloro-2-hydroxyphenoxy)-2-methylpropionic acid, which is a hydroxylated product of clofibric acid. This compound is detected neither using a BDD anode because it is quickly oxidized, nor in AO with a Pt anode and stainless steel cathode because it is a low oxidizing method. Reversed-phase chromatography for electrolyzed solutions of 179 mg L^{-1} clofibric acid of pH 3.0 at 100 mA cm^{-2} has been carried out for AO, EF and PEF using both Pt and BDD to know the different evolution of each aromatic. 4-Chlorophenol, 4-chlororesorcinol, 4-chlorocatechol, *p*-benzoquinone and 1,2,4-benzenetriol are identified and quantified using Pt, whereas only 4-chlorophenol, 4-chlorocatechol and *p*-benzoquinone are found when BDD is used. Hydroquinone is not detected in any case because it is quickly converted into *p*-benzoquinone. In AO with Pt or BDD all products are poorly accumulated and persist long time, as expected from the slow removal of clofibric acid. In contrast, they are much more quickly formed and destroyed under comparable EF and PEF degradations due to the greater $^{\bullet}OH$

production. 4-Chlorophenol is the aromatic intermediate that shows the highest accumulation in EF and PEF with Pt and BDD, being up to 7.3 and 9.0 mg L^{-1} quantified at 1 min for Pt and BDD, respectively, but it is removed in less than 10 min. All the rest of the aromatics are also removed in less than 10-12 min by EF and PEF, thus confirming the oxidizing ability of these processes. Moreover, the fact that all products show a similar evolution in both treatments confirms that they are not photolyzed under UVA illumination. Only *p*-benzoquinone seems to be influenced by UVA light, because it persists for 360 and 60 min without and with UVA irradiation, respectively.

Ion-exclusion chromatography analyses for the above AO, EF and PEF processes using Pt or BDD allow comparing the evolution of each carboxylic acid. Acids such as tartronic, 2-hydroxyisobutyric, maleic, fumaric, formic and oxalic are identified. Tartronic, fumaric, maleic and formic acids come from the oxidation of the aryl moiety of aromatics, whereas 2-hydroxyisobutyric acid is released in the early stages of the degradation process when 4-chlorophenol is formed. In AO large amounts of these carboxylic acids are slowly accumulated, but they are undetected or detected as traces for short time in EF and PEF because they are quickly degraded. In contrast, oxalic acid is always accumulated to a large extent and persists up to the end of the mineralization processes. This ultimate acid, formed from the independent oxidation of the precedent longer-chain carboxylic acids, as well as formic acid are directly coverted into CO_2. The production of the latter two acids is confirmed by GC-MS spectra after esterification with ethanol. Figure 8.-7 given below presents the evolution of oxalic acid, which is they key to understand the mineralization ability of EF and PEF processes. Fe^{3+} complexes of carboxylic acids are formed in both cases. In particular, Fe^{3+}-oxalato complexes are hardly oxidizable with $^{\bullet}OH$, and that is the reason why oxalic acid remains stable in EF using Pt, thus making it impossible to completely mineralize the treated solution. About 60 mg L^{-1} of this acid remain in the medium at 360 min, corresponding to 16 mg L^{-1} TOC, whereas the resulting solution

contains about 21 mg L^{-1}, so one can conclude that stable polyaromatics are formed. In contrast, complete oxalic acid degradation is achieved after 360 min in PEF using Pt thanks to the action of Reactions 5.-23 and 5.-24, thus leading to overall mineralization. When BDD is used, oxalic acid can be always destroyed, both in EF and PEF. This acid reaches high contents of 68 and 59 mg L^{-1} after 40 min of EF and PEF, respectively, due to the quick oxidation of organics with $^{\bullet}OH$. At longer time, this acid is gradually destroyed, until complete removal at 360 and 240 min in EF and PEF. It has been said that Fe^{3+}-oxalato complexes can not be oxidized with $^{\bullet}OH$ in EF, so they are slowly mineralized with BDD($^{\bullet}OH$). Finally, PEF using BDD is the most potent method, because hardly oxidizable complexes of oxalic acid can be simultaneously destroyed by BDD($^{\bullet}OH$) and UVA light.

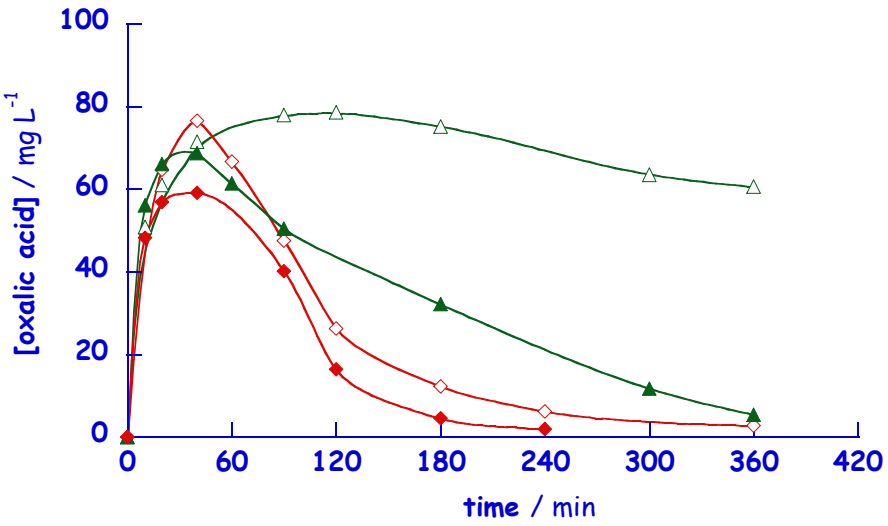

Figure 8.-7 Time-course of the amount of oxalic acid for the experiments in Fig.8.-6.

Considering all the intermediates reported above and accepting that hydroxyl radical is the main oxidizing species, plausible reaction schemes for the degradation of clofibric acid in acidic aqueous medium by EF and PEF with 1.0 mM Fe^{2+} are proposed. The pathway for the systems with Pt is very similar to that of AO with a stainless steel cathode already explained in section 8.2.2. Nevertheless, it includes something worth mentioning: $^{\bullet}OH$ can hydroxylate clofibric acid on its C(2)-position, yielding a 'hydroxy-clofibric acid'. Subsequent attack of $^{\bullet}OH$ releases

4-chlorocatechol and 2-hydroxyisobutyric acid. For the systems with BDD, the reaction pathway is a bit different. Here, the two kind of hydroxyl radicals widely discussed throughout this section are able to oxidize organics. Due to the greater oxidizing ability of BDD, a lower accumulation of intermediates is observed, so the sequence proposed is like a reduced version of the one with Pt: only 4-chlorophenol, 4-chlorocatechol, hydroquinone and *p*-benzoquinone are identified as aromatic intermediates. Also 2-hydroxyisobutyric is a primary product, generated when 4-chlorophenol is formed. Then, the oxidation of *p*-benzoquinone and 4-chlorocatechol can cause the opening of their benzenic rings to yield different carboxylic acids and, at the end, oxalic acid.

Figure 8.-8 given below shows a proposed degradation pathway for oxalic acid. This acid is oxidized to CO_2 with BDD($^{\bullet}OH$) at the anode surface either directly in AO or as Fe^{3+}-oxalato complexes in EF (because these complexes are not oxidized with $^{\bullet}OH$). It must be noted that BDD($^{\bullet}OH$) oxidizes more quickly free oxalic acid than its Fe^{3+} complexes. The latter species also undego a parallel quick photodecarboxylation under the irradiation of UVA light in PEF, with regeneration of Fe^{2+}. The action of UVA light justifies the fastest degradation rate and highest efficiency of PEF with BDD.

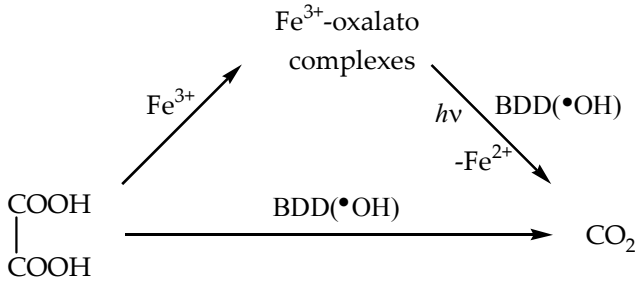

Figure 8.-8 Proposed reaction pathways for oxalic acid mineralization with a BDD anode and electrogenerated H_2O_2 by AO, EF and PEF.

The solution pH for the electrolyses at pH 3.0 remains practically constant throughout all the experiments, reaching final values between 2.8 and 3.0. Moreover, the starting pale yellow solution changes to pale orange color at the end of EF and PEF degradations using a Pt anode due to the formation of soluble colored polyaromatics to a small extent, which can not be destroyed by $^{\bullet}OH$. In contrast, in EF and PEF using a BDD anode the initial color changes to dark yellow, typical of the complexes between Fe^{3+} and H_2O_2, but orange color from polyaromatics is not observed because BDD($^{\bullet}OH$) is able to destroy them.

9. DESTRUCCIÓ D'UN FÀRMAC ANTIMICROBIAL: CLOROFÈ / *DESTRUCTION OF AN ANTIMICROBIAL DRUG: CHLOROPHENE*

This chapter is devoted to the study of the degradation of the antimicrobial drug chlorophene. In this case it is divided into two parts: (i) an introduction giving an overview on the characteristics of chlorophene, its environmental data and some results published in literature on its destruction, (ii) the results obtained for the destruction of this drug by electro-Fenton process, considering the use of two different C-based materials acting as the cathode, the O_2-diffusion and the carbon-felt electrodes.

This work has been carried out during a four-months stage in the research team *Chimie de l'Environnement* (*Laboratoire des Géomaériaux et Géologie de l'Ingénieur*, *Institut Francilien des Sciencs Appliquées*, *Université de Marne la Vallée*, Paris, France) under the supervision of Professor Mehmet Ali Oturan.

9.1. CARACTERÍSTIQUES DEL CLOROFÈ / *CHARACTERISTICS OF CHLOROPHENE*

The concerns regarding antimicrobials, especially as for the promotion of pathogenic resistance, and hormones in the environment are better established than for other PPCPs [378]. Antimicrobials, mainly at low concentrations, impose selective pressure for resistance (unabated growth), or more commonly, tolerance (temporary growth stoppage, but continued viability) among potentially pathogenic microorganisms. Promotion of antimicrobial resistance is at least partly caused by the proliferation or over-expression of cellular 'multidrug resistance' systems (efflux pump-mediated drug resistance), which serve to minimize the intracellular concentrations of contaminants. The acquired resistance or tolerance can be even permanent and genetically conserved, persisting in the absence of continued selective pressure by the antimicrobial. A straightforward evidence of this overuse and misuse is that diseases that once were easily cured by antimicrobials are becoming more difficult to treat, and the reason is simple: evolution. Over time, these hard strains come to predominate in the population and the drugs are no longer effective against them. Antimicrobials also have the potential to alter microbial species diversity, leading to altered successional consequences.

Chlorophene (*o*-benzyl-*p*-chlorophenol, Figure 9.-1) is an aryl halide biocide belonging to the therapeutical class known as antimicrobials (also referred as antibacterials or antiseptics), and was first registered in USA in 1948 as disinfectant. It is a white floury powder, with a slightly phenolic odour but with a clear specification of 'carcinogenic agent' stuck in the commercial can. It is a cutaneous irritant and it has been recognized to possess a weak skin tumor promoting activity in human beings. Chlorophene also appears to be nephrotoxic for rats and mice.

Some of the most remarkable properties of chlorophene are summarized in Table 9.-1.

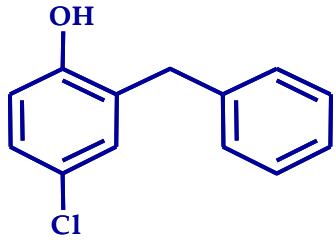

Figure 9.-1 Chlorophene.

Table 9.-1 Chlorophene data [379].

CAS number	120-32-1
Generic names	4-Chloro-2-(phenylmethyl)phenol *o*-benzyl-*p*-chlorophenol
Trade names	Santophen 1, Preventol BP, Nipacide
Molecular formula	$C_{13}H_{11}ClO$
Molecular mass (g mol^{-1})	218.68
Melting point (°C)	48.5
Boiling point (°C)	175
Solubility in H_2O (mg L^{-1})$_{25\ °C}$	149
Density (g cm^{-3})$_{20\ °C}$	1.188
pK_a	10.8

Chlorophene has been chosen since it is a widespread broad-spectrum antimicrobial pharmaceutical, commonly used in hospitals and households for general cleaning and disinfecting, as well as in industrial and farming environments as an active agent in disinfectant formulations [380-382]. It is also used as an algaecide, fungicide, microbicide/microbistat and virucide. There are currently 143 products registered by the EPA containing chlorophene active ingredients.

Although chlorophene is expected to pose a low toxicity for humans, evidence of its carcinogenic and mutagenic activity in animals is documented, so certain attention must be devoted to its behavior.

There are not available data regarding the usage of chlorophene and its salts, but these products account for a substantial share of household disinfectant products used in the mid-1980s. Industry has long relied on the lack of such data to justify inaction on the basis of its belief that the link between use of antimicrobials in animals and human health consequences was unproved. This has always been a cynical position, since industry possesses the data that would make the link more apparent. Antimicrobial agents can be found in sewage effluents, especially in places where they are used extensively, such as hospitals, pharmaceutical production plants, and near farms where animal feed containing antimicrobial agents is used.

Occurrence of chlorophene in the aquatic environment is not very well documented. Thomas et at. [383] have reported its detection in sediments collected from estuaries in the United Kingdom. Chlorophene has been routinely found in both influents (up to 0.71 μg L^{-1}) and effluents of STPs [384], but it has been detected even at concentrations up to 50 mg L^{-1} in activated sludge sewage systems, and up to 10 μg L^{-1} in sewage treatment plant effluents and rivers. It is known that its removal is not as extensive as for biphenylol, another common antimicrobial agent.

There is a great scarcity of information about the ways to avoid the dangerous accumulation of chlorophene in soils and the aquatic environment. Arnold et al. [381] have reported the photodegradation of its deprotonated phenolate form, as well as the reaction of chlorophene with hydroxyl radicals (showing a second-order rate constant, k_2 = 7.1 x 10^9 M^{-1} s^{-1}). Zhang et al. have described its oxidative degradation with MnO_2 and they have reported the conversion of chlorophene into polymeric intermediates. Precisely, Zhang has presented in his doctoral thesis the most extensive investigation on the degradation of antibacterial agents using metal oxides [385]. An interesting trait of this compound is that no previous works are found in literature on its removal from water by means of potent oxidation procedures such as AOPs, to mineralize chlorophene rather than transform it.

As in the case of paracetamol and clofibric acid, an important goal in the study of chlorophene is to design effective and optimized processes to remove it from wastewaters. Therefore, the present work deals with some of the fundamental aspects of the EF process: (i) the actual reduction ability of the cathode to regenerate Fe^{2+} from direct reduction of Fe^{3+}, (ii) the oxidation ability of Pt and BDD anodes to convert Fe^{2+} into Fe^{3+}, (iii) the action of weak oxidants formed at the anode on the Fe^{2+} content in solution and (iv) the role of Fe^{2+}/Fe^{3+} complexes with carboxylic acids to analyze the comparative rate removal of the pollutant.

9.2. TRACTAMENT MITJANÇANT ELECTRO-FENTON / *TREATMENT BY ELECTRO-FENTON*

9.2.1. Finalitat del treball / *Aim of the work*

All treatments were conducted at room temperature in an undivided glass cell by electrolyzing 200-mL chlorophene solutions of pH 3.0 containing 0.05 M Na_2SO_4 and different concentrations of Fe^{3+} as catalyst. Four EF systems were tested: Pt/O_2 diffusion, BDD/O_2 diffusion, Pt/carbon felt and BDD/carbon felt. The O_2-diffusion cathode was directly fed with pure O_2 at 20 mL min^{-1} to generate continuously H_2O_2, whereas the cells with a carbon-felt cathode were saturated of this gas by bubbling compressed air at 1 L min^{-1}, starting 15 min before electrolysis.

The first goal of this study was to clarify the catalytic behavior of the Fe^{3+}/Fe^{2+} system in the EF process in the absence of chlorophene. With this aim, first of all the oxidation ability of the Pt and BDD anodes to transform directly Fe^{2+} into Fe^{3+} was tested. Several electrolyses with 4.0 mM Fe^{2+} were made at 300 mA with Pt or BDD, using a stainless steel cathode to focus the study on the activity of the anode. Then, several experiments were performed to analyze the evolution of Fe^{2+} and Fe^{3+} ions, as well as the accumulation of H_2O_2, in the four EF systems pointed out above. Solutions with 4.0 mM Fe^{3+} were electrolyzed at 300 mA for 60 min using Pt and BDD anodes with an O_2-diffusion cathode, and solutions with 0.2 mM Fe^{3+} under the same conditions were treated with a carbon-felt cathode.

To confirm the behavior of the Fe^{3+}/Fe^{2+} system several degradations in the presence of chlorophene were carried out by the four EF processes aforementioned. Chlorophene destruction was followed by reversed-phase HPLC chromatography. First of all, the chlorophene decay was studied by electrolyzing 50 mg L^{-1} chlorophene solutions, with Fe^{3+} initial content between 0.2 and 8.0 mM, at pH 3.0

and at 300 mA using the Pt/O_2 diffusion cell. A chemical test using 50 mg L^{-1} chlorophene and 20 mM H_2O_2 was also performed to assess the oxidizing power of H_2O_2. The Pt/O_2 diffusion cell was then used to electrolyze a solution under the same conditions but in the absence of Fe^{3+} to observe the oxidation ability of AO with electrogenerated H_2O_2. A parallel study was carried out with the BDD/O_2 diffusion cell under the previous conditions to discuss the influence of the anode. After using the O_2-diffusion cathode, the carbon-felt cathode was tested with both anodes and Fe^{3+} concentration between 0.1 and 2.0 mM at 60 and 300 mA. Kinetic analysis of the above chlorophene decays was simultaneously done. In addition, the second-order-rate constant for the reaction between chlorophene and hydroxyl radical was determined through the method of competitive kinetics. To do this, 200-mL solutions of pH 3.0 containing 50 mg L^{-1} chlorophene, 122 mg L^{-1} benzoic acid (as a standard competition substrate) and 0.2 mM Fe^{3+} were electrolyzed at 60 mA using the Pt/carbon felt and BDD/carbon felt cells.

Once the ability of the four EF methods to destroy chlorophene was assessed, its mineralization power had to be demonstrated from the corresponding TOC decay to assure their complete efficacy. This study was carried out by electrolyzing 84-mg L^{-1} chlorophene solutions (i.e., 60 mg L^{-1} TOC) at pH 3.0 and at 60, 100, 200 and 300 mA, using the four EF cells pointed out above. Efficient Fe^{3+} contents of 4.0 and 0.2 mM were used for the cells with the O_2-diffusion and the carbon-felt cathode, respectively.

Chloride ion evolution was followed by recording the ion chromatograms corresponding to the treatment of 84-mg L^{-1} chlorophene solutions with 0.015 M Na_2SO_4 and 0.2 mM Fe^{3+} at pH 3.0 and at 150 mA for the four EF cells.

The evolution of intermediates was followed by reversed-phase chromatography and ion-exclusion chromatography. To identify the aromatics, several trials were made by applying low currents and using the Pt/O_2 diffusion system with low oxidizing

power. Carboxylic acids were identified and quantified in the four EF systems by treating 84-mg L^{-1} chlorophene solutions of pH 3.0 at 60 and 300 mA, with 4.0 and 0.2 mM Fe^{3+} for the cells using the O_2-diffusion and the carbon-felt cathode, respectively. GC-MS was also used to detect the aromatic intermediates during the degradation of 50 mg L^{-1} chlorophene in the Pt/O_2 diffusion cell at 60 mA for 30 min. For the identification of carboxylic acids, the same treatment was performed and prolonged for 2 h. Prior to injection of the samples, different preparative sequences were applied to the solutions obtained.

Finally, the possible reaction paths of oxalic acid, which is the ultimate by-product formed during the mineralization process before the total conversion of all the initial organic carbon into CO_2, could be schematized for the EF systems used.

The thorough results of this section are included in the following paper (Paper 7):

7. **Sirés, I.**, Garrido, J.A., Rodríguez, R.M., Brillas, E., Oturan, N., Oturan, M.A., Catalytic behaviour of the Fe^{3+}/Fe^{2+} system in the electro-Fenton degradation of the antimicrobial chlorophene. *Appl. Catal. B: Environ.* (accepted for publication)

The following presentation in congress is related to this work:

G. **Sirés, I.**, Oturan, N., Brillas, E., Oturan, M.A., Electrochemical degradation of antimicrobials by electro-Fenton process: Comparative performance of carbon felt cathode versus oxygen diffusion cathode, Vol. 1, page 28, 7th Electrochemistry Days (7. Elektrokimiya Günleri), Hacettepe Üniversitesi, Ankara, Turkey, 28-30 June 2006. (Oral presentation)

UNIVERSITAT DE BARCELONA

ARTICLE 7 / *PAPER 7*

Catalytic behaviour of the Fe^{3+}/Fe^{2+} system in the electro-Fenton degradation of the antimicrobial chlorophene

Elsevier Editorial System(tm) for Applied Catalysis B: Environmental

Manuscript Draft

Manuscript Number:

Title:
Catalytic behavior of the Fe3+/Fe2+ system in the electro-Fenton degradation of the antimicrobial chlorophene

Article Type: Full Length Article

Keywords:
Antimicrobials; Electro-Fenton method; Advanced oxidation processes; Degradation; Water treatment

Corresponding Author: Prof. Mehmet A. Oturan,

Corresponding Author's Institution: Université de Marne la Vallée

First Author: Ignacio Sirés

Order of Authors: Ignacio Sirés; José A. Garrido; Rosa M. Rodríguez; Enric Brillas; Nihal Oturan; Mehmet A. Oturan

Cover Letter

Please find attached a copy of the manuscript entitled “Catalytic behavior of the Fe^{3+}/Fe^{2+} system in the electro-Fenton degradation of the antimicrobial chlorophene" by Ignasi Sirés, José Antonio Garrido, Rosa María Rodríguez, Enric Brillas, Nihal Oturan and myself, which we submit to your consideration in order to be published in "Applied Catalysis B: Environmental". The corresponding author will be myself. I am available at oturan@univ-mlv.fr; mailing address: Laboratoire des Géomatériaux, Université de Marne la Vallée, 5 Boulevard Descartes, Champs-sur-Marne, 77454 Marne-la-Vallée Cedex 2 - France; phone: +33 1 49 32 90 65 ; fax: +33 1 49 32 91 37.

We present in this work a comparative study on oxidizing power and mineralization efficiency of four variants of electro-Fenton process which is developed by Brillas's and Oturan's team during the last decade. We show that the efficiency of different systems under study is determined by the nature of cathode/anode materials used and the catalytic behaviour of the Fe^{3+}/Fe^{2+} redox couple as catalyst. In this paper we demonstrate that the four electro-Fenton system studied can be successfully applied to the treatment of an antimicrobial (chlorophene) aqueous solution, which is an emergent environmental pollutant.

We think this manuscript is appropriate for publication in Applied Catalysis B: Environmental on account of the growing importance of advanced electrochemical oxidation process (AEOPs) in treatment of persistent organic pollutants (POPs). This innovative and environmentally friendly technology can have high potential impact on this field due to its very high mineralization efficiency.

*** Manuscript**

Catalytic behavior of the Fe^{3+}/Fe^{2+} system in the electro-Fenton degradation of the antimicrobial chlorophene

Ignasi Sirés [a], José Antonio Garrido [a], Rosa María Rodríguez [a], Enric Brillas [a], Nihal Oturan [b], Mehmet Ali Oturan [b]*

[a] *Laboratori d'Electroquímica dels Materials i del Medi Ambient, Departament de Química Física, Facultat de Química, Universitat de Barcelona, Martí i Franquès 1-11, 08028 Barcelona, Spain*

[b] *Université de Marne la Vallée, Laboratoire des Géomatériaux et Géologie de l'Ingénieur, 5 Boulevard Descartes, Champs-sur-Marne, 77454 Marne-la-Vallée Cedex 2, France*

Paper submitted to be published in Applied Catalysis B:Environmental

*Corresponding author: Tel.: + 33 149 32 90 65,

E-mail address: oturan@univ-mlv.fr (M.A. Oturan)

Abstract

Solutions of the antimicrobial chlorophene with 0.05 M Na_2SO_4 and Fe^{3+} as catalyst of pH 3.0 have been comparatively degraded by the electro-Fenton method using four undivided electrolytic cells containing a Pt or boron-doped diamond (BDD) anode and a carbon-felt or O_2-diffusion cathode at constant current. Under these environmentally friendly conditions, pollutants are oxidized with hydroxyl radical ($^{\bullet}OH$) formed at the anode from water oxidation and in the medium from Fenton's reaction between electrogenerated Fe^{2+} and H_2O_2 at the cathode. The catalytic behavior of the Fe^{3+}/Fe^{2+} system mainly depends on the cathode tested. In the cells with an O_2-diffusion cathode, H_2O_2 is largely accumulated and their Fe^{3+} content remains practically unchanged, while the chlorophene decay is enhanced when Fe^{3+} concentration rises due to the greater $^{\bullet}OH$ production from the higher quantity of Fe^{2+} regenerated at the cathode. When a carbon-felt cathode is used, H_2O_2 is electrogenerated in small extent with large accumulation of Fe^{2+}, because this ion is more rapidly regenerated at the cathode than oxidized to Fe^{3+} at the Pt or BDD anode, only being required the presence of 0.2 mM Fe^{3+} to obtain the maximum $^{\bullet}OH$ generation with the quickest chlorophene removal. Chlorophene is poorly mineralized in the Pt/O_2 diffusion cell due to the difficult oxidation of final Fe^{3+}-oxalate complexes with $^{\bullet}OH$. These species are completely destroyed using a BDD anode at high current due to the great $^{\bullet}OH$ generation on its surface. Total mineralization is also achieved in the Pt/carbon felt and BDD/carbon felt cells with 0.2 mM Fe^{3+}, where oxalic acid and its Fe^{2+} complexes are directly oxidized with $^{\bullet}OH$ in the medium. The highest oxidizing power for total mineralization at high current is attained for the BDD/carbon felt cell, because oxalic acid can be simultaneously destroyed on BDD.

Keywords: Antimicrobials; Electro-Fenton method; Advanced oxidation processes; Degradation; Water treatment

1. Introduction

A large variety of advanced oxidation processes (AOP's) have been recently proposed for the degradation of toxic and biorefractory organics in wastewaters [1-3]. They are chemical, photochemical, photocatalytic and electrochemical procedures characterized by the in situ generation of hydroxyl radical ($^{\bullet}OH$) as the main oxidizing agent of pollutants. This radical has a high standard potential ($E^{o}(^{\bullet}OH/H_2O)$ = 2.80 V vs. NHE) and it is the second most strong oxidizing species known, after fluorine. $^{\bullet}OH$ has enough ability to react non-selectively with organics yielding dehydrogenated or hydroxylated derivatives up to their final mineralization, i.e., their total conversion into CO_2, water and inorganic ions. One of the most popular AOP's for the treatment of acidic waters is the Fenton's reagent [2-4], composed of a mixture of Fe^{2+} and hydrogen peroxide that is added to the contaminated water to produce $^{\bullet}OH$ and Fe^{3+} according to the classical Fenton's reaction (1) with a second-order rate constant (k) of 63 M^{-1} s^{-1} [4]:

$$Fe^{2+} + H_2O_2 \rightarrow Fe^{3+} + {}^{\bullet}OH + OH^{-} \quad (1)$$

This method becomes effective because reactions between $^{\bullet}OH$ and organics are usually very fast, with k-values of 10^{8}-10^{10} M^{-1} s^{-1}. However, a part of the generated radical is lost due to its direct reaction with Fe^{2+} (k = 3.2x10^{8} M^{-1} s^{-1} [5]) and H_2O_2 (k = 2.7 x10^{7} M^{-1} s^{-1} [6]), as shown in reaction (2) and reaction (3), respectively:

$$Fe^{2+} + {}^{\bullet}OH \rightarrow Fe^{3+} + OH^{-} \quad (2)$$

$$H_2O_2 + {}^{\bullet}OH \rightarrow HO_2^{\bullet} + H_2O \quad (3)$$

An advantage of the use of the Fe^{3+}/Fe^{2+} system is its catalytic behavior, since Fe^{2+} is not completely removed by reactions (1) and (2) because it can be regenerated in small extent from the reduction of Fe^{3+} by H_2O_2 from reaction (4) with k = 8.4 x 10^{-6} M^{-1} s^{-1} [7], by hydroperoxyl radical ($HO_2^{\bullet}$) from reaction (5) with k = 2 x 10^{3} M^{-1} s^{-1} [8] and/or by organic

radical intermediates $R^{\bullet}$ from reaction (6). $HO_2^{\bullet}$ is an oxidant much weaker than $^{\bullet}OH$ and can also oxidize Fe^{2+} from reaction (7) with $k = 1.2x10^6\ M^{-1}\ s^{-1}$ [8].

$$Fe^{3+} + H_2O_2 \rightarrow Fe^{2+} + H^+ + HO_2^{\bullet} \quad (4)$$

$$Fe^{3+} + HO_2^{\bullet} \rightarrow Fe^{2+} + H^+ + O_2 \quad (5)$$

$$Fe^{3+} + R^{\bullet} \rightarrow Fe^{2+} + R^+ \quad (6)$$

$$Fe^{2+} + HO_2^{\bullet} \rightarrow Fe^{3+} + HO_2^- \quad (7)$$

Reactions (4)-(6) propagate Fenton's reaction (1) with the continuous production of $^{\bullet}OH$ for the destruction of organic pollutants.

Electro-oxidation methods such as anodic oxidation and electro-Fenton are also being developed for water remediation [9-45]. These environmentally friendly electrochemical techniques are more potent than chemical AOP's because they can produce greater amount of oxidant $^{\bullet}OH$ under control of the applied current. In anodic oxidation contaminants are destroyed by reaction with adsorbed hydroxyl radical generated at the surface of a high O_2-overvoltage anode from water oxidation [9-12], according to reaction (8):

$$H_2O \rightarrow {}^{\bullet}OH_{ads} + H^+ + e^- \quad (8)$$

Conventional anodes such as Pt, PbO_2, IrO_2, etc., lead to poor degradation of aromatics due to the formation of carboxylic acids that are difficultly oxidizable by $^{\bullet}OH$. These products can be destroyed using a boron-doped diamond (BDD) thin-film anode, which possesses much greater O_2-overvoltage and produces higher amount of effective $^{\bullet}OH$ from reaction (8) than the above anodes, thus leading to a quicker oxidation of organics [12]. Recent studies have confirmed the total mineralization of several aromatics and short carboxylic acids in waters by anodic oxidation with a BDD anode [9-22].

Electro-Fenton is an indirect electro-oxidation treatment based on the combined use of cathodically generated hydrogen peroxide and iron ions as catalyst [23-45]. The method consists in the continuous supply of H_2O_2 to the acidic contaminated solution from the two-electron reduction of oxygen gas given by reaction (9):

$$O_{2(g)} + 2\,H^{+} + 2\,e^{-} \rightarrow H_2O_2 \quad (9)$$

Reaction (9) can take place at reticulated vitreous carbon [23,24,26,27,44], carbon-felt [28-30,33-38,40,43], activated carbon fiber [41] and carbon-polytetrafluoroethylene (PTFE) O_2-diffusion [17,25,31,32,39,42,45] cathodes. Fe^{2+} or Fe^{3+} is then added to the solution to generate the oxidizing agent $^{\bullet}OH$ from Fenton's reaction (1).

In our laboratories we have previously studied the electro-Fenton degradation of some aromatic compounds, mainly pesticides, such as chlorophenoxy acids [17,28-31,32,39] and organophosphorus [34], dyes [37], industrial pollutants [33,38,40,45] and analgesic pharmaceuticals as emerging pollutants [42] using different undivided electrolytic cells. The outstanding oxidizing power of these electro-Fenton systems has been explained by the fast reaction of organics with $^{\bullet}OH$ formed in the medium from reaction (1) and in some cases, at the anode from reaction (8), being the former reaction enhanced by the additional regeneration of Fe^{2+} from cathodic reduction of Fe^{3+}:

$$Fe^{3+} + e^{-} \rightarrow Fe^{2+} \quad (10)$$

However, these previous works have not yet examined extensively some fundamental aspects of the Fe^{3+}/Fe^{2+} catalytic system involved in the electrolytic cell such as: (i) the actual reduction ability of the cathode to regenerate Fe^{2+} from reaction (10), (ii) the oxidation ability of the anode to convert Fe^{2+} into Fe^{3+} from reaction (11), (iii) the action of weak oxidants formed at the anode on the Fe^{2+} content in solution and (iv) the comparative removal rate of generated carboxylic acids and their complexes with Fe^{2+} and/or Fe^{3+} with regard to the oxidizing power of the system to achieve total mineralization.

$$Fe^{2+} \rightarrow Fe^{3+} + e^{-} \quad (11)$$

The understanding of these effects for different electro-Fenton systems is needed to establish their optimum operational conditions for the treatment of agricultural, industrial and urban

wastewaters containing aromatics. To clarify them, we have undertaken a comparative study on the behavior of the Fe^{3+}/Fe^{2+} system using four undivided electrolytic cells containing a Pt or BDD anode and a carbon-felt or O_2-diffusion cathode. The comparative oxidizing power of these cells was tested from the degradation of chlorophene (*o*-benzyl-*p*-chlorophenol, see chemical structure in Fig. 1). Pharmaceuticals belonging to several therapeutical classes are being continuously detected in the environment, but their effects on humans and aquatic fauna are not well known for the moment. Chlorophene was chosen since it is a widespread broad-spectrum antimicrobial pharmaceutical, commonly used in hospitals and households for general cleaning and disinfecting, as well as in industrial and farming environments as an active agent in disinfectant formulations [46-48]. It has been detected at concentrations up to 50 mg l^{-1} in activated sludge sewage systems and up to 10 μg l^{-1} in sewage treatment plant effluents and rivers. Although chlorophene is expected to pose a low toxicity for humans, evidence of its carcinogenic and mutagenic activity in animals is documented [49]. To avoid its dangerous accumulation in soils and the aquatic environment, this compound and its by-products need to be removed from wastewaters by potent and viable oxidation methods. In this sense, only its oxidative degradation with MnO_2 has been described [46].

This paper reports a detailed investigation on the catalytic behavior of the Fe^{3+}/Fe^{2+} system in the electro-Fenton degradation of chlorophene using undivided Pt/O_2 diffusion, BDD/O_2 diffusion, Pt/carbon felt and BDD/carbon felt cells. Comparative experiments were carried out with solutions containing 0.05 M Na_2SO_4 as background electrolyte and Fe^{3+} at pH 3.0, near the optimum pH of 2.8 for Fenton's reaction (1) [5]. The evolution of Fe^{2+}, Fe^{3+} and H_2O_2 in each cell was examined in the absence of pollutants to know the extent of reactions (10) and (11). Concentrated solutions of chlorophene (solubility in water 145 mg l^{-1}) were degraded to clarify better the effects of the Fe^{3+}/Fe^{2+} system. In each electro-Fenton system the influence of Fe^{3+} content and applied current on its degradation rate and oxidizing power for total mineralization was also explored. The kinetics of chlorophene decay and the evolution of its generated carboxylic acids were followed by chromatographic techniques.

2. Experimental

2.1. Chemicals

Chlorophene was reagent grade from Sigma-Aldrich, being used in the electrolytic experiments as received. Benzoic, maleic, fumaric, malonic, glycolic, glyoxylic, formic and oxalic acids were either reagent or analytical grade supplied by Sigma-Aldrich, Fluka and Acros Organics. Sulfuric acid, anhydrous sodium sulfate, heptahydrated ferrous sulfate and ferric sulfate were analytical grade purchased from Fluka and Acros Organics. All solutions were prepared with ultra-pure water obtained from a Millipore Milli–Q system with resistivity > 18 MΩ cm at room temperature. Organic solvents and the other chemicals used were either HPLC or analytical grade from Fluka, Panreac and Acros Organics.

2.2. Instruments

Electrolyses were performed either with a Hameg HM8040 triple power supply or a Micronics-Systems MX 30 V-10 A microlab power supply. The solution pH was measured with a Eutech Instruments CyberScan pH1500 pH-meter. The mineralization of chlorophene solutions was monitored by the abatement of their total organic carbon (TOC), determined on a Shimadzu VCSH TOC analyzer. The decays of chlorophene and benzoic acid were followed by reversed-phase HPLC chromatography using a Merck Lachrom liquid chromatograph equipped with a L-7100 pump, fitted with a Purospher RP-18 5 µm, 25 cm x 4.6 mm, column at 40 °C, and coupled with a L-7455 photodiode array detector selected at λ = 280 nm. Generated carboxylic acids were identified and quantified by ion-exclusion HPLC chromatography with a Merck Lachrom liquid chromatograph equipped with a L-2130 pump, fitted with a Supelco Supelcogel H 9 µm, 25 cm x 4.6 mm, column at 40 °C, and coupled with a L-2400 UV detector selected at λ = 210 nm. In both HPLC techniques 20 µl samples were injected into the liquid chromatograph and measurements were controlled through an EZChrom Elite 3.1 program. Cl^- concentration in treated solutions was determined by ion chromatography just injecting 25 µl aliquots into a Dionex ICS-1000 Basic Ion Chromatography System fitted with an IonPac AS4A-SC, 25 cm x 4 mm, anion-exchange column, linked to an IonPac AG4A-SC, 5 cm x 4 mm, column guard, and coupled with a DS6 conductivity detector containing a cell heated at 35 °C under control through a Chromeleon

SE software. The sensitivity of this detector was improved from electrolyte suppression using a SRS-ULTRA II self-regenerating suppressor. Colorimetric measurements were made with a Unicam UV4 Prisma double-beam spectrometer thermostated at 25.0 °C.

Oxidation products were detected by gas chromatography-mass spectrometry (GC-MS) using a Hewlett-Packard system composed of a HP 5890 Series II gas chromatograph fitted either with a HP-5 0.25 µm or a HP-Innowax 0.25 µm, both of 30 m x 0.25 mm, column and coupled with a HP 5989A mass spectrometer operating in EI mode at 70 eV. The temperature ramp for the HP-5 column was 35 °C for 2 min, 10 °C min^{-1} up to 320 ºC and hold time 5 min, and the temperatures of the inlet, transfer line and detector were 250 ºC, 250 ºC and 290 ºC, respectively. The temperature ramp for the HP-Innowax column was 35 ºC for 2 min, 10 ºC min^{-1} up to 250 ºC and hold time 15 min, and the temperature of the inlet, transfer line and detector was 250 ºC.

2.3. Electrolytic systems

All electrolyses were conducted in an undivided glass cell of 6 cm diameter and 250 ml capacity. Four different electro-Fenton systems were tested: (i) a Pt/O_2 diffusion cell, with a 3 cm^2 Pt sheet from SEMP as anode and a 3 cm^2 carbon-PTFE O_2-diffusion electrode from E-TEK as cathode, (ii) a BDD/O_2 diffusion cell, containing a 3 cm^2 BDD thin-film deposited on conductive single crystal *p*-type Si (100) wafers from CSEM as anode and the above O_2-diffusion cathode, (iii) a Pt/carbon felt cell, with a 4.5 cm^2 Pt cylindrical mesh as anode and a 70 cm^2 (17 cm x 4,1 cm) carbon felt from Carbone-Lorraine as cathode and (iv) a BDD/carbon felt cell, containing the above BDD anode and carbon-felt cathode. The preparation of the O_2-diffusion cathode has been reported elsewhere [25,31]. In the Pt/O_2 diffusion and BDD/O_2 diffusion cells, the interelectrode gap was about 1 cm and the cathode was directly fed with pure O_2 at 20 ml min^{-1} to generate continuously H_2O_2 from reaction (9). In the Pt/carbon felt and BDD/carbon felt cells, the corresponding anode was centered in them and each cathode covered their inner wall, where H_2O_2 was produced from reduction of O_2 dissolved in the solution, also from reaction (9). Continuous saturation of this gas at atmospheric pressure was ensured by bubbling compressed air at 1 l min^{-1}, starting 15 min before electrolysis.

Solutions of 200 ml containing up to 84 mg l^{-1} chlorophene with 0.05 M Na_2SO_4 and different concentrations of Fe^{3+} at pH 3.0 adjusted with H_2SO_4 were comparatively degraded in the above four electro-Fenton systems at constant current between 60 and 300 mA and at room temperature (20±1 °C). All solutions were vigorously stirred with a magnetic bar during treatment.

2.4. Analytical procedures

Reproducible TOC values were always obtained by injecting 100 µl aliquots into the TOC analyzer using the non-purgeable organic carbon method. The mineralization current efficiency (MCE) for treated solutions at a given time was then calculated from the following equation:

$$MCE = \frac{\Delta(TOC)_{exp}}{\Delta(TOC)_{theor}} \times 100 \qquad (12)$$

where $\Delta(TOC)_{exp}$ is the experimental TOC removal and $\Delta(TOC)_{theor}$ is the theoretically calculated TOC decay at a given time considering that the applied electrical charge (= current x time) is only consumed in the mineralization process of chlorophene.

Reversed-phase chromatography analyses were carried out was made under circulation of a 50:50 (v/v) acetonitrile/water mixture at 0.8 ml min^{-1} as mobile phase. For ion-exclusion chromatography, the mobile phase was 4 mM H_2SO_4 at 0.2 ml min^{-1}. Cl^- measurements were conducted with a solution of 1.8 mM Na_2CO_3 and 1.7 mM $NaHCO_3$ circulating at 1.0 ml min^{-1} as mobile phase. The concentration of H_2O_2 in electrolyzed solutions was determined from the light absorption of the titanic-hydrogen peroxide colored complex at λ = 408 nm [50]. The Fe^{2+} and Fe^{3+} contents in the same solutions were obtained by measuring the light absorption of their corresponding colored complexes with 1,10-phenantroline at λ = 508 nm [51] and with SCN^- at λ = 466 nm [52], respectively.

To detect the aromatic intermediates, 50 mg l^{-1} of chlorophene were degraded in the Pt/O_2 diffusion cell at low current for 30 min. The remaining organics were withdrawn with 45 ml of CH_2Cl_2 in three times. This solution was then dried with anhydrous Na_2SO_4, filtered and its volume reduced to 2 ml to concentrate the aromatics for their analysis by GC-MS using the

HP-5 column. For the identification of final carboxylic acids, the treatment of 50 mg l^{-1} of chlorophene in the same cell was prolonged for 2 h. The resulting solution was evaporated at low pressure and the remaining solid was dissolved in 2 ml of ethanol. The esterified acids were further analyzed by GC-MS using the HP-Innowax column.

3. Results and Discussion

3.1. Behavior of the Fe^{3+}/Fe^{2+} system without pollutants

A preliminary study was carried out to test the oxidation ability of the Pt and BDD anodes to transform Fe^{2+} into Fe^{3+} via reaction (11). Several electrolyses of 200 ml of a 0.05 M Na_2SO_4 solution with 4.0 mM Fe^{2+} at pH 3.0 and at 300 mA were made using undivided cells containing one of the above anodes and a 3 cm^2 stainless steel (AISI 304) sheet as cathode. A quick decay of Fe^{2+} concentration, along with the simultaneous increase in Fe^{3+} content, was found in both cases, indicating a very poor regeneration of Fe^{2+} at the stainless steel cathode from reaction (10) compared to its fast oxidation at each anode from reaction (11). Fe^{2+} was completely removed in 45 min using BDD (current efficiency 95%), whereas for Pt, a longer time of 64 min was required (current efficiency 67%). Kinetic analysis of these data showed a pseudo-first-order decay for Fe^{2+} during the initial 20-30 min of both electrolyses, with a pseudo-rate constant (k_1) of 9.05×10^{-4} s^{-1} (square linear regression coefficient $R^2 = 0.995$) for BDD and 5.87×10^{-4} s^{-1} ($R^2 = 0.991$) for Pt. The faster Fe^{2+} removal with BDD can be accounted for by its greater O_2-overpotential [12] that favors reaction (11) instead of O_2 evolution from water oxidation, a process taking place in larger extent in Pt. The greater O_2-overpotential of BDD causes an average cell voltage equal to 9.8 V, a value much higher than 5.7 V when it is replaced by Pt.

Several experiments were further performed to clarify the evolution of Fe^{3+}, Fe^{2+} and accumulated H_2O_2 in the four electro-Fenton systems with H_2O_2 electrogeneration considered in the present work. The time-course of these species during the electrolysis of 200 ml of a 0.05 M Na_2SO_4 solution with 4.0 mM Fe^{3+} at pH 3.0 and at 300 mA for 60 min using the Pt/O_2 diffusion and BDD/O_2 diffusion cells, is depicted in Fig. 2a. As can be seen, the Fe^{3+} concentration remains practically unchanged in both trials. In addition, no significant quantity

of Fe^{2+} was detected in the electrolyzed solutions, as expected if reaction (10) occurs in such a small extent at the O_2-diffusion cathode that the generated Fe^{2+} is rapidly converted into Fe^{3+} from reactions (1), (2) and (7) and mainly at the anode from reaction (11), thus preventing its accumulation in the medium. The predominant reaction in this cathode is the reduction of injected O_2 to electrogenerate H_2O_2 from reaction (9). This can be easily deduced from Fig. 2a because this species is continuously accumulated up to reach a steady concentration of about 9 mM after 45 min in both electrolyses, just when its electrogeneration and decomposition rates become equal. Under these conditions, H_2O_2 can be slowly decomposed with Fe^{2+} by reaction (1) and with Fe^{3+} by reaction (4), but it is much more rapidly oxidized to O_2 via formation of $HO_2^{\bullet}$ as intermediate at the anode surface [31,39]:

$$H_2O_2 \rightarrow HO_2^{\bullet} + H^+ + e^- \quad (13)$$

$$HO_2^{\bullet} \rightarrow O_2 + H^+ + e^- \quad (14)$$

Our results indicate that the rates of reactions (13) and (14) are practically independent of the anode used, despite the average cell voltage raises from 12.0 V for the Pt/O_2 diffusion cell to 19.0 V for the BDD/O_2 diffusion one.

A very different behavior of these species was found using the Pt/carbon felt and BDD/carbon felt cells. These trials were also performed at 300 mA, but with a smaller content of Fe^{3+} (0.20 mM) in the 0.05 M Na_2SO_4 solution of pH 3.0 to try to clarify better the extent of reactions (10) and (11). As can be seen in Fig. 2b, the use of the Pt/carbon felt cell gives rise to the reduction of all Fe^{3+} to Fe^{2+} in 20 min, indicating that reaction (10) is very fast at the carbon felt cathode. Its kinetic analysis allows determining a k_1-value of 4.05×10^{-3} s^{-1} for overall Fe^{2+} regeneration, corresponding to a reaction rate of 8.10×10^{-7} M s^{-1} for 0.20 mM Fe^{2+}. This value is much higher than 1.17×10^{-7} M s^{-1} expected from its oxidation at the Pt anode from reaction (11) with $k_1 = 5.87 \times 10^{-4}$ s^{-1}, as determined above. The parallel generation of H_2O_2 from reaction (9) in the carbon-felt cathode is rather slow, being detected at a concentration as low as 0.23 mM after 60 min of electrolysis in the Pt/carbon felt cell (not shown in Fig. 2b). This confirms the consumption of Fe^{2+} by reactions (1), (2) and (7) in parallel to reaction (11), although its regeneration from reaction (10) is so fast that only Fe^{2+}

is detected for electrolysis times longer than 20 min. In contrast, Figure 2b shows that Fe^{3+} is not totally converted into Fe^{2+} in the BDD/carbon felt cell under comparable conditions. The Fe^{2+} content in this cell immediately rises up to 0.058 mM in 2 min and thereafter, it is slowly removed to disappear in 60 min, when 0.20 mM of H_2O_2 is accumulated. This anomalous trend can be explained by the additional destruction of Fe^{2+} with weak oxidant species produced at the BDD anode, since its great O_2-overpotential causes an average voltage applied to the BDD/carbon felt cell at 300 mA equal to 12.5 V, a value much higher than 2.2 V using a Pt anode. Under these conditions, it is well-known that peroxodisulfate is competitively formed with $^{\bullet}OH$ at the BDD anode from the reaction (15) [12,14]:

$$2\ HSO_4^- \rightarrow S_2O_8^{2-} + 2\ H^+ + 2\ e^- \qquad (15)$$

and this ion can further react with Fe^{2+} to yield sulfate and Fe^{3+} from reaction (16), with k = 23 $M^{-1}\ s^{-1}$ [53]:

$$S_2O_8^{2-} + 2\ Fe^{2+} \rightarrow 2\ SO_4^{2-} + 2\ Fe^{3+} \qquad (16)$$

The slow disappearance of Fe^{2+} generated from reaction (10) in the BDD/carbon felt cell can then be accounted for by the increase in rate of reaction (16) due to the continuous accumulation of $S_2O_8^{2-}$ in the medium. However, Fe^{3+} does not seem to be completely regenerated in this cell, since its concentration undergoes a progressive abatement with electrolysis time (see Fig. 2b). An inspection of the carbon felt cathode after this trial revealed the presence of a yellow precipitate of $Fe(OH)_3$ on its large and porous surface (geometric area 70 cm^2). The decay in Fe^{3+} content can be related to the gradual formation of such precipitate due to the high OH^- concentration present in the vicinity of the cathode coming from the simultaneous water reduction to hydrogen. Note that no precipitation of $Fe(OH)_3$ was observed neither in the systems containing an O_2-diffusion cathode with much smaller geometric surface (3 cm^2), nor in the Pt/carbon felt cell where Fe^{3+} is completely reduced to Fe^{2+} at the cathode.

The above results are indicative of a main dependence of the Fe^{3+}/Fe^{2+} catalytic system on the cathode used. The fast generation of H_2O_2 from reaction (9) at the O_2-diffusion cathode favors the accumulation of large amounts of this species in the Pt/O_2 diffusion and BDD/O_2 diffusion cells. The regenerated Fe^{2+} by reaction (10) is then rapidly oxidized to Fe^{3+} by reactions (1), (2), (7) and (11), so Fe^{3+} concentration does not practically varies along electrolysis. In contrast, the carbon felt cathode yields a much smaller quantity of H_2O_2, but reaction (10) becomes so fast on its surface that Fe^{2+} is accumulated in large extent in the Pt/carbon felt cell. Under these conditions, a maximum production of $^{\bullet}OH$ from Fenton's reaction (1) is expected. For the BDD/carbon felt cell, however, regenerated Fe^{2+} is slowly removed by the weak oxidant peroxodisulfate formed at the BDD anode. This causes two negative effects: (i) a decay in rate of reaction (1) due to the accumulation of a lower quantity of Fe^{2+} and (ii) the enhancement of $Fe(OH)_3$ precipitation on the large surface of the carbon felt cathode with loss of soluble Fe^{3+}. To confirm the catalytic behavior of the Fe^{3+}/Fe^{2+} system in these four systems, their comparative oxidizing power under electro-Fenton conditions was evaluated by studying the degradation of chlorophene.

3.2. Chlorophene decay under electro-Fenton conditions

A series of electrolysis was carried out with 50 mg l^{-1} chlorophene solutions of pH 3.0 at 300 mA to determine the influence of Fe^{3+} concentration on its destruction rate in the Pt/O_2 diffusion cell. The kinetics for the reaction of the antimicrobial with generated oxidants was followed by reversed-phase HPLC chromatography, where it exhibits a well-defined peak with a retention time (t_r) of 16.5 min. The change of its concentration with time for an initial Fe^{3+} content between 0.2 and 8.0 mM is depicted in Fig. 3. A fast and complete removal of chlorophene can be observed in all cases. Its decay rate undergoes a gradual acceleration when Fe^{3+} concentration increases, disappearing from the medium in 20 min for 0.2 mM Fe^{3+}, but in only 3 min for 8.0 mM Fe^{3+}. This effect can be related to an increasing quantity of Fe^{2+} regenerated from reaction (10) that enhances the production of strong oxidant $^{\bullet}OH$ by Fenton's reaction (1) and hence, its reaction with chlorophene. However, in this system this compound could also react with $^{\bullet}OH$ produced at the anode surface from reaction (8) and other weaker oxidizing agents such as H_2O_2 and $HO_2^{\bullet}$. Note that greater amounts of $HO_2^{\bullet}$ are

formed from Fenton-like reaction (4) when Fe^{3+} content rises, although this species is also generated from H_2O_2 oxidation by reaction (13). The possible action of H_2O_2 as oxidant was discarded by confirming that the antimicrobial concentration does not vary in 200 ml of a solution of pH 3.0 prepared with 50 mg l^{-1} of chlorophene and 20 mM H_2O_2. To clarify the influence of $^{\bullet}OH$ and $HO_2^{\bullet}$ produced at the Pt anode, a 50 mg l^{-1} chlorophene solution of pH 3.0 was electrolyzed in the Pt/O_2 diffusion cell, but without Fe^{3+}, i.e., using anodic oxidation in the presence of electrogenerated H_2O_2. Figure 4 shows that this method yields a much slower removal of this compound, disappearing in 300 min, a time much longer than that needed in the presence of Fe^{3+} (see Fig. 3). Since in anodic oxidation organics are oxidized by $^{\bullet}OH$ formed from reaction (8) and in smaller extent by $HO_2^{\bullet}$ largely produced from reaction (13) [39], one can infer that the much faster destruction of the antimicrobial under the electro-Fenton conditions shown in Fig. 3 is due to its reaction with $^{\bullet}OH$ formed from Fenton's reaction (1), which is enhanced with raising Fe^{2+} regeneration when more Fe^{3+} is present in the solution.

A similar influence of Fe^{3+} concentration on chlorophene destruction was observed by electrolyzing 50 mg l^{-1} antimicrobial solutions of pH 3.0 at 300 mA in the BDD/O_2 diffusion cell when the Fe^{3+} content increased from 0.2 to 8.0 mM. However, its decay rate was significantly reduced in comparison to that found for the Pt/O_2 diffusion cell. Figure 4 illustrates that the time required for overall removal of chlorophene increases from 7 min for the Pt/O_2 diffusion cell to 90 min for the BDD/O_2 diffusion one using 4.0 mM Fe^{3+}. This trend seems surprising at first sight, since an acceleration of the destruction of this compound using BDD could be expected due to its much greater oxidizing power [12], as was corroborated by treating comparatively the antimicrobial solution by anodic oxidation in the presence of electrogenerated H_2O_2 either with a BDD or Pt anode. As can be seen in Fig. 4, anodic oxidation with BDD gives faster chlorophene decay, in agreement with the production of more reactive $^{\bullet}OH$ from reaction (8). The opposite effect found under electro-Fenton conditions can then be accounted for by the quicker oxidation of Fe^{2+} to Fe^{3+} at the BDD anode than at the Pt one from reaction (11), along with its additional destruction by reaction (16) with $S_2O_8^{2-}$ generated at the former anode. This causes a drop in the regeneration rate of Fe^{2+} from reaction (10) and consequently, in $^{\bullet}OH$ produced from Fenton's reaction (1),

411 reducing its reaction rate with chlorophene. These results also evidence that this compound is
412 not significantly oxidized by $S_2O_8^{2-}$.
413 When a carbon-felt cathode was used in the electrolytic cell, a more positive action of the
414 Fe^{3+}/Fe^{2+} system was found due to the much faster regeneration of Fe^{2+} at its surface (see Fig.
415 2b) leading to much greater •OH production. Figure 5a shows the chlorophene abatement for
416 50 mg l^{-1} of the antimicrobial solutions of pH 3.0 with Fe^{3+} contents between 0.1 and 2.0 mM
417 treated in the Pt/carbon felt cell at 60 mA. The quickest antimicrobial decay in this system is
418 achieved either with 0.1 or 0.2 mM Fe^{3+}, disappearing in 20 min in both cases, since its
419 removal rate undergoes a gradual drop at higher Fe^{3+} concentration up to needing a time as
420 long as 60 min for its destruction with 2.0 mM Fe^{3+}. This tendency can be associated with a
421 progressive fall of •OH content in solution, mainly due to the participation of non-oxidizing
422 reaction (2), which is strongly accelerated when much larger amounts of Fe^{2+} are formed from
423 reaction (10) as more Fe^{3+} is added to the starting solution. That means that the maximum
424 concentration of reactive •OH in the Pt/carbon felt cell at 60 mA is attained using 0.1-0.2 mM
425 Fe^{3+}, that is, when this radical formed from Fenton's reaction (1) is wasted in smaller extent
426 with regenerated Fe^{2+}. This effect was also found by applying higher currents. As an example,
427 Figure 5b presents the chlorophene removal in the same conditions as in Fig. 5a, but at 300
428 mA. By comparing both figures one can easily deduce that the destruction of this compound
429 is enhanced with raising current, because more amount of oxidant •OH is produced due to the
430 quicker H_2O_2 formation and Fe^{2+} regeneration at the cathode. At 300 mA, however, the
431 antimicrobial disappears in 5 min using 0.2 mM Fe^{3+}, whereas it undergoes a slower removal
432 for the other Fe^{3+} contents. These findings allow concluding that a small concentration equal
433 to 0.2 mM of Fe^{3+} in the starting solution is optimal for this electro-Fenton system. Note that
434 an increase in current also causes the production of more •OH at the Pt anode surface from
435 reaction (8) [20,39,42]. However, the reaction of this species with chlorophene on Pt is
436 insignificant in comparison to that of •OH formed from Fenton's reaction (1), as deduced
437 from Fig. 4. Similar results were obtained by electrolyzing the same solutions with the
438 BDD/carbon felt cell, although the antimicrobial was more slowly removed under comparable
439 conditions, as expected from the negative effect of reaction (16) on Fe^{2+} regeneration, as
440 discussed in section 3.1.

Kinetic analysis of the above chlorophene concentration decays only fit to a pseudo-first-order equation for the cells containing a carbon-felt cathode, where this compound and $^{\bullet}OH$ react very rapidly in solution. The second-order rate constant or absolute rate constant for the aforementioned reaction was then determined using these electro-Fenton systems from the proposed method of competitive kinetics [40], taking benzoic acid as standard competition substrate. Following this method, the pseudo-first-order rate constants for chlorophene ($k_{1,CP}$) and benzoic acid ($k_{1,BA}$) were simultaneously obtained in such systems for short electrolysis times, then calculating the second-order rate constant for chlorophene (k_{CP}) from that of benzoic acid ($k_{BA} = 4.30x10^9$ M^{-1} s^{-1} [55]) as follows:

$$k_{CP} = \frac{k_{1,CP}}{k_{1,BA}} \text{ x } k_{BA} \qquad (17)$$

Figure 6 shows the excellent linear correlations found for the pseudo-fist-order kinetic analysis of the decay of both compounds followed by reversed-phase HPLC chromatography ($t_{r,CP}$ = 15.4 min, $t_{r,BA}$ = 3.4 min) during the electrolysis of 50 mg l^{-1} of chlorophene and 122 mg l^{-1} of benzoic acid with 0.2 mM Fe^{3+} in the Pt/carbon felt and BDD/carbon felt cells at 60 mA. From these plots, values of $k_{1,CP} = 1.15x\ 10^{-3}$ s^{-1} ($R^2 = 0.997$) and $k_{1,BA} = 4.82x10^{-4}$ s^{-1} ($R^2 = 0.995$) for the first cell and $k_{1,CP} = 1.03x\ 10^{-3}$ s^{-1} ($R^2 = 0.996$) and $k_{1,BA} = 4.47x10^{-4}$ s^{-1} ($R^2 = 0.997$) for the second one were determined. Taking these data in Eq. 16, one obtains an average value for k_{CP} of $(1.00\pm0.01)x10^{10}$ M^{-1} s^{-1}, close to $7.1x10^9$ M^{-1} s^{-1} reported by Arnold et al. for chlorophene degradation with Fenton's reagent [47]. This k_{CP}-value allows calculating a steady $^{\bullet}OH$ concentration in solution of about 10^{-13} M at 60 mA.

3.3. TOC removal and mineralization current efficiency

The oxidizing power of the four electro-Fenton systems to mineralize chlorophene solutions was evaluated from their TOC decay. The change of this parameter with time represents the degradation rate of all pollutants. This study was carried out with solutions of pH 3.0 containing 84 mg l^{-1} of antimicrobial (corresponding to 60 mg l^{-1} of TOC) and an efficient Fe^{3+} content by applying different currents for 11 h as maximum. In all cases the

solution pH slightly decreased during electrolysis due to the formation of acidic products, up to a final value of 2.7-2.8.

Figure 7a shows selected TOC-time plots for the degradation of the above chlorophene solution with 4.0 mM Fe^{3+} using an O_2-diffusion cathode. A continuous, but slow, TOC abatement can be observed in the Pt/O_2 diffusion cell, only attaining 52% of mineralization after 660 min of electrolysis at 300 mA. This poor decontamination can be related to the formation of products, as short carboxylic acids and their complexes with iron ions, that are difficultly oxidizable with $^{\bullet}$OH produced in the medium from Fenton's reaction (1) and at the Pt anode surface from reaction (8) [31,32,39,42]. In contrast, these species can be completely removed in the BDD/O_2 diffusion cell at 300 mA (see Fig. 7a), indicating that they are oxidized by $^{\bullet}$OH on BDD. This agrees with the greater oxidation ability of this anode than that of Pt [12]. As can be seen in Fig. 7a, the degradation rate of the chlorophene solution in the BDD/O_2 diffusion cell rapidly increases with raising current from 60 to 300 mA, as expected from the concomitant production of more amount of $^{\bullet}$OH on the anode. After 11 h of treatment, its TOC is reduced by 33%, 45%, 85% and 97% at 60, 100, 200 and 300 mA, respectively. This electro-Fenton system then yields a rapid and total mineralization by applying high currents, when BDD has great oxidizing power.

A much faster degradation of the antimicrobial solution was found using the Pt/carbon felt cell. Figure 7b illustrates that this system is able to decontaminate completely the solution with an optimum concentration 0.2 mM of Fe^{3+} for all currents between 60 and 300 mA. An enhancement of the degradation rate with raising current can be observed, mainly for the first 60 min when aromatic intermediates are expected to be more easily destroyed. In all cases and after 540 min of treatment, more than 95% of mineralization is achieved. The great oxidizing power of this system can be ascribed to the rapid oxidation of all products (aromatics and carboxylic acids) with the high amounts of $^{\bullet}$OH formed from Fenton's reaction (1) due to the fast regeneration of Fe^{2+} at the carbon-felt cathode by reaction (10), without significant participation of $^{\bullet}$OH generated at the Pt anode. Figure 7b also shows that the BDD/carbon felt cell has even higher oxidizing power to decontaminate completely the same solution in a shorter time of 6 h at 300 mA, although TOC is more hardly reduced for the first 2 h and further, much more rapidly removed. The different degradation rate of the BDD/carbon felt

cell compared to that of the Pt/carbon felt one can be accounted for: (i) the slower oxidation rate of chlorophene and its aromatics products in the medium due to the lower production of $^{\bullet}OH$, since Fe^{2+} is accumulated in much less extent by its reaction with $S_2O_8^{2-}$ generated at the BDD anode, and (ii) the parallel quicker destruction of all pollutants with $^{\bullet}OH$ at the BDD anode, enhancing the mineralization of more persistent products such as final carboxylic acids. The much quicker TOC abatement in the BDD/carbon felt cell than in the BDD/O_2 diffusion one at 300 mA (see Figs. 7a and 7b) corroborates the oxidation path via $^{\bullet}OH$ in the medium.

The mineralization of chlorophene is expected to be accompanied by the loss of its chlorine atom in the form of inorganic ions. This was confirmed by treating 84 mg l^{-1} antimicrobial solutions with 0.015 M Na_2SO_4 and 0.2 mM Fe^{3+} of pH 3.0 in the four cells at 150 mA. Ion chromatograms of all electrolyzed solutions only displayed one peak related to chloride ion, discarding the formation of other ions such as chlorate and perchlorate. As can be seen in Fig. 8, Cl^- is rapidly accumulated for 120 min in the cells with a Pt anode and at longer time, it reaches a quasi-steady concentration of about 13 mg l^{-1}, a value very close to 13.6 mg l^{-1} corresponding to the initial chlorine contained in solution. This evidences that all chloro-organics are destroyed with the release of stable chloride ion. A very different behavior can be observed in Fig. 8 for the evolution of Cl^- in the cells with a BDD anode, where this ion reaches a maximum content between 5 and 9 mg l^{-1} at 180 min, further being slowly destroyed until disappearing at 540 min. The instability of Cl^- under these conditions is due to its oxidation to Cl_2 gas on BDD, as reported for the electrolysis of NaCl aqueous solutions with this anode [10].

The above results allow establishing that the mineralization of chlorophene by electro-Fenton involves its conversion into CO_2 and chloride ion as primary inorganic ion. Its overall reaction can be written as follows:

$$C_{13}H_{11}ClO + 25\,H_2O \rightarrow 13\,CO_2 + Cl^- + 61\,H^+ + 60\,e^- \qquad (18)$$

where 60 electrons are involved in the destruction of each molecule of the antimicrobial.

529 The mineralization current efficiencies for the experiments given in Figs. 7a and 7b were
530 then calculated from Eq. 12, considering reaction (18) to evaluate $\Delta(TOC)_{theor}$. The
531 corresponding MCE-time plots thus obtained are presented in Figs. 9a and 9b. In all cases this
532 parameter undergoes a dramatic fall with electrolysis time, as expected if products that are
533 more difficultly oxidizable with $^{\bullet}OH$ than the initial compound, such as short carboxylic
534 acids, are progressively formed. In contrast, all electro-Fenton treatments become much more
535 efficient when current drops. For example, Figure 9a shows that after 60 min of electrolysis in
536 the BDD/O_2 diffusion cell, increasing MCE values of 10%, 12%, 14% and 19% are obtained
537 for decreasing currents of 300, 200, 100 and 60 mA, respectively. Under these same
538 conditions, Figure 9b also shows a gradual rise in efficiency of 30%, 41%, 71% and ca. 100%
539 for the Pt/carbon felt cell. This trend is contrary to the concomitant fall in TOC removal found
540 in these systems due to the smaller production of $^{\bullet}OH$ from reactions (1) and (8) (see Figs. 7a
541 and 7b). The increase in efficiency with decreasing current can then be ascribed to the higher
542 decay in rate of non-oxidizing reactions of this radical, such as reaction (2), giving rise to a
543 larger relative proportion of $^{\bullet}OH$ with ability to react with pollutants. On the other hand,
544 comparison of Figs. 9a and 9b for the trials at 300 mA confirms that the efficiency for
545 chlorophene degradation in the cells, at least at the early stages of treatment, increases in the
546 order: Pt/O_2 diffusion < BDD/O_2 diffusion < BDD/carbon felt < Pt/carbon felt. This can be
547 easily deduced taking into account that after 60 min of electrolysis, for example, the
548 corresponding MCE values are 8.3%, 10%, 17% and 30%.

549 All these findings show that chlorophene can be totally mineralized in the Pt/carbon felt,
550 BDD/carbon felt and BDD/O_2 diffusion cells under electro-Fenton conditions, raising their
551 efficiency as current decreases. The action of the Fe^{3+}/Fe^{2+} catalytic system is optimal in the
552 Pt/carbon felt cell, which yields the highest degradation rate at the beginning of electrolysis
553 with efficiency close to 100% at low current. However, the BDD/carbon felt cell has the
554 highest oxidizing power for overall mineralization at high current due to the greater oxidation
555 ability of BDD than Pt. These systems are then viable for the treatment of wastewaters
556 containing this antimicrobial.
557
558
559

560 *3.4. Identification and time-course of intermediates*

561 Reversed-phase chromatograms of solutions treated by all electro-Fenton systems did not
562 display any identified peak related to aromatic intermediates coming from chlorophene
563 oxidation. Several attempts were then made to try to identify some of such products by
564 electrolyzing 50 mg l^{-1} of the antimicrobial with either 4 mM or 1 mM Fe^{3+} at 60 mA for 30
565 min using the Pt/O_2 diffusion cell with the lowest oxidizing power. However, the GC-MS
566 analyses of collected organics only showed the presence of the remaining chlorophene. These
567 findings evidence that its aromatic products are always oxidized at the same rate as formed,
568 without being accumulated in the solution.

569 Generated carboxylic acids were identified by analyzing the treated solutions by ion-
570 exclusion chromatography. These chromatograms displayed well-defined peaks ascribed to
571 oxalic acid at t_r = 7.8 min, maleic acid at t_r = 9.4 min, glyoxylic acid at t_r = 11.4 min, malonic
572 acid at t_r = 11.7 min, glycolic acid at t_r = 14.5 min, formic acid at t_r = 16.0 min and fumaric
573 acid at t_r = 17.0 min. Maleic, glycolic, malonic and fumaric acids come from the oxidation of
574 the aryl moiety of aromatic products, whereas glyoxylic acid is formed from the degradation
575 of glycolic acid [11,20,31,42]. Further oxidation of these products yields formic and oxalic
576 acids that are transformed into CO_2. The production of oxalic acid was corroborated by
577 treating 50 mg l^{-1} of chlorophene with 4 mM Fe^{3+} at 60 mA for 120 min in the Pt/O_2 diffusion
578 cell. The GC-MS analysis after esterification of the remaining acids with ethanol revealed the
579 presence of an intense peak related to diethyl oxalate (m/z = 146 (2, M^+)) at t_r = 7.9 min.

580 Once the identification of chromatographic peaks was made, the concentration of the
581 different carboxylic acids during the treatment of 84 mg l^{-1} chlorophene solutions in the four
582 electro-Fenton systems at 60 and 300 mA was determined as a function of electrolysis time
583 via external calibration by using standard compounds. The evolution of formic and oxalic
584 acids for these trials is presented in Figs. 10a and 10b, respectively.

585 For the cells containing an O_2-diffusion cathode and 4.0 mM Fe^{3+}, maleic, malonic and
586 fumaric acids were detected at concentrations < 3 mg l^{-1} only operating at 60 mA for 60 min
587 as maximum, similarly to formic acid (see Fig. 10a). In contrast, oxalic acid is largely
588 accumulated at 60 and 300 mA, remaining in solution up to the end of both treatments. Figure
589 10b shows that in the Pt/O_2 diffusion cell this acid reaches 88 mg l^{-1} after 240 min of

electrolysis at 300 mA, whereupon its concentration drops slightly to 68 mg l^{-1} at 540 min, corresponding to 18 mg l^{-1} of TOC, a value much lower than 30 mg l^{-1} found for the remaining solution (see Fig. 7a). This indicates that the solution also contains other undetected products that are hardly oxidized by $^{\bullet}OH$ produced in the medium by Fenton's reaction (1) and at the Pt anode by reaction (8). In this system all iron ions are accumulated as Fe^{3+} (see Fig. 2a) and hence, the majority of oxalic acid is expected to be in the form of Fe^{3+}-oxalate complexes, which can not be oxidized by $^{\bullet}OH$ in solution [5,54]. The quite slow destruction of these species in the Pt/O_2 diffusion cell can then be ascribed to their hard mineralization to CO_2 with $^{\bullet}OH$ at the Pt surface, thus confirming the low oxidation ability of this anode. A similar behavior can be seen in Fig. 10b for the BDD/O_2 diffusion cell at 60 mA, where oxalic acid attains a quasi steady-concentration of 45 mg l^{-1} at times longer than 180 min, corresponding to 12mg l^{-1} of TOC, a value very far from 40 mg l^{-1} of TOC determined for the final electrolyzed solution, as can be seen in Fig. 7a. At this low current, this system is unable to destroy Fe^{3+}-oxalate complexes and other undetected products. However, when the current rises to 300 mA, oxalic acid (see Fig. 10b) and the solution TOC (see Fig. 7a) are completely removed at 660 min. The overall mineralization of chlorophene in the BDD/O_2 diffusion cell at 300 mA can be explained by the efficient oxidation of final Fe^{3+}-oxalate complexes with $^{\bullet}OH$ on BDD, as expected from its great oxidizing power at high current [12-22].

Maleic, malonic, fumaric, glycolic, glyoxylic and formic acids were found in larger extent and during longer time in the Pt/carbon felt cell than in the BDD/carbon felt one using 0.2 mM Fe^{3+} at 60 mA, but were not detected at 300 mA due to their faster destruction. For example, Figure 10a shows a great accumulation of formic acid up to 17 mg l^{-1} at 120 min of electrolysis in the first system at 60 mA and its complete mineralization in ca. 360 min, whereas for the second system, this acid only persists for 120 min, reaching 1.5 mg l^{-1} as maximum. These results indicate that in the Pt/carbon felt cell all aromatic intermediates are transformed into carboxylic acids, because they react rapidly with the large amounts of $^{\bullet}OH$ formed from Fenton's reaction (1), which is enhanced by the fast regeneration of Fe^{2+} at the cathode from reaction (10). Even the persistent final oxalic acid can be totally converted into CO_2 under these conditions at ca. 540 min (see Fig. 10b), when all solution TOC is removed

620 (see Fig. 7b). The mineralization of this acid is accelerated with increasing current due to the
621 quicker production of oxidant •OH, as can be observed in Fig. 10b, attaining a maximum
622 content of 33 and 21 mg l^{-1} after 120 min of electrolysis at 60 and 300 mA, respectively. The
623 low concentration of iron ions, practically all of them as Fe^{2+} (see Fig. 2b), in the solution
624 treated in the Pt/carbon felt cell suggests the formation of quite a small proportion of Fe^{2+}-
625 oxalato complexes, and hence, this acid and its Fe^{2+} complexes are directly oxidized with •OH
626 in the medium, since they can not be destroyed by this radical on Pt [12].
627 The lower accumulation of carboxylic acids in the BDD/carbon felt cell can be related to
628 a slower destruction of aromatics since •OH is generated to a lesser extent from Fenton's
629 reaction (1), because of the parallel oxidation of Fe^{2+} with $S_2O_8^{2-}$ from reaction (16). This
630 agrees with the fact that the efficiency found in this cell is lower than in the Pt/carbon felt one
631 during the early stages for both treatments at 300 mA (see Fig. 9). However, in the
632 BDD/carbon felt cell the degradation of carboxylic acids is enhanced by their simultaneous
633 oxidation at the BDD surface, mainly at high current when this anode produces a large
634 amount of •OH from reaction (8). This behavior can be confirmed in Fig. 10b from the
635 corresponding evolution of oxalic acid, since it disappears in only 360 min at 300 mA, but in
636 contrast it needs more than 540 min to be removed at 60 mA, when it is mainly destroyed by
637 •OH in solution. The faster destruction of this acid in the BDD/carbon felt cell in comparison
638 to the other electro-Fenton systems at high current accounts for its highest oxidizing power
639 for total mineralization.
640 The possible reaction paths of oxalic acid, that is the ultimate by-product generated along
641 the mineralization before the conversion of all the initial organic carbon into CO_2, in the
642 electro-Fenton systems are schematized in Fig. 11. In the cells with an O_2-diffusion cathode
643 Fe^{3+}-oxalate complexes are accumulated in large extent, so the overall mineralization is
644 uniquely achieved by •OH on a BDD anode at high current. In the cells with a carbon-felt
645 cathode, oxalic acid can be directly transformed into CO_2 by •OH formed in solution. When a
646 Pt anode is used under these conditions, this oxidant can also destroy Fe^{2+}-oxalate complexes
647 present in small proportion, whereas for BDD, oxalic acid and its Fe^{2+} and Fe^{3+} complexes
648 can also be oxidized by the efficient •OH formed at the anode surface at high current.
649

4. Conclusions

The catalytic behavior of the Fe^{3+}/Fe^{2+} system in the electro-Fenton degradation of chlorophene solutions with 0.05 M Na_2SO_4 and different Fe^{3+} concentrations of pH 3.0 mainly depends on the cathode tested. The cells with either a Pt or BDD anode and an O_2-diffusion cathode yield a large accumulation of electrogenerated H_2O_2 while Fe^{3+} content remains practically constant. Chlorophene falls more rapidly with raising Fe^{3+} concentration up to 8.0 mM, since more amount of oxidant $^{\bullet}OH$ is formed from Fenton's reaction (1) due to the higher amount of Fe^{2+} regenerated at the O_2-diffusion cathode from reaction (10). In contrast, the latter reaction is so fast at a carbon-felt cathode that Fe^{2+} is largely accumulated, but H_2O_2 is electrogenerated in small extent. This is feasible by the much slower oxidation of Fe^{2+} at Pt and BDD from reaction (10), as explained by the pseudo-first-order rate constants determined. In these systems the antimicrobial decay is enhanced with raising current thanks to the higher generation of H_2O_2 and Fe^{2+} leading to greater amount of $^{\bullet}OH$ from Fenton's reaction (1), only being required 0.2 mM Fe^{3+} to obtain its maximum production under all applied currents. The removal rate of chlorophene is always lower in the cells with BDD than with Pt, because Fe^{2+} is less accumulated since it is also oxidized with peroxodisulfate generated at the BDD anode. A second-order rate constant of $(1.00\pm0.01)\times10^{10}$ M^{-1} s^{-1} is determined for the reaction between chlorophene and $^{\bullet}OH$ in solution from the method of competitive kinetics with benzoic acid. Concentrated solutions of the antimicrobial are poorly decontaminated in the Pt/O_2 diffusion cell with 4.0 mM Fe^{3+}, whereas total mineralization is achieved using the BDD/O_2 diffusion cell with 4.0 mM Fe^{3+} at high current and the Pt/carbon felt and BDD/carbon felt cells with 0.2 mM Fe^{3+}. The initial chlorine is completely released as chloride ion, which remains stable in solution using a Pt anode, but it is oxidized to Cl_2 on BDD. At the early stages of treatment, the efficiency for the degradation process in the cells increases in the order: Pt/O_2 diffusion < BDD/O_2 diffusion < BDD/carbon felt < Pt/carbon felt, although it always rises with decreasing current. The hard oxidation of final Fe^{3+}-oxalate complexes and other undetected products with $^{\bullet}OH$ in the medium and at the Pt surface accounts for the poor degradation in the Pt/O_2 diffusion cell. These species are completely mineralized at a BDD anode at high current due to the great production of reactive $^{\bullet}OH$ on its

surface. In the cells with a carbon-felt cathode oxalic acid and its Fe^{2+} complexes are directly oxidized with $^{\bullet}OH$ in the medium. The highest oxidizing power for total mineralization at high current is attained for the BDD/carbon felt cell, when this acid can be simultaneously destroyed on BDD. These results show that electro-Fenton is a viable environmentally friendly technology for the remediation of wastewaters containing chlorophene.

Acknowledgments

Financial support from MEC (Ministerio de Educación y Ciencia, Spain) under project CTQ2004-01954/BQU and from MJENR (Ministère de la Jeunesse, de l'Education Nationale et de la Recherche, France) under decision number 03V398 is acknowledged. The authors thank DURSI (Departament d'Universitats, Recerca i Societat de la Informació, Generalitat de Catalunya) for the grant given to I. Sirés to do this work.

694 **References**

695

696 [1] R. Andreozzi, V. Caprio, A. Insola, R. Marotta, Catal. Today 53 (1999) 51-59.
697 [2] M. Tarr (Ed.), Chemical Degradation Methods for Wastes and Pollutants.
698 Environmental and Industrial Applications, Marcel Dekker, Inc., New York, 2003.
699 [3] M. Pera-Titus, V. García-Molina, M.A. Baños, J. Giménez, S. Esplugas, Appl. Catal. B:
700 Environ. 47 (2004) 219-256.
701 [4] H. Gallard, J. De Laat, B. Legube, New J. Chem. 22 (1998) 263-268.
702 [5] Y. Sun, J.J. Pignatello, Environ. Sci. Technol. 27 (1993) 304-310.
703 [6] G.U. Buxton, C.L. Greenstock, W.P. Helman, A.B. Ross, J. Phys. Chem. Data Ref. 17
704 (1988) 513-886.
705 [7] J. De Laat, H. Gallard, Environ. Sci. Technol. 33 (1999) 2726-2732.
706 [8] J.D. Rush, B.H.J. Bielski, J. Phys. Chem. 89 (1985) 5062-5066.
707 [9] B. Marselli, J. García-Gomez, P.A. Michaud, M.A. Rodrigo, Ch. Comninellis, J.
708 Electrochem. Soc. 150 (2003) D79-D83.
709 [10] A. Kraft, M. Stadelmann, M. Blaschke, J. Hazard. Mat. B 103 (2003) 247-261.
710 [11] E. Brillas, I. Sirés, C. Arias, P.L. Cabot, F. Centellas, R.M. Rodríguez, J.A. Garrido,
711 Chemosphere 58 (2005) 399-406.
712 [12] M. Panizza, G. Cerisola, Electrochim. Acta 51 (2005) 191-199.
713 [13] J. Iniesta, P.A. Michaud, M. Panizza, G. Cerisola, A. Aldaz, Ch. Comninellis,
714 Electrochim. Acta 46 (2001) 3573-3578.
715 [14] M. Panizza, P.A. Michaud, G. Cerisola, Ch. Comninellis, J. Electroanal. Chem. 507
716 (2001) 206-214.
717 [15] S. Hattori, M. Doi, E. Takahashi, T. Kurosu, M. Nara, S. Nakamatsu, Y. Nishiki, T.
718 Furuta, M. Iida, J. Appl. Electrochem. 33 (2003) 85-91.
719 [16] M. Panizza, G. Cerisola, Electrochim. Acta 49 (2004) 3221-3226.
720 [17] E. Brillas, B. Boye, I. Sirés, J.A. Garrido, R.M. Rodríguez, C. Arias, P.L. Cabot, Ch.
721 Comninellis, Electrochim. Acta 49 (2004) 4487-4496.
722 [18] P. Cañizares, C. Sáez, J. Lobato, M.A. Rodrigo, Ind. Eng. Chem. Res. 43 (2004) 1944-
723 1951.

724 [19] C.A. Martinez-Huitle, S. Ferro, A. De Battisti, Electrochim. Acta 49 (2004) 4027-4034.
725 [20] C. Flox, J.A. Garrido, R.M. Rodríguez, F. Centellas, P.L. Cabot, C. Arias, E. Brillas,
726 Electrochim. Acta 50 (2005) 3685-3692.
727 [21] B. Nasr, G. Abdellatif, P. Cañizares, C. Sáez, J. Lobato, M.A. Rodrigo, Environ. Sci.
728 Technol. 39 (2005) 7234-7239.
729 [22] X. Chen, G. Chen, Sep. Purif. Technol. 48 (2006) 45-59.
730 [23] Y.L. Hsiao, K. Nobe, J. Appl. Electrochem. 23 (1993) 943-946.
731 [24] C. Ponce de Leon, D. Pletcher, J. Appl. Electrochem. 25 (1995) 307-314.
732 [25] E. Brillas, E. Mur, R. Sauleda, L. Sánchez, J. Peral, X. Domènech, J. Casado, Appl.
733 Catal. B: Environ. 16 (1998) 31-42.
734 [26] A. Alverez-Gallegos, D. Pletcher, Electrochim. Acta 44 (1999) 2483-2492.
735 [27] T. Harrington, D. Pletcher, J. Electrochem. Soc. 146 (1999) 2983-2989.
736 [28] M.A. Oturan, J.J. Aaron, N. Oturan, J. Pinson, Pestic. Sci. 55 (1999) 558-562.
737 [29] M. A. Oturan, J. Appl. Electrochem. 30 (2000) 475-482.
738 [30] J.J. Aaron, M.A. Oturan, Turk. J. Chem. 25 (2001) 509-520.
739 [31] B. Boye, M.M. Dieng, E. Brillas, Environ. Sci. Technol. 36 (2002) 3030-3035.
740 [32] E. Brillas, M.A. Baños, J.A. Garrido, Electrochim. Acta 48 (2003) 1697-1705.
741 [33] B. Gözmen, M.A. Oturan, N. Oturan, O. Erbatur, Environ. Sci. Technol. 37 (2003)
742 3716-3723.
743 [34] E. Guivarch, N. Oturan, M.A. Oturan, Environ. Chem. Lett. 1 (2003) 165-168.
744 [35] G. Kaichouh, N. Oturan, M.A. Oturan, K. El Kacemi, A. El Hourch, Environ. Chem.
745 Lett. 2 (2004) 31-33.
746 [36] M.C. Edelahi, N. Oturan, M.A. Oturan, Y. Padellec, A. Bermond, K. El Kacemi,
747 Environ. Chem. Lett. 1 (2004) 233-236.
748 [37] E. Guivarch, T. Trévin, C. Lahitte, M.A. Oturan, Environ. Chem. Lett. 1 (2003) 39-44.
749 [38] M.A. Oturan, N. Oturan, C. Lahitte, S. Trévin, J. Electroanal. Chem. 507 (2001) 96-
750 102.
751 [39] E. Brillas, M.A. Baños, S. Camps, C. Arias, P.L. Cabot, J.A. Garrido, R.M. Rodríguez,
752 New J. Chem. 28 (2004) 314-322.
753 [40] K. Hanna, S. Chiron, M.A. Oturan, Water Res. 39 (2005) 2763-2773.

754 [41] A. Wang, J. Qu, J. Ru, H. Liu, J. Ge, Dyes Pigments 65 (2005) 227-233.
755 [42] I. Sirés, J.A. Garrido, R.M. Rodríguez, P.L. Cabot, F. Centellas, C. Arias, E. Brillas, J.
756 Electrochem. Soc. 153 (2006) D1-D9.
757 [43] S. Irmak, H.I. Yavuz, O. Erbatur, Appl. Catal. B: Environ. 63 (2006) 243-248.
758 [44] Y.B. Xie, X.Z. Li, Mat. Chem. Phys. 95 (2006) 39-50.
759 [45] C. Flox, S. Ammar, C. Arias, E. Brillas, A.V. Vargas-Zavala, R. Abdelhedi, Appl.
760 Catal. B: Environ. 67 (2006) 93-104.
761 [46] H. Zhang, C.H. Huang, Environ. Sci. Technol. 37 (2003) 2421-2430.
762 [47] W.A. Arnold, K. McNeil, J.L. Packer, D.E. Latch, A.L. Boreen, Report of the USGS-
763 WRRI 104G National Grants Competition, 2003, p. 18.
764 [48] W. Boehmer, H. Ruedel, A. Wenzel, C. Schroeter-Kermani, Organohalogen Comp. 66
765 (2004) 1489-1494.
766 [49] T.A. Yamarik, Int. J. Toxicol. 23 (2004) 1-27.
767 [50] F.J. Welcher, (Ed.), Standard Methods of Chemical Analysis, R.E. Krieger Pub. Co.,
768 Huntington, New York, 1975, Vol. 2 (Part B), 6th ed., p. 1827.
769 [51] N.H. Furman, (Ed.), Standard Methods of Chemical Analysis, R.E. Krieger Pub. Co.,
770 Huntington, New York, 1975, Vol. 1, 6th ed., p. 553.
771 [52] E.B. Sandell, in: B.L. Clarke, P.J. Elving, I.M. Kolthoff (Eds.), Chemical Analysis,
772 Interscience Publishers, Inc., New York, 1959, Vol. III, 3rd ed., p.522.
773 [53] S.S. Gupta, Y.K. Gupta, Inorg. Chem. 20 (1981) 454-457.
774 [54] Y. Zuo,J. Hoigné, Environ. Sci. Technol. 26 (1992) 1014-1022.
775 [55] M.A. Oturan, J. Pinson, J. Phys. Chem. 99 (1995) 13948-13954.

Figure captions

Fig. 1. Chemical structure of chlorophene.

Fig. 2. Time-course of Fe^{3+}, Fe^{2+} and H_2O_2 concentrations during the electrolysis of 200 ml of 0.05 M Na_2SO_4 solutions with different Fe^{3+} contents at pH 3.0, 300 mA and room temperature in a one-compartment cell. Plots: (a) 4.0 mM Fe^{3+} and a 3 cm^2 O_2-diffusion cathode; (b) 0.20 mM Fe^{3+}, air saturated solutions and a 70 cm^2 carbon-felt cathode. Species: (○) Fe^{3+}, (□) Fe^{2+} and (Δ) H_2O_2 using a 3 cm^2 Pt anode; (●) Fe^{3+}, (■) Fe^{2+} and (▲) H_2O_2 using a 3 cm^2 BDD anode.

Fig. 3. Effect of Fe^{3+} concentration on chlorophene concentration decay during the electro-Fenton treatment of 200 ml of 50 mg l^{-1} antimicrobial solutions in 0.05 M Na_2SO_4 of pH 3.0 at 300 mA and room temperature using a Pt/O_2 diffusion cell. $[Fe^{3+}]_0$: (●) 0.2 mM, (■) 1.0 mM, (♦) 2.0 mM, (▲) 4.0 mM, (▼) 6.0 mM, (◣) 8.0 mM.

Fig. 4. Chlorophene abatement with electrolysis time for 200 ml of 50 mg l^{-1} antimicrobial solutions in 0.05 M Na_2SO_4 of pH 3.0 degraded at 300 mA and room temperature by: anodic oxidation (without Fe^{3+}) in the presence of electrogenerated H_2O_2 with a (●) Pt/O_2 diffusion and (■) BDD/O_2 diffusion cell; electro-Fenton with 4.0 mM Fe^{3+} using a (▲) Pt/O_2 diffusion and (♦) BDD/O_2 diffusion cell.

Fig. 5. Influence of current and Fe^{3+} content on chlorophene concentration decay during the electro-Fenton treatment of 200 ml of 50 mg l^{-1} of this antimicrobial and 0.05 M Na_2SO_4 at pH 3.0 and room temperature using a Pt/carbon felt cell. Each solution was previously saturated with air. Current: (a) 60 mA, (b) 300 mA. $[Fe^{3+}]_0$: (○) 0.1 mM, (■) 0.2 mM, (♦) 0.5 mM, (▲) 1.0 mM, (▼) 2.0 mM.

Fig. 6. Kinetic analysis for the pseudo first-order reaction of (○,□) chlorophene and (●,■) benzoic acid with hydroxyl radical. Electro-Fenton experiments were carried out with 200 ml

of an air saturated solution containing 50 mg l^{-1} chlorophene, 122 mg l^{-1} benzoic acid, 0.05 M Na_2SO_4 and 0.2 mM Fe^{3+} at pH 3.0, 60 mA and room temperature using a (○,●) Pt/carbon felt and (□,■) BDD/carbon felt cell.

Fig. 7. TOC removal vs. electrolysis time for 200 ml of 84 mg l^{-1} chlorophene solutions in 0.05 M Na_2SO_4 with different Fe^{3+} contents of pH 3.0 treated by electro-Fenton at room temperature. In plot (a), solutions with 4.0 mM Fe^{3+} in a (©) Pt/O_2 diffusion and (●,■,▲,♦) BDD/O_2 diffusion cell. In plot (b), air saturated solutions with 0.2 mM Fe^{3+} in a (●,■,▲,♦) Pt/carbon felt and (©) BDD/carbon felt cell. Current: (●) 60 mA, (■) 100 mA, (▲) 200 mA, (♦,©) 300 mA.

Fig. 8. Concentration of chloride ion accumulated during the electro-Fenton treatment of 200 ml of an 84 mg l^{-1} chlorophene solution with 0.015 M Na_2SO_4 and 0.2 mM Fe^{3+} of pH 3.0 at 150 mA and at room temperature using a (●) Pt/O_2 diffusion, (■) Pt/carbon felt, (♦) BDD/O_2 diffusion and (▲) BDD/carbon felt cell.

Fig. 9. Dependence of mineralization current efficiency calculated from Eq. 11 on electrolysis time for the experiments reported in: (a) Fig. 7a, (b) Fig. 7b.

Fig. 10. Evolution of the concentration of (a) formic and (b) oxalic acids detected as final carboxylic acids during the electro-Fenton degradation of 200 ml of 84 mg l^{-1} chlorophene solutions in 0.05 M Na_2SO_4 of pH 3.0 at room temperature. System: Pt/O_2 diffusion cell with 4.0 mM Fe^{3+} at (●) 60 mA and (○) 300 mA; BDD/O_2 diffusion cell with 4.0 mM Fe^{3+} at (♦) 60 mA and (©) 300 mA; Pt/carbon felt cell with 0.2 mM Fe^{3+} at (■) 60 mA and (□) 300 mA; BDD/carbon felt cell with 0.2 mM Fe^{3+} at (▲) 60 mA and (Δ) 300 mA.

Fig. 11. Reaction paths of oxalic acid in the electro-Fenton systems. $^{\bullet}OH$ denotes the hydroxyl radical generated in solution and BDD($^{\bullet}OH$) represents the hydroxyl radical formed on the BDD anode surface.

*** List of Three (3) Potential Reviewers**

Possible reviewers

Prof. André Savall : savall@chimie.ups-tlse.fr
Laboratoire de Génie Chimique, Université Paul Sabatier, 118 route de Narbonne, 31062 Toulouse, France

Dr. Birame Boye : b.boye@mbi-consultin.com
Istituto di Chimica Fisica ed Elettrochimica, Università degli Study di Padova, Via Marzolo 14, 35131 Padova, Italy

Prof. Dr. Christos Comninellis : christos.comninellis@epfl.ch
Groupe de génie Electrochimique, Ecole Polytechnique Fédérale de Lausanne,
SB-ISP-UGEC, 1015 Lausanne - SWITZERLAND.
Fax : +41-21 693 3190

Figure(s)

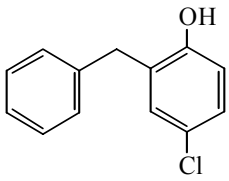

Fig. 1

Figure(s)

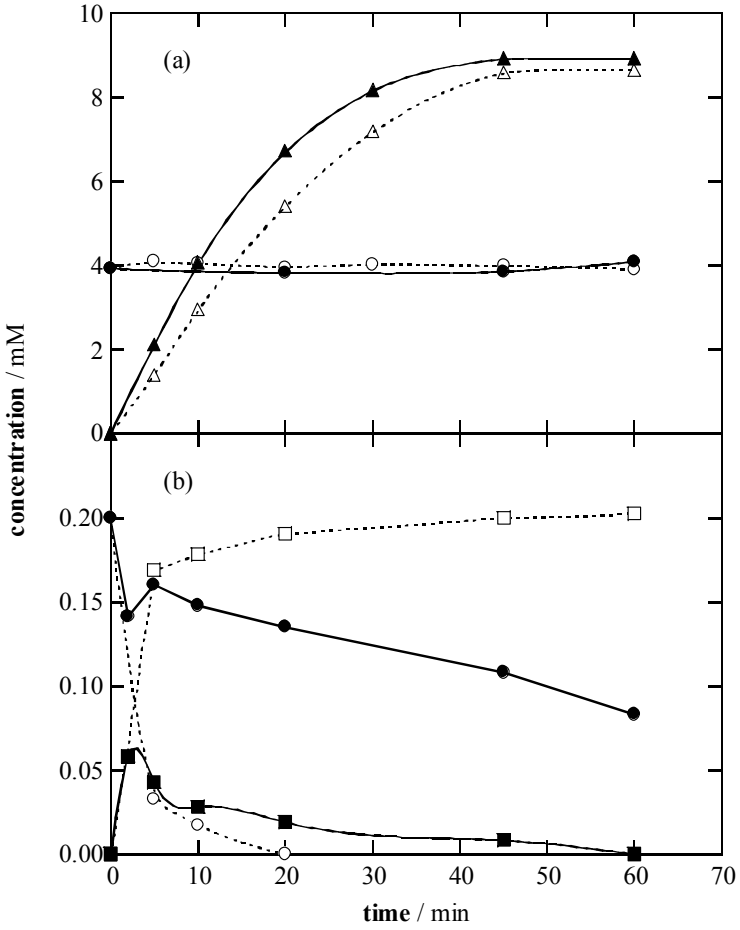

Fig. 2

Figure(s)

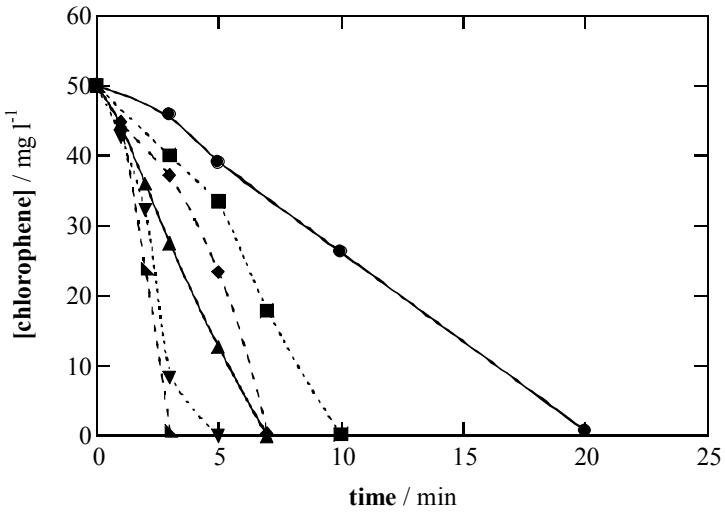

Fig. 3

Figure(s)

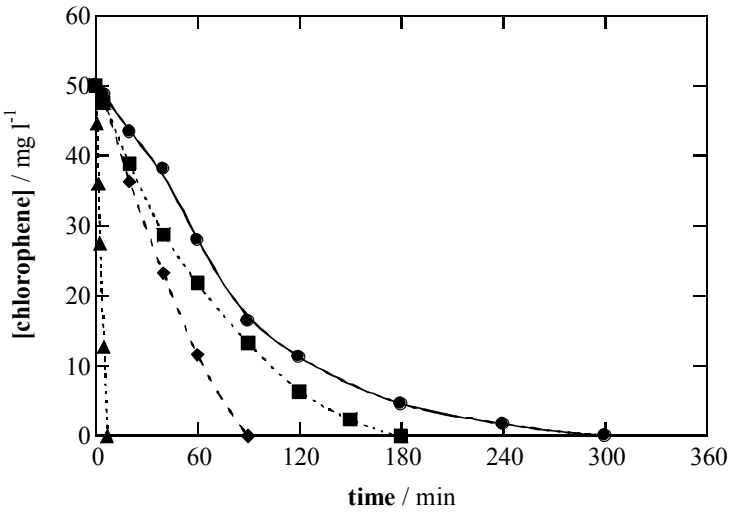

Fig. 4

Figure(s)

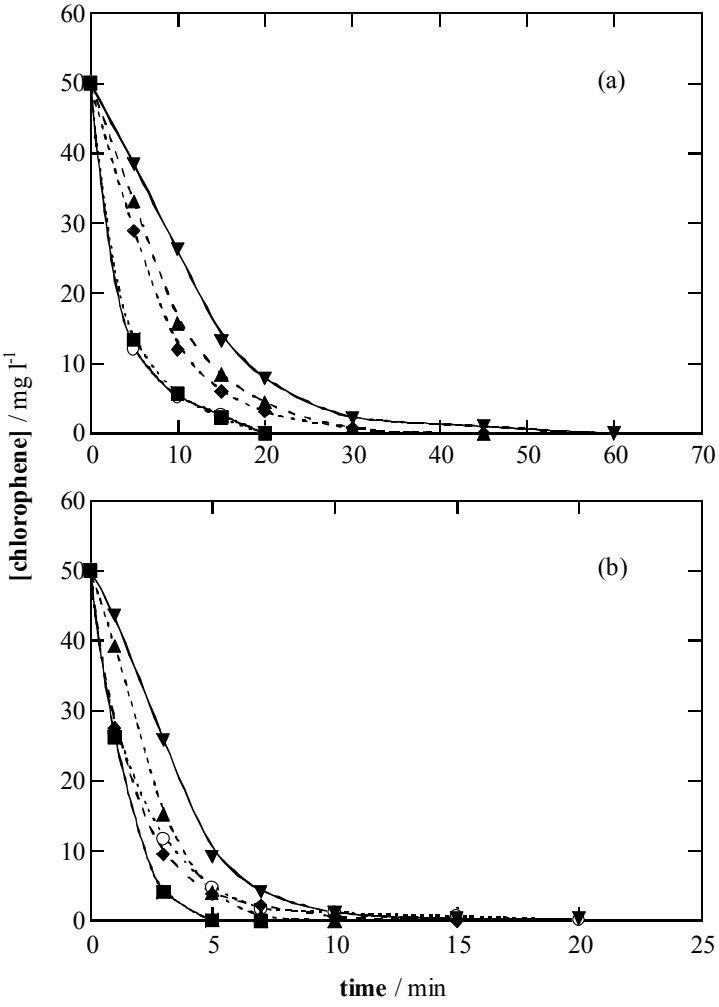

Fig. 5

Figure(s)

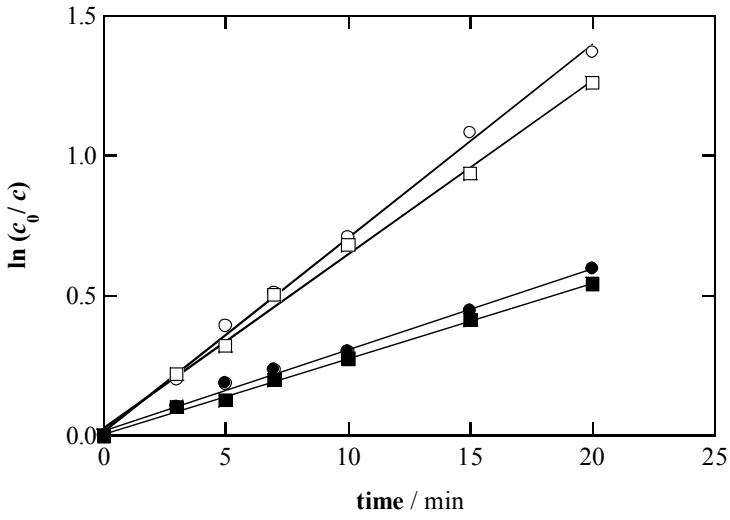

Fig. 6

Figure(s)

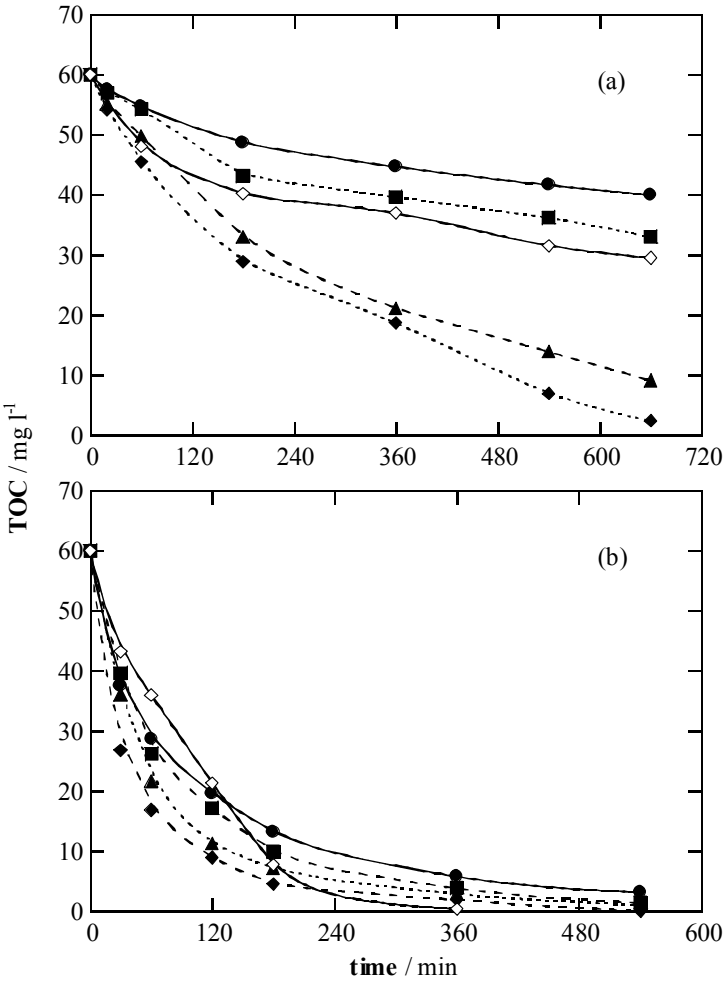

Fig. 7

Figure(s)

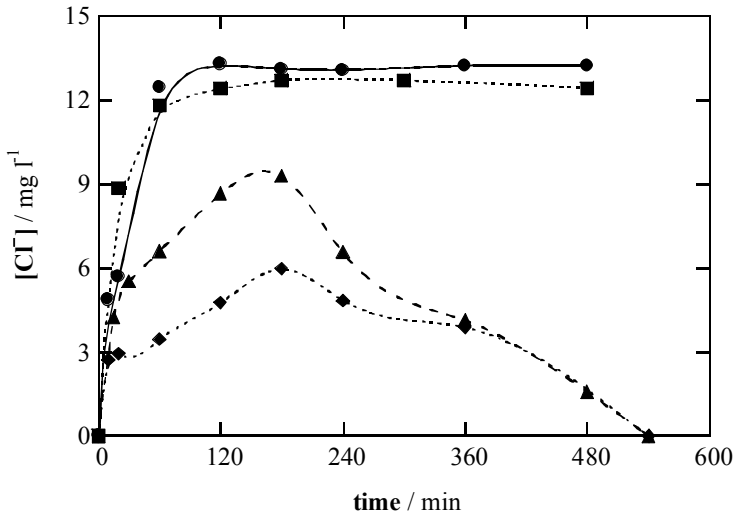

Fig. 8

Figure(s)

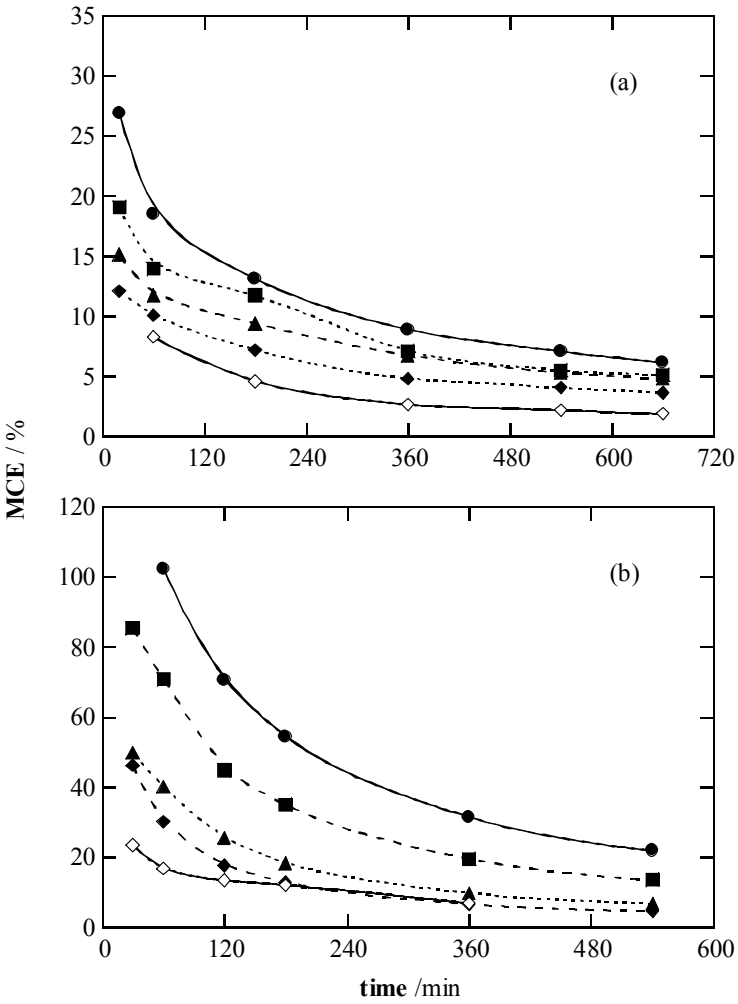

Fig. 9

Figure(s)

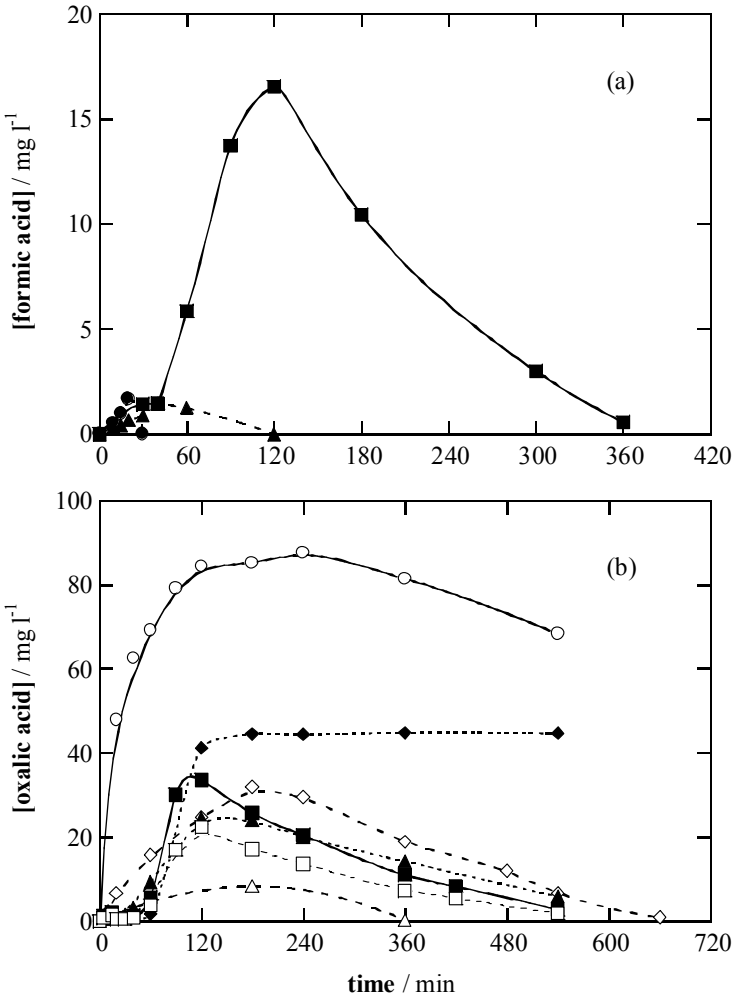

Fig. 10

Figure(s)

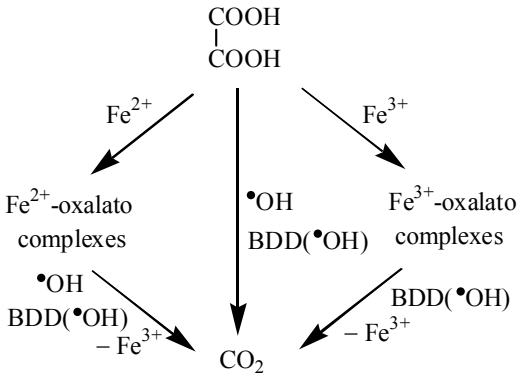

Fig. 11

9.2.2. Resultats i Discussió / *Results and Discussion*

First of all, the catalytic behavior of the Fe^{3+}/Fe^{2+} system in the EF process has been tested in the absence of chlorophene. The oxidation ability of Pt and BDD to transform directly Fe^{2+} into Fe^{3+} has been examined by electrolyzing 200-mL solutions of 0.05 M Na_2SO_4 with 4.0 mM Fe^{2+}, at pH 3.0 and at 300 mA, using a stainless steel cathode. A quick decay of Fe^{2+} concentration and a simultanous increase of Fe^{3+} is found using both anodes, thus indicating a fast direct oxidation at each anode. Fe^{2+} is completely removed after 45 and 64 min using BDD and Pt, respectively. This fact can be explained considering that BDD favors the direct oxidation of Fe^{2+} instead of O_2 evolution. A pseudo-first-order decay is found in both cases at their early stages.

Several electrolyses of 0.05 M Na_2SO_4 solutions at pH 3.0 have been performed for 60 min at 300 mA using Pt and BDD anodes, with 4.0 and 0.2 mM Fe^{3+} in O_2-diffusion and carbon felt cells, respectively, in order to assess the evolution of Fe^{2+}, Fe^{3+} and H_2O_2. The results for the O_2 diffusion cells allow concluding that Fe^{3+} concentration remains unaltered, so the amount of Fe^{2+} accumulated is insignificant. This means that direct reduction of Fe^{3+} occurs to a very small extent at the O_2-diffusion cathode and the regenerated Fe^{2+} is quickly converted into Fe^{3+} from Reactions 5.-3, 5.-5 and 5.-14, as well as from direct oxidation at the anode. In addition, H_2O_2 is continuously accumulated up to reach a steady concentration of about 9 mM after 45 min using both anodes. The latter behavior was widely described in section 7.2.1. The results for the carbon felt cells present significant differences depending on the anode used. The use of Pt/carbon felt cell causes the reduction of all the initial Fe^{3+} to Fe^{2+} in 20 min, thus indicating that direct reduction at the carbon-felt cathode is considerably fast: a reduction rate of 8.10×10^{-7} M s^{-1} is obtained, a value much higher than the direct oxidation rate of 1.17×10^{-7} M s^{-1} calculated for Fe^{2+} at the Pt anode. The amount of H_2O_2 accumulated is rather low (0.23 mM after 60 min). On the other hand, overall Fe^{3+} reduction is not achieved in the BDD/carbon felt cell, since Fe^{2+} immediately rises

up to 0.058 mM after 2 min, further being slowly removed until its disappearance after 60 min. The concentration of H_2O_2 after 60 min is again very low, ca. 0.20 mM. This surprising trend can be explained by the important role of the weaker oxidizing species produced at the BDD anode (see section 8.2.2), which are able to oxidize Fe^{2+} significantly. For example, $S_2O_8^{2-}$ ions can oxidize Fe^{2+} to Fe^{3+} with k = 23 M^{-1} s^{-1}. However, Fe^{3+} is not completely regenerated from the oxidizing reactions because it undergoes a gradual abatement, which can be accounted for by the precipitation of $Fe(OH)_3$ on the large surface of the carbon-felt cathode. This precipitate is favored by the OH^- formed from water reduction near the cathode in the BDD/carbon felt system.

In conclusion, the Pt/carbon felt system accumulates Fe^{2+} able to react largely with H_2O_2 to produce high amounts of $^{\bullet}OH$ from Fenton's reaction, whereas in the BDD/carbon felt system Fe^{2+} is slowly destroyed, thus causing a lower production of $^{\bullet}OH$ as well as a decrease of soluble Fe^{3+} concentration due to $Fe(OH)_3$ precipitation. In contrast, the O_2-diffusion systems accumulate H_2O_2 and lower amounts of Fe^{2+}.

To confirm the above comments, the degradation of chlorophene by the four EF processes has been thoroughly studied. The influence of Fe^{3+} concentration on chlorophene decay has been studied by reversed-phase HPLC chromatography. Firstly, several 50-mg L^{-1} chlorophene solutions, with Fe^{3+} contents between 0.2 and 8.0 mM have been electrolyzed at pH 3.0 and at 300 mA using the Pt/O_2 diffusion cell. Results show a fast and complete removal of the pharmaceutical whatever the initial Fe^{3+} amount may be. Its destruction rate undergoes a progressive acceleration as Fe^{3+} concentration increases, disappearing after 20 and 3 min for 0.2 and 8.0 mM, respectively. This trend can be related to an increasing amount of Fe^{2+} regenerated from direct cathodic reduction of Fe^{3+}, thus enhancing the oxidation of chlorophene with $^{\bullet}OH$ produced from Fenton's reaction (Reaction 5.-3). $^{\bullet}OH_{ads}$ formed at the Pt surface (Reaction 5.-44) and a weaker oxidizing species such as $HO_2^{\bullet}$ (Reactions 5.-4 and 5.-48) could contribute to the destruction of this pharmaceutical as well.

In contrast, the oxidizing power of H_2O_2 can be discarded because a chemical test carried out with 20 mM H_2O_2 reflects no alteration of chlorophene concentration. The role of $^{\bullet}OH_{ads}$ and $HO_2^{\bullet}$ produced at the anode has been clarified by electrolyzing a chlorophene solution under the conditions given above, but without Fe^{3+}, using the Pt/O_2 diffusion cell. The results of this degradation by AO with electrogenerated H_2O_2 indicate that the initial compound disappears much more slowly, after about 300 min. It can be concluded that the main oxidizing agent in this electrolytic system is $^{\bullet}OH$ produced from Fenton's reaction. The greater oxidizing power of BDD, previously discussed for paracetamol and clofibric acid mineralization, is also demonstrated for chlorophene, where AO with electrogenerated H_2O_2 using the BDD/O_2 diffusion cell causes the total chlorophene destruction after 180 min. The effect of Fe^{3+} concentration is similar to that described above using Pt, but it is worth noting that the destruction rate of chlorophene is significantly reduced. A chlorophene removal time of 7 and 90 min is obtained for the Pt and BDD systems, respectively, using 4.0 mM Fe^{3+}. This effect can be explained by the quicker oxidation of Fe^{2+} to Fe^{3+}, and even to ferrate ions (see section 8.3.2), at the BDD anode in comparison to that taking place at the Pt anode, along with its additional destruction by reaction with $S_2O_8^{2-}$ ions, involving $SO_4^{\bullet-}$ (see section 8.3.2). Fe^{2+} disappearance leads to a drop in the production of $^{\bullet}OH$ from Fenton's reaction, thus making the chlorophene decay much slower. At this point it must be mentioned the huge influence of the iron source used in EF on the $^{\bullet}OH$ production: Figure 8.-6 in section 8.3.2 shows a very similar decay of clofibric acid in the Pt/O_2 diffusion and BDD/O_2 diffusion cells when Fe^{2+} is used, because in both cases the amount of $^{\bullet}OH$ generated from Fenton's reaction is high enough to yield an analogous oxidation during the early stages (i.e., clofibric acid is destroyed after 7 min). On the contrary, Fe^{2+} regeneration is so difficult in such an oxidizing system as BDD/O_2 diffusion when Fe^{3+} is used, that the destruction rate for chlorophene is significantly lower compared to that of the Pt/O_2 diffusion cell. The use of the carbon-felt cathode leads to a greater production of $^{\bullet}OH$ due to the fast Fe^{2+} regeneration, so chlorophene destruction

should be accelerated. Thus, chlorophene is removed after 5 min at 300 mA with 0.2 mM Fe^{3+} using the Pt/carbon felt cell, and its decay becomes slower with rising Fe^{3+} concentration. This is due to the action of the non-oxidizing reactions involving an ever increasing Fe^{2+} concentration regenerated at the cathode. With 0.1-0.2 mM Fe^{3+} the hydroxyl radical formed from Fenton's reaction is wasted to a small extent in those parasite reactions. In addition, an increase in current causes a quicker decay due to the production of more oxidizing species. The same trends are found by electrolyzing the above solutions with the BDD/carbon felt cell, and again a negative effect on chlorophene removal is observed because the oxidizing power of BDD hinders the Fe^{2+} regeneration.

The above concentration decays can be fitted to a pseudo-first-order kinetic equation. The reaction between chlorophene and $^{\bullet}OH$ is especially fast for the cells containing a carbon-felt cathode due to the high constant concentration of this radical in the medium, so the absolute rate constant (k_2) for this reaction has been determined in those cells using Pt and BDD anodes. Taking benzoic acid as standard competition substrate, pseudo-first-order rate constants (k_1) are obtained for chlorophene and benzoic acid, so considering $k_2 = 4.30 \times 10^9$ M^{-1} s^{-1} for benzoic acid, an average value of $k_2 = (1.00 \pm 0.10) \times 10^{10}$ M^{-1} s^{-1} is obtained for chlorophene. This value is very close to 7.1×10^9 M^{-1} s^{-1} reported by Arnold et al. [381] for chlorophene degradation with Fenton's reagent. From this k_2-value, a steady reactive $^{\bullet}OH$ concentration ca. 10^{-13} M at 60 mA can be calculated.

The ability of the four EF cells to mineralize 84-mg L^{-1} chlorophene solutions has been assessed from their TOC decay in the range 60-300 mA with an efficient content of 4.0 and 0.2 mM Fe^{3+}, deduced from the previous study by HPLC, using the O_2-diffusion and carbon-felt cathode, respectively. A continuous slow TOC removal is found in the Pt/O_2 diffusion cell, only attaining 52% mineralization after 660 min of electrolysis at 300 mA. This low oxidizing power can be explained by the formation

of products hardly oxidizable with $^{\bullet}OH$, as discussed for EF treatment of paracetamol and clofibric acid. In contrast, these Fe^{3+}-carboxylics complexes can be slowly but completely destroyed with BDD($^{\bullet}OH$) in the BDD/O_2 diffusion cell at 300 mA, as also found for clofibric acid (see section 8.3.2). It can also be observed that in the latter system the mineralization rate increases as current rises from 60 to 300 mA, and 33%, 45%, 85% and 97% TOC abatement is achieved at 60, 100, 200 and 300 mA after 11 h, respectively, due to the higher production of $^{\bullet}OH$ and BDD($^{\bullet}OH$). Total mineralization can not be attained at all currents after 11 h because $^{\bullet}OH$ from Fenton's reaction are slowly produced from the difficult Fe^{2+} regeneration. Using the carbon-felt cathode, however, a fast and complete degradation (> 95%) is always reached after 540 min of electrolysis. The process is accelerated as current rises, mainly for the first 60 min, because aromatic intermediates can be quickly destroyed. The greater oxidizing ability of the systems with the carbon-felt cathode in comparison to those with the O_2-diffusion cathode can be ascribed to the great amounts of $^{\bullet}OH$ formed from Fenton's reaction due to the fast Fe^{2+} regeneration at the cathode. Appart from this, when the two carbon felt cells are compared, it can be seen that the use of BDD does not lead to a much more relevant TOC abatement. This happens because regardless the important contribution of BDD($^{\bullet}OH$), the production of $^{\bullet}OH$ is more difficult than using Pt.

Ion chromatography displays a unique peak corresponding to chloride ion. The results confirm that Cl^- is quickly accumulated in the cells with Pt, reaching a quasi-steady concentration of about 13 mg L^{-1} (very close to the maximum value of 13.6 mg L^{-1} corresponding to 84 mg L^{-1} chlorophene), whereas in the cells with BDD this ion only attains between 5 and 9 mg L^{-1} and further it is destroyed until disappearing. This behavior agrees with that observed for the EF degradation of clofibric acid.

The above results allow concluding that the overall mineralization of this pharmaceutical by EF involves 60 F for each mol of chlorophene, with chloride ion as primary inorganic ion (Reaction 6.-4). Therefore, MCE can then be determined using Equation 6.-1. As usual, plots show a dramatic fall of efficiency with electrolysis time due to the formation of hardly oxidizable products. In addition, the efficiency rises when current decreases. For example, efficiencies of 10 and 19% values are obtained at 300 and 60 mA, respectively, after 60 min using the BDD/O_2 diffusion cell. Comparison between the four EF systems at 300 mA allows ordering their efficiency on the basis of increasing degradation ability: Pt/O_2 diffusion < BDD/O_2 diffusion < BDD/carbon felt < Pt/carbon felt. In fact, the latter cell presents the greatest MCE values among all the systems tested during this thesis, reaching an efficiency close to 100% at the early stages with a low current applied.

The clarification of the reaction pathway turns out to be a bit more complicated for chlorophene than for the other pharmaceuticals studied in this thesis. Any aromatic intermediate has been identified by chromatographic techniques, not even under the mildest experimental conditions. The remaining chlorophene is the only benzenic compound detected in the chromatograms. This can be accounted for by: (i) the lack of stabilty of these aromatics in its oxidizing surroundings, which prevents their accumulation in the solution, and/or (ii) the formation of soluble polyaromatics that are difficult to characterize due to the lack of standards and the complexity of the mixture. Zhang et al. [385] have reported that chlorophene tends to form this kind of polymers through a radical mechanism. Fortunately, it has been possible to identify and quantify some short-chain carboxylic acids such as glycolic (HOH_2C-HOOC), fumaric (*trans*, H_2C-CH=CH-CH_2), maleic (*cis*, H_2C-CH=CH-CH_2), malonic (HOOC-CH_2-COOH), glyoxylic (CHO-COOH), formic (HCOOH) and oxalic (HOOC-COOH) acids. The former four come from the oxidation of the aryl moiety of aromatic products, whereas glyoxylic acid is formed from the oxidation of glycolic acid. All of them lead to formic and oxalic acids that can be transformed into CO_2 by

the most oxidizing EF systems. Electrolyses using the O_2-diffusion cathode evidence an accumulation of maleic, fumaric, malonic and formic acids at concentrations < 3 mg L^{-1}, and uniquely for 60 min at 60 mA. In contrast, oxalic acid is largely accumulated up to the end of the electrolysis with Pt and BDD anodes. Since Fe^{3+} is largely accumulated in both systems, this acid is expected to be in the form of Fe^{3+}-oxalato complexes, which can not be oxidized by $^{\bullet}OH$ in the bulk solution, thus confirming the mineralization behavior explained above. The slow decay observed using Pt can be ascribed to the role of $^{\bullet}OH_{ads}$ at the anode surface. Similarly, BDD is not able to destroy some of the Fe^{3+} complexes at 60 mA, but at 300 mA, these complexes and solution TOC are completely removed at 660 min through the action of BDD($^{\bullet}OH$). Higher amounts of carboxylics can be found at 60 mA using the carbon-felt cathode. For example, formic acid attains 17 mg L^{-1} at 120 min in the Pt/carbon felt cell. This trend confirms the oxidizing power of the systems with this cathode, which produce such a high concentration of $^{\bullet}OH$ that the aromatics are quickly converted into significant amounts of carboxylics. In addition, the production of this oxidizing species is so high that oxalic acid can be totally destroyed even in the system with Pt. A worth remarking aspect of the systems with the carbon-felt cathode is that a high concentration of iron ions are in the form of Fe^{2+}, thus generating Fe^{2+}-oxalato complexes which are liable to be destroyed by $^{\bullet}OH$. When BDD is coupled to the carbon-felt cathode, Fe^{2+}-carboxylic complexes can be simultaneously oxidized by BDD($^{\bullet}OH$), leading to a slightly faster TOC removal.

Figure 9.-2 given below shows the proposed degradation pathway for oxalic acid. In the cells with the O_2-diffusion cathode, this acid mainly yields Fe^{3+}-oxalato complexes, which can not be destroyed by $^{\bullet}OH$ in the solution, so uniquely BDD($^{\bullet}OH$) at high current is able to destroy them. In contrast, in the cells with a carbon-felt cathode this acid is free or forming Fe^{2+}-oxalato complexes. Both of them can be destroyed by $^{\bullet}OH$ even when Pt is used. Coupling with BDD leads to simultaneous destruction of free oxalic acid and its iron complexes by the combined action of $^{\bullet}OH$ and BDD($^{\bullet}OH$).

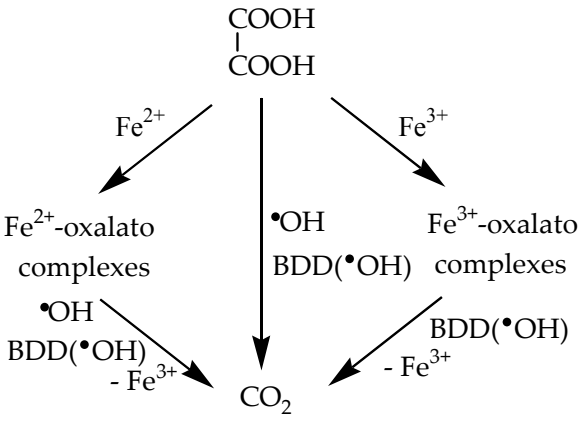

Figure 9.-2 Proposed reaction pathways for oxalic acid in the EF systems. $^{\bullet}OH$ is produced in the bulk solution from Fenton's reaction and BDD($^{\bullet}OH$) is adsorbed on the anode surface.

10. *SUMMARY AND GENERAL CONCLUSIONS*

Paracetamol, clofibric acid and chlorophene are paradigms of NSAIDs, blood lipid regulators and antimicrobials, respectively, which are three of the top sales PPCPs therapeutical groups all throughout the world.

During the last decades, the impact of chemical pollution has focused almost exclusively on the conventional 'priority' pollutants, mainly pesticides and industrial intermediates exhibiting persistence in the environment. Another group that has received comparatively little attention includes both human and veterinary pharmaceutical compounds and personal care products (PPCPs). Nowadays, these compounds are also considered as persistent pollutants because they are continually introduced in the environment at ng-μg L^{-1} level through several routes due to their high worldwide consumption. In contrast to agrochemicals, most of these products are disposed or discharged into the environment via domestic/industrial sewage systems, being the main souces the metabolism and the treatment in the STPs.

Aquatic pollution is particularly troublesome considering that survival of living organisms, including human beings, is based on the water-cycle. PPCPs can pose a huge risk, under assessment at present, because long exposure to trace levels leads to unpredicted and unknown subtle effects that can accumulate so slowly that the changes can become irreversible and be even attributed to natural evolution.

The enormous diversity of chemical composition of pollutants in waters excludes the possibility of using an universal treatment method and suggests the requirement of special treatment technologies for water decontamination. Many treatment processes including several AOPs reported in literature have been shown to be inefficient towards total mineralization of the pharmaceuticals pointed out above. Therefore, more effective processes must be developed as a plausible alternative. In this sense, electrochemical processes such as EAOPs and AO using effective anodes appear to be an appealing environmentally friendly choice, since the main oxidant species is thought to be hydroxyl radical. EF and PEF processes using an O_2-diffusion or a carbon-felt cathode are able to electrogenerate hydroxyl radicals in the bulk solution through Fenton's reaction, whereas in AO using a Pt or a BDD anode the same oxidizing agent is chemisorbed or physisorbed, respectively, at the electrode surface.

Several experimental systems have been studied by combining different cathodes and anodes and by using several catalysts. For each pharmaceutical, optimum conditions for the mineralization process at laboratory scale have been established from the analysis of the TOC abatement and the corresponding MCE values. Subsequently, the degradation kinetics for the reaction between each drug and hydroxyl radicals has been reported. Lastly, the aromatics, carboxylics and inorganic ions have been identified and quantified in order to reveal their trends along the mineralization process and, consequently, the possible pathways for the electrochemical degradation of paracetamol, clofibric acid and chlorophene. In addition, some particularities of the EF process have been clarified.

To sum up, the main conclusions of this thesis are:

1. The oxidation ability of the systems under study depends on the kind of oxidizing agents formed in each one: in AO with Pt only low amounts of $^{\bullet}OH_{ads}$ are involved, whereas in AO with BDD a high effective concentration of $^{\bullet}OH_{ads}$ (also noted as BDD($^{\bullet}OH$)) is reached and weaker oxidizing species are also identified (O_3, H_2O_2 and $S_2O_8^{2-}$ ions). In EF and PEF using a Pt anode the main oxidizing agent is $^{\bullet}OH$ generated in the medium from Fenton's reaction, although hypervalent iron species as well as less powerful oxidizing species such as $HO_2^{\bullet}$ and H_2O_2 are also present in the bulk solution. Coupling between a BDD anode and H_2O_2 electrogeneration in the presence of Fe^{2+} ions and UVA light leads to a **multi-oxidizing-species mixture** responsible for the best performance of such a process towards total mineralization: $^{\bullet}OH$ in the bulk solution and $^{\bullet}OH_{ads}$ at the BDD surface are the main agents, but parallel oxidation of pollutants with weaker oxidizing species formed in the bulk solution such as $HO_2^{\bullet}$, H_2O_2, $SO_4^{\bullet-}$, ferrate ions and other hypervalent iron species, as well as at the BDD surface, as for example O_3, H_2O_2 and $S_2O_8^{2-}$ ions, is also possible. In addition, whenever BDD anode is used and chlorinated compounds are treated, the oxidizing substance Cl_2 is formed in the medium. Such an 'oxidizing cocktail' shapes a water treatment process with the best performance among all the electrochemical procedures studied. The effect of all those oxidizing species different from $^{\bullet}OH$ produced from Fenton's reaction is less significant when the carbon-felt cathode is used, because this reaction has a prevailing role due to the high Fe^{2+} accumulation in the medium.

2. A synergistic combination of Fe^{2+}, Cu^{2+} and UVA light is the key to the degradation behavior of complexes of oxalic and oxamic acids during the total mineralization of paracetamol: Cu^{2+}-oxalato and Cu^{2+}-oxamato complexes can be efficiently oxidized by $^{\bullet}OH$, whereas Fe^{3+} complexes can be destroyed uniquely

by photodecomposition with UVA light. The optimal conditions to mineralize 100-mL solutions containing up to 400 mg L^{-1} paracetamol by EF and PEF are 300 mA, 35 ºC and pH = 3.0.

3. The formation of Fe^{3+}-oxalato complexes is the limiting step regarding overall mineralization whenever an O_2-diffusion cathode and Fe^{2+} ions are used to degrade clofibric acid, because they can not be oxidized with $^{\bullet}OH$ in the bulk solution. BDD($^{\bullet}OH$) is able to slowly destroy these complexes, which are even more quickly oxidized under UVA irradiation in the PEF process mainly due to: (i) the photodecomposition of Fe^{3+} complexes with carboxylic acids, and (ii) the regeneration of Fe^{2+} from photoreduction of $Fe(OH)^{2+}$. The action of UVA light justifies the greatest degradation rate and highest efficiency of PEF using BDD.

4. A poor mineralization is achieved by AO with a Pt anode, whereas the alternative use of a BDD anode leads to total mineralization of paracetamol and clofibric acid up to close to saturation in all media due to the efficient production of $^{\bullet}OH_{ads}$. The mineralization rate is pH-independent, increasing when both temperature and applied current rise, but decreasing when drug concentration rises. Coupling between BDD and O_2-diffusion cathode enhances the mineralization rate and increases the efficiency.

5. Paracetamol and clofibric acid are destroyed after 6-7 min, exhibiting similar pseudo-first-order or complex kinetics by EF and PEF due to the great amount of $^{\bullet}OH$ from Fenton's reaction, whereas they remain in the solution for 150-240 min by AO. Parent compounds and their intermediates are oxidized at similar destruction rate by AO with BDD in acidic and alkaline media, thus justifying the low accumulation of the products and the pH-independence for their TOC decay. The different adsorption of each pollutant at the electrode surface justifies the decay kinetics in AO using Pt and BDD anodes.

6. The comparative performance of O_2-diffusion and carbon-felt cathode in EF shows that an increasing Fe^{3+} initial content causes a slower destruction of chlorophene when the carbon-felt cathode is used, because non-oxidizing reactions are gradually enhanced, but high Fe^{3+} amounts are required with the O_2-diffusion cathode to increase the amount of Fe^{2+} regenerated at the cathode. Overall mineralization of chlorophene solutions at pH 3.0 can always be attained using a carbon-felt cathode, whereas a BDD anode must be used when the O_2-diffusion cathode is tested. This can be related to the formation of Fe^{3+}-oxalato complexes that are hardly oxidized with $^{\bullet}OH$ in the Pt/O_2-diffusion system, whereas they can be slowly but completely destroyed with BDD($^{\bullet}OH$). In contrast, in the systems with a carbon-felt cathode Fe^{2+}-oxalato complexes are formed and directly oxidized in the medium with $^{\bullet}OH$, and its coupling with BDD leads to a slight increase in the oxidation ability at the end of the treatment. On the other hand, the efficiency sequence during the early stages in the four cells used increases in the order:

Pt/O_2 diffusion < BDD/O_2 diffusion < BDD/carbon felt < Pt/carbon felt.

7. MCE calculated on the basis of the primary inorganic ions released from the initial pollutant (Cl^- for clofibric acid and clorophene and NH_4^+ for paracetamol) always rises with increasing temperature and initial pollutant concentration, and with decreasing working current density. The MCE values for AO with BDD are comparable to those of EF and PEF at high initial pollutant concentration because the process is mass-transfer controlled. The highest MCE values are obtained in the cells with a the carbon-felt cathode due to the efficient production of $^{\bullet}OH$ from Fenton's reaction. In all cases the efficiency decreases at long electrolysis time due to both parallel non-oxidizing reactions and the generation of hardly oxidizable products.

8. General reaction pathways for the mineralization of paracetamol and clofibric acid by electro-oxidation methods, including the aromatic, carboxylic and ionic intermediates detected, have been proposed. For chlorophene, carboxylic intermediates formed as a result of the cleavage of the benzenic rings have been identified, and their total destruction has been demonstrated.

9. The electrochemical technologies discussed in this thesis are potent enough to decontaminate wastewaters containing paracetamol, clofibric acid and chlorophene in a wide range of experimental conditions. All of them are suitable to destroy the initial pollutant, and most of them are even able to completely mineralize the solutions treated. Therefore, direct and indirect electro-oxidation processes can be an effective, simple and versatile alternative compared to other less oxidizing methods reported in literature to remove these pharmaceuticals. EF and PEF processes are complex, since pH must be adjusted at ca. 3.0 and O_2 must be supplied continuously. However, wastewaters usually contain the required amounts of Fe^{2+} and Cu^{2+} ions and then EF and PEF with acceptable efficiency are suitable methods to degrade both the parent compounds and their aromatic intermediates in a few minutes just releasing carboxylic acids and inorganic ions. Coupling with biological treatments could be easily and quickly carried out if total mineralization was not required by means of EF and PEF. On the other hand, AO with a BDD anode can be applied in a larger variety of conditions than the above methods and notwithstanding the comparatively lower MCE values at early stages for low-loaded wastes, it gives an insignificant accumulation of reaction intermediates that could be even more dangerous than the pharmaceutical treated. Combination with an O_2-diffusion cathode enhances both the mineralization rate and efficiency. Unfortunately, the cost of BDD electrodes is at present a major drawback of this technology.

11. RESUM I CONCLUSIONS GENERALS

El paracetamol, l'àcid clofíbric i el clorofè són exemples representatius de tres dels grups terapèutics més comercialitzats de *PPCPs* en tot el món: fàrmacs antiinflamatoris no esteroídics, fàrmacs reguladors de lípids en sang i fàrmacs antimicrobials, respectivament.

En els últims temps, l'impacte de la pol·lució química en el medi s'ha centrat de manera quasi exclusiva en els anomenats contaminants convencionals 'prioritaris', principalment pesticides i intermedis industrials molt persistents un cop alliberats en els diversos ecosistemes. Un grup de substàncies també presents en les aigües, i al qual s'ha dedicat poca atenció fins fa poc temps, inclou els compostos farmacèutics d'ús humà i veterinari i tot un conjunt de productes de cura personal (*PPCPs*). Actualment aquests compostos també es cataloguen com a contaminants persistents, donat que són introduïts en el medi de manera continuada a nivell de ng-µg L^{-1} a través de vàries rutes mercès al seu consum àmpliament extès a nivell mundial.

En moltes ocasions, aquestes substàncies entren en el medi provinents d'aigües residuals domèstiques i industrials, trobant-se l'origen primari en el metabolisme per part dels éssers vius i en els tractaments en les *STPs*. La contaminació del medi aquàtic és especialment preocupant si hom té en compte la importància del cicle de l'aigua en la conservació del planeta i dels éssers que hi habiten. En darrer terme, els *PPCPs* poden implicar un risc enorme, que avui dia es troba en fase d'avaluació, ja que un temps d'exposició prolongat a traces de compostos exògens d'aquest tipus podria conduir a efectes molt subtils i difícils de predir sobre els éssers vius, tot acumulant-se lentament i provocant alteracions biològiques de diversa magnitud.

Avui dia l'estratègia aplicada en l'àmbit dels tractaments d'aigües residuals amb un ampli ventall de contaminants presents en elles es fonamenta en la combinació de procediments successius, incloent-hi tecnologies especials que siguin efectives contra compostos molt particulars. Diversos autors han dut a terme estudis d'eliminació de fàrmacs mitjançant varis dels *AOPs* comentats àmpliament en el capítol 5 d'aquesta tesi, però habitualment aquests mètodes no són capaços de mineralitzar completament les dissolucions tractades. Per tant, cal desenvolupar processos més potents i efectius. Amb aquesta intenció, diversos procediments electroquímics que inclouen la *AO* i els *EAOPs* es presenten com a una atractiva alternativa compatible mediambientalment, ja que la principal espècie oxidant que intervé és el radical hidroxil. S'han realitzat varis experiments tot combinant diversos càtodes i ànodes, i utilitzant diferents catalitzadors. A través de la reacció de Fenton, els processos EF i PEF emprant càtodes de difusió d'oxigen o de feltre de carbó permeten produir radicals hidroxil en el si de la dissolució tractada. En la *AO* amb ànodes de Pt o *BDD* l'agent oxidant és el mateix, si bé es troba quimisorbit o fisisorbit, respectivament, en la superfície de l'elèctrode.

Per al paracetamol s'ha fet un estudi dels processos *EF* i *PEF* amb un ànode de Pt i un càtode de difusió d'oxigen, i s'ha constatat el paper rellevant que tenen els diferents

complexos formats entre els catalitzadors metàl·lics emprats i els àcids carboxílics generats durant la degradació. També s'ha aplicat el procès de *AO* amb dos tipus d'ànodes, Pt i *BDD*, i emprant un càtode de grafit.

En el cas de l'àcid clofíbric s'ha seguit un esquema anàleg, però a més s'ha introduït la combinació de l'ànode de *BDD* amb el càtode de difusió d'oxigen, fet que ha conduït a una millora significativa dels resultats. En l'estudi d'aquest compost s'ha posat de manifest la importància d'espècies oxidants diferents del radical hidroxil de cara a la destrucció dels contaminants orgànics.

I quant al clorofè, s'ha dut a terme una anàlisi profunda del procès *EF*, desenvolupada principalment en el Laboratori d'Electroquímica dels Materials i del Medi Ambient i en el laboratori del professor Oturan durant l'estada a la Universitat de Marne la Vallée (París). Fruit de la col·laboració entre ambdues parts s'ha pogut explicar l'efecte del sistema catalític Fe^{3+}/Fe^{2+} sobre l'efectivitat de les cel·les amb ànodes de Pt i *BDD* i càtodes de difusió d'oxigen i feltre de carbó.

Per a cadascun dels tres fàrmacs estudiats s'han definit els processos òptims de mineralització a escala de laboratori a partir de l'evolució amb el temps d'electròlisi del *TOC* de la dissolució i dels valors de *MCE* corresponents. En aquest sentit, s'ha estudiat la influència de les variables experimentals (intensitat de corrent, pH, *T*, concentració de catalitzadors). Mitjançant l'*HPLC* en fase inversa s'han analitzat i comparat en profunditat les cinètiques de degradació per a la reacció entre cada fàrmac i els radicals hidroxil. I per últim, amb l'*HPLC* en fase inversa i d'exlusió iònica, la cromatografia iònica i la *GC-MS* s'han identificat i quantificat els intermedis aromàtics i carboxílics i els ions inorgànics alliberats, i d'aquesta manera s'han pogut discutir les evolucions observades i, finalment, s'han proposat els possibles camins de reacció per a la mineralització electroquímica del paracetamol, l'àcid clofíbric i el clorofè. A més, s'han aclarit de forma detallada algunes particularitats del procès *EF*.

Les principals conclusions de la tesi es presenten a continuació:

1. La capacitat oxidativa de cadascun dels sistemes estudiats depèn dels diversos agents oxidants que es formen en cada cas: en *AO* amb Pt es genera una quantitat molt baixa de $^{\bullet}OH_{ads}$, mentre que en *AO* amb *BDD* s'assoleix una concentració efectiva de $^{\bullet}OH_{ads}$ (altrament identificats com *BDD*($^{\bullet}OH$)) elevada i es detecta també la presència d'espècies oxidants més febles (O_3, H_2O_2 i ions $S_2O_8^{2}$). En *EF* i *PEF* amb Pt, el principal agent oxidant és el radical $^{\bullet}OH$ generat en el medi a partir de la reacció de Fenton, tot i que també cal tenir en compte la presència en el si de la dissolució d'espècies hipervalents de ferro i d'agents menys potents, com per exemple el H_2O_2 i el radical $HO_2^{\bullet}$. L'acoblament entre l'ànode de *BDD* i l'electrogeneració de H_2O_2 amb presència d'ions Fe^{2+} i llum UVA condueix a una **mescla de multi-oxidants** que és la responsable de la major capacitat de mineralització d'aquest procediment: els principals agents oxidants són els radicals $^{\bullet}OH$ en el si de la dissolució i els $^{\bullet}OH_{ads}$ en la superfície del *BDD*, si bé no cal oblidar la possible oxidació paral·lela dels contaminants mitjançant espècies menys poderoses formades en el medi, com per exemple $HO_2^{\bullet}$, H_2O_2, $SO_4^{\bullet-}$, ions ferrat i altres espècies hipervalents de ferro, així com en la superfície del *BDD*, com els esmentats O_3, H_2O_2 i ions $S_2O_8^{2-}$. A més, sempre que s'utilitza l'ànode de *BDD* per a tractar compostos clorats, es genera en el medi una altra espècie oxidant com és el Cl_2. En definitiva, mercès a aquest 'còctel oxidant' s'aconsegueix un procés de tractament d'aigües amb el qual s'obtenen els millors resultats d'entre tots els procediments electroquímics estudiats. L'efecte de totes aquestes espècies oxidants diferents del radical $^{\bullet}OH$ produït a partir de la reacció de Fenton és menys significatiu quan s'empra el càtode de feltre de carbó, ja que, a causa de l'acumulació d'una gran quantitat d'ions Fe^{2+} en el medi, aquesta reacció juga un paper preponderant.

2. La combinació sinèrgica de Fe^{2+}, Cu^{2+} i llum UVA és la clau del comportament degradatiu dels complexos dels àcids oxàlic i oxàmic generats durant la mineralització completa del paracetamol: tants els complexos Cu^{2+}-oxalat com els Cu^{2+}-oxamat són oxidats eficientment per part del radical $^{\bullet}OH$, mentre que els complexos de Fe^{3+} únicament poden ser destruïts per fotodescomposició amb llum UVA. Les condicions òptimes per a mineralitzar dissolucions de 100 mL amb concentracions de fins 400 mg L^{-1} de paracetamol mitjançant *EF* i *PEF* són 300 mA, 35 ºC i pH = 3,0.

3. La formació dels complexos Fe^{3+}-oxalat és l'etapa limitant quant a la mineralització total de l'àcid clofíbric sempre que s'usen el càtode de difusió d'oxigen i ions Fe^{2+}, ja que no poden ser oxidats per part del radical $^{\bullet}OH$ en el si de la dissolució. L'agent *BDD*($^{\bullet}OH$) és capaç de destruir lentament aquests complexos, que encara són més ràpidament eliminats en irradiar amb llum UVA en l'anomenat procès *PEF*. Aquest darrer comportament es pot atribuir principalment a: (i) la fotodescomposició dels complexos formats pels àcids carboxílics amb Fe^{3+}, i (ii) la regeneració de Fe^{2+} a partir de la fotorreducció de $Fe(OH)^{2+}$. L'acció de la llum UVA justifica que la velocitat de degradació i l'eficiència més elevades s'obtinguin amb el procès *PEF* amb *BDD*.

4. La mineralització assolida mitjançant *AO* amb ànode de Pt és pobra, mentre que l'ús de l'ànode de *BDD* condueix a la mineralització total de dissolucions fins i tot saturades de paracetamol i àcid clofíbric en un ampli rang de pH, gràcies a la producció eficient de radicals $^{\bullet}OH_{ads}$. La velocitat de mineralització és independent del pH inicial, tot augmentant quan s'apliquen intensitats i temperatures més elevades, però disminuint a mesura que la concentració inicial de fàrmac és major. L'acoblament entre el *BDD* i el càtode de difusió d'oxigen provoca un increment tant de la velocitat de mineralització com de l'eficiència del procès.

5. El paracetamol i l'àcid clofíbric són destruïts en 6-7 min mitjançant *EF* i *PEF*, amb cinètiques de pseudo-primer ordre o bé complexes que són similars a causa de la gran quantitat de radicals $^{\bullet}OH$ generats per la reacció de Fenton en ambdós casos. En canvi, mitjançant *AO* romanen en dissolució durant 150-240 min. El compost inicial i els seus intermedis de reacció són oxidats a velocitats de destrucció semblants en *AO* amb *BDD*, en medi àcid i alcalí, tot justificant la baixa acumulació d'intermedis i la independència del descens de *TOC* respecte el pH inicial. La diferent cinètica observada en *AO* amb Pt i *BDD* es pot atribuir a la diferència d'adsorció de cada fàrmac en la superfície de cadascun dels ànodes.

6. La comparació entre l'actuació dels càtodes de difusió d'oxigen i de feltre de carbó en el procès *EF* revel·la que un augment del contingut inicial de Fe^{3+} causa un alentiment de la destrucció del clorofè quan s'empra el càtode de feltre de carbó perquè les reaccions no oxidants prenen progressivament més notorietat. En canvi, es requereixen quantitats elevades de Fe^{3+} quan s'empra el càtode de difusió d'oxigen, per tal d'incrementar la concentració Fe^{2+} regenerat al càtode. En utilitzar el càtode de feltre de carbó, sempre s'assoleix la mineralització completa de les dissolucions de clorofè a pH 3,0, mentre que en usar el càtode de difusió d'oxigen cal recórrer a la combinació amb l'ànode de *BDD*. Aquesta diferència es pot relacionar amb la formació de complexos Fe^{3+}-oxalat, que són difícils d'oxidar amb el radical $^{\bullet}OH$ en el sistema Pt/difusió, i que poden ser destruïts de manera completa però lenta amb el *BDD*($^{\bullet}OH$). D'altra banda, en els sistemes amb el càtode de feltre de carbó es formen complexos Fe^{2+}-oxalat que són directament oxidats pel radical $^{\bullet}OH$ en el si de la dissolució, i l'acoblament amb l'ànode de *BDD* dóna com a resultat un lleuger increment en la capacitat oxidativa al final del tractament. Per altra part, l'eficiència del procès en les primeres etapes del tractament en les quatre cel·les utilitzades augmenta en l'ordre:

Pt/difusió < *BDD*/difusió < *BDD*/feltre < Pt/feltre.

7. La *MCE* calculada en base als ions inorgànics primaris provinents del contaminant inicial (Cl^- per a l'àcid clofíbric i el clorofè i NH_4^+ per al paracetamol) sempre augmenta en incrementar la temperatura i la concentració inicial de fàrmac, i en disminuir la densitat de corrent de treball. A concentracions inicials de fàrmac elevades, els valors de *MCE* per a *AO* amb *BDD* són comparables als obtinguts en *EF* i *PEF* perquè el procès està controlat per transferència de matèria. Els valors més alts de *MCE* s'obtenen en les cel·les amb el càtode de feltre de carbó mercès a l'eficient producció de radicals $^{\bullet}OH$ a partir de la reacció de Fenton. En tots els casos, l'eficiència disminueix a temps d'electròlisi llargs degut a les reaccions paral·leles no oxidants i a la generació d'intermedis difícils d'oxidar.

8. S'han proposat camins de reacció generals per a la mineralització del paracetamol i l'àcid clofíbric mitjançant mètodes d'electro-oxidació, tot incloent-hi els intermedis aromàtics, carboxílics i iònics detectats. En el cas del clorofè s'han identificat els intermedis carboxílics generats a partir de la ruptura dels anells benzènics, i s'ha demostrat la seva destrucció completa.

9. Les tecnologies electroquímiques discutides en aquesta tesi són prou potents com per descontaminar aigües residuals que continguin paracetamol, àcid clofíbric i clorofè en un rang ampli de condicions experimentals. Tots els processos estudiats són adients per a destruir el fàrmac inicial, i molts d'ells a més són capaços de mineralitzar totalment les dissolucions tractades. Per tant, aquests procediments d'electro-oxidació directa o indirecta poden suposar una alternativa efectiva, simple i versàtil en comparació amb altres mètodes que tenen una capacitat oxidativa menor en tractar aquests tipus de compostos. Els processos *EF* i *PEF* són complexos, ja que cal ajustar el pH inicial a un valor de 3,0 aproximadament, i a més cal sumministrar O_2 continuament al càtode o a la dissolució. De tota manera, les aigües residuals contenen habitualment una

quantitat suficient d'ions Fe^{2+} and Cu^{2+}, i per tant aquests mètodes acostumen a ser adients i presenten una eficiència acceptable pel que fa a la degradació dels contaminants inicials i dels seus intermedis aromàtics de reacció en uns pocs minuts, tot alliberant àcids carboxílics i ions inorgànics. En cas que no es requereixi la mineralització total mitjançant *EF* i *PEF*, aquests processos es poden plantejar com a mètodes de pretractament per a un posterior trasvasament fàcil i ràpid cap a reactors biològics. D'una altra banda, el procès *AO* amb ànode de *BDD* es pot aplicar en una varietat de condicions més àmplia que els mètodes *EF* i *PEF* i, malgrat presentar uns valors de *MCE* comparativament menors durant les etapes inicials quan es tracten efluents poc carregats, dóna lloc a una menor acumulació d'intermedis de reacció que podrien ser inclús més perillosos que el fàrmac estudiat. La combinació amb un càtode de difusió d'oxigen fa que s'incrementin la velocitat de mineralització i l'eficiència del procès. Malauradament, el cost dels elèctrodes de *BDD* és encara avui dia un inconvenient important d'aquesta tecnologia.